In vivo characterisation of Hippocampal Neuroinflammatory Pathology in Patients with Multiple Sclerosis using novel Multimodal quantitative MR imaging

Prince Nwaubani

Department of Clinical Neuroimaging and Neuroscience

Clinical Imaging Sciences Centre

Brighton and Sussex Medical School

University of Brighton

A thesis submitted for the degree of Doctor of Philosophy

February 2023

CHAPTER OVERVIEW

This thesis describes a multi-modal approach for molecular imaging of hippocampal neuroinflammation in Multiple Sclerosis (MS). The major aims were to test the sensitivity of high-resolution diffusion weighted imaging (DWI-MRI) in the identification and quantification of microstructural alterations within selected hippocampal sub regions in neuroinflammatory pathology. I also additionally sought to explore the potential of Diffusion Weighted Magnetic Resonance Spectroscopy (DWMRS) in the detection of cell specific morphological alterations within the anterior hippocampus.

My thesis comprises 8 key chapters. The first chapter gives a broad insight into the background of MS and the available phenotypes, the complexities surrounding imaging of the hippocampus in inflammatory states, the imaging techniques utilized in this research and also introduces an innovative post acquisition resolution enhancing algorithm (Imaging quality transfer) which was applied to enhance resolution of my imaging data.

In my second chapter, I carried out a comprehensive systematic review which elaborated on the in-vivo quantitative imaging of hippocampal inflammation in prototypical autoimmune neuroinflammatory states, focusing on three conditions; MS, Systemic lupus erythematosus (SLE) and Autoimmune Encephalitis (AE).

The third chapter tests the effectiveness of the resolution enhancing algorithm protocol on 11 downloaded preliminary imaging data from the Human connectome project, and in the fourth chapter, I begin to describe the general methodology employed in the characterization and analysis of the recruited clinical data.

15 MS patients and 10 healthy controls underwent high-resolution diffusion weighted MRI scans. Structural, functional and spectroscopy sequences were utilized in imaging the hippocampus in recruited participants with the application of image quality transfer to further enhance spatial resolution, and the subsequent use of manual and automatic segmentation methods to deduce diffusion indices reflective of alterations in hippocampal subfield microstructure.

The fifth chapter describes the clinical and behavioural characterisation of my recruited participants, while my chapter six looks at a preliminary analysis of microstructural

pathological alterations of relapsing and progressive MS with healthy controls, and potential correlations within the hippocampus.

Chapter seven reports exploratory findings of DWMRS of the recruited participants and demonstrates the distribution of the apparent diffusion coefficient of three key metabolites (Creatinine, N-acetyl aspartate and Choline) within the anterior hippocampus.

My findings provide preliminary support to the utility of resolution enhanced DW MRI, and of DWMRS for the assessment of MS hippocampal pathology, particularly in PPMS, a form of MS characterised by progressive neurological worsening from the onset. My findings also inform design of future studies of therapeutics targeting symptoms related to hippocampal pathology.

To conclude, chapter eight provides a detailed summary, and highlights on the limitations, hinderances and the potential future directions of this research.

ABSTRACT

Background

Evidence indicates that the hippocampus is a site of neuroinflammatory pathology and glial activation in Multiple Sclerosis (MS). Cognitive and affective sequelae of hippocampal involvement in MS are disabling and difficult-to-treat with available disease modifying treatments. Although hippocampal subregions display differential pathological vulnerability, clinical routine MR techniques are unable to characterise hippocampal subfields due to insufficient spatial resolution. The work presented in my thesis investigated the use of novel multi-modal MRI techniques to characterize hippocampal neuroinflammatory pathology in patients with MS.

Aims

In my PhD studies I tested two novel approaches: 1) the application of a post-acquisition resolution enhancing technique on diffusion-weighted MR imaging data to enable assessment of tissue microstructure separately across different hippocampal subfields. 2) the study of the hippocampus with diffusion-weighted Magnetic Resonance Spectroscopy (DWMRS), to detect cell-specific morphological alterations. My aim was to test whether the application of

these imaging techniques to the hippocampus in MS patients is feasible and sensitive to detect neuroinflammatory changes.

Using collected MS and control data, I also intend to test the statistical significance amongst depression, cognitive and disability scores and explore correlations with imaging variables.

Methods

For my first study, I used diffusion-weighted imaging datasets (n=11) from the Human Connectome Project (HCP) database of healthy subjects, and I applied image quality transfer (IQT) to enhance post-acquisition resolution before segmentation of hippocampal subfields. Diffusion parameter estimates were obtained from diffusion tensor imaging (DTI) and neurite orientation dispersion and density imaging (NODDI) models. For my second study, I recruited a cohort of 15 MS patients (PPMS n=6; RRMS, n=9), and 10 healthy subjects and applied a similar imaging protocol to compare DTI and NODDI parameters across hippocampal subfields. In the third study, I applied DW-MRS to the same cohort to estimate hippocampal apparent diffusion coefficients (ADC) of cell-specific metabolites. Clinical outcomes, including cognitive and affective symptoms, were recorded.

Results

The application of IQT protocol on DW imaging data enabled effective segmentation of hippocampal subfields on both HCP datasets and clinical cohort. There were significant differences in DTI and NODDI parameters between subfields. In the clinical study, I found differences in diffusivity parameters in specific subfields between PPMS and controls. The DW-MRS study provided preliminary evidence that assessment of hippocampal metabolites ADC was feasible, and potentially sensitive to detect differences in PPMS patients. Finally, I estimated effect sizes to inform power and sample size calculation for future studies.

Conclusions

My findings provide preliminary support to the utility of resolution-enhanced DTI and DW-MRS for the assessment of MS hippocampal pathology, particularly in PPMS. These results will inform design of future studies of therapeutics targeting symptoms related to hippocampal pathology.

TABLE OF CONTENTS

COPYRIGHT DECLARATION

Prince Nwaubani

November 2021

DECLARATION OF ORIGINALITY

I declare that the work described in this thesis is that of the author and that all work by others are appropriately referenced.

None of this work has been submitted for any other qualification at this or any other University.

Prince Nwaubani

November 2021

STATEMENT OF CONTRIBUTION

I was the principal contributor to the research project illustrated in this thesis from the

earliest phases of the design and preparation of the studies. I prepared the initial draft

of the project and outlined the plan for the studies in the "research proposal" of my

CISC- Clinical Research Fellowship. I designed and wrote the first drafts of the

study protocol under the close supervision of my research supervisor. I submitted the final study protocol to the Research Ethics Committee (REC). I also designed and completed all the additional documentation for the ethics application, including the IRAS form, the Site-Specific application forms, the R&D application form, the Participant Information Sheet, the letter to General Practitioners/ Neurologists, and the advertisement material.

I processed the application to the REC and presented the application at the REC meeting. I replied to the REC committee comments and finally obtained definitive approvals.

I have been the Doctoral Researcher of the study reported here (study protocol reference: 277501). I have continuously ensured compliance with Good Clinical Practice and I held the ultimate responsibility for the study conduct and management of all research sites involved in the research, for the entire duration of the study.

I have set up, coordinated, and actively managed the identification and recruitment of

study subjects. I conducted initial phone-based pre-screening interviews with all subjects interested in taking part in the study. I met all subjects for explanation of the study procedures, and obtained the informed consent and approved their inclusion in the study based on the review of the inclusion criteria. I have been responsible for the medical governance of the study. I have led the screening process, interviewed and conducted a complete medical examination of all subjects. I reviewed any clinical incidental findings, and liaised with General Practitioners and consultant neurologists to share any useful clinical information based on incidental findings. I have administered questionnaires, clinical rating scales and psychiatric diagnostic interviews. I was responsible for all phases of MRI

scanning. I was present and supervised the scanning procedures for all MRI scans. Specifically, my involvement included:

- the inspection of all individual MRI imaging study data

- the comparison of various modelling methods for selection of the quantification method to be used in the final analysis.

- the exploration of various methodologies for identification of a suitable pseudo-reference region

- the manual and automatic segmentation of the hippocampus of patients with multiple sclerosis as well as healthy controls.

I conceived and ran all statistical analyses, including statistical tests on group comparisons and on correlations between clinical and demographic data, MRI data, in addition to structural and functional MRI parameters, as well as clinical parameters.

I provided the initial interpretation of all findings, and coordinated the discussion and review of the findings with all collaborators to the project. I have been the principal author and drafted the first version of the articles on which Chapters 1, 2, 4, 5, 6 and 7 are based.

PUBLICATIONS DERIVED FROM THIS WORK

- Nwaubani P, Cercignani M, Colasanti A. Invivo Quantitative Imaging of Hippocampal Inflammation in Autoimmune Neuroinflammatory Conditions: A Systematic Review. Published in the Journal of Clinical and Experimental Immunology. DOI: 10.1093/cei/uxac058

- Nwaubani P, Warner A, Colasanti A, Cercignani M. MRI Analysis: Optimization of parameters for diffusion MRI to enhance hippocampal subfield analysis and segmentation (Preliminary Data). Published in the Journal of European Psychiatry.

- P Nwaubani, A Warner, N Dowell, AW Barritt, I Ronen, M Cercignani, A Colasanti. Multi-modal Imaging in Multiple Sclerosis. Abstract accepted at the Faculty of Neuropsychiatry Conference (2022).

ACKNOWLEDGEMENTS

SUMMARY OF FIGURES AND TABLES

LIST OF ABBREVIATIONS

AD	Axial Diffusivity
ADC	Apparent Diffusion Coefficient
AE	Autoimmune Encephalitis
ANAM	Automated Neuropsychological Assessment Metric
anx	Anxiety
ASE	Asymmetric spin echo
ASHS	Automatic Segmentation of Hippocampal Subfields
ATP	Adenosine triphosphate
AVLT	Auditory Verbal Learning Test
BDI	Becks Depression Inventory
B_{max}	Benzodiazepine receptor concentration
BBB	Blood Brain Barrier
BICAMS	Brief International Cognitive Assessment for MS.
BMS	Benign Multiple Sclerosis
BOLD	Blood-oxygen level dependent
BRB-N	The Brief Repeatable Battery of Neuropsychological Tests
BVMT-R	Brief Visuospatial Memory Test- Revised

CA	Cornu Ammonis
CBF	Cerebral Blood Flow
CHO	Choline
CIS	Clinical Isolated Syndrome
CISC	Clinical Imaging Sciences Center
COX	Cyclooxygenase
Cr	Creatine
CVLT	California Verbal Learning Test
DCE	Dynamic Contrast Enhanced
dep	Depression
DG	Dentate Gyrus
DIT	Disseminated in time
DIS	Disseminated in space
dMRI	Diffusion MRI
DMT	Disease modifying treatment
DNRAB	*N*-methyl-D-aspartate receptor
DTI	Diffusion Tension Imaging
DVR	Distribution Volume Ratio
DW-MRI	Diffusion Weighted Magnetic Resonance Imaging
DW-MRS	Diffusion Weighted Magnetic Resonance Spectroscopy
EAE	Experimental autoimmune encephalomyelitis
EDSS	Expanded Disability Status Scale
EPI	Echo-planner imaging
ESS	Epworth Sleepiness Scale
FA	Fractional Anisotropy
FASTMAP	Fast automatic schimming technique by mapping along projections.

FLAIR	Fluid attenuated inversion recovery
FOV	Field of view
FSS	Fatigue Severity Scale
GABA+	Gama-aminobutyric acid (contains contributions from both macromolecules and homocarnosine
GAD-7	Generalized Anxiety Disorder Assessment
GASE	Modified asymmetric spin echo
GL	Glycine
Glu	Glutamate
GM	Grey Matter
HADS	Hospital Anxiety and Depression Scale
HC	Healthy Control
HCP	Human Connectome Project
HPA	Hypothalamic pituitary axis
HV	Healthy Volunteer
IL	Interleukin
Ins	Inositol
ICVF	Intracellular volume fraction
IQT	Image Quality Transfer
K^{trans}	Volume transfer constant
LH	Left Hippocampus
LLT	Location Learning Test
LPS	Lipopolysaccharide
LPSVD	Linear prediction singular value decomposition
Lt	Left
LTP	Long term potentiation
MADRS	Montgomery-Asberg depression rating scale

MAP	Mean apparent propagator
MD	Mean Diffusivity
MDD	Major Depressive Disorder
MINI	Mini International Neuropsychiatric Interview
MMSE	Mini-Mental State Examination
MPRAGE	Magnetization Prepared-Rapid Gradient Echo
MRS	Magnetic Resonance Spectroscopy
MS	Multiple Sclerosis
MTL	Medial temporal region
MTR	Magnetization Transfer Ratio
NAA	N-acetylaspartate
NAWM	Normal appearing white matter
NCV	Normalized Cortical Volume
neg /pos correl	Negative/Positive Correlation
NODDI	Neurite Orientation Dispersion and Density Imaging
NS	Not Specified
ODI	Orientation Dispersion Index
PASAT	Pace Auditory Serial Addition Test
PET	Positron Emission Tomography
PHC	Parahippocampal Cortex
PMS	Progressive Multiple Sclerosis
PPMS	Primary Progressive Multiple Sclerosis
Rad Dist	Radial Distance
RAFF4	Relaxation Along a Fictitious Field in the rotating frame of rank 4
RAVLT	Rey Auditory Verbal Learning Test
RD	Radial Diffusivity

RH	Right Hippocampus
ROCF/RCF/RCFT	Rey-Osterrieth Complex Figure Test
ROI	Region of interest
RRMS	Relapsing Remitting Multiple Sclerosis
Rt	Right
RWFT	Regensburger Word Fluency Test
SD	Standard Deviation
SDMT	Symbol Digit Modalities Test
SLE	Systemic Lupus Erythematosus
SLRM	Stratum lacunosum, radiatum and moleculare
SNR	Signal to noise ratio
SPMS	Secondary Progressive Multiple Sclerosis
SRT	Selective Reminding Test
SS	Short Story
SSCI	Simple Spinal Cord Involvement
STAI	State Trait Anxiety Inventory
SUV_R	Mean radioactivity/ injected dose/weight
$T1_P$	Adiabatic Longitudinal relaxation method
$T2_P$	Transverse Relaxation Method
TE	Echo time
TMT	Trail Making Test
TR	Relaxation time
TSPO	Translocator Protein (18kDa)
Ve	Volume in the extravascular extracellular space per unit of tissue volume
VEPCASL	Vessel encoded psudo-continuous arterial spin labelling
VHS	Vestigial hippocampal sulcus

V_T	Volume of Distribution
WAIS	Wechler Adult Intelligence Scale
WCST	Wisconsin Card Sorting Test
WL	Word Learning

CHAPTER 1. BACKGROUND

1.1 MULTIPLE SCLEROSIS

1.1.1 Brief history

The contents of the diary of Sir Augustus Frederick d'Este (Grandson of King George III of England) was probably the first known legitimate case record of Multiple Sclerosis (Landtblom et al., 2010). The 26-year ordeal of the disease condition that befell d'Este at the age of 28 years was vividly described as transient visual loss, accompanied later on by episodic bouts of weakness and clumsiness in the limbs, dizziness, numbness, urinary problems, muscle spasms, tremors and erectile dysfunction. Following further progression of symptoms, d'Este would become confined to a wheelchair after approximately 20 years. He died in 1848 at the age of 54 years (Landtblom et al., 2010). There would be further misconceptions arising from similar presentations, until the turn of the 19th century when French neurologist, Jean Martin Charcot gave the first explicit description of Multiple Sclerosis (MS) through his famous lectures on "la sclérose en plaques" in Paris. This established the earliest insight into the pathophysiology and clinical diagnosis of MS (Kumar et al., 2011). With further advancements in clinical investigatory modalities and the ushering in of sophisticated diagnostic tools in the 20th century, MS is currently reckoned to be one of the most common reasons for admission onto a neurological ward.

1.1.2 Epidemiological and clinical considerations

MS is a chronic, debilitating disease and represents the major, non-traumatic, cause of neurological disability especially within societies that lie along northern geographic latitudes. Globally, an estimated 2.5 million people are considered to have MS. Based on GP records analysed by (Mackenzie et al., 2014), accumulated between periods 1990 and 2010, approximately 126.000 individuals were known to be affected by MS in the UK alone, with a rising trend of approximately 2.4% per annum, possibly attributable to better diagnostic acumen. More recent data emerging from Public Health England 2020, depict prevalence

counts with records of 105.800 individuals in England (about 190 cases per 100.000), and a two-fold presence in women than men (276 versus 106 per 100.000 population). Total UK prevalence figures are portrayed to be over 130.000. Highest prevalence figures are reported in the 60-69 age category for both sexes. In terms of incidence rates across England, there are approximately 10 new cases diagnosed each year per 100.000 population and 4950 new cases of MS are reported to be diagnosed annually. A cross-sectional retrospective study estimates the average cost of MS per person, per year, in the UK to increase proportionally to the levels of disability; £11.400, £22.700 and £36.500 for mild, medium and advanced levels of disability respectively (A. Thompson et al., 2017). A possible estimated 1.2 billion expenditure per annum in the UK (Compston & Coles, 2002).

For approximately 85% of MS patients the disease starts with a course of recurrent and reversible neurological deficits. Relapses usually last no more than a few months and the patient regains neurological function. This phase of the disease is termed relapsing-remitting MS (RRMS). After 8-20 years, the majority of RRMS patients enter a second phase of the disease, secondary progressive MS (SPMS) characterised by continuous, irreversible neurological decline without intermittent relapses. The Primary Progressive MS (PPMS), a distinct clinical entity, which could also precede the SPMS, is without the relapsing-remitting characteristics of RRMS, and consists of gradually progressive worsening symptoms from the outset. Unlike RRMS which is more common in females and is usually diagnosed under the age of 40, PPMS occurs in equal numbers of males and females and is commonly diagnosed in the 40s or 50s.

The signs and symptoms of MS comprise sensory, motor, visual, cognitive, as well as affective alterations. Sensory symptoms include; numbness, burning, prickling, tightness, itching, tingling, experiences of pins and needles. Visual related symptoms include; double vision, blurred vision, involuntary rapid eye movements, optic neuritis and in some cases, total sight loss in affected eye. Approximately 25-50% of MS patients will suffer with major depression in their life time, a 3-5 times increase compared to the population in general (Feinstein et al., 2014). More regular symptoms of depression include, concentration difficulties, irritability, insomnia, anorexia and fatigue. Rarer symptoms include a sense of guilt and low self-esteem (Minden et al., 1987a). Anxiety disorders also occur in approximately 13 to 31% of cases, with generalized anxiety, panic disorders and obsessive-compulsive disorder being the more common types (Korostil & Feinstein, 2007). Up to 50%

of MS patients tend to experience varied forms of decline in cognition during illness course (Calabrese, 2006). Incidence rates of cognitive impairment are 20-40% in MS patients with a benign course, and approximately 50-60% in more progressive MS types (Benedict et al., 2006; Glanz et al., 2007; Patti, 2009). Sustained attention, complex visuospatial tasks, short/long term retrieval functions, working memory and conceptual reasoning are usually impacted upon (Savettieri et al., 2004).

Evidence of damage to the central nervous system (CNS) that are disseminated in time (DIT) and space (DIS) are the key requirements for a diagnosis of MS. DIT and DIS represent damage that has occurred at different dates and to different locations of the central nervous system. With particular emphasis on the necessity for early diagnosis in the disease course and prompt access to the right treatment, the International Panel on Diagnosis of Multiple Sclerosis reviewed the 2010 McDonald criteria in 2017 and incorporated the following changes, which allow for a confirmed diagnosis. These apply firstly, if there is an additional existence of CSF-specific oligoclonal bands with clinical isolated syndrome plus clinical/MRI affirmation of dissemination in space. Secondly, in patients with infra/supra tentorial or spinal cord syndromes, dissemination in space and time could be demonstrated by symptomatic lesions and thirdly, dissemination in space can be demonstrated by cortical lesions (A. J. Thompson et al., 2018).

A vast majority of patients (about 80%) initially present with a clinically isolated syndrome which signifies acute episodes affecting one or several sites. Additional MRI evidence of white matter damage at clinically unaffected locations are indicative of relapsing-remitting multiple sclerosis. Spinal disease are usually suggestive of primary and secondary progressive MS, however, syndromes attributable to optic, cerebral or brainstem dysfunction can also occur. Compared to affected adult populations, affected children take longer to get to the secondary progressive stage, from the time of onset. Female children are more often affected than their male counterparts and encephalopathy is usually the main presentation in such cases. While there is speculation that persistent parasitic infections tend to confer some degree of protection from disease activity via T-regulatory cell activity, respiratory and gastrointestinal viral infections are thought to double the risks of relapse. Mortality reflects a total reduction in life expectancy of about 5-10 years and is often resultant from complications of infections in persons with advanced neurological disability. The risk of

suicide is pronounced in people with MS, and also reflects an increased lifetime frequency of depression in people with MS (Compston & Coles, 2008).

Current treatment modalities do not provide an outright cure, but can be effective in combating the unremitting physical, cognitive, and quality-of-life deterioration that many MS patients inevitably face, and may also be useful in alleviating symptomatology. Regular exercises, a healthy sleep pattern and cognitive behavioural therapy are beneficial for individuals with fatigue; Regular physiotherapy is also useful for spasms and muscle stiffness and special exercises and adaptation aids are helpful with impairments in mobility. In terms of pharmacology, Gabapentin is reported to be useful in some cases of involuntary eye movements and steroids have been effectively utilized for optic neuritis and relapses in general. Amantadine is also suggested to have some effect on fatigue and the SSRI's are noted to be effective when there is co-morbid depression (Stamoula et al., 2021). Disease modifying therapies are mostly indicated in RRMS and are targeted towards reductions in relapses and slowing of disability. Current treatments include Lemtrada, Interferon beta, Cladrabine, Dimethyl fumarate, Fingolimod, Natalizumab and Ocrelizumab.

The complex interplay between convenience, safety and efficacy of interventions (pharmacological or psychological) also further complicates decision making in terms of existing and future therapies. The impact of MS is not only felt by the patient but also extends to the families and caregivers. The symptom complex are intense and can be quite disruptive to both occupational and social functioning even in the early stages. Disability in MS is commonly quantified in half-point increments using a clinician-measured scale, the Kurtzke Expanded Disability Status Scale (EDSS) (Kurtzke, 1983). The EDSS quantifies disability in a number of functional systems and allows raters to assign a score for each functional system using a 0–10 scale. The functional systems are pyramidal, cerebellar, brainstem, sensory, bowel and bladder, visual, and cerebral. EDSS scores of ≤ 6.5 refer to people with MS who are ambulatory whereas EDSS scores of > 6.5 are defined by the impairment to ambulation. The scale measures disease progression predominantly by focusing on deficits in ambulation.

1.1.3 MS Neuropathophysiology

To fully comprehend and appreciate the pathophysiological mechanisms behind MS, a considerable understanding of neuroaxonal physiology and neuronal membrane activity is required. The stages of neuronal development, synaptic function and signal propagation along the axons are three fundamental roles applicable to neuronal and non-neuronal cells (glia) which support the neurons. Electrical excitability is expedited across neuronal cell membranes when an action potential is generated and when the homeostatic balance between intra and extra cellular neuronal compartments, as well as the separation of charges are altered. As expected, sodium influx and potassium efflux which characterise these alterations precede the generation of action potentials, facilitating signal conduction across the axons. The myelin sheath, a proteinous, fatty insulating layer which serves to protect the axons, increase the speed of conduction, and is indeed responsible for the preservation of energy during this process. In a nutshell, MS pathology is characterised by damage to myelin structures, disruption in neuro conduction and a resultant neurodegenerative sequalae.
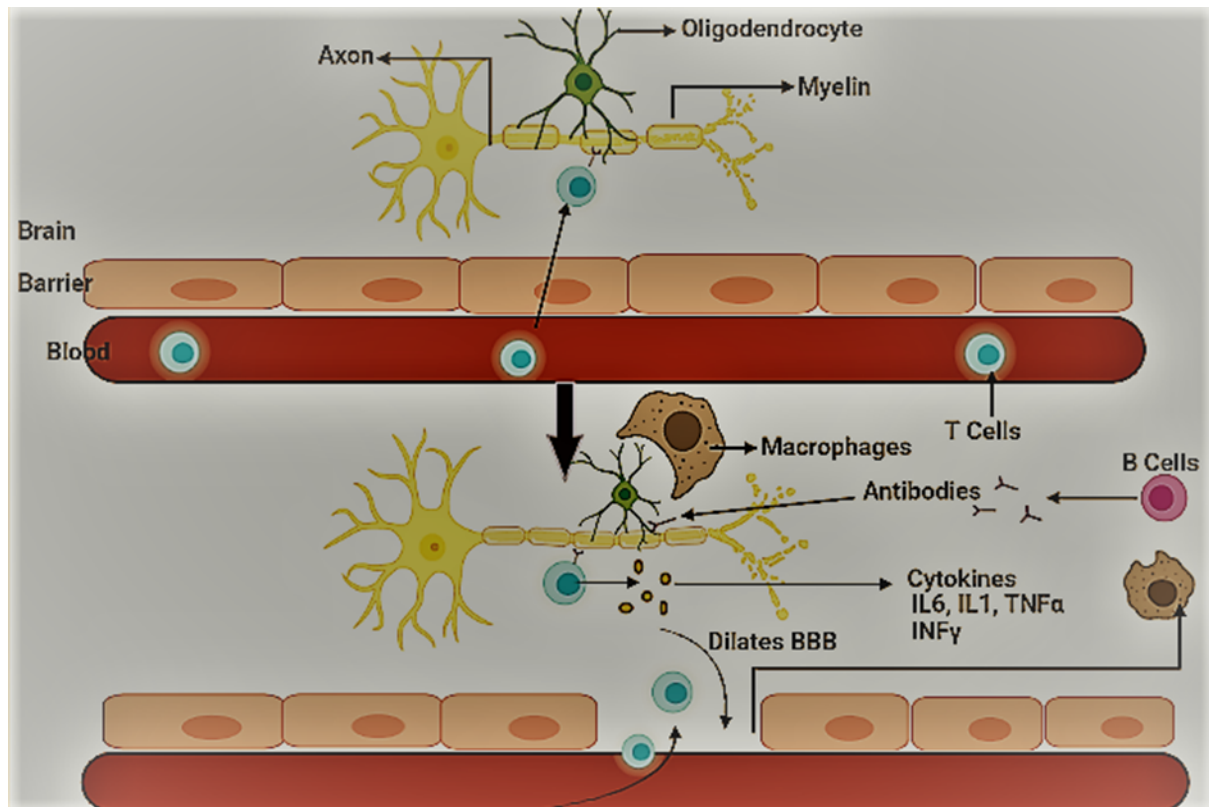
Figure 1. 1 Schematic representation of MS neuropathophysiological process showing the activity of T and B cells (Created with BioRender.com).

The clinical symptoms of MS (sensory and motor) are characterised by plaque of demyelination within the CNS with relative conservation of axons (Huang et al., 2017). Classed as a type IV hypersensitivity, T-cell mediated reaction; local inflammation, which precedes demyelination, gliotic scaring and later on axonal injury, is mediated by autoreactive lymphocytes crossing the blood brain barrier (BBB). Activation of the myelin reactive T cells causes a release of specific cytokines and chemokines, which exert proinflammatory effects and directly cause injury to the oligodendrocytes and neurons, as well as dilate the BBB, further allowing more immune cells to pass through (see figure 1). In addition, and as part of the inflammatory reaction, B-cells and macrophages become involved. B-cells secrete myelin reactive antibodies, which target the myelin sheet proteins, thus inducing phagocytotic activity by the macrophages, which engulf oligodendrocytes, exerting further deleterious effects on myelin and axons.

1.1.4 MS Neuroinflammatory Pathology

The neuroinflammatory process is a dynamic biological response employed to destroy pathogens, enhance tissue repair and ultimately remove surrounding debris at the site of tissue damage. The activation and invitation of innate and adaptive immune cells characterise aspects of the protective mechanisms involved in the neuroinflammatory process, albeit a shift to more chronic and aggressive responses could ensue, endangering survival and repair of neurons, which may then enhance or progress the pathological processes (Kempuraj et al., 2016; Russo & McGavern, 2016; Wyss-Coray, 2016). This diverse process primarily involves the activation of Microglia and Astrocytes; Resident immunocompetent cells, which are proposed to exist in heterogeneous phenotypes (neuroprotective and neurotoxic) based on activation status, regulatory capacity and the presence of influencing triggers (endogenous or environmental) (Kwon et al., 2020). In addition, and with regards to the type, stage, severity and regional location of neurodegenerative pathology; multiple reactive phenotypes involving astrocytes and microglia are reported to exist, as well as their pro-inflammatory or immunoregulatory mediators, all of which are suggested to contribute to the overall pathological process (Kwon et al., 2020).

In MS pathology, the destruction of myelin, oligodendrocytes and axons are initiated by infiltrating lymphocytes, which gain access to the perivascular spaces leading to focal areas of inflammatory demyelination. The blood-brain barrier (BBB) is further compromised resulting in oedematous swelling around lesional areas. Consequently, gliosis (scarring) results, following the process of astrogliosis in the demyelinating plaques. Histologically, resulting damage is defined by a hypercellular margin, characterised by high density of activated microglia surrounding demyelinating plaques and reactive gliosis. This is a consistent finding in MS pathology according to varying neuropathological studies (Boyle & McGeer, 1990; Lucchinetti et al., 2000; Marik et al., 2007).

During MS pathology lesional damage and acute relapses are primarily driven by adaptive immune responses (Robinson et al., 2018). Specific relapse pathomechanisms are characterised by BBB permeability changes and subsequent infiltration of inflammatory cells, while remission is thought to occur with the initiation of immune regulatory functions, where repair of CNS, resolution of inflammation and initiation of remyelination processes contributes to some degree of clinical recovery. This characterises and encompasses the relapsing-remitting phase of MS (Kutzelnigg & Lassmann, 2014). A subsequent phase known

as the secondary progressive phase follows clinical progression and more advanced brain atrophy, and is usually characterised by a relatively intact BBB, where compartmentalization of inflammatory processes is increasingly confined to the subarachnoid and perivascular spaces, and associated with the impact of transected axons and damaged neurons (Trapp & Nave, 2008).

Myelin debris clearance facilitated by microglia, and promotion of the health of neurons are reported to be extremely vital for remyelination, and quite central to the avoidance of progression (Kotter et al., 2006; Lampron et al., 2015; Sosa et al., 2015; Wujek et al., 2002).

1.1.5 Anatomical distribution of MS Pathology

MS is historically described as a demyelinating CNS condition, associated with chronic inflammation and the development of white/ grey matter focal lesions, which could culminate in diffuse neurodegeneration across brain regions, including the basal ganglia, brain stem and the spinal cord (Lassmann et al., 2018, Charcot 1880). In early phases, established lesions with perivenous extensions fuse with confluent demyelinated plaques, expanding into normal appearing white matter (NAWM), and give rise to finger-like shapes referred to as Dawson fingers (Dawson, 1916). Other primary distributions of MS disease pathology include inflammation of the meninges which have been suggested to drive white matter cortical injuries and involvement of subarachnoid spaces.

Though focal demyelinated plaques in MS pathology are more typically located, and characteristically identified in the juxtacortical and periventricular white matter regions, it is now becoming increasingly evident that the cortical grey matter, the archicortex (especially the hippocampus), and other deep grey matter structures also undergo extensive demyelination (Brown and Hughes 1962); are associated with motor and cognitive deficits, and are suggested to be the initial sites of MS disease pathology (Klaver et al., 2013).

1.2 THE HIPPOCAMPUS

The hippocampus is a complex limbic structure anatomically embedded in each medial temporal lobe of the cerebral cortex (Dhikav & Anand, 2012). The functional role of the

hippocampus has been well characterised and includes critical roles in learning, memory processes, spatial navigation, regulation of the hypothalamic, pituitary axis (HPA axis) function and modulation of emotional behaviour (E. J. Kim et al., 2015; Rubin et al., 2014). Several notable connections in and around the hippocampus are central to these functions. Polysynaptic pathways effectively regulate the learning/memory loop, and reciprocal and direct projections to the hypothalamus and amygdala, via a ventral striatal loop are elemental in influencing motor and emotional behaviour, as well as the release of adrenocorticotropic hormones (Dhikav & Anand, 2012).

The hippocampus is implicated in the orchestration of numerous critically important allostatic processes that facilitate neurodevelopment through the life span, adaptation to challenging environments and response to stress, as well as insults and injury. These processes include neurogenesis and synaptic plasticity (LTP); excitation/inhibition balance and neuronal excitability, and a tight and dynamic feedback regulation of HPA axis function. The functional consequences of hippocampal neurodegeneration, the most obvious being seen in neuropsychiatric conditions such as Alzheimer's disease (AD), have enormous clinical relevance and impact in terms of general functional impairment and disability, reflecting the central role to the above-mentioned critical processes and systems.

1.3 HIPPOCAMPAL NEURO-INFLAMMATION AS A CANDIDATE CAUSAL MECHANISM UNDERLYING THE COMORBIDITY BETWEEN DEPRESSION AND MS

Current research evidence suggests that treatments or experimental challenges that raise pro-inflammatory cytokines induce symptoms of psychological distress, and potentially lead to depressive syndromes in the general population. Depression is found associated with higher levels of inflammatory biomarkers, cytokines, and expression of genes involved in the inflammatory response (Farooq et al., 2017). Furthermore, there is an increased incidence of affective disorders in immune mediated inflammatory disease cohorts (Marrie et al., 2017). These findings suggest that immune dysregulation and the activation of the inflammatory response system might play a causal role in the development of major depression. Mechanisms underlying the link between inflammation and depression include role of

cytokines directly crossing the blood brain barrier, crosstalk between peripheral and central immune systems and the dysregulation of the hypothalamic-pituitary-adrenal axis (Miller & Raison, 2016). Based on this evidence, we hypothesize that affective and cognitive symptoms in MS might be caused by the neuro-inflammatory processes associated with MS. The hippocampus is a candidate brain structure potentially involved in the etiopathogenesis of MS depression. The hippocampus is associated with affective regulation; its distinct connections and associations to the anterior nuclei of the thalamus, cingulate cortex, the entorhinal cortex and the amygdala show involvement in the affective and emotional experience. The Hippocampus is also especially vulnerable to neuroinflammation. It is subject to extensive demyelination in MS (Geurts et al., 2007b). Demyelinated hippocampi, which have been identified in 53-79% of post-mortem MS brains, have also been linked to possible mechanisms behind cognitive dysfunction and decrease in synaptic density in MS patients (Dutta et al., 2011). Subregional analysis have particularly implicated volume loss in the cornu ammonis (CA) 1 subregion in RRMS with further worsening in SPMS (Sicotte et al., 2008). Furthermore, pro-inflammatory activity of the resident immunocompetent CNS cells (Microglia) is widely accepted to interfere with hippocampal neurogenesis (Vasic & Schmidt, 2017). In addition, impairment of long-term potentiation of the hippocampus and inhibition of neurotrophic factor signalling by the activities of inflammatory cytokines is known to negatively influence synaptic plasticity and memory formation. Indeed, impairment in synaptic plasticity and a reduction in hippocampal dendritic spine density have been duly observed after the activation of central and peripheral immune responses (Jurgens et al., 2012; Vasek et al., 2016). To further confirm the importance of the hippocampus in the genesis of depression associated to MS, Imaging studies found altered hippocampal morphology (Gold et al., 2014) to be associated with depression in MS , and hippocampal microglial activation (as measured with TSPO PET) associated with depressive symptoms as well as the strength of hippocampal functional connectivity (Colasanti et al., 2016). In the later study, TSPO uptake indicative of microglial activation in the hippocampus of MS patients strongly corelated with increased BDI scores, and also with functional connectivity (from fMRI) in the prefrontal and parietal regions.

1.4 AFFECTIVE SYMPTOMS IN MS

Since the famous lectures in Paris by French neurologist, Jean Martin Charcot on "la sclérose en plaques", now referred to as Multiple Sclerosis (MS); there have been numerous research on the aetiology, pathophysiology and co-morbid impact of MS. Charcot's anatomo-clinical methods and applications played an initial role in unravelling the early knowledge of the clinical pathology of MS, as well as depicting the presence of neuropsychiatric symptoms associated with the condition. Among some of his notable descriptions, was an associated fit of 'Lypemania' or severe depression, which was adequately described in one of his affected patients (Mademoiselle V). Other co-morbid psychiatric symptoms noted by Charcot comprised weeping, paranoia, euphoria, mania and pathological laughing (Siegert & Abernethy, 2005). During a systematic evaluation of 100 patients attending an MS clinic in the late eighties, it was found that 13% fulfilled the criteria for manic depressive illness while a lifetime history of depression was identified in 42% (Joffe et al., 1987). The prevalence of bipolar affective disorder in MS is believed to be twice that in the general population (Minden & Schiffer, 1990). Currently; the known psychiatric co-morbidities and affective conditions of clinical concern in MS include Bipolar disorder, Anxiety disorder and of primary interest in this research, depression.

The neuropsychiatric comorbidities (especially Major Depression) in MS tend to worsen overall prognosis and quality of life (Haussleiter et al., 2009). Reported lifetime prevalence of MDD is up to 50%. The annual prevalence is about 25.7% for major depression among people with MS aged between 18-45-year-old (Siegert & Abernethy, 2005), Compared to the general population and when matched with other chronic debilitating conditions, the prevalence of major depression is increased (Patten et al., 2003). Consistent data from various previous studies have also demonstrated these findings (Chwastiak et al., 2002; Joffe et al., 1987; Minden et al., 1987b; Minden & Schiffer, 1990; Sadovnick et al., 1996). Even in the presence of a number of methodological lapses, the variation of studies depicting the high prevalence and frequency of depression in MS give credence to arguments for the possibility of other responsible mechanisms that may precede the development of depression in MS, other than just functional response to chronic or disabling illness. There appears to be limited

understanding and a lack of consensus amongst the research community as to what these other mechanisms may entail, or the reasons underlying the high prevalence.

1.5 AIMS AND RATIONALE OF THESIS

1.5.1 Aim of the Thesis

The purpose of our study is to use diffusion MRI techniques to characterise hippocampal pathology associated with neuroinflammation, specifically microstructural alterations and cellular changes, in MS phenotypes (PPMS and RRMS). Quantitative changes in the parameters derived from diffusion MRI have been found to be reflective of tissue microstructural alterations, hence are able to assess CNS tissue integrity and detect neuroinflammatory/ neurodegenerative pathology at quite early concealed stages (Granziera et al., 2021). Considering evidence described above, the development of neuroimaging biomarkers of hippocampal pathology is of crucial importance to shed light on the biological mechanisms involved in MS pathogenesis and of cognitive and affective illness in MS, and therefore, subsequently enabling direct assessment of the anti-inflammatory effects of novel immune modulating treatments. Given the recognised role of neuroinflammatory processes in primary, or idiopathic depression (ie not associated to MS), and the importance of the hippocampus in affective psychopathology, this study could also inform more generally on the etiopathology of depression.

1.5.2 Rationale of Thesis

MRI is the gold standard for the diagnosis and treatment assessment of demyelination in MS. Traditional MRI are not able to precisely assess the extent of hippocampal pathology associated with MS, because grey matter lesions tend to be MRI-invisible, and diffuse damage can only be picked up when using quantitative imaging approaches. Quantitative methods such as diffusion MRI, on the other end typically use coarse resolution, which is

suboptimal for the hippocampus. Newer techniques such as High-Resolution Diffusion MRI (Treit et al., 2018) are promising tools to image hippocampal neuroinflammation as they enable a better definition of the internal microanatomy of the hippocampus, or Diffusion Weighted Magnetic Resonance Spectroscopy (Ingo et al., 2018) are able to quantify brain tissue changes that are specifically related to inflammatory cells such as microglia and astrocytes.

 Considering the anatomical complexities attributable to the hippocampus, the study methods employed were potentially predicted to better analyse and describe subregional hippocampal pathology with the application of a combination of both modalities. Post-mortem research evidence supports this prediction, as it does suggest that subregional pathological variations do exist within the demyelinated hippocampus of MS patients with relevance for clinical presentation. Indeed, particular areas of the hippocampal formation (CA1, CA3) and the molecular layer of the dentate gyrus are reported to have been mostly affected in MS pathology (Geurts et al., 2007b). Evaluation of intrinsic micro-changes could in effect capture the early stages of neurodegeneration and could also be useful in monitoring future therapeutic strategies (Crombe et al., 2018).

Pre-clinical applications also indicate analogous findings; Multi-modal techniques have been found sensitive in rodent experimental models of MS to detect hippocampus microstructural alterations resulting from neuroinflammatory processes (Crombe et al., 2018). Crombe et al challenged the capacity of two models (Diffusion tension imaging-DTI and Neurite orientation dispersion and density imaging-NODDI) to effectively delineate, compute and quantify microstructural alterations in specific hippocampal layers of 18 experimental autoimmune encephalomyelitis mice (EAE mice) and 18 control mice. Both modalities were equally effective in delineating specific layers but DTI showed more prospects with regards quantification. A decrease in axial diffusivity (AD) and mean diffusivity (MD) was noted in the molecular layer of the hippocampus of EAE mice.

 My study effectively combines High Resolution Diffusion MRI and Diffusion weighted Spectroscopy with an innovative post acquisition resolution-enhancing algorithm (Image Quality Transfer) (Alexander et al., 2017), which enables regional hippocampal manual segmentation and enhances automatic methods.

Quantitative imaging techniques that were potentially capable of providing quantitative assessment of brain oxidative metabolism (ie pCASL, ASE), and could allow for

simultaneous characterization of inflammatory processes in hippocampal subfields as well as the oxidative energy alterations associated with inflammation were also collected from recruited participants but data from these later techniques and modalities were not analysed within the remit of this study.

1.5.3 Diffusion Weighted Imaging

Diffusion magnetic resonance imaging (dMRI) can be described as the process of probing, along a defined direction, the random motion of water molecules in tissues (Andica et al., 2019). Typically, sensitivity to diffusion is achieved by adding magnetic field gradients to either side of a refocusing pulse in a spin echo sequence. The difference in the phase accumulated by spins during either gradient results in a signal attenuation, which is proportional to the diffusion coefficient of tissue in the gradient direction (O'Donnell & Westin, 2011). The effect of the gradients can be summarised by the so-called b factor, which results from the amplitude, the duration and the separation between gradients. In order to quantify diffusion, appropriate signal models are needed. Diffusion tensor imaging (DTI) is one of the most common and widely utilized diffusion MRI techniques. It was introduced to account for the dependency of the diffusion coefficient upon the measurement direction. This "anisotropy" could not be accounted by a scalar diffusion coefficient, and the diffusion tensor was thus introduced (Basser et al., 1994). Scalar parameters deduced from DTI have shown favourable potential in the understanding and evaluation of microstructural changes that are expected in neuroinflammatory pathology. According to extensive literature, such metrics (Fractional anisotropy, Mean, Axial and Radial diffusivities- FA, MD, AD, RD) serve as potential biomarkers of brain abnormalities in patients with neurological conditions and also provide a means of non-invasive, in vivo quantification and characterisation of tissue microstructure (Sbardella, Petsas, et al., 2013). Fractional anisotropy (FA) and Mean diffusivity (MD), parameters from Diffusion Tension Imaging (DTI) represent the degree of anisotropy of water molecules and microstructural integrity, while AD and RD are measures of axonal and myelin integrity. Extensive literature signifying alterations in these parameters are evident in MS which invariably reflects demyelination and axonal loss.
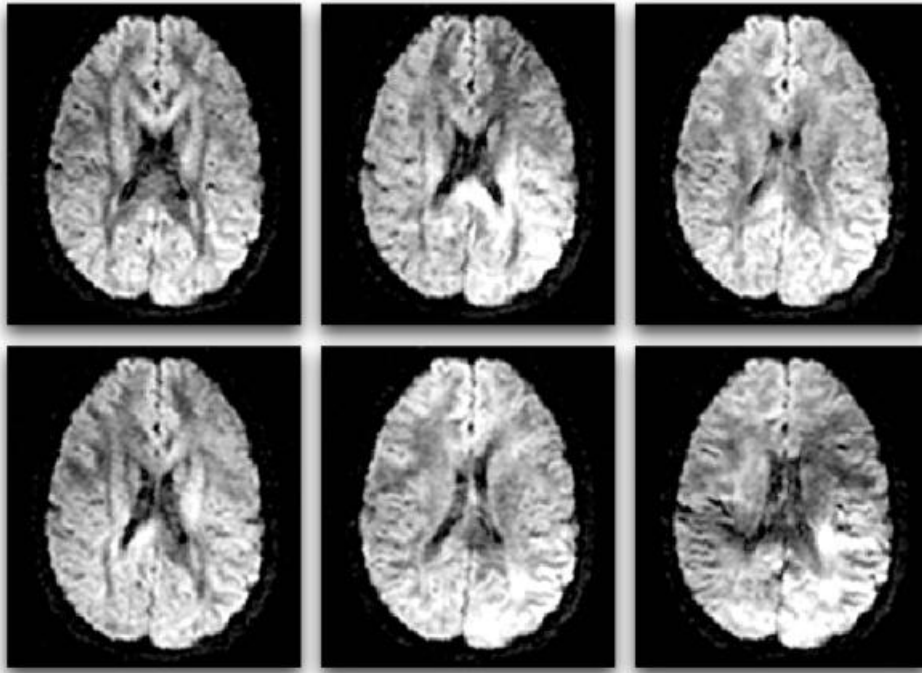
Figure 1. 2 Tensor calculation in six Diffusion weighted images. The diffusion image is sensitised in specific directions by induction of magnetic field gradients with signal loss occurring in varying patterns due to anisotropic diffusion (O'Donnell & Westin, 2011).
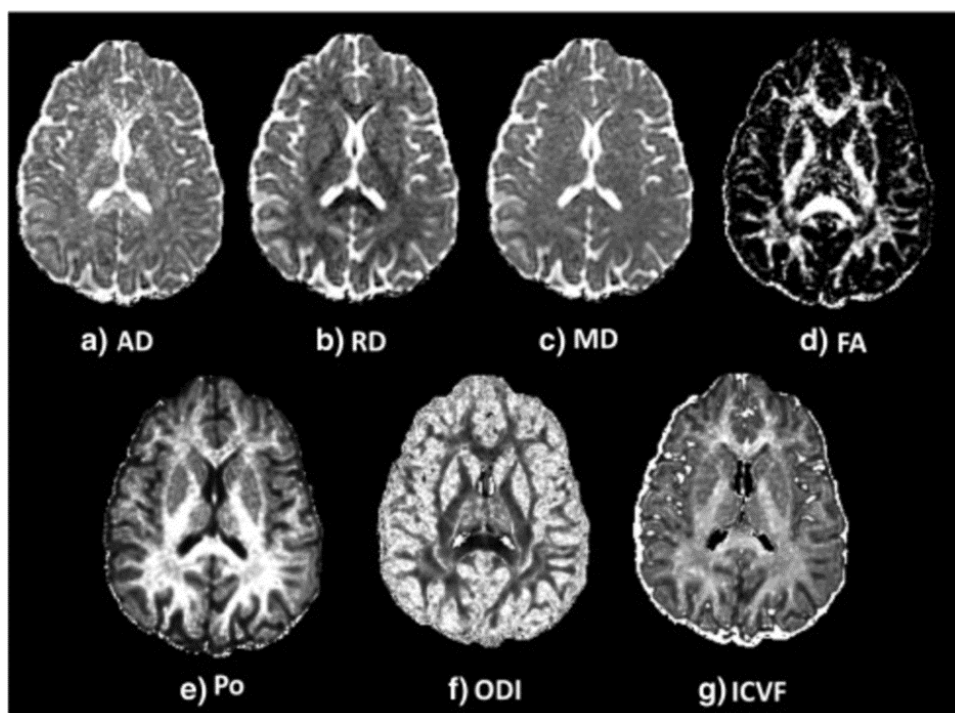
Figure 1. 3 DTI and NODDI maps (Kodiweera et al., 2016)

DTI assumes a single water compartment, and a Gaussian diffusion propagation, which results in a monoexponential signal decay. At the end of the 90's it became clear that such assumption only held for b values < 1500 smm^{-2}. In order to measure diffusion at higher b values, new, so-called, higher order models started to appear, often classified as biophysical models (i.e., linking the measured signal directly with some biophysical parameters such as, for example cell density) or signal representations (which simply attempt to derive parameters that describe the signal). For the purpose of this thesis, 2 signal models must be briefly described: Neurite orientation dispersion and density imaging (NODDI) and mean apparent propagator MRI (MAP MRI).

NODDI (Zhang et al., 2012) is a hierarchical biophysical model that assumes that tissue is made up of 3 water compartments with differing diffusion characteristics. First of all, it separates isotropic diffusion (free water) and tissue. The tissue is then also split between intra neurite (restricted diffusion) and extra neurite (hindered diffusion). The former is modelled using a combination of sticks, while the latter is modelled via a tensor. NODDI enables the estimation of the isotropic and neurite compartment fractions (fiso, NDI), and the orientation dispersion (ODI).

MAPMRI (Özarslan et al., 2013) is a signal representation that models the dMRI signal as a series expansion of basic functions. MAPMRI can provide useful indices that characterise diffusion, but is also a handy way of manipulating the signal, with the option to easily simulate the acquired signal repeatedly. This is the method we used to increase the resolution via IQT.

Overview of Diffusion indices and alterations in MS include:

    a.   Fractional Anisotropy (FA)

FA is usually mathematically defined as; $(3/2)^{1/2} \times [((\lambda_1 - \lambda_{av})^2 + (\lambda_2 - \lambda_{av})^2 + (\lambda_3 - \lambda_{av})^2) / (\lambda_1^2 + \lambda_2^2 + \lambda_3^2)]^{1/2}$, where λ_n signifies the eigenvalues describing the diffusion tensor, and λ_{av} signifies the mean diffusivity $((\lambda_1 + \lambda_2 + \lambda_3)/3)$ (Grieve et al., 2007). In the diffusion process, a measure of FA is equivalent to the degree of anisotropy, and represents scalar values of between zero and one, where zero is indicative of unrestricted or equally restricted movement of water molecules (eg CSF) and 1, a more anisotropic movement of water molecules, in one axis, as seen in fiber bundles or within axons. An approximate inference

which reflects pathological alterations in the diameter of the axons, density of fiber and structure of myelin is thus considered feasible when the FA is measured under such conditions (González-Reimers et al., 2019). Converging evidence has generally shown that in MS patients, there is a significantly lower average of FA than compared to healthy controls (Nusbaum 2000; Cercignani et al., 2000; Iannucci et al., 2001; Inglese & Bester, 2010). There is also the widespread view that these measures become more sensitive with MS progression.

    b.   Mean Diffusivity (MD)

MD, ADC, or trace, can be calculated by the mean of the three eigenvalues and correspond to the molecular diffusion rate (lower values mean low diffusivity) (J. M. Soares et al., 2013). Mathematically represented as $((\lambda_1 + \lambda_2 + \lambda_3)/3)$, MD can be further described by the average quantity of diffusion in each principal direction as determined or calculated in the tensor (Salat, 2013). Aside from the diffusivity of water, MD quantification also reflects the presence of cellular structures and is expected to be of lower average in the presence of more cellular structures (inhibition to the free diffusion of water molecules) (Assaf & Pasternak, 2008; Ni et al., 2010; Sagi et al., 2012). Hence, pathological mechanisms that degenerate tissue barriers and lead to unrestricted diffusion are seen to increase MD (Stebbins, 2010). In MS, where there is axonal loss and demyelination, MD has been noted to increase (Cercignani et al., 2001).

    c.   Orientation Dispersion Index (ODI)

There are two comprehensive applications of ODI. The evaluation of axonal fanning and bending in the white matter or the quantification of the pattern of sprawling dendritic processes in grey matter. Grey matter complexity are suggested to be better reflected using this procedure, and are reckoned to provide more specific markers of tissue microstructure when compared to tensor indices (Zhang et al., 2012)

    d.   Intra-cellular volume fraction/ Neurite density index (ICVF/ NDI)

In brain tissue, this models the full spectrum of neurite orientation patterns and comprises coherently oriented white matter structures, axons that are composed of fanning and bending, as well as sprawling dendritic processes such as the cerebral cortex and subcortical grey matter. The compartment alludes to the spaces generated by the boundaries of neurite membranes. (Zhang et al., 2012)

1.5.4 Image Quality Transfer

Image quality transfer, or IQT (Alexander et al., 2017) is a computational technique that uses machine learning to transfer information between imaging datasets. It was originally proposed to learn mappings from low-quality to corresponding high-quality images. Here we used it to increase the resolution of existing dataset, with the purpose of creating reference scans that can be used to segment the hippocampus subfields but are at the same time inherently co-registered with dMRI maps. This enables subfield-specific dMRI indices to be estimated in vivo. A detailed description of IQT is provided in (Alexander et al., 2017). For the purpose of this thesis, we follow an approach similar to that described by Alexander et al for tractography. Essentially, we fit the MAPMRI model (detailed above) to the original data, and then enhance the resolution of MAP coefficient maps. Those coefficient maps are then used to produce synthetic diffusion weighted images through equation 24 in (Özarslan et al., 2013). Directionally averaged images are then obtained for all b values. The b=1000 mean is the best compromise between signal-to-noise ratio (SNR) and contrast, and is therefore chosen to conduct manual and automated segmentation of the hippocampal subfields. Additional details are provided in the dedicated chapters.
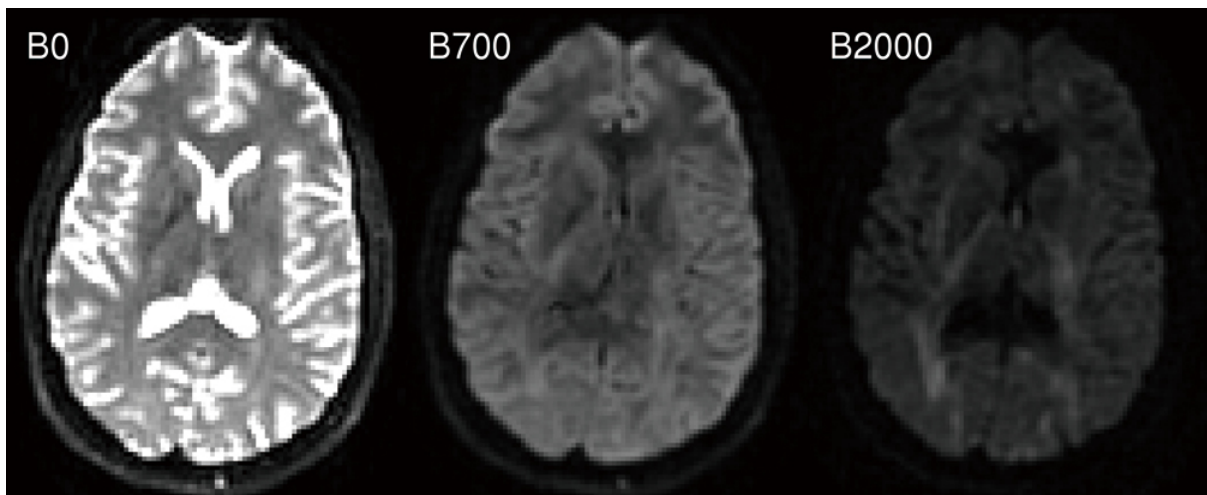
Figure 1. 4 Different degrees of weighting in DWI (Winston et al., 2012)
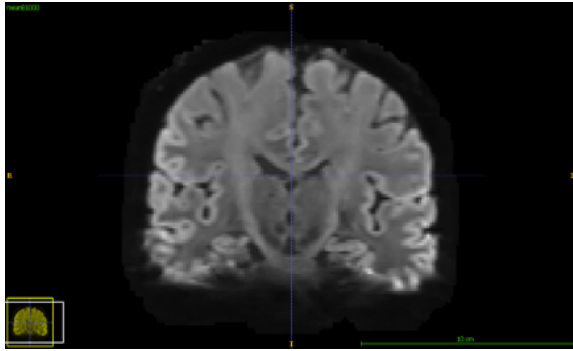
Figure 1. 5 Mean B=1000 image

1.5.5 Diffusion Weighted Spectroscopy

There is existing evidence with experimental models that advanced neurological disability in MS are determined by axonal loss (Wujek et al., 2002). Prior correlational studies have also depicted axonal injury as principal pathological mechanisms associated with the progression of MS pathology (Mews et al., 1998; Van Waesberghe et al., 1999). According to further research evidence, healthy neurons require metabolic and homeostatic support from glial cells to sustain fundamental functions, with dysfunctional glial activity contributing to neuronal injury, and hence, progression of MS pathology.

Physiologically and in order to maintain mitochondrial health, provide homeostatic balance in membrane potential, and also reduce oxidative stress; neurons make use of lactate over glucose to sustain adenosine triphosphate (ATP) production which is required in large proportions to power ion transporters (Harris et al., 2013). To fully sustain this process and keep up with ATP requirements, neurons depend steadily on the production of metabolic intermediates i.e lactate by glial cells (Astrocytes and Microglia).

Following myelin damage during MS pathology, further increases in ATP demands outstrips supply leading to mitochondrial injury, glutamate excitotoxicity and mitochondrial transport defects; a state described in research literature as Virtual hypoxia (Trapp & Stys, 2009; Veronica Witte et al., 2014).

There is indeed increasing and abundant evidence to show that MS can indirectly affect levels of intermediate metabolites produced in the CNS, which can be quantitatively estimated by advanced spectroscopy imaging applications (Cianfoni, Niku and Imbesi, 2007)**.** Proton

magnetic resonance spectroscopy (^{1}H-MRS) and Diffusion weighted magnetic resonance spectroscopy (DWMRS) form parts of the multi-modal applications utilized in this study to characterise MS pathology, with the Hippocampus as specific region of interest. The Hippocampus is particularly vulnerable to the effects of neuroinflammation in MS and also has limited perfusion reserve, hence a propensity to higher metabolic vulnerability and hypoxic injury (Perosa et al., 2020). Providing both physiological and chemical information (compared to only anatomy alone), and with results usually expressed as metabolic ratios; there is great and widely untapped potential for MRS to increase the sensitivity of routine diagnostic imaging (Hamsini et al., 2018).

An overview of alterations in specific grey matter metabolites during MS pathology include;

a) N-Acetyl Aspartate (NAA): Physiologically known to have one of the largest peaks on MRS scans, NAA is regarded as one of the most concentrated metabolites produced in the brain (Moffett et al., 2013). NAA are synthesised in most part by mature neurons from acetyl coenzyme A and acetate, and the enzymes responsible for their production are chiefly expressed in oligodendrocytes and neurons (Moffett et al., 2013; Swanberg et al., 2019). Due in part to their acetate reservoir role, a reduction in the availability of NAA as a result of brain pathology is depicted to have an impact on acetyl coenzyme A production, there by impairing vital cellular functions related to protein acetylation, lipid synthesis and energy derivation (Moffett et al., 2013; Swanberg et al., 2019). Acetyl moieties are usually identified in spectral peaks of around 2.0 ppm and 4.0ppm (Bulik et al., 2013; de Graaf et al., 2007). Compared to controls, reductions in NAA (creatine referenced in some reports) have been identified in grey matter mixed and unspecified lesions in relation to RRMS and progressive MS (Chard et al., 2002; Inglese et al., 2004; Kapeller et al., 2001; Tiberio et al., 2006; Wylezinska et al., 2003).

b) Creatine (Cr): By virtue of kinase enzymatic functions, Cr is vital for maintaining energy homeostasis and energy metabolism within the cell (Stagg et al., 2014). From the kidneys where they are originally synthesised, they are transported via the blood stream to peripheral organs. Total creatine (Phosphocreatine and creatine together) are found in neuronal and glial cells and can be identified at spectra peaks of 3.0ppm, and in some instances, visible at peaks of 3.9ppm (Bulik et al., 2013). Cr usually serves as reference metabolite for invivo MRS. Quantification of Cr metabolite during MS

pathology is still widely indefinite as there are variations in the alteration of CNS concentrations during MS pathology. Reports indicate Cr reductions in the grey matter in RRMS lesions and also in the progressive grey matter (Bodini et al., 2018; Helms, 2001; Sijens & Oudkerk, 2005)

c) Choline (Cho): Widely recognised as metabolic by-products of the phospholipid membrane, choline plays a significant role in the synthesis of cellular membrane phospholipid components (Michel et al., 2006). Increasing cell membrane synthesis and degradation which are tenable during inflammatory processes are suggested to also reflect increased choline levels. Much of Cho are not visible, but have been identified at MRS peaks of between 3.0 and 4.0 ppm. Decreases in Cho have been noted in grey matter lesions in MS pathology (Mathiesen et al., 2005).

d) Myoinositol (Myo): Two of the nine separate isomers of inositol identified (myoinositol and scylloinositol) are the most abundant in human tissue. They are cyclic organic molecules primarily synthesised in glial cells, predominantly in Astrocytes, where they function as precursors and osmolytes to distinct signalling molecules (Stagg et al., 2014). Elevations in Myo have been noted in marked gliosis which is present in advanced and progressive MS lesions. Increases are also noted in grey matter lesions (Geurts et al., 2006).

e) Glutamate (Glu), Glutamine (Gln), ɣ-Aminobutyric Acid (GABA): Isolating and separating these metabolites is usually complex and difficult at magnetic field strengths of either 1.5 T and 3 T (Stagg et al., 2014), and will require additional spectral editing methods in the case of isolating GABA. A complex peak (Glx) for all three can be identified on MRS at the range of 2.05-2.50 ppm (Bertholdo et al., 2013). A decrease in Glu levels have been reported in RRMS mixed tissue lesions (Muhlert et al., 2014). Decreases in RRMS and progressive mixed tissue lesions have also been reported for edited GABA metabolite concentrations (Cao et al., 2018; Cawley et al., 2015).

f) Gluthathione (GSH): Similar to GABA, MRS GSH quantification requires additional spectral editing methods for accuracy due to its low amplitude spectral signature. With regards brain pathology in general, there have been limited reports in literature. In MS grey matter lesions; there are suggestions of a decrease in GSH metabolites (Srinivasan et al., 2010).

g) Lactate (Lac): During alternative energy production within cells (anaerobic glycolysis), Lac is synthesised as a by-product of pyruvate breakdown. Elevated levels are significant with healthy brain tissue whereas sustained presence usually reflects pathology (Stagg et al., 2014). Increased concentrations have been identified in RRMS lesions (Kocevar et al., 2018).
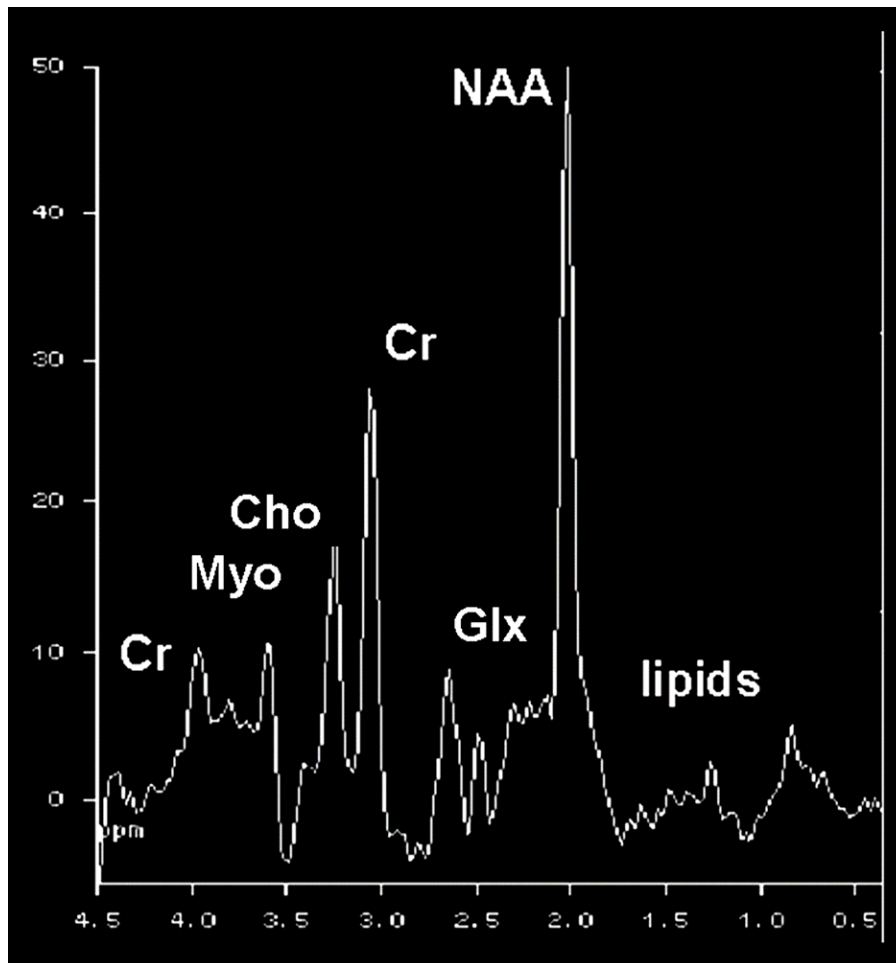
Figure 1. 6 MRS Spectrum demonstrating major metabolites (D. P. Soares & Law, 2009)

Diffusion preparation can be added to MRS to compute the apparent diffusion coeffient of specific metabolites (De Marco et al., 2022). This is of interest because, thanks to the cell-specificity described above, DW MRS makes it possible to infer about cell-specific morphological changes (De Marco et al., 2022).

1.5.6 PPMS: Changes on MRI and MRS.

About 10-15% of patients experience an MS clinical phenotype characterised by gradual progression from the onset and an absence from the episodic pattern of relapses and remissions (A. J. Thompson et al., 1997). PPMS remains a highly disabling MS subtype to which none, or only a licensed few disease modifying treatment (DMT) exists (Ingle et al., 2003). Distinctions from the more common RRMS subtype also remain speculative and conventional MRI findings (lesion load) display poor correlations with clinical state.

Admittedly, PPMS relative rarity, sporadic occurrences and non-episodic nature has meant an absence of relevant clinical trials and a consequent degree of lack of knowledge, in terms of discovering novel therapeutic end points. Hence, fully understanding the underlying patho-physiologic mechanisms and rationale behind progression and disability in PPMS will prove key to this effect, and may indeed be vital in understanding MS and its complications as a whole.

Essentially, there have been some research studies to distinguish PPMS from SPMS. Compared to SPMS, patients with PPMS tend to have fewer and smaller lesions on T2 weighted MRI, with even fewer lesions in the periventricular area (Filippi et al., 1999; Foong et al., 2000; Stevenson et al., 1999; Van Walderveen et al., 1998; Wolinsky et al., 2001). Fewer rates of enhancement of lesions on application of gadolinium contrast have also been observed (A. J. Thompson et al., 1991). In contrast, a greater percentage of total lesion load is observed on the spinal cord in PPMS compared to other MS phenotypes, hence the higher levels of disability (Kidd et al., 1993; Thorpe et al., 1996).

With regards to diffusion weighted imaging, much older studies involving PPMS and other MS subtypes found no differences in diffusion measures and no correlations with disability (Droogan et al., 1999). More current research found differences in diffusion measures in the internal capsule and corpus callosum between PPMS and controls (Filippi et al., 2001). Ciccarelli et al., 2001 also reported correlations of diffusion measures with disease duration.

Not many current studies have been carried out with MRS, but most prior MRS studies have observed reductions in NAA in high signal T2 lesions in PPMS and also in normal appearing white matter (NAWM), with some correlations with EDSS (Cucurella et al., 2000; Davie et al., 1997; Leary et al., 1999). Due to the presence of NAA in the neurons and axons, such

reductions are usually suggestive of neuro-axonal loss, axonal damage and disease progression in PPMS (Aboul-Enein et al., 2010).

1.5.7 Objectives

Primary

• To carry out a systematic review aimed at broadly exploring quantitative imaging of hippocampal inflammation in autoimmune neuroinflammatory conditions (Methodology displayed in Chapter 2).

• Assess the sensitivity of novel MRI techniques (DWI and DW-MRS) to detect hippocampal pathology in patients with MS relative to non-affected participants.

• To examine the application of novel high-resolution diffusion MRI techniques (Human connectome project [HCP] like diffusion imaging) to define the internal microanatomy of the hippocampus in healthy volunteers and in MS neuroinflammatory processes. Such techniques have already been found sensitive in experimental models (Crombe et al., 2018; Treit et al., 2018).

• To test whether MRI measures of hippocampal pathology are able to differentiate MS phenotypes.

1.5.8 Secondary/Exploratory

• To study the characteristics, intensity and severity of Depression, Cognition and Fatigue in RRMS and PPMS.

• To estimate effect sizes to inform power and sample size calculation for future studies.

• To explore correlations between hippocampal imaging parameters and clinical measures from the cognitive and affective domains that might reflect hippocampal involvement.

1.5.9 Impact of the Covid-19 Pandemic

Apart from the emotional and psychological impact of the pandemic which was in itself a setback with the entire study, the significant effect of the pandemic was mostly experienced with recruitment. It became practically and almost impossible to identify eligible participants, undertake screening, or where these had already been concluded, to perform scanning (expanded further in Chapter 8).

Hence, in the event that the entire PhD study might be redefined, relevant mini-projects were undertaken which I will highlight in this section. Firstly, a literature review on the potential role of Covid-19 in neuroinflammation and Demyelination which sought to elucidate a possible viral post delayed neurobiological link with MS and depression; and Secondly, the inception of a novel proposed online computer app projected as a potential psychological intervention for chronic neuroinflammatory and disabling illnesses with an initial focus on MS. The later idea was borne out of my experience with prior in-person focus groups with MS patients. (See Appendices i and ii for further elaboration).

CHAPTER 2. INVIVO QUANTITATIVE IMAGING OF HIPPOCAMPAL INFLAMMATION IN AUTOIMMUNE NEUROINFLAMMATORY CONDITIONS: A SYSTEMATIC REVIEW.

2.1 Introduction

Hippocampal pathology has been the subject of extensive preclinical mechanistic characterisation. A large body of experimental animal and histopathological research established that the hippocampus is subject to neuroinflammatory pathology (Geurts et al., 2007b; Papadopoulos et al., 2009) and that hippocampal neuroinflammation can have direct impact on its main roles and functions, culminating in alterations in neurogenesis such as reduction in synaptic density, (Dutta et al., 2011) and alterations in synaptic plasticity, (Nisticò et al., 2013) indicating plausible mechanisms that underlie cognitive and affective sequalae of neuroinflammatory pathology.

This exquisite vulnerability of hippocampus to neuroinflammation is related to several converging factors, including its plasticity and involvement in neuroimmune cross talks (McEwen et al., 1999; Williamson & Bilbo, 2013). The hippocampal proximity to the choroid plexus for instance is presumed to facilitate, via alterations in CSF composition and CNS inflammatory immune signal processing, activated lymphocytic cell entry during neuroinflammatory pathology (Brown & Sawchenko, 2007; Marques et al., 2009; Reboldi et al., 2009). The hippocampus also contains a very high density of interleukin 1 receptors (IL1) which mediate inflammatory processes (Farrar et al. 1987), with the highest expression of IL1 receptors located in the granule layer of the dentate gyrus and pyramidal cell layer (CA1-4) of the hippocampus. Microglia in the hippocampal neuronal system of adult mice have a higher proliferative capability against LPS-induced inflammatory stimulation, relative to other brain regions examined (Fukushima et al., 2015).

More so, immune signalling molecules such as cytokines and chemokines, produced within the hippocampus in response to any perturbations of CNS homeostasis, are implicated in normal hippocampal neurogenesis processes (Pérez-Rodríguez et al., 2021). Adult neurogenesis is defined as a process whereby adult neural precursors in the CNS produce

functional neurons (Ming & Song, 2011). Recognised as a continuing process, Hippocampal neurogenesis is characterised by the introduction of new neurons in the memory processing circuits, and is a vital determinant of cognitive reserve (Valero et al., 2017). Impact of adult hippocampal neurogenesis has consistently been linked to the development of depression and anxiety (Anacker, 2014). Neurogenesis in the subgranular zone of the dentate gyrus (DG) in particular appears to be readily impaired in a transgenic mouse model of neuroinflammation secondary to IL6 overexpression (I. L. Campbell et al., 2014). In a mouse model of Experimental Autoimmune Encephalitis (EAE), these impairments of neurogenesis and neuroplasticity could be linked to specific microstructural modifications in the molecular layer (ML) of the DG, such as alterations in the dendritic tree and decreases in dendritic length, which manifest in diffusion-weighted MRI as reductions in axial diffusivity (AD, ie water diffusion along tracts) and mean diffusivity (MD). Interestingly, the reductions were only visible to the ML of DG, and not in other subfields (Crombe et al., 2018), implying subregional variability to neuroinflammatory mechanisms, with potential relevance to the definition of specific anatomical neuroimaging endpoints.

The hippocampus also has high metabolic vulnerability due to limited perfusion reserve. In the presence of cerebral small vessel pathology, the already miniature arterial supply (posterior cerebral and anterior choroidal vessels), especially when only independently supplied (by the posterior cerebral artery) are compromised, leading to hypoxic injury in the hippocampal region (Perosa et al., 2020). Indeed, when compared to the neocortex, experimental studies indicate notable reductions in blood flow, blood oxygenation and neurovascular coupling in the hippocampus as a consequence of distinct alterations in endothelial cell function and vascular network, such as lower capillary density and marginal pericyte contractile morphology (Shaw et al., 2021). Accordingly, there are observed varying individual subfield vulnerabilities with respect to hypoxic/ischaemic injury. Specifically, CA1 pyramidal neurons are found to be more vulnerable to ischemic effects, due in part to reduced metabolic capabilities and excess glutamate release, compared to other hippocampal subfields (Bartsch et al., 2010, 2015). These findings are paralleled by the notion of an extremely high metabolic requirement of a specific subgroup of hippocampal interneurons functioning at near limit of their mitochondrial metabolic capacity to continuously provide fine-tuning of the neuronal excitatory-inhibitory balance of hippocampal circuits (Pinna & Colasanti, 2021). Considering the increased neurometabolic demands generally associated with neuroinflammatory processes, the sensitivity of hippocampus to inflammation and its

limited oxygen supply reserve, it would be expected that the hippocampal metabolic vulnerability would be further exaggerated and amplified in neuroinflammatory pathology.

Although abundant animal research provided full characterisation of inflammatory pathology of the hippocampus, there has been comparatively less research on the pathological characteristics of human hippocampal neuroinflammation. A few post-mortem studies provided evidence of neuroinflammatory demyelination of human hippocampus in the prototypical neuroinflammatory condition, multiple sclerosis (MS) (Dutta et al., 2011; Geurts et al., 2007a; Papadopoulos et al., 2009). However, no study so far has directly correlated post-mortem pathological findings to neuroimaging, to enable in vivo characterisation of hippocampal neuroinflammation. The ability to identify neuroimaging biomarkers of hippocampal inflammation in vivo would be crucial to characterise its pathology, but also would help in the identification of endpoints for clinical trials with therapeutics targeting neuroinflammatory processes.

Over the past two decades, there have been promising advances in the field of quantitative neuroimaging, in terms of sensitivity to detect neuroinflammation. For example, PET targeting 18 kDa translocator protein (TSPO) as well as novel MRI approaches claim to have good sensitivity and some degree of specificity for measuring brain inflammatory processes (Albrecht et al., 2016; Colasanti et al., 2016; De Marco et al., 2022; Herrera-Rivero et al., 2015; Lee et al., 2020). However, various methodological aspects complicate the characterisation of the hippocampus with neuroimaging. For instance, the complex sub structural organization of the hippocampal formation, which comprise subfields, have individual vulnerability to physiological and pathological processes. (Pereira et al., 2014) observed a correlation between ageing, diffusion tensor imaging measures and volumes of varying subfields. (Zheng et al., 2018) also observed volume alterations of differing hippocampal subfields at different ages with positive correlations to delayed and immediate recall measures. Specifically, CA1-4, DG are impacted upon. Indeed, some studies have emphasized distinct links between biological ageing, elevated inflammatory markers and chronic inflammation, a phenomenon known as inflammageing or accelerated aging (Ferrucci & Fabbri, 2018; Yegorov et al., 2020).

Given the above evidence of aging-related processes impacting differentially on hippocampal subfields, it is plausible to expect similar subfields-specific vulnerability to neuroinflammatory processes.   In particular and as highlighted above; such mechanisms

may comprise the interplay between glial activation and the rate of neurogenesis in DG, and under perfusion induced metabolic modifications made more prominent in CA1.

The unique anatomical location of the hippocampus also makes it vulnerable to partial volume artefacts (when more than one tissue type is present in a voxel, invalidating the quantitative accuracy). Use of segmentation techniques employing automated coregistration of quantitative maps on high-resolution anatomical images might therefore be suboptimal. Further, separation of subfields is difficult due to low resolution of imaging techniques. Conventional MRI approaches have also failed to accurately discriminate between varying subfield layers.

Despite these challenges associated in general to hippocampal neuroimaging methods, there has been an increasing number of applications of novel quantitative approaches to study neuroinflammation in the hippocampus. In the present overview, I will provide details on how these quantitative techniques might inform on various aspects of neuroinflammatory pathology. I also aim to summarise the state of the art on hippocampal imaging of neuroinflammation by systematically reviewing studies that employed quantitative imaging techniques to assess hippocampal neuroinflammatory processes. I will focus on MS, systemic lupus erythematosus (SLE), and autoimmune encephalitis (AE) as prototypical examples of autoimmune neuroinflammatory diseases that might involve the hippocampus. I include studies that used imaging techniques targeting neuroinflammation-specific pathological processes, namely:

1. the activation of resident immunocompetent cells (TSPO PET; MRS (Lactate, Myo-inositol, Choline);
2. BBB disruption/permeability (dynamic contrast enhanced or DCE MRI);
3. Interstitial modifications consequent to neuroinflammation, such as oedema and modifications to the relative size of the extra-cellular water compartment, which can be detected using diffusion-weighted (DW) MRI, magnetization transfer ratio (MTR), or magnetic resonance spectroscopy (MRS) by quantifying metabolites such as Lactate, Choline, and Lipids.

Furthermore, I will also separately report findings from quantitative neuroimaging studies that assessed hippocampal morphology differentially across hippocampal subfields. These studies will be useful to reveal the sequelae of neuro-inflammation such as neuronal loss / neurodegeneration.

2.2 Overview of relevant imaging techniques

Over the past two decades, there have been promising advances in the field of quantitative neuroimaging, in terms of sensitivity to detect neuroinflammation. For example, PET targeting 18 kDa translocator protein (TSPO) and other novel MRI approaches claim to have good sensitivity and some degree of specificity for measuring brain inflammatory processes (Albrecht et al., 2016; Colasanti et al., 2016; De Marco et al., 2022; Herrera-Rivero et al., 2015; Lee et al., 2020). However, various methodological aspects complicate the characterisation of the hippocampus with neuroimaging. And, as highlighted above, the subfields of the hippocampal formation have differential vulnerability to physiological and pathological processes.

The most frequently used imaging tool in routine clinical settings to identify *in vivo* biomarkers in neuroinflammatory conditions such as MS, is MRI. For example, MRI is established as gold standard in the diagnosis of MS, and is used to investigate the natural course of the disease and monitor treatment effects in clinical trials. MRI "lesions" appear as hyperintensities on T2-weighted images and, in the relapsing-remitting phase of MS (RRMS), the effect of a treatment on MRI lesions and its effect on the frequency of relapses are strongly correlated, supporting the use of MRI parameters as surrogates for clinical end points (Sormani et al., 2009). However, conventional MRI measures are limited by lack of neuropathological specificity, and for example, non-specifically reflects demyelination, oedema, or gliosis (Arnold & Matthews, 2002). Furthermore, as disability progresses in the secondary progressive phase of MS (SPMS), the strength of the relationship between T2-hyperintensities and clinical severity becomes weaker. Importantly, conventional MRI measures, including T2-weighted FLAIR, is only able to detect a minority of cortical or sub-cortical grey matter lesions. This may be due to the different pathophysiology of cortical grey matter lesions, compared to those in the white matter, with less inflammatory cell infiltration and absent blood–brain barrier damage (Peterson et al., 2001). All these factors impact the value and utility of conventional MRI measures for the assessment of hippocampal neuroinflammation. We have therefore focused our review on alternative molecular imaging techniques that provide higher, although not absolute, specificity to the pathological

processes that are relevant for hippocampal neuroinflammation. Here we provide a brief description of the imaging techniques used in the studies we reviewed.

2.2.1 Neurite orientation dispersion and density imaging (NODDI)

A good compromise between complexity and acceptable scan time is neurite orientation dispersion and density imaging (NODDI) (Zhang et al., 2012), which provides estimate of the intra-neurite and the isotropic volume fractions. NODDI also provides a more specific characterisation of tissue microstructure in the whole brain by means of a multishell diffusion technique and a clinically feasible protocol. As a three compartment tissue model, NODDI measures the intracellular volume fraction (ICVF), the orientation dispersion index (NDI) and a CSF water fraction (IsoVF) (McCunn et al., 2019; Zhang et al., 2012). The biophysical tissue models of NODDI may provide specific biomarkers of brain microstructural alterations, and allude to properties of neurites such as density and orientation dispersion (Zhang et al., 2012). Histological measures of CNS neurite orientation dispersion have been noted to correlate with ODI, and there have also been reported correlations of ICVF with myelin (Grussu et al., 2017; Mollink et al., 2017). In MS pathology, reduced ICVF fractions and increased ODI measures have been observed in the brain and spinal cord, compared to healthy controls and are usually more evident with RRMS and SPMS (Granberg et al., 2017; Spano et al., 2018; Toschi et al., 2019).

2.2.2 Magnetic resonance spectroscopy (MRS)

MRS aims to quantify the concentration of tissue metabolites, by exploiting a phenomenon known as chemical shift. In molecules more complex than water, the negatively charged electrons can oppose the external static magnetic field resulting in a small shift of the resonance frequency of each metabolite. As these molecules are fairly mobile, their signal results in relatively narrow peaks in frequency, which can be easily identified. By measuring the area under each peak, it is possible to estimate their concentration. The main metabolites visible in the brain are N-acetyl aspartate (NAA), only present in neurons, and often regarded

as a neuronal marker; choline (Cho), a marker of membrane turnover, which resides in glial cells and neurons; and creatine (Cr), a marker of cellular energetics, often used as a reference for other peaks. Other metabolites of interests, which are, however, more difficult to measure, are glutamate (Glu), glutamine (Gln), myo-inositol (mI), and lactate (Lac). The last two are of interest in the context of neuroinflammation, as mI is only present in glial cells, while Lac is virtually invisible in healthy brain but increases in conditions of hypoxia, poor perfusion and other pathologies. More details can be found in (Tognarelli et al., 2015).

2.2.3 Resting-state functional MRI

Resting state functional MRI (RS-fMRI) examines brain functions by the application of oxygen level-dependent contrast (Barkhof et al., 2014). The technique makes use of a short acquisition time of less than 10 minutes. The modality is based on the concept that BOLD signals (Oxygen level dependent) fluctuate at rest and represents brain neuronal baseline activity, as well as resting state network of relevance (Damoiseaux et al., 2006). Generally; in research and clinical practice, focus is on the variations in BOLD signals during a task that is controlled externally (Damoiseaux et al., 2006). In MS pathology, consistency between cerebral region activities during an external task, a phenomenon known as functional connectivity of the brain can be analysed with a view to understanding brain functional alterations and their roles in clinical impairment and progression of disease (Sbardella et al., 2015).

2.2.4 Modified Asymmetric spin echo (GASE)

Oxygen delivery to Oxygen consumption ratios constitute the oxygen quantity derived from the circulatory system that inevitably gets into the brain tissue. This is defined as oxygen extraction or R2, and is regarded as a vital and relevant marker of healthy brain tissue. The measurement could directly represent both brain activity and viability (Gupta et al., 2014; Liu

& Li, 2016; Yanyan et al., 2018). MRI R2 measurements exploit the characteristics of deoxygenated haemoglobin in the veins and capillaries via tissue, blood and CSF MR signals.

2.2.5 Arterial spin labelling (VEPCASL)

Arterial spin labelling (ASL) employs a freely diffusible intrinsic tracer to determine perfusion of tissue (Petcharunpaisan, 2010). Specifically, ASL is an MRI technique utilized in the quantification of blood flow in the tissue (Ferré et al., 2013). The procedure involves magnetic labelling, by non-invasive means, the protons in arterial blood, using radio frequency pulses. Two acquisitions are necessary, with one acquisition as control (without labelling). Inversion time corresponds to the time taken for the labelled protons to perfuse brain tissue. A perfusion weighted image is obtained from the subtraction of labelled and controlled acquisitions (Detre et al., 1992). VEPCASL which stands for vessel-encoded pseudocontinuous arterial spin labelling is reported to be a highly efficient for both non-invasive vascular territory imaging and dynamic angiography (Okell et al., 2019).

2.2.6 Positron Emission Tomography (PET)

Positron Emission Tomography imaging, based on the in vivo administration of radiolabelled ligands that bind selectively to a target of interest, offers the potential of high specificity for molecular markers of cellular and metabolic processes. The high selectivity of PET allows microdosing of the radiotracer, ensuring high safety and tolerability for the subjects who undergo the procedure. Although for over two decades there have been intense research in the identification of suitable PET targets for neuroinflammation imaging, only a limited number of targets have been investigated in living patients to date, and the only extensively characterised target in clinical populations is the 18 KDa Translocator Protein (TSPO). TSPO, formerly known as the peripheral benzodiazepine receptor (PBR), is a protein primarily (but not exclusively) localized on cells outer mitochondrial membrane. In normal conditions TSPO is highly expressed in peripheral tissues, particularly where steroids are

synthesized, consistent with its role in steroidogenesis (Owen et al., 2017). In the normal human brain, the expression of TSPO is low. TSPO expression is observed in macrophages and microglia, astrocytes, oligodendrocytes, endothelial cells and smooth muscle cells, platelets, subpial and subependymal glia, meninges (vessels, macrophages and sometimes, arachnoid cells), ependymal cells, and choroid plexus. Furthermore, recent evidence confirmed TSPO is also expressed in neurons (Notter et al., 2021; Vicente-Rodríguez et al., 2021). Autoradiography studies using radiolabelled TSPO ligands demonstrate that the expression of TSPO is dramatically enhanced in response to microglia proliferation or activation, in the case of a disrupted blood brain barrier, on invading cells of mononuclear-phagocyte lineage (Chen & Guilarte, 2008; Nutma et al., 2019, 2021; Venneti, Sriram; Lopresti, Brian J; Wiley, 2006). The precise role of TSPO in the inflammatory processes of microglia during such disease states remains unclear, with accumulating evidence suggesting an allostatic role of TSPO in the orchestration of bioenergetic, and more specifically, redox responses that accompany neuroinflammatory processes.

In neuroinflammation, the areas of focal tissue damage and demyelination, such as for example in active or chronic active MS lesions, are characterized by dramatically increased microglia density, therefore TSPO represents an attractive target for imaging focal lesional neuroinflammatory pathological processes. However, TSPO PET also enables assessment of neuroinflammation in non-lesional areas providing clinically relevant information that is not available with conventional routine MRI approaches (Colasanti et al., 2016). An important caveat to consider relates to the notion that the specificity of TSPO to each cellular type is not uninform across species, brain regions and disease processes (Nutma et al., 2019, 2021; Owen et al., 2017; Vicente-Rodríguez et al., 2021). Therefore, the application of TSPO PET imaging should be informed by histopathological studies that reveal, for each specific target and application, which cellular types, and immunopathological processes are contributing the greatest proportion of TSPO signal. In parallel to developments in the TSPO PET field, I note promising results from first-in-human applications of other emerging PET radiotracers targeting neuroinflammatory processes, such as for example the COX-1 targeting [11C]PS13 which displays exquisitely high hippocampal uptake (M. J. Kim et al., 2020). Furthermore, promising data are emerging from novel human applications of [11C]-deuterium-L-deprenyl ([11C]-DED) (Rodriguez-Vieitez & Nordberg, 2018) and [11C]-BU99008 (Calsolaro et al.,

2021), which bind respectively to Monoamine Oxidase B, and the non-adrenergic imidazoline-2 binding site, both of which are overexpressed in reactive astrocytes.

2.2.7 Dynamic Contrast-Enhanced MRI (DCE MRI)

The aim of DCE MRI is to assess the integrity of the blood brain barrier (BBB) by measuring the distribution of a paramagnetic contrast agent (typically, gadolinium chelates) injected intra-venously. When the BBB is intact, the contrast agent stays in the vasculature, while in the presence of increased permeability, it leaks in the tissue altering the MRI signal. Alterations to the BBB are known to occur in the presence of neuroinflammation, for example in acute MS lesions (Kermode et al., 1990). More subtle increases in permeability have also been reported in conditions such as dementia (Starr et al., 2009), and have been linked to the presence of underlying chronic inflammation. The transfer constant K_{trans} can be estimated by fitting analytical models of tissue compartmentalisation to serial T1-weighted acquired after the injection. K_{trans} tends to increase with increased BBB permeability. Please see (Chi et al., 2019; Ibrahim et al., 2021) and Figure 2.1 for more information and illustration.
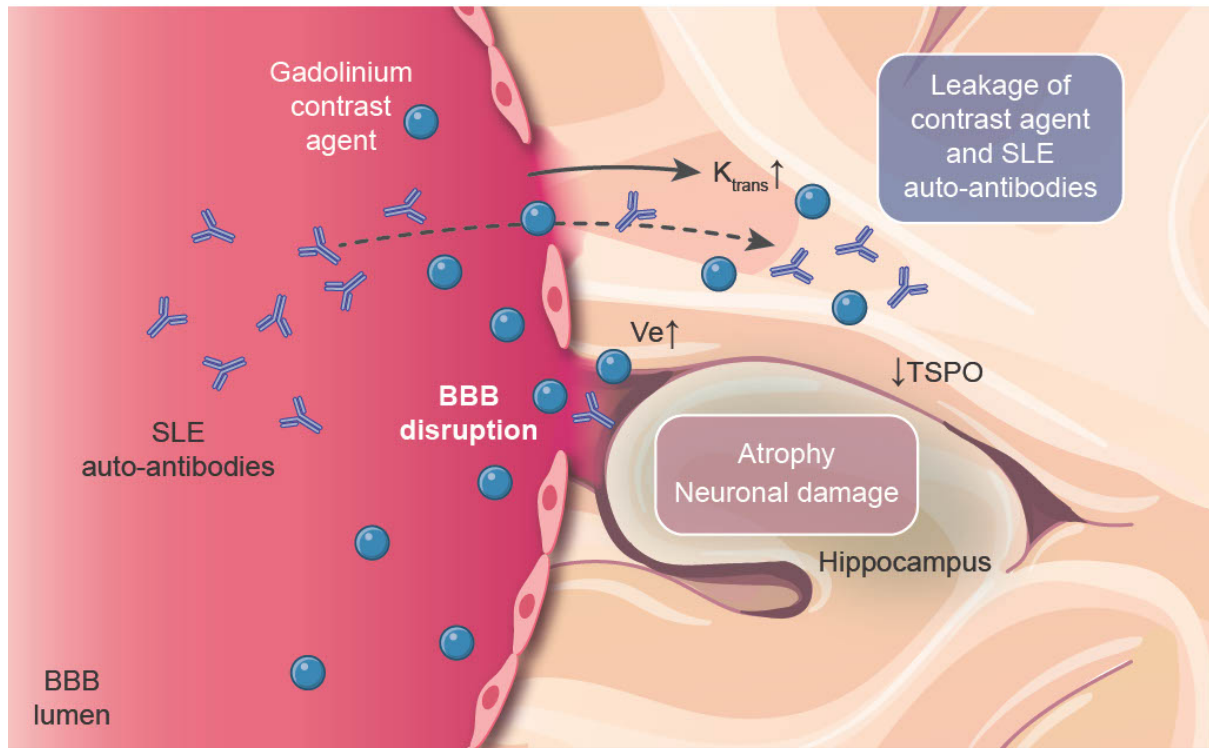
K_{trans}: Volume transfer constant
Ve: Volume per unit tissue
TSPO: Translocator protein

Figure 2. 1 Immunopathology of BBB disruption in SLE (Nwaubani et al., 2022). Diagrammatic representation showing rationale for Dynamic Contrast Enhanced MRI of Neuropsychiatric lupus pathology with impact on the Hippocampus. Neuronal damage within the hippocampus is induced following breach of the blood-brain barrier (BBB) and access of SLE Auto-Antibodies. Accumulation of gadolinium-based contrast agent, as measured by increasing capillary permeability (K_{trans}), and accumulation in the extravascular space (V_e) have been reported (Chi et al., 2019). Significant decrease in TSPO distribution in the Hippocampus has also been reported using PET (Wang et al., 2017).

2.2.8 Magnetization Transfer Imaging & MTR

MRI is only sensitive to the signal from small, mobile hydrogen-containing molecules, as the signal from larger ones (lipids, proteins) decays too fast to be probed. Nevertheless, hydrogen protons in differing chemical environments can exchange magnetization, thus enabling the indirect probing of macromolecular protons through an MRI measurement. This forms the basis of magnetization transfer (MT) imaging. MT uses radiofrequency pulses far from the resonance frequency of water to saturate macromolecular protons without affecting water

protons directly. Thanks to the exchange of magnetization between the two, such saturation is transferred to the water protons and results in a signal attenuation, which depends on the local density of macromolecules. Early attempt to quantify these effects led to the development of the MT ratio (MTR), a percentage difference between the signal measured with and without MT saturation. Larger MTRs typically indicate tissue rich in protein and lipids (including myelin), while reduced MTR values suggest either a reduction in macromolecular content, or an increase in the extracellular water compartment. The interested reader is referred to (Cercignani et al., 2001). In the rodent, MT imaging has demonstrated sensitivity to the effects of peripheral inflammation on the brain (Serres et al., 2009) and sciatic nerve (Stanisz et al., 2004), primarily through its sensitivity to increased water content.

2.2.9 MESH MODELLING

Three-dimensional renderings of brain structures also known as mesh models can be obtained from structural MRI data via finite element modelling. These digital 3D-renderings are obtained by combining simple elements (typically tetrahedral or hexahedral ones). The advantage of mesh models is that they enable relevant properties of the brain, such as cortical folding and structural shape, to be captured better than using standard image volumes. Several image analysis packages include similar options, and are typically used to compare morphological structures within or between groups (Pain et al., 2005). In the context of hippocampal inflammation, mesh modelling can be used to compare the hippocampal shape and volumes, as well as those of its subfields.

2.3 SYSTEMATIC REVIEW METHODOLOGY (QUANTITATIVE IMAGING OF HIPPOCAMPAL NEUROINFLAMMATION)

A systematic review was conducted following PRISMA guidelines (Moher et al., 2009).

PubMed

Identification

Records identified from*:

Databases (n = 621)

Records from other sources (n=0)

Screening

Titles/ Abstract screened (after duplicates, non-English language, case reports, case series and reviews were removed (n= 580)

Records excluded for non-meeting criteria

(n = 551)

Eligibility

Full-text articles assessed

(n = 29)

Study protocol and study methodology did not meet criteria (n = 4)

Primary pathology not

Included

Studies included in review

(n = 18)

Divided into 2 groups

- Studies directly examining neuroinflammatory pathology (n=15)
- Studies measuring in separate hippocampal subfields neurodegenerative changes secondary to

Figure 2. 1 PRISMA flow chart

2.4 STUDY SELECTION

Prior to the review, I defined the search terms and data to be extracted as highlighted in Tables 2 and 3 below. I employed the free search engine pubmed.ncbi.nlm.nih.gov to search the literature from June 1988 to July 2021. Start year was selected based on when selected articles began to meet relevant criteria as per PubMed search. I also manually searched the references of relevant and related articles. In terms of target clinical populations, I decided to focus the search of studies on quantitative neuroimaging measures of hippocampal neuroinflammation with a focus on three prototypical neuroinflammatory autoimmune conditions for which post-mortem pathology reports clearly confirm hippocampal involvement namely MS; AE; SLE (Ballok et al., 2004; Hughes et al., 2010; Papadopoulos et al., 2009; Schnider et al., 1995). Eligible studies were then further split in two categories; the first group (15 studies in total) comprised studies that used imaging techniques to target primary neuroinflammatory processes, and the second group (3 studies in total) included studies of morphological alterations of hippocampal subfields reflecting neuroinflammatory sequalae, such as neuronal loss/neurodegeneration. I did not include studies focused on conditions such as temporal lobe epilepsy (TLE) and Alzheimer's disease (AD) with well characterised hippocampal involvement but whose primary pathology is non-neuroinflammatory. From the selected studies, I reported on each ability to differentiate between patients and normal brain.

Search Terms:	Key Words:	**("multiple sclerosis" or MS or "autoimmune encephalitis" or "limbic encephalitis" or "systemic lupus erythematosus" or SLE)**
	AND	**(MRI or "Magnetic Resonance Imaging" or Diffusion or DWI or DWMRI or DTI or NODDI or MTR or QSM) or (MRS or Magnetic Resonance Spectroscopy) or ((TSPO or Translocator Protein or PBR) AND (PET or "Positron Emission Tomography"))**
	AND	**(hippocamp* or cornu ammonis or CA1 or CA3 or CA4 or "dentate gyrus")**
	Selection:	English Language Humans Year: 1988 – 2021
	Inclusion Criteria:	- Human participants - Patients affected by at least one of the three pre-selected neuroinflammatory diseases (MS or AE or SLE) - Group of non-affected control participants present - Employing quantitative imaging techniques (such as TSPO PET, DW-MRI, MRS, etc.) - Reporting data on the hippocampus or one of the hippocampal subregions, separately from other brain ROIs
	Exclusion Criteria:	- Non-English language studies - Case reports - Case series - Reviews - Meta-analysis - Studies on experimental models of neuroinflammation (human or animal) - Only reporting qualitative MRI findings (such as reporting only either presence or absence of T2-weighted hyperintensities) - Only reporting volumetric analysis of hippocampus or its subfields - Primary pathological process was not neuroinflammation, such as in AD or Epilepsy

Table 1: Literature Search Methodology

2.4.1 Article Selection

All articles included are original research papers and are all in English language. The study designs of selected articles comprised longitudinal studies, case controls and cross-sectional studies. Primary search was conducted by myself and experienced supervisors. Only studies, which were eligible, based on inclusion and exclusion criteria were selected.

2.4.2 Data Extraction

I extracted the data which was later reviewed by supervisors (Prof Mara Cercignani- Imaging physicist). Key data included clinical population, imaging methods, outcome measures and effect sizes. Effect sizes were estimated by calculating the Cohen's *d*, which was determined by calculating the mean difference between two groups (affected participants and controls), and dividing obtained result by the standard deviation. **Cohen's *d* = (M₂ – M₁)/SD.** Complete table of data information is available in Table 3.

Author
Year
Clinical Population (i.e. number of cases, mean age/ standard deviation, gender)
Imaging Methods (i.e. Imaging type, hippocampal segmentation, subfield analysis)
Outcome Measures (i.e. Imaging, affective/ cognitive measures
Findings (i.e. Difference cases vs controls, effect size, p values, correlations to cognitive/ affective measures.

Table 2 : List of Data extracted

2.4.3 Quality Assessment

The quality of each study included, was independently assessed by an experienced imaging physicist (Prof Mara Cercignani). The Rayyan software was utilized in screening relevant search results against selected criteria, and was equally employed in discarding irrelevant studies (Ouzzani et al., 2016). The strength of evidence in each paper selected was also manually analyzed and thoroughly checked for biases.

2.5 RESULTS

During the initial search, I came up with 621 articles (See Prisma flow diagram in Fig 2.3). I excluded conference extracts, non-human studies and non- English language articles. Case reports, case series and reviews were also removed. A further 551 articles were excluded upon review of their titles and abstracts. 216 article titles did not match criteria. 73 of theses articles were not based on human studies, and the other 143 articles did not employ quantitative imaging techniques. 335 articles from the 551 had been excluded mostly due to a non-focus on the hippocampus and also for only reporting qualitative MRI findings. The remaining 29 articles were further screened by three reviewers. 4 articles were excluded due to imaging methodology not meeting eligibility criteria and a further 7 were excluded because their target disease was not primary neuroinflammatory pathology. A total of 18 studies met the criteria for inclusion. Fifteen of these used imaging techniques directly examining neuroinflammatory pathology, whilst three applied imaging techniques measuring morphological changes in separate hippocampal subfields, reflecting neurodegenerative changes such as neuronal loss secondary to neuroinflammation. See illustration in figure 2.2 below;
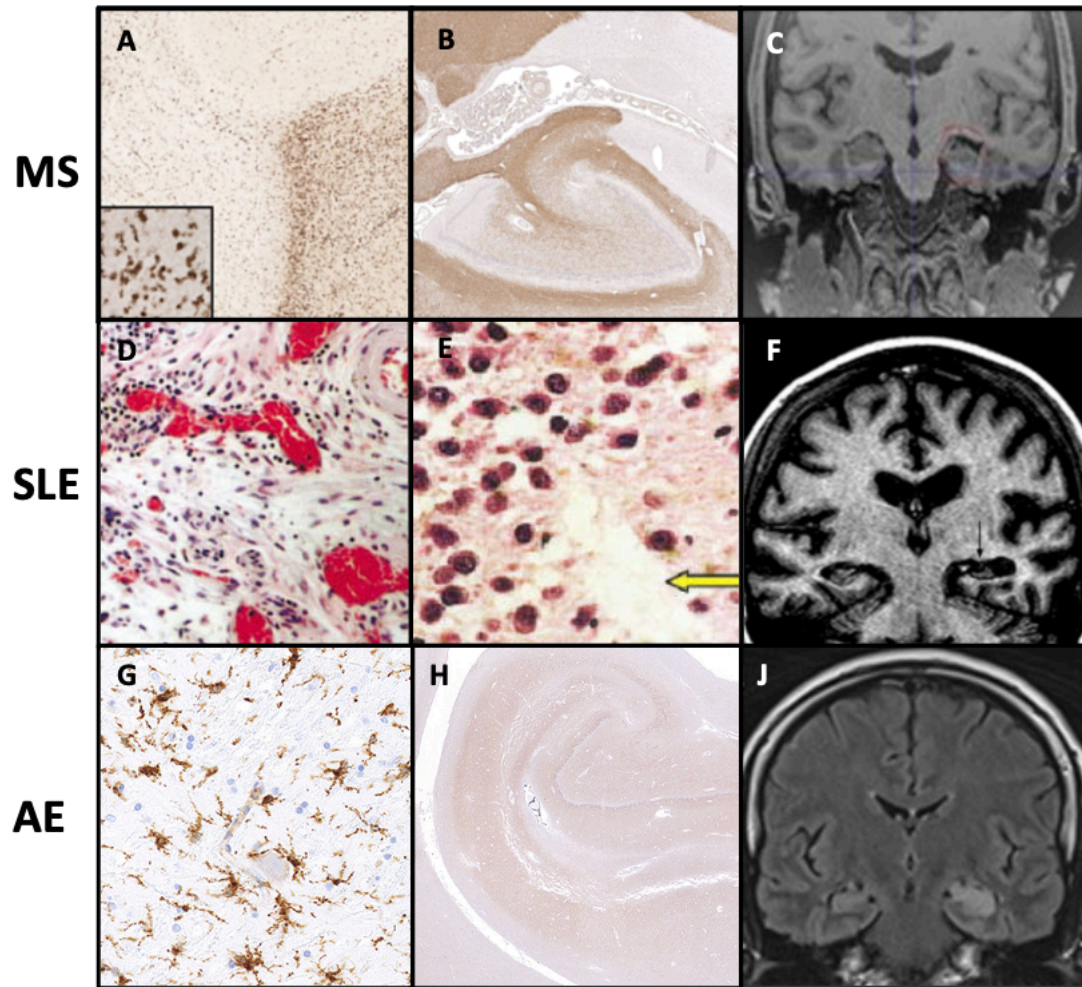
Figure 2. 2 Immunopathological and Neuroimaging features of hippocampal neuroinflammation across neuroinflammatory diseases. **A, B, C**: Multiple Sclerosis (MS): reduced density of ramified Microglia (HLA class II staining) in a lesion centre with increased density of activated microglia and macrophages in the lesion edge (A); Pattern of hippocampal demyelination in the DG of a MS patient (B) [from (Papadopoulos et al., 2009)]. Reduced Hippocampal volume in patient with MS (C) (unpublished data). D, E, F: Systemic Lupus Erythematous (SLE): Lymphocytes infiltrates in the Choroid Plexus (D). Evidence of neuronal loss in DG (E) [from (Ballok et al., 2004)]. Hippocampal atrophy in SLE patient (F)[from (Appenzeller et al., 2006)]. G, H, J: Autoimmune Encephalitis (AE): Hippocampal microglial activation (HLA class II staining) (G) and reduced NMDAR-expression (H) in a patient with NMDAR encephalitis [from (Zrzavy et al., 2021)]. FLAIR MR image showing hyperintense swelling of the left hippocampus (J) [from (Dekeyzer et al., 2017)].

Of the 18 studies included in the systematic review, 14, 2, and 2 studies focused on MS, AE and SLE respectively. The overall study cohorts included 729 MS, 16 SLE and 166 patients with autoimmune encephalitis, giving a total number of 911 patients. Healthy controls were

497 in total. Ages ranged from 28-66 years and SD between 4 and 13. Female to male ratio was 467/262 for MS patients, and 101/65 for AE patients. The gender of participants was unspecified in the SLE studies. Comprehensive details of demographics and results can be found in Tables 3 and 4. In our review of studies (n=15) targeting primarily neuroinflammatory processes, 4 studies used TSPO PET, 8 studies used DW MRI, whilst one study used DCE, MRS, MTR respectively. There was high heterogeneity in terms of techniques and specific imaging methodology employed, and virtually no study replicated exactly the same methodology within the same condition, with the exception of five studies in MS that all used DW MRI. The three PET studies in MS used three different 2nd generation TSPO radiotracers and reported different outcome measures (SUVr; Vt; DVR)

All neuroinflammation – targeting studies revealed at least one significant signal change in the hippocampus, relative to the control group. The effects sizes varied greatly across studies (range 0.1 to 1.6). Across conditions, the largest effect sizes were seen with TSPO PET and DW MRI, indicating respectively increases in hippocampal TSPO binding and in the Diffusion based MD parameter; and a reduction in diffusion-based FA. These changes appeared consistent across MS studies and were evident in various MS sub-types, although increase in TSPO PET signal (Colasanti et al., 2016; Herranz et al., 2016), as well as changes in diffusion FA and MTR appeared more prominent in progressive forms of MS relative to relapsing-remitting, and even more to CIS (Cappellani et al., 2014; Planche et al., 2017; Vrenken et al., 2007). The direction of the changes observed in AE which revealed an increase in MD as reported in two studies (Finke et al., 2016/17), was thus consistent with findings in MS, whilst the two studies in SLE revealed TSPO binding changes opposite to those seen in MS, and alterations in BBB permeability that no other studies had examined. Only two studies (both DW MRI studies on AE) examined separately, individual hippocampal subfields (Finke et al., 2016, 2017). No other studies reported regional subfield analysis.

In MS, increased TSPO binding and elevations in mean diffusivity parameter (MD) correlated with neurological disability and impaired cognitive performance. For instance, SDMT z-scores negatively correlated with TSPO uptake in the hippocampus (Herranz et al., 2016). Increase in diffusion-based MD parameter also negatively correlated with SDMT and CVLT scores in MS and CIS respectively and was also able to effectively discriminate between memory impaired and memory preserved patients with CIS. In contrast, a decrease

in the FA parameter had positive correlations with SDMT (Planche et al., 2017). Negative correlations were observed with the following: BBB parameters in SLE and elevated MD in AE correlated with varying neuropsychological assessment scores (ANAM; RAVLT and ROCF respectively) (Chi et al., 2019; Finke et al., 2016, 2017). There were also correlations observed with imaging measures and scores on the affective scales in MS and SLE patients. TSPO hippocampal distribution volume ratio in MS and BBB parameters in SLE were positively correlated with BDI scores (Chi et al., 2019; Colasanti et al., 2016). Decrease FA parameter correlated with HAMD scores (Shen et al., 2014).

In the second group of studies examining separate hippocampal subfields and reporting neurodegenerative changes due to neuroinflammation, I included 3 studies using MESH modelling. Regional changes were detected between subfields. In MS patients there was surface expansion of the hippocampal dentate gyrus (DG) as measured by radial distance (RD) enlargement (Rocca et al., 2015). This was also observed in the (Cacciaguerra et al., 2019) study looking at serial regional measurements, and was more pronounced in later months. In contrast, there was a reduction in RD in the CA1 subfield after 3 months progressing to the subiculum. Across MS and AE, deformation overlap corresponded to damage within the CA1 subfield (Heine et al., 2020).

Authors; year	Clinical population		Imaging Methods			Outcome Measures		Findings	
	Disease	n cases; mean age (SD) ; gender	Imaging type	Hippocampal Segmentation	Subfields analysis	Imaging	Affective / Cognitive	Difference Cases vs controls effect size (ES); p value	Correlations to cognitive / affective measures
(Colasanti et al., 2016)	MS	MS: n=11; 45(8) yrs; 10F HC: n=22; 49(10) yrs; 14F	TSPO PET [18F]PBR111	Automated (CIC Atlas)	No	[18F]PBR111 DVR (cortical GM as pseudo-reference region)	BDI-II	MS: [18F]PBR111 DVR: 0.8 (p=0.024)	MS cohort: [18F]PBR111 DVR (p=0.037) pos correl to BDI
(Herranz et al., 2016)	MS	RRMS: n=12; 43(10) yrs; 10F SPMS: n=15; 52 (7) yrs; 11 F HC: n=14; 48 (13) yrs; 6 F	TSPO PET [11C]PBR28	Automated (First/FSL)	No	[11C]PBR28 SUV$_R$; DVR	SDMT; TMT-A & B; CVLT-II; BMVT-R; WCST	RRMS: [11C]PBR28 SUV$_R$: 1.1 (p=NS) [11C]PBR28 DVR: 0.8 (p=NS) SPMS [11C]PBR28 SUV$_R$: 1.6 (p<0.003) [11C]PBR28 DVR: 1.2 (p<0.005)	Whole MS cohort: [11C]PBR28 SUVR (p=0.05) neg correl to SDMT
(Singhal et al., 2019)	MS	RRMS: n=7; 33(7)yrs; 5 F SPMS: n=5; 55(4)yrs; 3F HC: n=5; 38 (13)yrs; 3F	TSPO PET [18F]PBR06	Automated (PNEURO)	No	[18F]PBR06 SUV$_R$	No	MS: [18F]PBR06 SUV$_R$: 1.4 (p=0.03)	NA
(Cappellani et al., 2014)	MS	RRMS: n=210; 46(9) yrs; 149 F PMS: n=75; 49 (7) yrs; 57 F HC: n=110; 47 (13) yrs; 76 F	DW-MRI	Automated (First/FSL)	No	FA, MD, RD, AD	No	RRMS: FA 0.4 (p=0.047) MD 0.6 (p<0.001) AD 0.5 (p<0.001) RD 0.6 (p<0.001)) PMS: FA 0.3 (p=0.047) MD 0.7 (p<0.001) AD 0.6 (p<0.001) RD 0.7 (p<0.001))	NA

(Geurts et al., 2006)	MS	MS: n=33; 48 (12) yrs ; 16 F HC: n=10; 43 (9); 7 F	MRS	NS	No	Ins	BRB-N	MS: Ins 0.7 (p<0.05) SPMS Ins 0.9 (NS)	No correlation with BRB-N
(Planche et al., 2017)	MS	CIS: n=37; 37(10) yrs; 29F MS: n=32; .41 (6) yrs (SD); 23 F HC: n=36; .38 (10); 24 F	DW-MRI	Automated (First/FSL)	No	MD, FA	SDMT, WAIS-III, SRT, CVLT, BDI	CIS: FA: 0.5 (p<0.050) MS FA: 1.05 (p<0.0001) MD: 1.21 (p<0.0001)	CIS MD CVLT/SRT (DR) r= -0.57 (p=0.0002) MS FA SDMT r= 0.36 (p=0.004)n.s[a] MD SDMT r= -0.52 (p=0.002) (p=0.012)[a]
(Roosendaal et al., 2010)	MS	MS: n=25; 39 (8) yrs; 17 F HC: n=30; 41 (10) yrs; 20 F	DW-MRI	Automated (First/FSL)	No	MD	LLT, HADS-A, HADS-D,	MS MD LH: 0.7 (p=0.01) MD RH: 0.5 (p<0.03)	NA
(Shen et al., 2014)	MS	RRMS: n=15; 38 (12) yrs; 11 F HC: n=15; 37 (13) yrs; 11 F	DW-MRI	Automated (First/FSL)	No	FA	HAMD	MS FA: ES (p<0.05)	MS LH FA HAMD r= 0.5742 (p=0.025)
(Vrenken et al., 2007)	MS	RRMS: n=35; 39(7) yrs; 24 F PPMS: n=12; 58(6) yrs 5 F SPMS: n=19; 44 (11) yrs ; 11 F HC: n=23; 31 (7) yrs; 11 F	MRI-MTR	Automated (First/FSL)	No	MTR	PASAT	RRMS: MTR 0.1(p=NS) PPMS: MTR 0.7(p=NS) SPMS: MTR 0.9(p<0.05)	No observed corr.
(Yin et al., 2018)	MS	MS-SSCI: n=22; NS (7) yrs; 13 F HC: n=22; NS (13) yrs; 13 F	DW-MRI	SPM8	No	FA, ADC	NA	MS-SSCI: RH FA 0.1 (p=0.042) LH FA 1.4 (p=0.000) MS-SSCI:	NA

								RH ADC ES (p=0.047) LH ADC ES (p=NS)	
(Filip et al., 2020)	MS	MS: n=10; 47(12) yrs; 8 F HC: n=10; 46 (13) yrs; 8 F	DW-MRI and susceptibility	Automated (FreeSurfer)	No	RAFF4, T1p, T2P, FA, MD, AD, RD	SDMT CES-D	MS: RAFF4: 1.6 (p=0.007) T1p: 1.1 (p=0.041) T2P: 1.5 (p=0.004) FA: 0.6 (p=NS) MD: 1 (p=0.099) AD: 0.5 (NS) uncorr RD: 1.1 (P=0.0184) uncorr	No observed correl
(Chi et al., 2019)	SLE	SLE: n=6; 38(13) yrs; (NS) F HC: n=5; .34 (11) yrs; .(NS) F	DCE-MRI	No	No	K^{trans}, Ve, CBF	ANAM, BDI, STAI	SLE: ;K^{trans}: 0.9 (p=0.04) Ve : 0.9 (p=0.04) CBF : 1.1 (p=0.013)	3 SLE had elevated DNRAB titres with pos correl to BDI, STAI. neg correl to ANAM (not stat sig).
(Wang et al., 2017)	SLE	SLE (n=10; 41(9) yrs; (NS) F HC (n=11; 39 (11);. (NS) F	TSPO PET [^{11}C]DPA-713	Automated (FreeSurfer)	No	[^{11}C]DPA-713 V_T	ANAM	SLE: [^{11}C]DPA-713 $V_{T;}$: 0.8 (p<0.05)	NA
(Finke et al., 2016)	Anti-NMDAR Encephalitis	anti-NMDAR encephalitis (n=40; 28(12) yrs; 36 F HC (n=25; 28 (11) yrs; 23 F	DW-MRI	Automated (First/FSL)	Yes (Subfields: CA1, CA2/3, CA4/DG, presubiculum, subiculum, fimbria	MD	RAVLT, ROCF	Anti-NMDAR Encephalitis: LH MD 0.09 (p=0.004) RH MD 0.7 (p=0.019)	RAVLT LH MD r= -0.524 (p=0.001) RH MD r= -0.470 (p=0.004) ROCF LH MD r= -0.45 (p=0.008) RH MD r= -0.44 (p=0.009)
(Finke et al., 2017)	Anti-LGI1 Encephalitis	anti- LGI1 encephalitis (n=30; 66(12) yrs; 11 F HC (n=27; 64 (2) yrs; 9 F	DW-MRI	Automated (FreeSurfer)	Yes (Subfields: CA1, CA2/3, CA4/DG, pre-subiculum, subiculum, fimbria	MD	RAVLT, ROCF	Anti- LGI1 Encephalitis: LH MD 1.1 (p=0.001) RH MD 1 (p<0.001)	RAVLT LH MD r= -0.41 (p=0.04) RH MD r= 0.57 (p=0.03)

Table 3 : Neuroinflammatory changes in the hippocampus

Authors; year	Clinical population		Imaging Methods			Outcome Measures		Findings	
	Disease	n cases; mean age (SD) ; gender	Imaging type	Hippocampal Segmentation	Subfields analysis	Imaging	Affective / Cognitive	Difference Cases vs controls effect size (ES); p value	Correlations to cognitive / affective measures
(Heine et al., 2020)	MS Anti-NMDAR Encephalitis Anti-LGI1 Encephalitis	RRMS (n=30; .43 (6) yrs (SD); 18 F HC (n=30; .42 (8); .18 F anti-NMDAR encephalitis (n=30; .28 (8) yrs (SD); 26 F HC (n=30; .29 (8); .26 F anti-LGI1 encephalitis (n=30; .66 (9) yrs (SD); 9 F HC (n=30; .63 (10); .9 F	MRI	Automated (First/FSL)	Mesh Modelling	Post MRI: Surface based analysis: Scalar values	NMDA/ LGI1 : RAVLT, RWFT RRMS: BRB-N, SRT All: BDI-II	NMDA LH Scalar 0.9 (p=0.001) RH Scalar 0.6 (p=0.070) RRMS LH Scalar 0.8 (p=0.003) RH Scalar 0.6 (p=0.071) LGI1 LH Scalar 0.8 (p=0.003) RH Scalar 0.9 (p=0.002)	NMDA RAVLT Scalar r= 0.335 (p=0.035) RWFT Scalar r= -0.033 (p=0.432) BDI-II Scalar r_s= -0.100 (p=0.356) RRMS BRB-N Scalar r= 0.540 (p=0.010) LGI1 RAVLT LH Scalar r= 0.348 (p=0.041)- No such obs in controls.
(Rocca et al., 2015)	MS	BMS (n=26; .44 (7) yrs (SD); 18 F RRMS (n=28; .40 (11) yrs (SD); 20 F SPMS (n=34; .46 (11) yrs (SD); 24 F HC (n=28; .45 (11); .18 F	MRI	Manual Tracing (MNI) Space	Mesh Modelling	Post MRI: Vertex based analysis: Radial Dist. (DG)	WL test, SS test	BMS Lt DG Rad Dist 0.6 (p=NS) Rt DG no vertices (p=NS) RRMS Lt DG Rad Dist 0.8 (p=NS) Rt DG Rad Dist 0.7 (p=NS) SPMS	BMS WL Lt DG Rad Dist r= -0.43 (p=NS) RRMS WL Lt DG Rad Dist r= 0.50 (p=NS) SS Lt DG Rad Dist r= 0.47 (p=NS) SPMS WL Lt DG Rad Dist r= -0.41 (p=NS)

								Lt DG Rad Dist 0.7 (p=NS) Rt DG Rad Dist 0.6 (p=NS)	SS Lt DG Rad Dist r= -0.38 (p=NS) WL Rt DG Rad Dist r= -0.39 (p=NS)
(Cacciaguerra et al., 2019)	MS	CIS (n=36; .31 (7) yrs (SD); 29 F HC (n=14; .34 (8) yrs (SD); 10 F	MRI	Manual Tracing (MNI) Space	Mesh Modelling	Post MRI: Radial mapping analysis: Radial Dist. HSRV (CA1, Presubiculum, CA4, DG)	PASAT	CIS (M3) Rt CA1 HSRV 0.2 (p=0.009) Rt mol layer HSRV 0.1 (p=0.003) Rt gran layer DG HSRV 0.2 (p=0.002) Rt Presubiculum HSRV 0.3 (p=0.026) Rt CA4 HSRV 0.3 (p=0.007)	No correlation with PASAT

Table 4 : Neurodegenerative changes associated to inflammation in Hippocampal subfields

Summary of Table 3 and 4: Column chart showing individual study main effect sizes
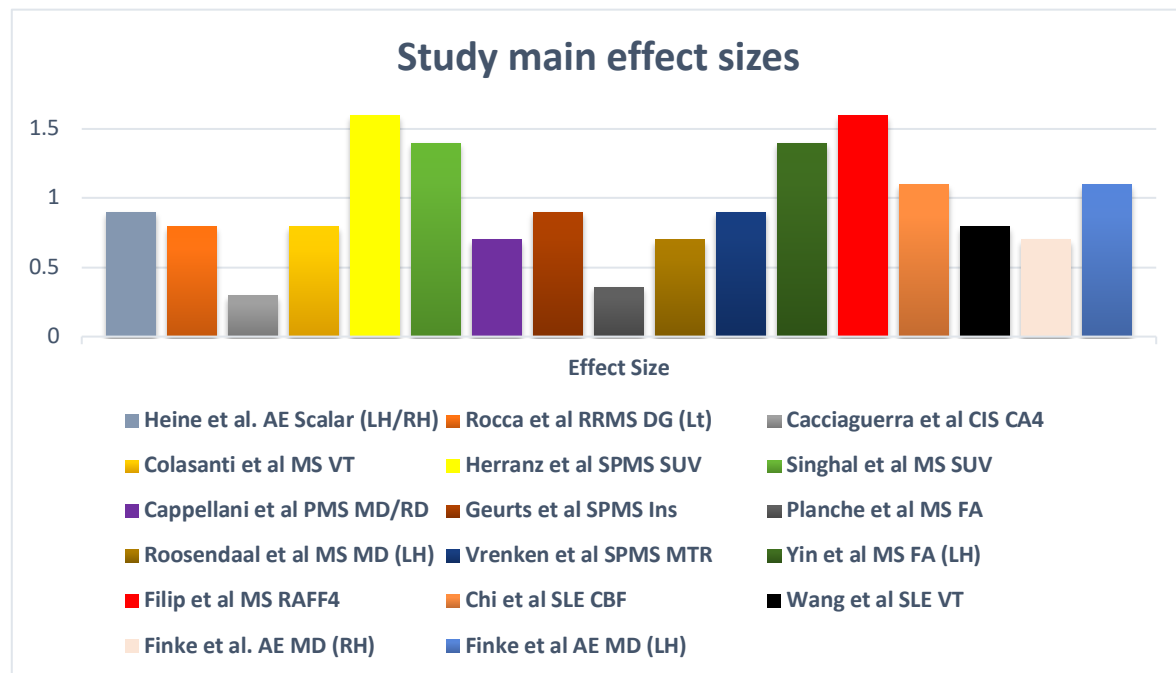
KEY: AE- Autoimmune echephalitis, LH-Left Hippocampus, VT- Volume of distribution, PMS-Progressive MS, MD-Mean Diffusivity, RD-Radial Diffusivity, RAFF4-Relaxation Along a Fictitious Field in the rotating frame of rank 4, RH-Right Hippocampus, RRMS-Relapsing Remitting MS, DG-Dentate Gyrus, Lt- Left, SPMS-Secondary Progressive MS, SUV-

Mean radioactivity/injected dose/weight, Ins-Myo-inositol, MTR-Magnetization Transfer Ratio, SLE-Systemic Lupus Erythematosus, CBF-Cerebral Blood Flow, CIS-Clinical Isolated Syndrome, FA-Fraction Anisotropy.

2.6 DISCUSSION

The systematic review of the literature focused on imaging measures of hippocampal neuroinflammation in 3 prototypical autoimmune neuroinflammatory conditions. It revealed the largest and most consistent significant differences between cases and controls in MS patients, particularly those with the more progressive forms, as shown by studies using TSPO PET and DW MRI. Preliminary results from studies employing other techniques, such as susceptibility, MTR, DCE, appeared promising but require replication in larger samples.

All studies reported global hippocampal imaging measures, and no information specifically related to immunocompetent cells density (e.g. TSPO) or microstructural integrity (e.g. DWI) was reported for separate hippocampal subfields. Although two studies in AE depicted individual sub regional atrophy in CA1, CA2/CA3, CA4/DG and in the subicula regions of the hippocampus, diffusion changes were only reported in the hippocampus as a whole. The separate analysis looking at effect on morphological changes, resulting from neurodegeneration, in neuroinflammatory conditions confirmed our predicted differential vulnerability of subfields to inflammation. For instance, there were specific contrasting measurements in radial distance observed between DG and CA1.

The value of correlations to functional deficits and clinical manifestation were limited by small samples but overall provided preliminary evidence that signs of hippocampal neuroinflammation, capable of causing functional alterations such as in processing speed, semantic organisation, attention, concentration, visuospatial constructional ability, depression and anxiety, might be detected using quantitative imaging markers (Filip et al., 2020; Geurts et al., 2006) and (Colasanti et al., 2016; Vrenken et al., 2007).

Although these correlational data suggest that these quantitative imaging measures are potentially related to clinical phenomena, the lack of specific correspondence between imaging signals and underlying histopathology limit their precise interpretability. For instance, although a large proportion of the TSPO PET signal increases observed in the acute phase of inflammation in MS can be attributed to an increased density of TSPO expressing

macrophages/microglia resulting from their infiltration, proliferation and activation (Nutma et al., 2019, 2021); it is possible that as time progresses, astrocytes contribute to an increasingly substantial proportion of observed hippocampal signal (Nguyen et al., 2018). The discrepancy between findings in MS relative to SLE studies might reflect unique and disease-specific changes in constitutive binding to TSPO expressed by non-inflammatory cells (including for example platelets, endothelia, or other TSPO expressing peripheral cell types), which might be particularly relevant to conditions with systemic and generalised inflammatory responses such as SLE.

Furthermore, TSPO PET presents challenges to quantification of the specific radiotracer binding which become particularly difficult to address in presence of systemic inflammatory responses (Woodcock et al., 2020) , and might contribute to variability of results between studies due to inconsistencies in methodological approaches.

DW MRI was frequently utilized especially in MS. The specificity of its applications and the extent to which it captures and quantifies hippocampal microstructural alterations in neuro-inflammatory pathology have been frequently investigated using pre-clinical and experimental models. Göbel-Guéniot and coworkers (Göbel-Guéniot et al., 2020) observed CA1 pyramidal cell degeneration and granular cell layer dispersions correlated significantly with alterations in tissue diffusivity parameters in murine models of Mesial temporal lobe epilepsy (MTLE), a common type of epilepsy affecting inner aspects of the temporal lobes, which can present in the hippocampus. The findings support the capability of high resolution DW MRI in measuring quantitative changes in epileptic hippocampal tissue consistent with histopathological features in MTLE. Crombe (Crombe et al., 2018) assessed two diffusion-related imaging measures (DTI and NODDI) in terms of their sensitivity to effectively delineate, compute and quantify microstructural alterations in specific hippocampal layers in mice with EAE, a murine experimental model of RRMS. NODDI employs a multishell tissue modality in the characterisation of tissue microstructure while DTI is a simpler approach that assumes a single water compartment characterised by anisotropic diffusion. Both modalities were equally effective in delineating specific hippocampal layers and the quantification of diffusivity parameters presented with differences within 3 specific layers (SR, SLM, ML). DTI showed more prospects with regards to quantification. The same study assessed histopathological correlations between EAE pathology and DW-imaging measures and identified a reduction in AD and MD in the molecular layer of the hippocampus of mouse

model of EAE, corresponding histologically to microglial activation and a reduction in dendritic density, consistent with early neuroinflammatory and neurodegenerative processes respectively. This interestingly contrasts with findings of the studies we reviewed here, where both MS and AE were associated with increased hippocampal MD across studies. A logical explanation here may indeed be due to progression from the MD reduction, reflecting the early neuroinflammatory and neurodegenerative disease processes characteristic of EAE, to more sustained and progressive neurodegenerative pathology seen in MS patients where the expansion of extracellular fluid and microscopic barrier disruptions become progressively more prominent (Finke et al., 2016). Similar distinctive observations were a sole reduction in FA in Clinically isolated syndrome (CIS), considered the first neurological onset of potential MS, and an additional increase in MD seen in MS patients (Planche et al., 2017). However, the impact of partial volume effects with CSF should not be excluded, as human MRI data are typically acquired with much lower resolution.

Due to indirect measures between tissue architecture and DW parameters, DW MRI does lack levels of specificity in neuroinflammatory pathology (Crombe et al., 2018). Both MD and FA are sensitive to increases in extracellular water, reduction in myelin, changes in microstructure and changes in cell density. It is therefore difficult to associate the observed changes with a specific pathological substrate. More so, human applications have also revealed considerable limitations in acquisition due to low resolution protocols specifically designed for whole brain (Treit et al., 2018). To mitigate against these effects and limitations, Treit developed a simple DTI protocol which employed standard single-shot 2D Echo-planar imaging (EPI) at 3T, to obtain high spatial resolution images ($1x1x1mm^3$) of the human hippocampus. In order to compensate for the SNR loss induced by the small voxels, they proposed to use relatively low b-value (thus reducing the amount of diffusion weighting), at the price of limiting the sensitivity to microscopic water environment. As already noted, this may potentially decrease or limit the certainty in identifying vital micro-image details in neuroinflammatory pathology, in an already complex structure such as the hippocampus.

There are other notable methodological concerns in processing hippocampal neuroinflammatory imaging data, which may arise post MRI acquisition such as proposed methods of segmentation, risk of poor precision in co-registration of DW maps if segmentation is done on T1 and resolution limits that can effectively distinguish hippocampal subfields or layers. DW MRI is typically acquired using echo-planar imaging (Schmitt,

2015), a pulse sequence insensitive to bulk motion, but characterised by geometric distortions induced by magnetic susceptibility (Brun et al., 2019). As a consequence, the anatomy on DW EPI does not match the corresponding T1-weighted scans, making image coregistration between the 2 modalities challenging.

Even if perfect coregistration could be achieved, due to the morphological complexities and extremely small structural sizes of the hippocampal compartments, segmenting the subregions of the hippocampus is indeed fraught with difficulties and immense challenges in the analysis of MRI images (Shi et al., 2019). Hippocampal segmentation might be obtained by either automated or manual methods: most of the studies included in the review have utilized automated methods, such as FSL and Free Surfer. Only the studies by (Rocca et al., 2015) and (Cacciaguerra et al., 2019) employed manual tracing for hippocampal segmentation. While manual segmentation by adequately trained human raters is generally regarded as the gold standard (Dalton et al., 2017), semi-automated and more automatic methods appear to be gaining traction with a view to reducing workload, increasing reproducibility and avoiding inter/intra rater variability which is also common with manual methods of segmentation. Automated methods are however not without limitations, which range from a lack of public availability of software, and the limited appropriate training image data sets. Methods can also be subject to error in significant disease states and require parameter tuning (Goubran et al., 2020).

Taking resolution into consideration, a future approach could be computational imaging techniques, which enhances contrast and resolution of lower resolution images. One such application is the Image Quality Transfer (IQT) approach, which mitigates the challenges resulting from spatial resolution, lengthy acquisition protocols, slow translation, interpolation and complex processing pipelines. IQT technique adapts clinically low-quality mappings to experimental high-quality images applying the likeness of images across scales, modalities, regions and subjects (Alexander et al., 2017). With the avoidance of artefacts comprising hot-spots and blurring, and the reduction of partial volume effects, finer details are recovered which were lost at low resolution, hence, allowing for easier identification of hippocampal architecture including morphology, digitations, landmarks, boarders and separation of sub regional layers. Zooming into desired region (MTL for instance) allows for adequate manual segmentation directly on diffusion images, with subsequent computation of desirable

diffusion parameters. The need for co-registration to anatomical or histological images is hence diminished.

The poor specificity of diffusion MRI is caused by its sensitivity to all water compartments (intra and extra cellular). A way to overcome this limitation is by combining the sensitivity to microstructure offered by diffusion MRI with the cell-specificity of MRS. Diffusion-weighted MRS (DW-MRS) offers a promising and cheaper alternative for non-invasively characterising the effects of inflammation in the brain (De Marco et al., 2022). In De Marco's study, DW-MRS was able to provide cell specific information about cellular morphology and equally, was found sensitive to systemic inflammation induced glial cytomorphological changes in grey matter. It should be re-iterated, however, that the hippocampus is an exceptionally challenging region to capture with this technique, which is inherently characterised by very poor spatial resolution.

2.7 CONCLUSION

In the review, I explained why the hippocampus is an important site of neuroinflammation and highlighted possible reasons underlying its vulnerability, which differentially affects hippocampal subfields. I also reported challenges associated to the application of hippocampal imaging of neuroinflammation using both conventional and novel imaging techniques. The review did provide confirmatory evidence that a few imaging markers that reflect neuroinflammatory tissues changes, such as DW-MRI and TSPO PET, were able to detect signal alterations in the hippocampus in prototypical neuroinflammatory conditions. However, no study as yet has examined hippocampal subfields separately.

I propose that this could be addressed by use of higher resolution acquisitions, or alternatively the adoption of particular post-processing techniques, which represent promising approaches to gain better insight into neuroinflammatory pathology in vivo, ultimately enabling more precise and sensitive characterisation of hippocampal pathophysiology.

In order to fill this gap, I evaluated the use of Image quality transfer for increasing the resolution of dMRI (chapter 3 and chapter 6), and DW MRS for improving the specificity of non-invasive MR techniques (Chapter 7).

CHAPTER 3. MRI ANALYSIS: OPTIMIZATION OF PARAMETERS FOR DIFFUSION MRI TO ENHANCE HIPPOCAMPAL SUBFIELD ANALYSIS AND SEGMENTATION.

3.1 INTRODUCTION

The hippocampus is a morphologically complex region of the brain limbic system centrally involved in important cognitive, affective and behavioural regulatory roles. It has exquisite vulnerability to neuroinflammatory processes, with some of its subregions found to be specific sites of neuroinflammatory pathology in ex-vivo studies. The study of in vivo neuroimaging correlates of hippocampal neuroinflammation would enable direct study of functional consequences of hippocampal neuroinflammatory pathology, as well as the definition of therapeutic endpoints for treatments targeting neuroinflammation, and their related affective or cognitive sequelae. However, in vivo quantitative imaging of the hippocampus and its subregions is fraught with difficulties, due to methodological challenges deriving from its unique anatomical characteristics. Relevant post-acquisition and processing of structural images, which involves delineation of substructures within the human hippocampus (by manual or automated means), and also vital for subregional analysis, could also prove extremely complicated in clinical pathology. Extensive lesional pathology in progressive MS for instance, is expected to induce limitations in the specificity of automated hippocampal segmentation methods. Most automated segmentation methods rely on either T1 or T2 weighted images. However, co-registration between these images and quantitative techniques, such as dMRI, is challenging due to the geometric distortions that characterise the latter images. The desired rigid alignment of diffusion images to high-resolution T1 weighted anatomical maps during co-registration is thus deemed suboptimal when automated segmentation techniques are employed. Further, partial volume effects arising from the neuro-anatomical location and the subregional inhomogeneity of the hippocampal interior, as well as the limited spatial resolution applicable to diffusion weighted images in general, invariably contribute to analytical restrictions and also introduces deviations in diffusion tensor measurements due to partial volume effects (Ma & Peng, 2021).

Indeed, till date, there are only brief descriptions of hippocampal subregional segmentation procedures in existing literature (Dalton et al., 2017) and fewer studies have focused on the characterisation of the MRI neuroimaging signatures of highly physio- pathologically relevant subfields of the hippocampus (CA1, CA2/CA3, CA4-DG and SLRM). Recent research advances have been centred around the development of image acquisition techniques where spatial resolution is enhanced with a bid to creating subregional specific masks, facilitating more comprehensive hippocampal subfield analysis (DeKraker et al., 2021; Ekstrom et al., 2009; Pan et al., 2022; Winterburn et al., 2013). However, such approaches are inherently SNR limited leading to a trade-off between resolution and the amount of diffusion weighting applied.

I evaluated a different approach, which relies on resolution enhancement of previously acquired data. The advantage of this approach is that it retains the original SNR. This novel imaging analysis approach, called Image Quality Transfer, or IQT (Alexander et al., 2017), enhances spatial resolution of images obtained with standard MRI acquisitions, and enables pathological characterisation of different hippocampal subfields, by deducing region specific quantitative parameters.

IQT operations avoid the challenges resulting from spatial resolution, lengthy acquisition protocols, slow translation, interpolation and complex processing pipelines. IQT technique learns clinically low-quality mappings to experimental high-quality images applying the likeness of images across scales, modalities, regions and subjects (Alexander et al., 2017). In terms of microstructural imaging relevant in anatomically identifying, delineating and segmenting minute patho-physiologically relevant hippocampal formation and subfields, IQT has the potential in enhancing the spatial resolution of dMRI data (Alexander et al., 2017).

With the avoidance of artefacts comprising hot-spots and blurring, and the reduction of partial volume effects, finer details are recovered which were lost at low resolution, hence, allowing for easier identification of hippocampal architecture including morphology, digitations, landmarks, boarders and separation of sub regional layers. Zooming into desired region (Medial temporal region- MTL for instance) on diffusion maps, with adequate software, does not obscure desired structures and allows for adequate manual segmentation with subsequent computation of desirable diffusion parameters. The need for co-registration to anatomical or histological images is hence diminished.

The original implementation of IQT is available at https://github.com/ucl-mig/iqt. This version does not include the MAPMRI fit (it is limited to the resolution enhancement of parametric DTI images), and for the purpose of this thesis, I used a modified version, kindly provided by Dr Matteo Figini from UCL (University College London). The software is implemented in Matlab, and uses random forests, a machine learning regression technique. IQT is made up of 2 stages: training and application. For the purpose of this thesis, I used the random forest models that were trained for the original IQT paper (Alexander et al., 2017), where more details about the technique can be found.
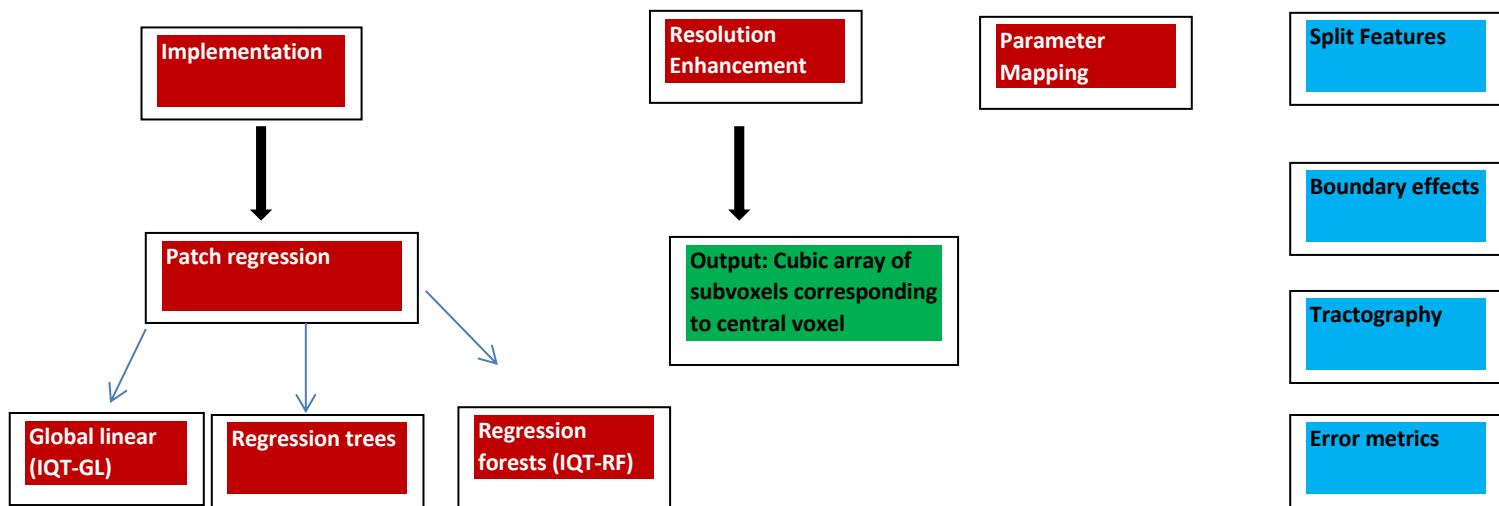
Figure 3. 1 Summary IQT methods grid (Alexander et al., 2017)

3.2 AIMS AND OBJECTIVES

The aims of this proof-of-concept study were 1) to apply IQT to increase the spatial resolution of the diffusion-weighted data of healthy controls; 2) to derive DTI and NODDI maps from the resulting high-resolution diffusion data; 3) to manually segment the high-resolution average diffusion weighted data obtained at b=1000 smm^{-2}; 4) to estimate DTI and NODDI parameters from selected hippocampal subfields. With the application of self-guided manually segmented, Diffusion weighted and NODDI maps created from data obtained from the Human Connectome Project (HCP), I attempted to directly obtain diffusion MRI-based quantitative imaging parameters (MD, FA, ODI, ISOVF, ICVF), indicative of microstructural

characteristics of major hippocampal subfields (CA1, CA2/CA3, SLRM and DG-CA4). The ultimate goal/ hypothesis behind the project was to enable and apply the use of more precise quantitative measurements for hippocampal micro-structural alterations (as expected in MS) which will reveal aspects of neuroinflammatory pathology that are not measurable with traditional MRI techniques.

Primary Objective

- To test for differences in diffusion parameters between selected hippocampal subfields

Secondary Objective

- To test whether the above diffusion parameters differ between age groups and correlate with hippocampal global and subfield volumes.

Endpoints (primary outcome measures)

- To obtain diffusion (DTI and NODDI-based) parameters within each of the selected hippocampal subfields, per hippocampus (left and right), per subject.

3.3 METHODS

3.3.1 Human Connectome Project Data (HCP Data)

We used images from the public HCP data (updated April 2018), exploring subjects with the 3T MRI session obtainable from the WU-Minn HCP Data section. For the purpose of this study, I selected and downloaded 11 imaging datasets based on age variability in the following ranges (26-30, 31-35 and 36+). 6 females and 5 males. Each data set is composed

of 3 shells of diffusion weighted images: 18 with b=0, and 270 split into 3 sets of 90 directions, each with a nominal b value of 1000, 2000, and 3000 smm^{-2}. Each volume is acquired twice with reversed phase encoding direction. The original resolution is 1.25 mm isotropic. More details on the acquisition can be found in (Sotiropoulos et al., 2013).

The images had been already pre-processed using tools from the FMRIB Software Library (FSL) to compensate for susceptibility-induced distortions (using TopUp) and for eddy-currents and involuntary motion (eddy).

The super-resolution algorithm was employed to double the resolution (i.e. to obtain images with a voxel size of 0.625 mm isotropic). See figure 3.4 for a schematic representation. As described in the thesis introduction, this was obtained by fitting MAPMRI (Özarslan et al., 2013) up to order 4 to the full dMRI dataset using linear least square. This yielded 22 coefficient maps. IQT applies the mapping learned during the training to produce high resolution versions of the coefficient maps. The corresponding synthetic DWIs (according to the same acquisition protocol as the original images, but with double resolution) are computed as described in the paper by Ozarslan et al., 2013.

The resulting images were then processed as follows. First, I computed the directionally averaged b=1000 smm^{-2}. These images provide a good contrast between anatomical structures and were used as a reference for manual segmentation of the hippocampus. Second, I fit both DTI (using the tool dtifit from FSL) and NODDI (using the linear implementation provided with Accelerated Microstructure Imaging via Convex Optimization (AMICO), available from https://github.com/daducci/AMICO) to the data, to yield high resolution maps of MD, FA, AD, RD and kurtosis, as well as of NDI, fISO and ODI.

The latest version of ITK-SNAP (version 3.8.0) was employed for image viewing, contrast adjustments, manual segmentation and obtaining quantitative estimates. Segmentation protocol was adapted from Dalton et al; 2017.

One-way Anova analysis was used to compare average diffusion parameters amongst subfields. Post hoc testing using Tukeys was also utilised when main effects were found. Means and standard deviation were reported and interpreted for the Anova analysis (see table 6). To ensure accuracy of manual segmentation processes, the same segmentation technique was carried out separately by myself and another individual with good knowledge of hippocampal neuroanatomy and having both individually thoroughly studied the adapted

segmentation manual. An approximately 90% degree of agreement based on the volumes obtained from the right and left hippocampal subregions was achieved using a joint probability agreement measure of inter-rater reliability. We were both able to agree on the reliability of 80 volumetric parameters, out of 88, after completing segmentation.

3.4 SUMMARY OF STEPS

I summarise here the steps of analysis

A. Data Acquisition

I randomly selected DWI images from the Public connectome data, exploring subjects with the 3T MRI session obtainable from the WU-Minn HCP Data section, Q3 release (Van Essen et al., 2013). Each data set contained 288 diffusion weighted images.

B. Diffusion Models

I obtained the Mean Apparent Propagator (MAP) MRI, which was able to capture orientational variance across multiple b-values (See Ozarslan et al., 2013); and further obtained the diffusion tensor model and the NODDI model

C. Image Reconstruction

I then applied a version of the IQT algorithm, modified to work with MAPMRI, to the data set. (See Alexander et al.,2017)

D. Hippocampal Subfield Segmentation

ITK-SNAP (version 3.8.0) [See (Yushkevich et al., 2006)] was utilized for image viewing, contrast adjustments, manual segmentation and obtaining quantitative diffusion estimates. Manual segmentation of hippocampal subfields (CA1, CA2/CA3, DG/CA4 and SLRM) was carried out following standard segmentation protocol, See (Dalton et al., 2017) , and was done directly on diffusion map (directionally averaged b = 1000 smm^{-2}). Created masks were uploaded to individual models.

3.5. STATISTICAL ANALYSIS

Using a General linear model, Multivariate Tests were performed to compare average diffusion (DTI and NODDI) parameters between subfields. To further understand group wise comparisons, post hoc tests were also conducted.

3.6 SEGMENTATION PROCESS

Before commencing segmentation, it was necessary to scroll through the image slices from acquired data set in order to identify relevant neuro- anatomical landmarks. See figures 3.6, 3.7 below. Notable important anatomical landmarks include:

- The Vestigial Hippocampal Sulcus (VHS), a band that forms a boundary between the dentate gyrus (DG) and Subiculum inferior-medially and between DG and CA inferiorly, laterally and superiorly.
- The Fimbria which forms the dorsal wall of the hippocampus and is visible as a large dark structure over the DG.
- The Lateral External Digitation (LED) whose flattening identifies the emergence of the DG.
- The Uncus (not always visible) whose apex help identify the hippocampal head.

3.7 RESULTS

Selection of appropriate Image

Fig. 3.2 C demonstrates the selected mean b=1000 image (averaged across multiple directions) employed for manual hippocampal segmentation. Compared to other potential images (Fig 3.2 A, B), it provided the best compromise between signal-to-noise ratio (SNR) and contrast. Selection of the appropriate image was required before implementation of IQT.

A   **B**   **C**
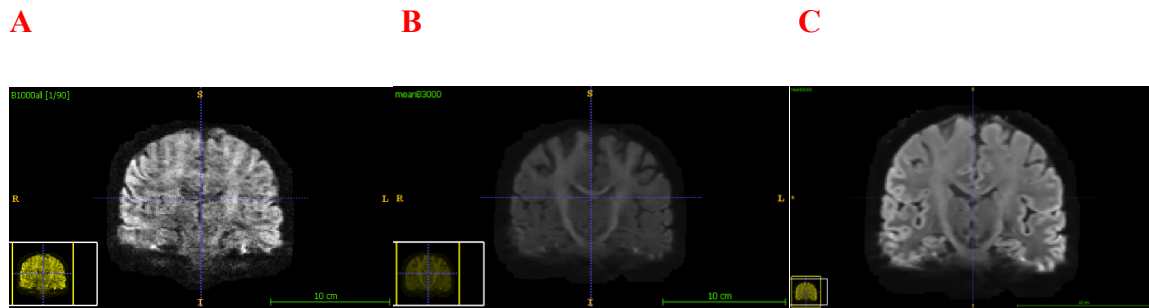
Figure 3. 2 Interpolated Images (A – original resolution b=1000 image, B – mean b=3000 image, C – mean b=1000 image after resolution enhancement)

In fig 3.2, to generate diffusion-weighted images, the strength and timing of gradients are reflected by the b-value. B-values are directly proportional to the diffusion effects, so that the higher the b-value, the stronger the diffusion effects (Burdette et al., 2001). Increasing the gradient duration, the amplitude and also expansion of the gradient pulses intervals increases the b-values (Portnoy et al., 2013). The choice of b-values is usually dependent on predicted pathology, features of anatomy and averaged signals. A single b value is sufficient for fitting models like DTI, but more shells (i.e. more b values) are needed for other models, such as NODDI. For the purpose of hippocampal segmentation, the mean b=1000 (averaged across multiple directions) is the best compromise between signal-to-noise ratio (SNR) and contrast and was therefore chosen to conduct manual and automated segmentation of the hippocampal

subfields. Fig 3.4 demenostrated in appropriate section below depicts image enhancement of resolution by IQT on selected data.

IQT implementation and Resolution enhancement

Patch regression and super resolution are demonstrated in Fig 3.3. This consists of an input and output patch. As seen in Fig 3.3, a cubic array of subvoxels (represented by the yellow patch structure) correspond to the output patch. In diffusion resolution enhancement, independent elements of diffusion tensor in the lower resolution patch (represented in green) are contained in the input vector, while the output vector contains elements of each diffusion tensor in the higher resolution patch. Higher dimensional mappings are thus achieved.
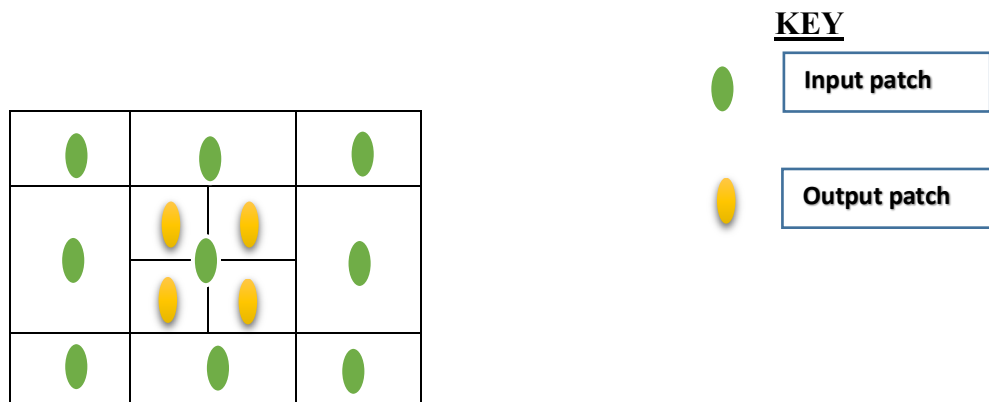
Figure 3. 3 Super resolution step of IQT

Fig 3.3 illustrates IQT resolution enhancement mapping which consists of an input and output patch. A cubic array of subvoxels (represented by the yellow patch structure) correspond to the output patch. In diffusion resolution enhancement for instance, independent elements of diffusion tensor in the lower resolution patch (represented in green) are contained in the input vector, while the output vector contains elements of each diffusion tensor in the higher resolution patch. Higher dimensional mappings are thus achieved (Alexander et al., 2017).

Fig 3.4 demenostrates image enhancement of resolution by IQT on selected data. Fig 3.4 A shows an unenhanced mean B 1000 image (1.25 mm isotropic). Fig 3.4 B shows same image

after reconstruction by IQT (0.675 mm isotropic). Same linear contrast adjustments applied to both images. Cortical areas became visually much more appreciable on Fig 3.4 B with much clearer anatomical landmarks, less blurriness and much more distinctness around both medial temporal regions, compared to the unenhanced Fig 3.4 A. Zooming into relavant region of interest (medial temporal zone) did not introduce blurring in IQT resolved image as demonstrated in Fig 3.5 B.

A   **B**
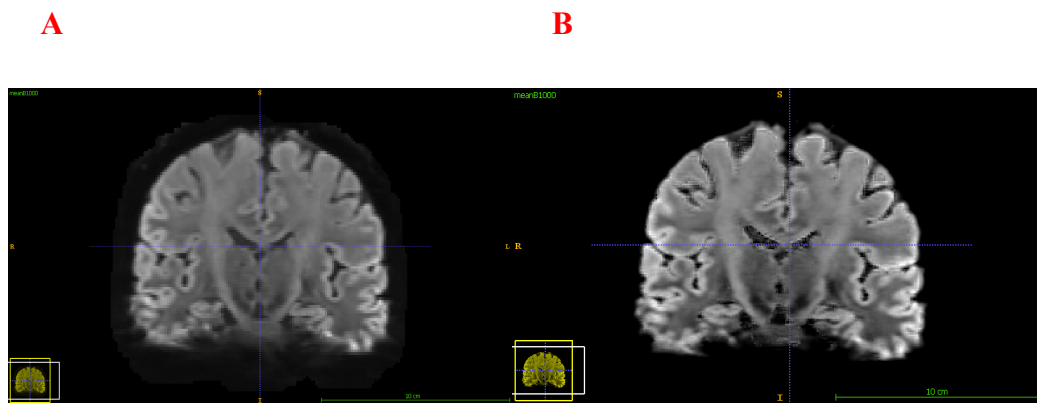
Figure 3. 4 Application of IQT to Image A (mean B 1000) enhances resolution, providing better visual perception and appreciation of anatomical landmarks essential for segmentation (Image B)

Fig 3.4 demenostrates image enhancement of resolution by IQT on selected data. Figure A shows an unenhanced mean B 1000 image (1.25 mm isotropic). Figure B shows same image after reconstruction by IQT (0.675 mm isotropic). Same linear contrast adjustments applied to both images. Cortical areas visually much more appreciable on figure B with much clearer, less blurriness and much more distinctness around both medial temporal regions, compared to unenhanced fig A (Alexander et al., 2017).

A   **B**

Figure 3. 5 Unenhanced (A) and Enhanced (B) Images showing the Hippocampus

Fig 3.5 shows closer views of both unenhanced and enhanced images. Zooming into relevant region of interest (medial temporal zone) does not introduce blurring in IQT resolved image (B) compared to unresolved image (A). Yellow arrows indicating hippocampal location.

Subfield Segmentation

Thanks to the enhanced resolution, I was able to perform the manual segmentation following the protocol suggested by Dalton et al (2017). An example is shown in Fig 3.6 below.

As demonstrated in Fig 3.6, contrast intensity and geometric applications was applied to the coronal planes of the images, with the sagittal plane used as guides and also for validation (bottom figures from left to right). Available figures on (http://ww.fil.ion.ucl.ac.uk/Maguire/Dalton_Maguire_BNA_Figures_1-29.pdf) were utilized as tools for troubleshooting (top figures, left to right). DG/CA4 were the first masks to be created following (Dalton et al., 2017). Delineation of subsequent masks was dependent on the DG/CA4 mask. Process of segmentation was initiated when the DG was seen to clearly fill the centre of the hippocampal lateral section, at the most anterior point. The VHS represented by the dark line in (Fig 3.6), surrounds the DG in an inverted 'C' like shape (Dalton et al., 2017).
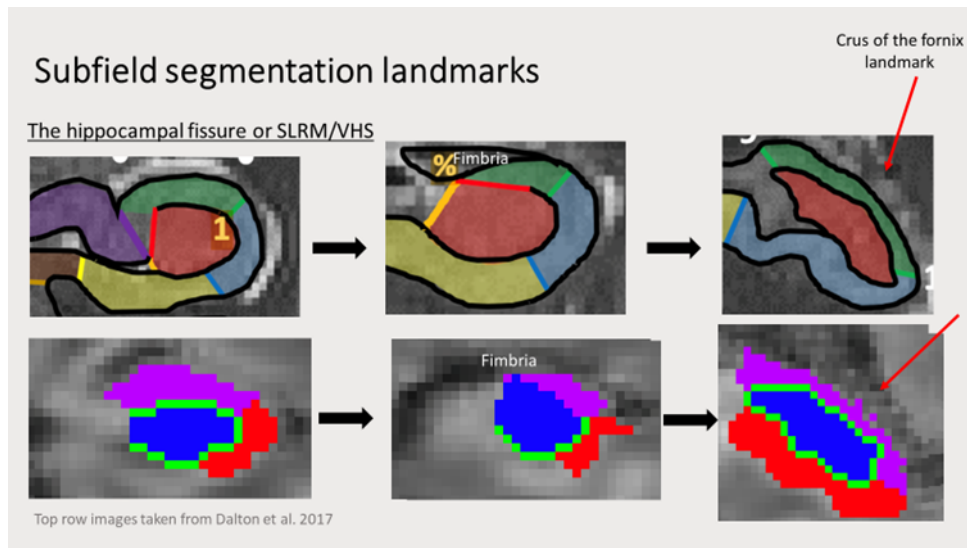
Figure 3. 6 Subfield Segmentation. Top row indicating subfield segmentation landmarks (Dalton et al., 2017). Bottom row indicating equivalent visible landmarks during manual segmentation, using ITK-SNAP software.

As illustrated in fig 3.6, to deduce approximate boundary locations of the hippocampal subfields, the knowledge of important neuro-anatomical landmarks was utilized. Contrast intensity and geometric applications was applied to the coronal planes of the images, with the sagittal plane used as guides and also for validation (bottom figures from left to right).

Available figures on (http://ww.fil.ion.ucl.ac.uk/Maguire/Dalton_Maguire_BNA_Figures_1-29.pdf) were utilized as tools for troubleshooting (top figures, left to right). DG/CA4 were the first masks to be created following (Dalton et al., 2017). Delineation of subsequent masks was dependent on the DG/CA4 mask. Process of segmentation begins when the DG is seen to clearly fill the centre of the hippocampal lateral section, at the most anterior point. The VHS represented by the dark line in (figure 3.6- 1), surrounds the DG in an inverted 'C' like shape. (Dalton et al., 2017).

Quantitative Computation of Subfield volumes and Diffusion Indices.

Complete segmentation of left and right hippocampal subfields is demonstrated in Fig 3.7, after IQT reconstruction and image resolution enhancement. Volumes of each subfield were derived, and diffusion indices computed automatically by the ITK-snap software.

Fig 3.7 below shows the images from a representative participant.
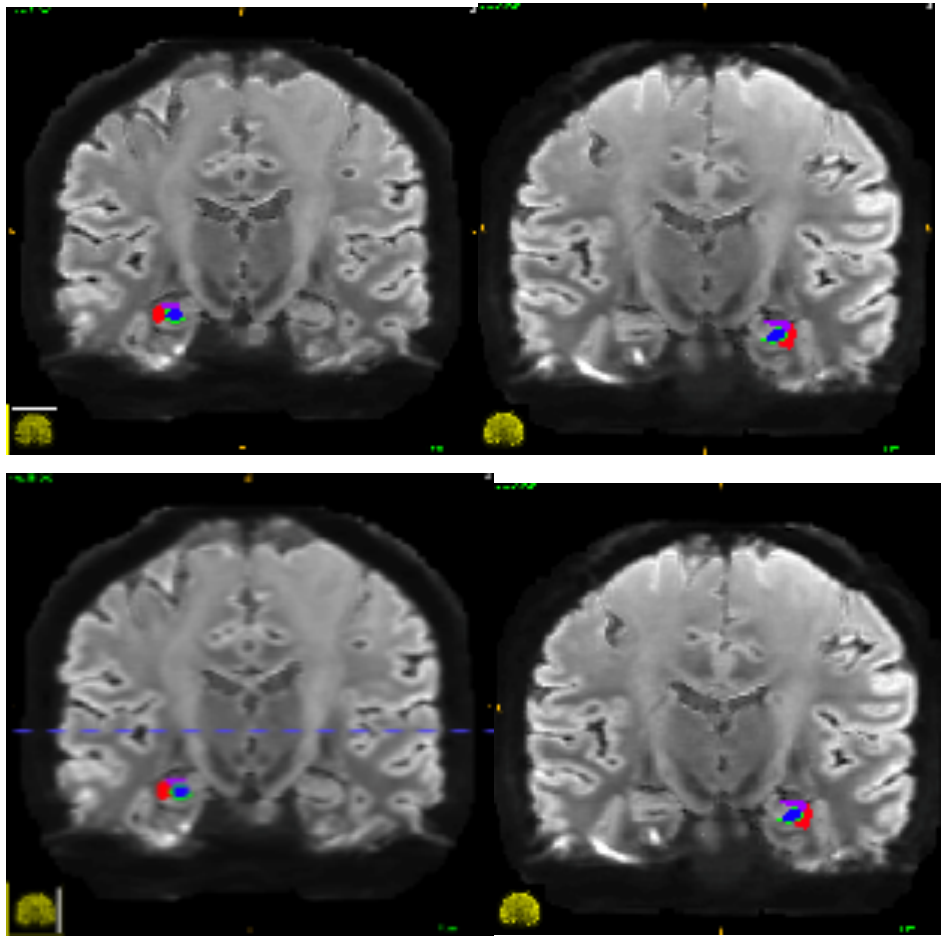
Figure 3. 7 Segmented diffusion maps (Left and right hippocampal locations)

In fig 3.7 complete segmentation of left and right hippocampal subfields is demonstrated after IQT reconstruction and image resolution enhancement. Volumes of each subfield were derived and diffusion indices computed by the ITK-snap software.

In order to ensure a reliable segmentation, I evaluated the average volume of each hippocampal subfield, and compared them against existing literature (Zheng et al., 2018). Fig 3.8 and Table 5 below summarises the results of this analysis.
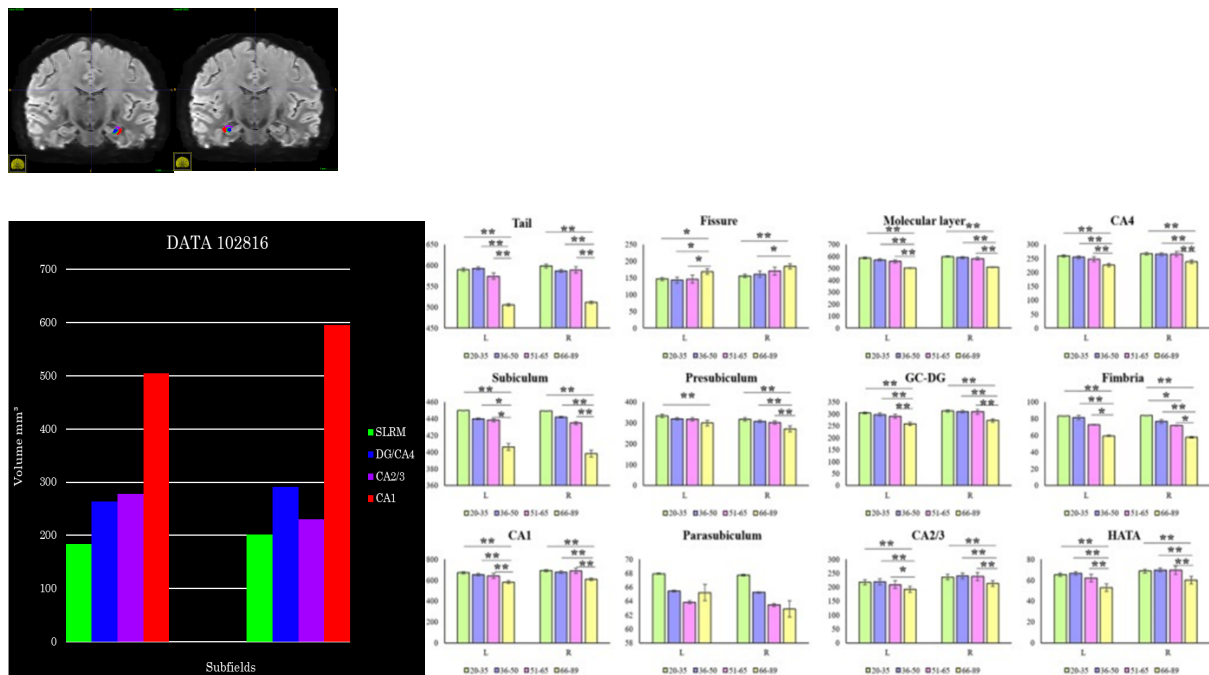
Figure 3. 8 Comparing deduced subfield volumes with available data from literature (Zheng et al., 2018)

In fig 3.8, range of volumes obtained in the left CA1 and left DG/CA4 was between 412 and 621 mm[3] and 289-503mm[3] respectively. CA1 volumes deduced after manual segmentation were similar to what is available in literature when compared (Zheng et al., 2018). See Table 5 below for complete table of volumes and tables 6 and 7 for means and standard deviation.

S/N	Age (Years)	Left CA1 Volume (mm³)	Left CA2/3 Volume (mm³)	Left DG/CA4 Volume (mm³)	Left SLRM Volume (mm³)	Right CA1 Volume (mm³)	Right CA2/3 Volume (mm³)	Right DG/CA4 Volume (mm³)	Right SLRM Volume (mm³)
1	26-30	446	337	503	187	563	464	569	209
2	31-35	552	383	411	212	668	335	411	237
3	26-30	505	278	263	184	596	230	291	201
4	31-35	399	355	491	200	436	352	587	217
5	26-30	621	323	454	264	709	387	495	249
6	31-35	502	374	475	225	564	381	487	244
7	26-30	562	322	482	237	694	417	459	219
8	31-35	542	541	476	191	563	456	471	196
9	26-30	493	249	453	211	641	345	397	221
10	36-	452	283	298	212	522	298	359	234
11	36-	412	234	289	169	483	377	367	195

Table 5: Age distribution of the data and volumes derived from the left and right subfields of the Hippocampus.

	FA		ICVF		ODI	
	Mean	SD	Mean	SD	Mean	SD
SUBFIELDS						
CA1	0.093	0.00783	0.3951	0.02035	0.5283	0.08001
CA2/CA3	0.115	0.1445	0.4365	0.02089	0.4147	0.0603
DG/CA4	0.09	0.00871	0.3648	0.01982	0.498	0.2799
SLRM	0.076	0.00702	0.3964	0.02712	0.5387	0.0301
AVERAGE		0.042015		0.022045		0.112578

Table 6: Averaged mean of FA, ICVF and ODI with standard deviations

Measure	subfields	Mean	Std. Error	95% Confidence Interval	
				Lower Bound	Upper Bound
FA	CA1	0.092	0.002	0.086	0.097
	SLRM	0.076	0.002	0.071	0.082
	CA2/CA3	0.115	0.005	0.103	0.127
	DG/CA4	0.090	0.003	0.083	0.097
ODI	CA1	0.531	0.006	0.517	0.544
	CA2/CA3	0.412	0.022	0.362	0.462
	SLRM	0.543	0.010	0.520	0.566
	DG/CA4	0.498	0.010	0.475	0.521
ICVF	CA1	0.395	0.007	0.378	0.412
	CA2/CA3	0.433	0.007	0.417	0.449
	SLRM	0.396	0.010	0.374	0.418
	DG/CA4	0.363	0.007	0.347	0.379

Table 7: Estimated Marginal Means, Standard error and Confidence intervals.

NODDI and DTI fit

Fitting DTI and NODDI applications provided high resolution maps of MD, FA, ODI, ICVF, ISOVF (demonstrated in Fig 3.9, 3.10, 3.11), and again, with ITK-snap applications, representative diffusion parameters were derived from these maps. Fig 3.12 demonstrates the distribution of the indices across subfields.

NODDI was fit using the linear implementation provided with Accelerated Microstructure Imaging via Convex Optimization (AMICO). Accuracy and precision were achieved with this framework, and times in obtaining maps were also accelerated (Daducci et al., 2015)

DTI maps (FA and MD) were derived using the FSL routine dtifit. Example maps can be seen in Figs 3.9, 3.10 and 3.11. The mean and standard deviation of these parameters for each subfield, together with other statistical descriptors are summarised in Tables 6 and 7.
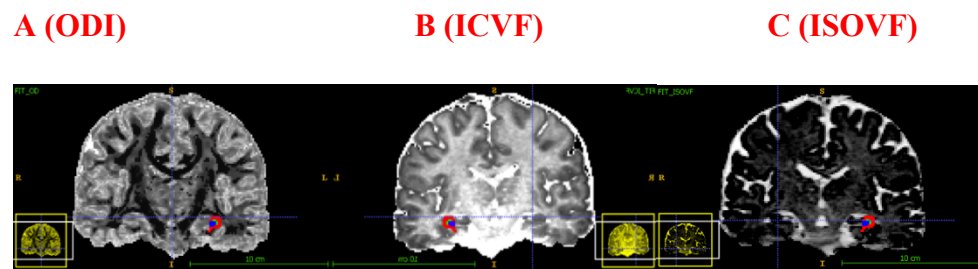
Figure 3. 9 Creation of NODDI maps using cluster computing and shell scripts: NODDI FIT (A- orientation dispersion index, B-Intracellular volume fraction and C-Isotropic volume fraction)
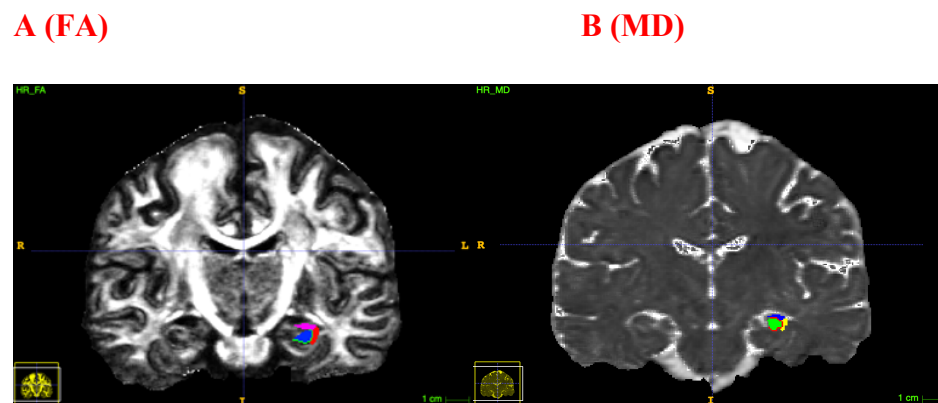
Figure 3. 10 Fractional anisotropy (FA) and Mean diffusivity (MD) maps
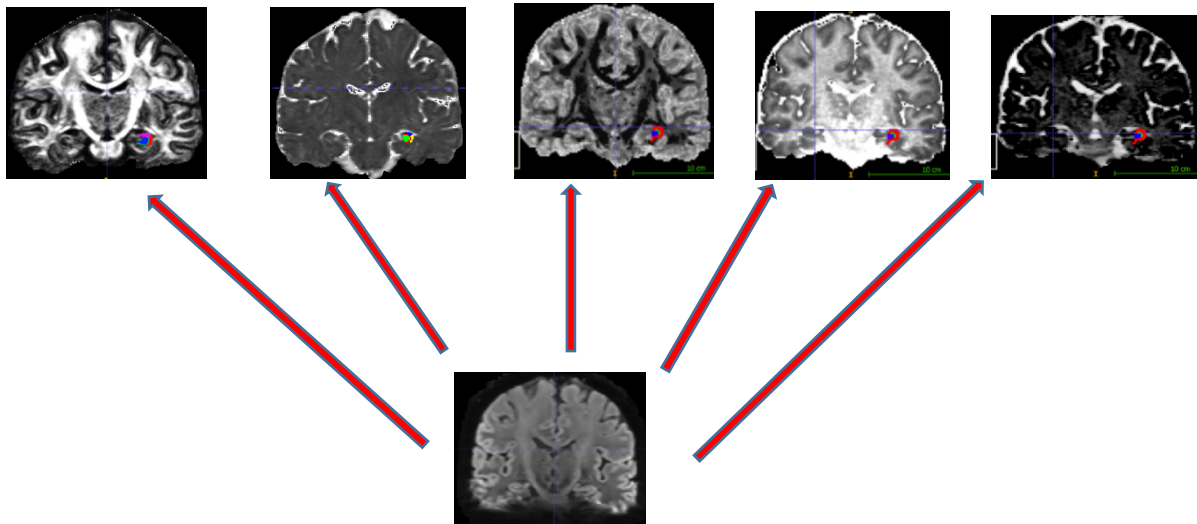
Figure 3. 11 Diffusion Images. Illustrates the derived diffusion models. Beneath the (MAP) MRI, and above from left to right (FA, MD, ODI, ICVF, ISOVF).

Outcomes

Outcomes depicted that there were significant differences for FA within 3 subfields ($p<0.01$), except SLRM which was not significant ($P=0.63$). There were also significant differences in MD parameters mostly in the DG/CA4 subfields ($p<0.05$). Similarly, for the NODDI parameters, there were significant differences in all subfields ($p<0.01$, for CA1, CA2/CA3 and DG/CA4; $p<0.05$ for SLRM), and main differences noted for ICVF in the SLRM subfield ($p<0.01$).

The median indices across subregions appeared to differ for each diffusion parameter, more so with some parameters than others. For instance, there were distinct differences in ODI, and MD compared to ICVF and FA. Medians were slightly similar in the later (See figures 3.12 and 3.13 below). Additionally, there was more variability in the diffusion indices obtained across the CA2/CA3 subfields compared to the indices from other subfield groups.
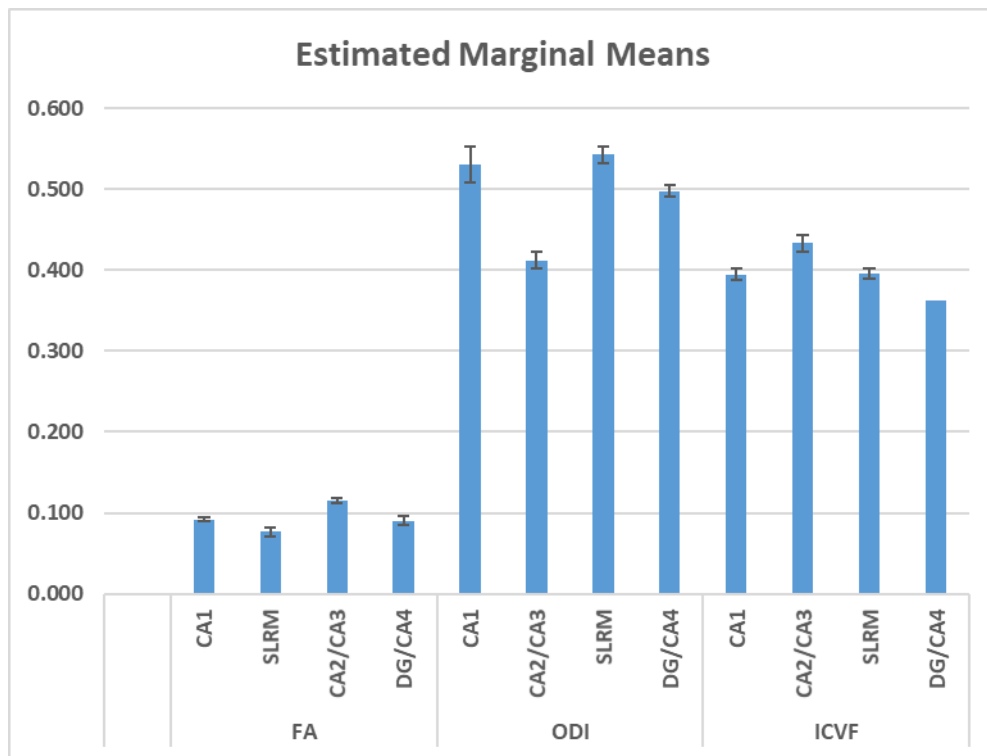
Figure 3. 12 Cluster representation of estimated marginal means. Error bars represent standard errors.
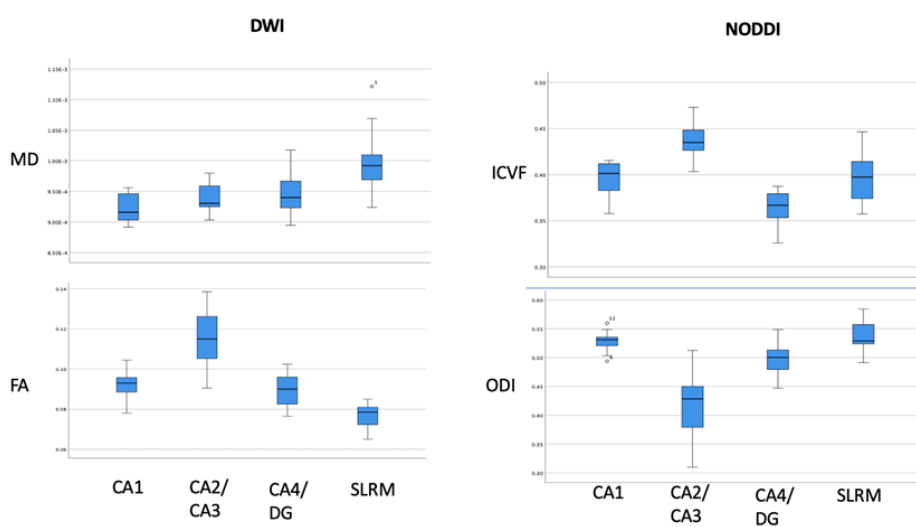
Figure 3. 13 Box and Whiskers plot showing significant differences in DWI and NODDI parameters (FA, MD, ODI and ICVF) in the selected four individual subfields (CA1,

CA2/CA3, CA4/DG, SLRM). FA (CA1, CA2/CA3, CA4/DG, $p < 0.01$), MD (CA4/DG, $p < 0.05$), ODI (CA1, CA2/CA3, CA4/DG, $p < 0.01$), ODI (SLRM $p < 0.05$), ICVF (SLRM, $p < 0.01$).

3.8 DISCUSSION

In prior chapters, there was emphasis on the importance of studying neuroimaging correlates of hippocampal neuroinflammation. I subsequently introduced IQT, an innovative post acquisition resolution enhancing algorithm which enables effective computation and deduction of hippocampal subfield diffusion parameters after methodical delineation and segmentation. Having also accentuated potential subfield vulnerabilities during pathology in the previous chapter, I set out to explore the degree of alterations in diffusion parameters (DTI and NODDI) across selected hippocampal subfields. Both classes of imaging parameters exhibited significant distinct variations across subfield groups which could either represent bio-physiological signatures, or when altered, could provide baseline reference values for measuring pathological mechanisms in disease states.

The complex and heterogenous hippocampal architecture is comprised of convoluted and interconnecting subregions which consists of the formation (CA1-CA3) and the dentate gyrus (Schultz & Engelhardt, 2014). Densely packed pyramidal cells are crammed into the CA regions, while a tightly packed smaller granular layer is sheathed around the terminal aspect of hippocampus proper. Morphologically, CA2 pyramidal neurons are identical to CA3. In terms of size, the pyramidal neurons in this region are somewhat larger but less densely packed in comparison to CA1 (Dudek et al., 2016). Experimentally and in addition, it has been observed that there is much heavier presence of axonal input spanning the CA2/CA3 regions when compared to CA1. Mean diffusivity which measures the rate of diffusion is inversely proportional to cellular membrane density, hence its possible lower scores in the CA regions in this study, particularly the densely packed CA1, with slightly increased measures as we approach the DG and SLRM, where rates of diffusion are expected to be marginally more. Across grey matter, MD values are notably regarded as similar (Winston, 2012) and diffusion is predominantly isotropic (Moseley et al., 1990). FA on the other hand examines the degree of deviation from isotropy (Pierpaoli et al., 1996) and appears to have

much larger distributions in the CA2/CA3 regions, which was observed in our data. Axons emanating from the granular cellular layer of the dentate gyrus make their way to CA3, after traversing the stratum giving rise to higher levels of directional diffusion, in essence increasing anisotropy.

The dentate gyrus which contributes to new memory formation is stratified further to contain a molecular aspect which is void of cells and comprises commissural and perforant fibres as well as dendrites from the granule layer; A polymorphic layer where CA4 is situated; and lastly the principal granular layer densely packed with granule cells. There are also a mix and variety of cellular structures; granular cell dendrites, pyramidal basket cells, polymorphic layer cells and axons from the entorhinal cortex, the presubiculum and the parasubiculum. Our data reflects a varied distribution of diffusion indices in the dentate gyrus possibly due to the heterogenous complexities and stratification as highlighted above.
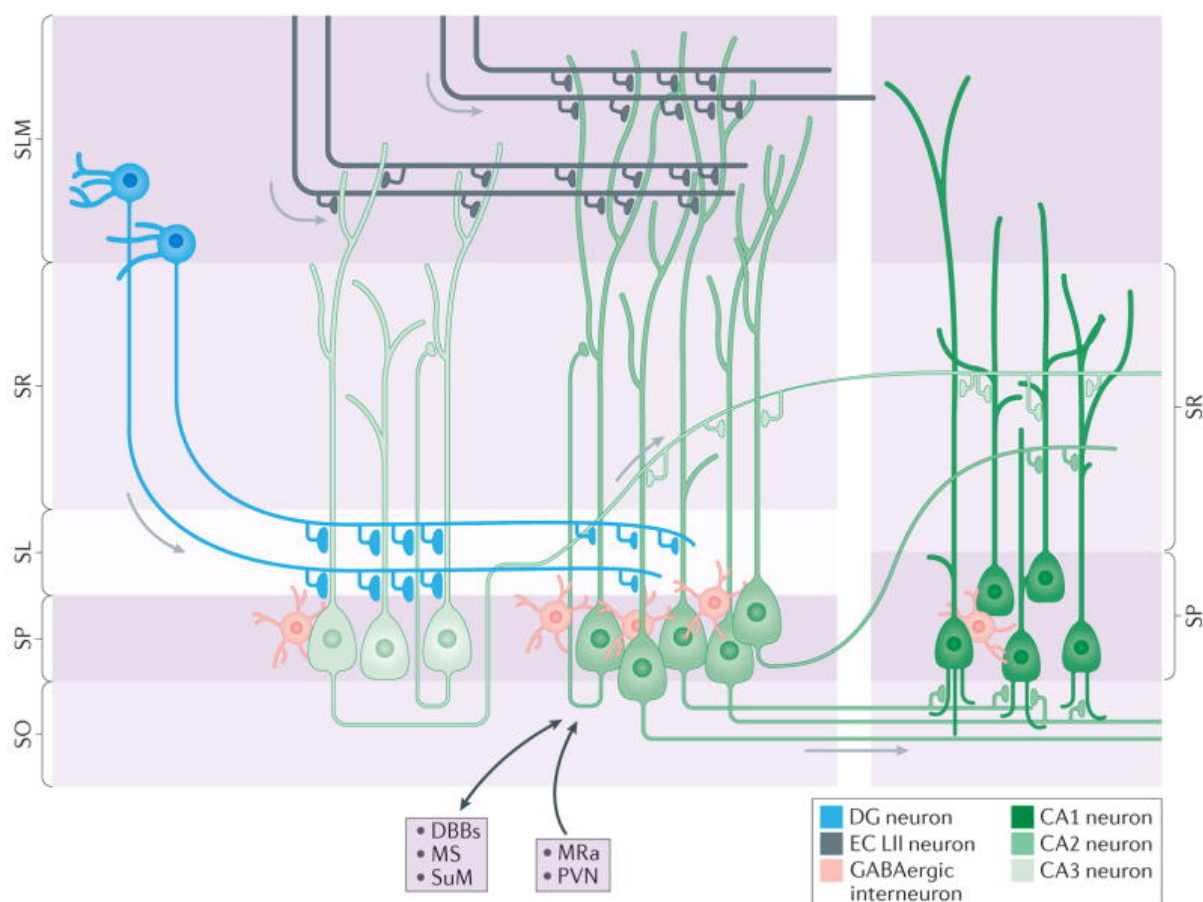
Figure 3. 14 Schematic representation of stratification and cellular characteristics of hippocampal sub-regions in rodents. **SLM (stratum lacunosom-moleculare), SR (stratum**

radiatum), SL (stratum lucidum), SO (stratum oriens), SP (stratum pyramidale) (Dudek et al., 2016).

During neuroinflammatory disease conditions such as MS, underlying tissue myeloarchictecture and cytoarchitecture disruption generally have an impact on the organization of tissue microstructure, further disintegrating intracellular organelles. Occurring in grey matter (hippocamapal interior), the diffusivity milieu of affected tissue are altered (Weston et al., 2015), potential antecedents of microscopic volumetric modifications. Interestingly, studies have reported that these modifications are not directly linked to macroscopic volume loss (Canu et al., 2010; Montal et al., 2018; Ridha et al., 2006; Ringman et al., 2007).

Several research literatures indicate measured altered DTI indices as generally reflective of microstructural disorganisation in hippocampal pathology, however, the inhomogeneity of the hippocampal interion, the gaussian assumption of DTI and the expected contamination of voxels by partial volume effects imply deficiencies in DTI to effectively capture grey matter heterogeneity (Gong et al., 2014; Henf et al., 2018; Nazeri et al., 2015; Parker et al., 2018). Hence, the NODDI multi-compartment model is speculated to possess greater sensitivity in the grey matter (Venkatesh et al., 2020). The neurite density index or intracellular volume fraction (ICVF) measures restricted diffusion and is generally associated with axons and dendrites in the intracellular space. Our data shows similar distribution to FA in subfields CA1 and CA2/CA3, but inverse distribution across DG and SLRM. This is possibly due to stratification complexities in the later regions. Another compartment, orientation dispersion index (ODI) measures hindered diffusion and looks at the influence of neurite dispersion on water diffusivity (Yi et al., 2019). ODI covers the extracellular space and is associated with cell bodies and glial cells. According to our findings, distributions in these regions have higher values in CA1, DG and SLRM and a wider variability in CA2/CA3. ODI are reported to be sensitive to microglial density and cellular activation changes in neuroinflammatory disease states (Yi et al., 2019). Experimental studies in MS (Crombe et al., 2018) gave more credence to DTI measures in terms of sensitivity to microstructural alterations.

Regarding MS, where there is cellular damage and less boundaries to the flow of water protons, MD measures tend to rise, with measured increases more profound on disease

progression, and FA measurements tend to fall (ElSayed et al., 2019; Razek et al., 2018; Sbardella, Tona, et al., 2013; Testaverde et al., 2012).

Possible limitations to this preliminary research stemmed from failure to also manipulate the dependents of voxel size which include slice thickness, the matrix elements, and the field of view (FOV) which was limited. IQT acts on post-acquisition maps, so limitations due to types of instruments, signal to noise ratios and considerations for relaxation times do not apply. Accuracy of manual segmentation was also contentious. This was carried out by two individuals with a thorough understanding of the neuroanatomy and intense study of segmentation manual (Dalton et al.,2017), in a bid to promote inter-rater reliability.

3.9 ENHANCED AUTOMATED VS MANUAL SEGMENTATION

The manual segmentation process employed after utilization of the IQT protocol, though effective in delineating the required subfields, was slow and labour-intensive, and required approximately 5-6 months to segment 11 HCP data by one rater. Clinically, this might be untenable. Consequently, it became critical to explore automated hippocampal segmentation techniques that can accurately delineate hippocampal subfields, especially considering more clinical scenarios and with respect to large data sets, while requiring minimal human operator input to quality check (as utilized in chapter 6). Faster semi-automated hippocampal segmentation methods have been reported to be commensurate with labour intensive manual segmentation methods (Hurtz et al., 2019). Hence, I carried out an initial proof of concept study comparing (descriptively) segmented HCP data (n=8) to randomly selected healthy volunteer cohort from the segmented Prisma data (n=8). Further employing single measure intraclass correlation statistics (smICC) (Koo & Li, 2016); I sought to also compare segmentation outputs based on anticipated neuroinflammatory and pathological imaging sensitivity and regional significance. I used CA1 segmentation volumes and diffusivity parameter values obtained from both selected manually segmented HCP data and automatically segmented Prisma data in the calculations.

Results are presented below;

	Prisma_Vol	HCP_Vol
Mean	689	516.13
Std. Deviation	112.76	69.71
Minimum	530.86	399
Maximum	910.05	621

Table 8: Table of mean and standard deviation. PRISMA_VOL- segmentation volumes from Prisma data, HCP_VOL- segmentation volumes from HCP data.
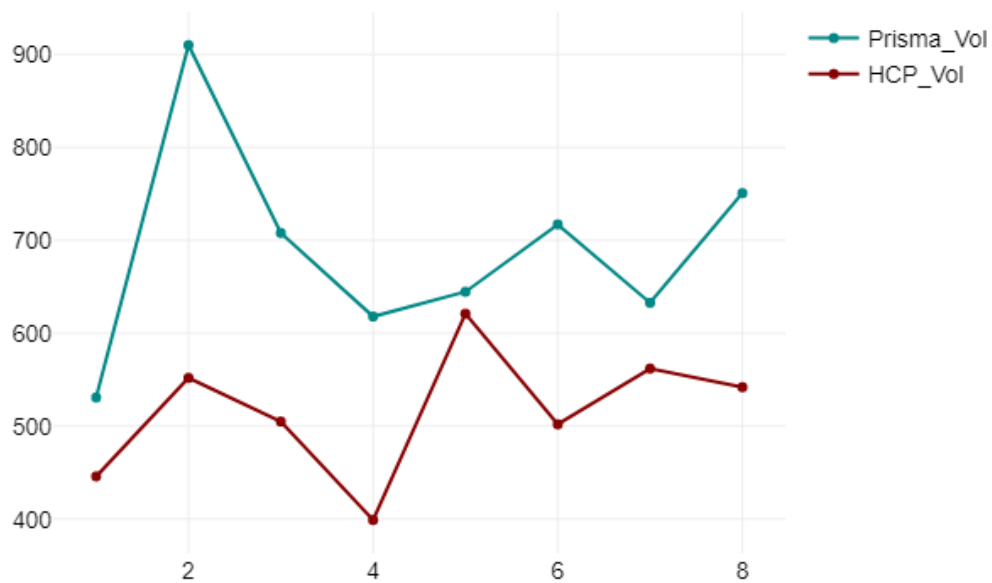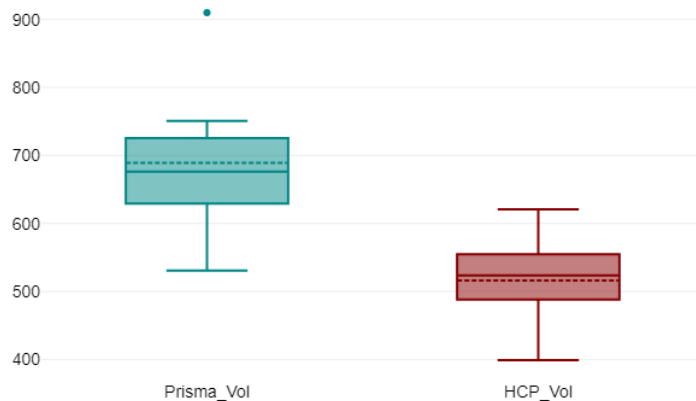
Figure 3. 15 Line chart above, and box plot below comparing manually segmented HCP volume data to automatically segmented Prisma data. PRISMA_VOL- segmentation volumes from Prisma data, HCP_VOL- segmentation volumes from HCP data.

The volumes from the automatically segmented data are more in keeping with sizes (around 600-700 mm^3 Left hippocampal CA1) from standard literature (Zheng et al., 2018), which informed it's use in later chapters. There was no agreement between segmentation outputs of the manual and automated comparisons using smICC. [smICC = 0.21 (95% CI -0 - 0.04)], indicating differences in the segmentation outcomes from both techniques.

Segmentation on unenhanced data was unachievable as I was unable to visually locate important neuro-anatomical landmarks necessary for hippocampal segmentation due to lower resolution.

3.10 CONCLUSION

Compared to conventional MRI methods, dMRI is able to employ measurements of diffusion indices to investigate concealed damage to tissue in MS patients. These indices are found to be somewhat sensitive, pertinent, and additionally are found to be correlated to progression and clinical status. An evaluation of tissue damage remote from conventional MRI visible lesional activity which can occur in the different phases of MS pathophysiology (and seen as

damage to normal appearing brain tissue or indeed, early grey matter involvement) is plausible with the quantification of DTI indices. Common approximations include fractional anisotropy (FA) and mean diffusivity (MD). Post-mortem studies looking at patients with chronic lesions and progressive MS indicate stronger correlations of FA and MD with myelin content compared to fibrillary gliosis and axonal count (Cercignani et al., 2003). NODDI is proposed to provide more practical measures in vivo and focuses on the microstructural estimations of dendrite and axon complexities (Zhang et al., 2012). NODDI employs a compartmental tissue model and a protocol that optimizes acquisition times, making the technique more adaptable for clinical use. Neurite indices such as the orientation dispersion index (ODI) and the Intracellular volume fraction (ICVF) have been reported to relate more directly to brain tissue microstructure, and when compared to standard DTI indices, are expected to provide more specific biomarkers to this effect. However, experimental models with EAE induced mice indicate superior sensitivity of the DTI indices in detecting microstructural alterations within hippocampal subfields (Crombe et al., 2018).

Image Quality Transfer (IQT) was used to enhance spatial resolution in a small HCP-derived dataset of controls (n=11), followed by manual hippocampal subfields segmentation. I observed that hippocampal subfields differed in terms of DWI and NODDI parameters distribution. It is possible that the inter-subject's variability for some of the parameters, gets smaller when looking at subfields independently, compared to whole hippocampus observations, and this might increase our sensitivity to detect changes. Considering that in other similar studies, MD and FA changes have been repeatedly observed in the whole MS hippocampus and speculating on the idea that specific subfields have differential sensitivity to neuroinflammatory damage, assessment of diffusion parameters after enhancement of spatial resolution and subfield segmentation might result in more precise characterisation of microstructural changes resulting from MS pathology.

CHAPTER 4. MS STUDY: GENERAL METHODS

In the previous chapter, I applied an imaging pipeline that enhanced spatial resolution and enabled assessment of microstructure-related DTI parameters individually across subfields. In the studies presented in the rest of my thesis, I will show clinical application of this imaging pipeline in the MS patient population. Here in Chapter 4, I will present details on the clinical protocol, specifically on design of the study protocol for recruitment of study subjects, study procedures, clinical characterisation of patients and selection of rating scales and questionnaires.

4.1 DESIGN OF THE STUDY

The study took an open label approach, with observational and longitudinal aspects to study healthy volunteers and patients with relapsing-remitting multiple sclerosis (RRMS) and primary progressive multiple sclerosis (PPMS).

This study consists of a between subject cross-sectional study design. Clinical and imaging parameters will be compared between MS patients and recruited healthy controls, and between the RRMS vs PPMS phenotypes. I will also explore whether the imaging parameters are associated with the presence of depression or cognitive dysfunction in the cohort of MS recruited patients.

4.2 STUDY SUBJECTS

4.2.1 Healthy Volunteers

Healthy volunteers were recruited from the local area using advertisements (online, including social media, and paper). It was incumbent upon those people interested in taking part to contact the study team. Participants were also recruited from the pool of students at

Universities of Sussex and Brighton. People who had previously indicated that they would be interested in participating in such studies were also contacted. Potential participants were contacted by phone, email or letter. After participants were sent or emailed the Patient Information Sheet, they were given as long as needed to decide if they wished to participate. Similar to patients with MS, healthy participants were also approached by a member of the study team for a phone pre-screening interview to assess eligibility criteria. The original sample size was expected to be 30 subjects in each group (MS patients and healthy volunteers respectively), however, due to the pandemic I was unable to complete recruitment.

For healthy volunteers, exclusion criteria included any medical, neurological, or psychiatric illness at screening or any concomitant pharmacological treatments. All structural MRI images were inspected for unexpected findings of potential clinical significance or features that might confound quantitative analysis by an experienced imaging physicist.

4.2.2 Participants with MS

Participants with MS were identified from the practices of consultant neurologists (Hurstwood park- University hospital Sussex NHS Trust, East Sussex health NHS Trust, Department of Neurology- Royal Sussex County hospital) and also MS peer support groups (MS Society, Eastbourne and South Wealden group, Hastings and Rother group, Uckfield, Heatfield and Lewes group). Some participants were also identified via MS Society organised interview blog and relevant twitter feeds.

All patients either had RRMS or PPMS based on neurological history, diagnosis and previous evaluations.

Participants were selected amongst those who were waiting to start a "higher impact" Disease modifying treatment (DMT) prescribed by their neurologists. In essence, drug naïve patients who were about to start any of the higher impact treatments. For "higher impact" DMT, we selected the treatments listed in the MS society website as having "High" or "Good" impact on MS, and included any of; alemtuzumab, natalizumab, ocrelizumab, cladribine, dimethyl fumarate and fingolimod.

Participants expressing interest in taking part were given a detailed patient information sheet (PIS) and were asked to contact (either by email or phone) a member of the study team. After

contact by study participants, I ran a pre-screening interview to assess eligibility criteria, using the pre-screening questionnaire which also addressed any questions on the PIS. If the participant was willing to take part, a screening visit to the Clinical Imaging Sciences Centre (CISC) was either organised or screening was conducted remotely via video call. During the pre-screening interview, participants were also screened for the likely presence of depression using the Emotional Thermometer (A. G. B. Thompson et al., 2019).

4.3 ELIGIBILITY CRITERIA

All participants were pre-screened over the telephone and fully screened either partially by remote video consultation or in person to check eligibility and requirements of criteria.

The study took place at the Clinical Imaging Sciences Centre, Knightsgate road, Falmer campus, University of Sussex, Brighton, East Sussex. All recruited participants underwent Diffusion weighted MRI and Diffusion weighted MRS in one session.

For MS participants, Disability had been pre-assessed by the patients treating Consultant Neurologist using the EDSS; and baseline cognition, mood, sleep and fatigue were also measured with appropriate scales prior to scanning.

The study was approved by the London-Camberwell St Giles Research Ethics Committee (Ref no: 20/LO/1303) and the Health Research Authority and Health and care Research, Wales (HCRW).

 All participants gave written informed consent and those requiring, were given financial compensation for the time spent in participation in the study.

I ensured that the study did not affect any clinical care that the participant may have been receiving. DMTs were prescribed by neurologist independent of participation in the research. Our study did not investigate a novel clinical intervention and did not involve randomisation between treatment groups. Participation in the study did not affect any aspect of existing clinical care for patients.

4.3.1 Inclusion criteria for all subjects

• Participants have the capacity to consent and have given their informed consent before any trial-related activity

• Participants are able to understand verbal and written information given in English.

• Age between 18 and 80 years inclusive

• No contraindications for MRI scanning requirements

• Not being pregnant or breastfeeding

 MS participants were eligible for inclusion into the study, if all of the following criteria applied:

• Male or Female, aged 18-80 at the time of signing informed consent

• Clinical or clinical and laboratory supported diagnosis of multiple sclerosis, with the following characteristics:

• Relapsing remitting or Primary progressive MS

• EDSS score up to and including 5.5 and below at screening evaluation

• If they were currently waiting to start a DMT's prescribed by responsible Neurologist

 • Able to stand unaided and transfer themselves onto the scanning table.

• Able to read, comprehend and record information written in English.

• Capable of giving written informed consent, which includes compliance with the requirements listed in the consent form.

4.3.2 Exclusion criteria for all subjects:

Participants were deemed ineligible for inclusion into the study if any of the following criteria applied:

• If female, positive urine pregnancy test

• History or presence of a neurological diagnosis (not limited to but including for example, stroke, epilepsy, space occupying lesions, Parkinson's disease, vascular dementia, transient ischemic attack) other than MS that may influence the outcome or analysis of the scan results.

• Currently being treated with one of DMTs for MS

• Any subject the investigator deemed unsuitable for the study (e.g., due to either medical reasons, laboratory abnormalities or subject's unwillingness to comply with all study-related procedures).

• Contraindications to MRI scanning including, but not limited to:

➢ Intracranial aneurism clips (except Sugita)
➢ History of intra-orbital metal fragments that have not been removed by an MD (as confirmed by orbital X-Ray);
➢ Pacemakers and non-MR compatible heart valves;
➢ Inner ear implants;
➢ Any physical abnormality or functional disability which prevents the subject from acquiring a suitable position for scanning.
➢ History of or participants suffering from claustrophobia or unable to lie still on his back in the MRI scanner for a period of at least 45mins.
➢ Unwillingness or inability to follow the procedures outlined in the protocol.

4.4 SCREENING AND INFORMED CONSENT

4.4.1 Screening visit

Screening of participants took place at a site of Sussex Partnership Foundation Trust or at CISC or at the adjacent Trafford Centre, both located at the Brighton and Sussex Medical School.

4.4.2 Informed consent procedure

I took the written informed consent from all subjects. The procedure included the explanation of aims, rationale, methods, and potential adverse effects of the study and was followed by completion of the informed consent form. The participant was allowed as much time as wished to consider the information, and the opportunity to question the Investigator, their GP, Consultant or other independent parties to decide whether they will participate in the study. I explained to the potential participant that they were free to refuse any involvement within the study or alternatively withdraw their consent at any point during the study and for any reason. The consent of the participant was recorded and retained at the study site in locked drawers. A copy of the signed Informed Consent was also made available to the participant. No study procedure was carried out until informed consent had been obtained from the participant.

4.4.3 Screening procedures

I conducted and carried out all screening processes

The following procedures took place during screening:

 • Collection of demographic data

• Medical history and assessment of medication use

• Physical examination

• Psychiatric interview: Administration of the MINI Neuropsychiatric Interview (Lecrubier et al., 1997), and rating of clinical symptoms using a self-report questionnaire, Beck depression Inventory-Second edition (BDI-II) (Beck et al., 1996) and a clinician-administered interview (Montgomery-Asberg Rating Scale, MADRS) (Montgomery SA, 1979). The MINI is a brief psychiatric structured diagnostic interview during which participants were asked to answer either 'yes' or 'no' to the presence of symptoms in the different diagnostic categories.

Depressive symptoms were rated using the BDI-II and the MADRS. Clinically relevant depression was determined by BDI-II scores in the range of 18-63 and MADRS scores > 20.

I was trained in the use of the MINI and of the clinical scales and I carried out the interviews for each participant.

• Cognitive testing: I used the Brief International Cognitive Assessment for MS (BICAMS), recommended by a panel of twelve neuropsychologists and neurologists adapted and recommended a brief battery of tests for the cognitive assessment and evaluation of MS, (Langdon et al., 2012). The primary focus of initiating BICAMS was to promote international use and standardise comparison across various settings. Selected tests are administered with ease and under a short period of time. The BICAMS comprises tests of memory and mental processing speed (Benedict et al., 2012), and consists of three components:

➢ The Symbol digit modalities test-SDMT (Smith et al., 1982) which measured the participants concentration and decision-making abilities, by asking participants to substitute and pair specific numbers for given geometric figures within a given time frame (90 seconds).

➢ The Brief visuospatial memory test- BVMT (Benedict et al., 1997) which tested for visual and spatial memory and required participants to draw as many figures as possible in their correct locations after viewing a given sample for about 10 seconds.

➢ The California verbal learning test- CVLT (Benedict et al., 1996) which assesses verbal learning and memory. This test required participants to recall as many words as possible from a read-out list over five different trials.

• Clinical questionnaires to measure Fatigue, Sleep and Anxiety. Questionnaires were handed out to participants (both MS and healthy controls) during full screening and before baseline scans. They were also handed out again to the MS participants that returned for their post treatment scans. Individuals who were unable to attend the centre during screening were assessed remotely via video links.

➢ The Fatigue Severity Scale- FSS (Krupp et al., 1989) is a questionnaire of 9 statements ranked on a scale of 1-7, based on strongly disagreeing with the statement (1) or strongly agreeing with the statement (7).
Robust research and clinical evidence indicate a high prevalence of fatigue in MS, associated with negative impact on activities of daily living and overall quality of life (Nagaraj et al., 2013). Originally devised for patients with MS and SLE (Krupp et al., 1989), the Fatigue Severity Scale (FSS) which was utilized in this study, is designed to measure mental and physical fatigue as well as establish its impact on social aspects. It represents a unidimensional generic fatigue rating scale and focuses on the function influence of fatigue (Martinez-Martin, 2017). Minimum and maximum scores of 9 and 63 respectively could be obtained, with scores between 9 and 35 considered normal. For this study, scores above 35 were clinically perceived as reflecting a high degree of fatigue (Goodwin et al; 2019). FSS scores have been linked with functional and structural changes in patients with MS and are credited with being quite straightforward to complete (Filippi et al., 2002; Roca et al., 2014). Research evidence has shown exceptional test-test reliability when utilized in neurological and gastrointestinal related conditions with significant positive correlation to depressive symptomatology (Valderrames et al; 2012, Rossi et al., 2017). A supposed pitfall of the FSS is its lack of distinction between motor and cognitive fatigue symptoms.

➢ Epworth Sleepiness Scale- ESS (Johns, 1991) is a self-administered questionnaire with 8 questions. Participants were asked to rate on a 4-point scale (0-3), their usual chances of dozing off or falling asleep while engaged in 8 different everyday activities like watching the TV or being stuck in traffic for instance.

➢ Generalized Anxiety Disorder scale- GAD-7 (Spitzer et al., 2006) is a self-administered 7-point questionnaire which serves a screening tool for anxiety symptoms. Participants were asked to rate on a 4-point scale (not at all, to nearly every day) how bothered they are with general anxiety symptoms in the past two weeks.

• Assessment of Inclusion/Exclusion criteria including the MRI safety questionnaire

 The screening visit lasted up to approximately 2 hours. All subjects that underwent screening were logged into a screening log associated with the study. If deemed eligible at screening, participants were asked to return to CISC for the scanning visit. We ensured that the first scanning visit took place prior to beginning the DMT prescribed by the neurologist.

4.4.4 Neurological assessments

The neurological assessments were done prior to the screening visit by the referring or treating neurologist, after necessary examinations and using the Expanded Disability Status Scale (EDSS). EDSS scores were provided to us on request, and were part of screening for eligibility criteria.

The Kurtzke Disability Status Scale was a widely used 10 step, objective process designed to measure functionality and invariably, the disability status of individuals with MS. Established by Dr John Kurtzke in the early 50's, the scale has been further modified severally and overtime to a more accurate clinically commemorate representation of levels of disability. The now familiar Kurtzke Expanded Disability Status Scale (EDSS) was hence developed in

1983, as a product of subsequent refinement to this effect (Kurtzke, 1983). Currently the prior 10 step scale gave way to a 2-part grade like system with lower scores (1 to 4.5) reflecting mobility without aid, and scores higher than 4.5 indicating some degree of gait impairment. Lower scores are also based on functional impairment in eight systems; pyramidal, cerebellar, brainstem, sensory, bowel and bladder, visual, and cerebral; and higher scores on both gait abilities and functional system scores. Contemplating future prospects of EDSS measures in MS, Cohen et al., 2012 highlighted on potential adjuncts to the disability scale. He mentions the use of composite end points, patient reported outcomes and indeed, the use of biomarkers for future references. The article also elaborates on the scale's underestimation of other relevant and important symptoms such as fatigue, depression and cognitive symptoms. The inclusion criteria were an EDSS score < 5.5 to ensure sufficient mobility of participants undergoing MR scanning. Though EDSS serves as a principal disability measure in this study for eligibility assessment purposes, we employed several other scales (FSS, ESS, BDI and MADRS) to account for these other symptoms.

4.6 MRI SCANNING PROTOCOL

There was one MRI session for healthy volunteers and two MRI sessions for MS patients to take place approximately 4-6 months apart. Scans took place at the CISC, a specialist environment for neuroimaging research. The procedures are listed in details in the Table of Events (Table 8 below). Prior to the baseline MRI scan, eligibility criteria were reviewed, including administration of the MRI safety questionnaire and a pregnancy test if participant was female and within child bearing age. During Post-treatment MRI scanning visits, procedures included a review of eligibility criteria, administration of the MRI safety questionnaire, pregnancy test as well as psychiatric diagnostic interview (MINI) and rating of clinical symptoms using the same questionnaires administered at screening (BDI-II, MADRS, FSS, ESS, GAD-7) as well as cognitive testing (BICAMS).

While in the scanner, subjects underwent the following MR sequences; High resolution anatomical T1 weighted MPRAGE (TR/TE: 2400.0ms/2.22ms); T2 FLAIR (0.4mm Isotropic); Diffusion weighted MRS of Hippocampus, MRS of Hippocampus, High resolution Diffusion Imaging (Voxel resolution was 1.35mm with B values of 1000 and 3000

s/mm^2), Resting state Functional Connectivity BOLD, Pseudo-Continuous Arterial Spin Labeling (pCASL), post-labelling delay (PLD 0 = 1800ms), and modified Asymmetric spin echo sequence (GASE) to measure irreversible transverse relaxation rate R2' ($\simeq$5min). Voxel was placed on the left hippocampus in all three planes (axial, sagittal and coronal). Slight variations in VOI positioning across participants was necessary for adjustments to different patterns of anterior, posterior curvature. The head and body of the hippocampus which contained the selected regions (CA1-4, DG) were targeted. Voxel size: 30 x 15 x 10 mm was utilised.

A.

B.
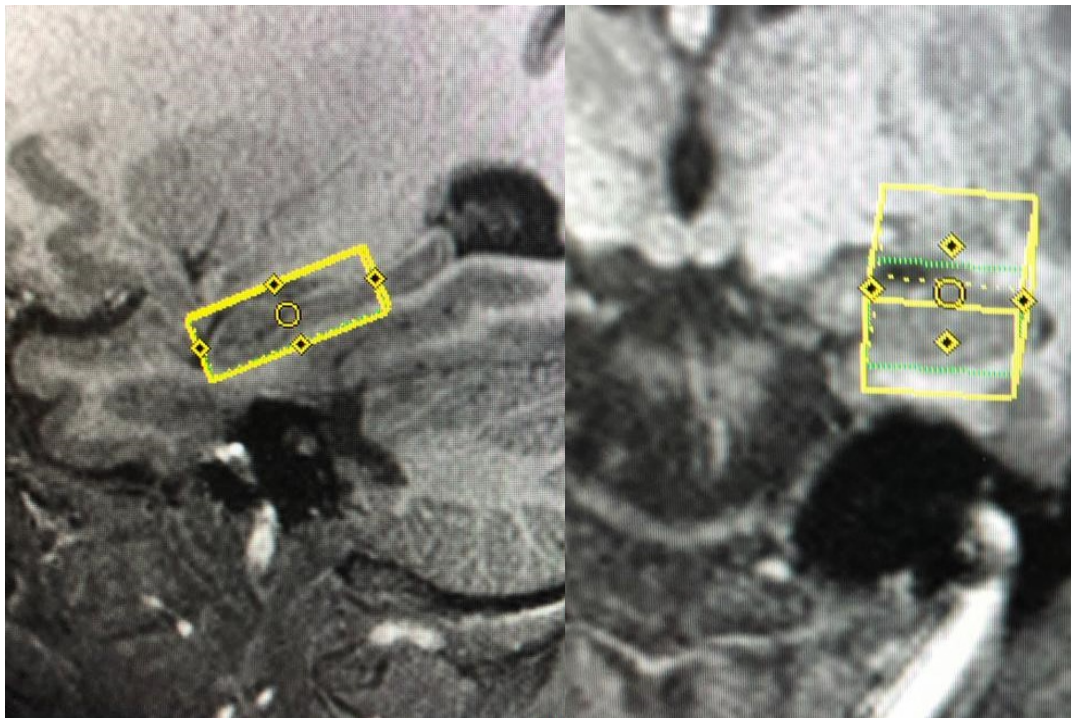
Figure 4. 1 Positioning of 3D Voxels on the left anterior hippocampus. Sagittal (A) and Coronal (B) views.

The total scan duration was approximately one hour, but the option to be split into two MRI scans each of approx. 45 minutes on the same day, or separate days within a 2 weeks period was also made available. The whole MRI scanning visit, including pre-scan preparation, MRI scan, and post-scan checks lasted for a period of approximately 3 hours. After the MRI scans, participants underwent brief physical checks prior to discharge.

	Pre-screening phone session	Screening Visit	MRI Scanning Visit (baseline)*		MRI Scanning Visit (post-treatment) *	
			Pre-scan	Post-scan	Pre-scan	Post-scan
Pre-screening eligibility questionnaire	X					
Emotional Thermometer (ET) (MS patients only)	X					
Informed consent		X				
Demographics		X				
Medical History		X			X	
Physical examination		X				
Clinical questionnaires (MINI, BDI-II, FSS, ESS, GAD-7, MADRS)		X			X	
Cognitive Tests (BICAMS)		X			X	
Pregnancy test		X	X		X	
MRI safety questionnaire		X	X		X	

Table 9: Table of Scanning and Screening events.

CHAPTER 5. CLINICAL AND BEHAVIOURAL CHARACTERISATION OF RECRUITED PARTICIPANTS

5.1 INTRODUCTION

Hippocampal involvement has been readily linked with manifestations of depression and cognitive impairment in multiple sclerosis (Rocca et al., 2018). Along with its well substantiated physiological role in memory function, the hippocampus also has established roles in processing speed, executive function, intelligence, path integration, spatial processing and also in emotional regulation (Papp et al., 2014; Reuben et al., 2011; Yamamoto & Tonegawa, 2017; Ruiz et al., 2014). Declarative memory and spatial relationships, both of which are heavily reliant on hippocampal circuitry and plasticity (Schinder et al., 2020) are the two likely cognitive aspects that are most readily affected during hippocampal dysfunction (Burgess et al., 2002); Shrager et al., 2007). In MS, prevalence rates of cognitive impairment range from 40-70% (Heaton et al., 1985; Maurelli et al., 1992). Involvement is generally around complex attention, episodic memory, information processing speed and executive function (Jongen et al., 2014), and all phases of MS are usually implicated. In some clinical scenarios, cognitive impairment presents as the first manifestation, and can also occur quite early in the MS course (Klonoff et al., 1991, Jensen et al., 1989, Ruggieri et al., 2003). SPMS and PPMS are reported to typically display greater severity with tendencies to impact more on attention and processing speed (Huijbregts et al., 2004) when compared to RRMS. While cognitive reserves are speculated to provide some degree of protection in MS patients, other clinical variables such as anxiety, depression, fatigue, disease duration as well as medication, can influence the degree and course of cognitive impairment and in co-morbid scenarios, could also invariably worsen symptoms (Jongen et al., 2012, Rogers et al., 2007). Impact cuts across personal life and vocational status and could initiate social impairment, vocational disability and as a whole, induce poorer quality of life (Rogers & Panegyres, 2007). Therapeutic effects of immunomodulatory treatments are currently not fully established (Montalban & Rio, 2006), though most benefit is reportedly observed with RRMS (Barak & Achiron, 2002; Fischer et al., 2000) where improvements in processing speed, learning, attention and memory have been reported.

Depression is predominantly regarded as one of the commonest, largely undetected, psychiatric ailments associated with MS, and additionally serves as a significant determinant of quality of life in MS patients (Siegert and Abernathy 2005). As seen in prior chapters, vast literature reports a lifetime prevalence of depression in approximately 50% of MS patients and an annual prevalence of approximately 25%. Worryingly, comorbidity of depression with MS is also deemed to be directly related to the increased risk of suicide in individuals with MS. A combination of psycho-social and functional related factors has been suggested to contribute to the development and high prevalence of depression in MS, however, robust and converging evidence are also indicative of the role of underlying neuroinflammatory and immune mediated related mechanisms. There is growing evidence that classical mediators of inflammation such as IL6, TNFα, and prostaglandins also play significant roles in major depression and stress induced disturbances (Khandaker et al., 2018; Pucak et al., 2007). Indeed, raised levels of inflammatory biomarkers, cytokines and the expression of genes involved in inflammatory responses have been found to be associated with depression (Farooq et al., 2017). Experimental challenges also suggest that psychological distress and depressive syndromes in the general population could be induced by treatments that raise pro-inflammatory cytokines (Felger et al., 2013, Roman et al., 2020). Clinically, the incidence of affective disorders in immune mediated inflammatory disease cohorts are observed to be increased (Marrie et al., 2017). Clinical presentations range from core symptoms, like low mood and anhedonia to more variable and atypical presentations such as irritability, anxiety and a profound sense of guilt. Overlapping symptoms that may result from distinct neurological manifestations of MS such as fatigue, cognitive difficulties, impaired sleep patterns, loss of appetite and poor concentration also make for diagnostic inaccuracies.

The main objective of this chapter is to provide clinical and behavioural characterisation of the recruited participants. I tested statistical significance amongst the depression, cognitive and disability scores between controls and MS subtypes and further compared the clinical effects of a group of returning participants at baseline and post treatment of DMT's. This chapter will help to prepare for the correlations between clinical and imaging variables in the following chapter (Chapter 6).

5.2 SUMMARY OF CLINICAL ASSESSMENTS

Study procedures have been described in details (previous chapter). In summary, participants had been duly informed of study conditions and informed consents were received. Eligibility and clinical assessment were conducted at screening. General Inclusion criteria was newly diagnosed RRMS or PPMS by treating neurologists according to the McDonald criteria, and currently awaiting disease modifying treatment. Severity of participant depression was estimated by BDI-II and MADRS, and confirmation of depressive and other psychiatric diagnoses was done using the MINI. Cognition was assessed using the three sections of BICAMS (described in 4.4.3). Raw scores of each BICAMS component were accumulated and total scores were obtained. Other clinical assessments carried out included the GAD-7, FSS and ESS (details in previous Chapter). To mitigate for any evaluation differences, self-administered, clinician-led and cognitive tests were all performed by me on the same day.

5.3 STATISTICAL ANALYSIS

Statistical analysis of data was accomplished by the Statistical Package for the Social Sciences (SPSS 23, IBM Corporation, Somers, New York.) statistical program. Spearman's rank correlation was utilized to test for associations between variables. Generalised linear model (Multivariate and Univariate analysis) was used to compare groups (RRMS and PPMS), Chi-square test were also employed in the analysis to compare the groups on categorical variables. Paired sample t-test was used to compare the depression scores and cognitive performance of 5 selected participants at baseline and after commencement of DMT's.

5.4 RESULTS

25 participants in total were recruited into the research project. 15 participants had MS and 10 participants were healthy controls (HC). Of the 15 MS participants, 9 participants had a

diagnosis of RRMS and 6 had a diagnosis of PPMS. The MRI scans of 2 HC's had technical issues and although their clinical data were included, they were subsequently excluded from the MRI analysis.

5 MS participants were asked to return back to the centre for post treatment scans in the 5th month after their base line scan. They included 4 males and 1 female. The 4 males were PPMS participants while the female had the RRMS subtype. They had all received Ocrevus and had had the first dose (comprising 300mg half infusions i.e 600mg in total but given as 300mg 2 weeks apart.) before having the post treatment scan. Essentially, all MS participants who returned for a second scan had their first dose and were awaiting the second dose of Ocrevus which is usually prescribed as one infusion (600mg) 6 monthly. Only clinical data from the 5 returning participants were analysed. Analysis of Imaging data from this cohort are beyond the scope of this thesis.

Demographic and clinical data are presented in Table 9. Comparisons of clinical variables across groups are presented in figure 5.1 and 5.2

Demographics

The categorical demographic variables were compared using chi-square statistics and no differences were detected for gender, p = 0.08, or employment, p = 0.23. There was no significant difference in age between MS and HV (mean age difference: 3.39 years) and neither between individual MS subtypes and HC. Mean age varied between PPMS and RRMS subtypes, although only at trend-level, and was 49.16 and 36.88 years respectively. 26% of the MS patients were unemployed (4/15).

Disability and Fatigue

The range of EDSS values in the recruited MS patient cohort (n=15) was between 1 and 5.5. The mean (±SD) was calculated as 2.2 ±1.5. Within our recruited participants, MS patients with PPMS type had higher EDSS values, with mostly visual and muscular related symptomatology. Significant main effects were detected between PPMS and RRMS (PPMS > RRMS) for EDSS, p = 0.006. Interestingly, mean duration of disease for PPMS was 3.8 years while that of RRMS was approximately 7 years.

The presence of severe fatigue in our recruited MS cohort was approximately 53% (8/15). Mean (±SD) fatigue scores were calculated as 33.3 (±19). Significant main effects were detected between MS and HC's for the FSS, $p = 0.001$. There was a mixed pattern of scores pertaining to MS type with no distinct trend. In post hoc analyses, significant differences were found both between the controls and PPMS group, $p = 0.000$, and controls and the RRMS group, $p = 0.001$.

Depressive symptoms

Forty percent of participants with MS met diagnostic criteria for current MDD. All patients with MDD had RRMS phenotype (6 cases, approximately 66% of RRMS patients), whilst no PPMS had a diagnosis of MDD. This appeared in contrast with levels of disability which were lower in RRMS relative to PPMS. There were no participants meeting criteria for any other DSM diagnosis.

Significant main effects were detected between MS and HC's (MS > HC) for the BDI, $p = 0.002$, the MADRS, $p = 0.004$, the FSS, $p = 0.001$. Subtypes compared to controls found significant post hoc differences between the controls and PPMS participants, $p = 0.001$, as well as between controls and RRMS, $p = 0.001$, for the BDI. Similar post hoc differences were found for the MADRS, with significant differences between controls and the PPMS group, $p = 0.02$, and the RRMS group, $p = 0.001$.

With regards to contrasts between MS types, there was no significant difference in BDI depression scores, t (8) = 0.73, P= 0.49. Mean BDI scores for clinical types of MS was 18.5 (±2.5) for PPMS and 23 (±18) for RRMS. The difference in scores for MADRS amongst the MS groups was also not significant, t (11) = 0.85, P= 0.41. Mean MADRS scores were 13.5 (±4.9) for PPMS and 17.8 (±14) for RRMS. Group variances for both were unequal. Correlation was statistically significant and positive at the 0.01 level (2-tailed) for MADRS scores and the levels of fatigue (p<.01) and was also significant for BDI and levels of fatigue at the 0.05 level (2-tailed), (p<.05). There was no significant correlation between the depression scores and cognition, levels of disability, age and gender. 6/9 (66%) participants with RRMS had higher depression scores indicative of depressive illness, and the mean (± SD) was 33.6 (±12) for BDI and 26 (±8) for MADRS. All participants with PPMS (40%) did not have depression.

Of the four MS patients who were unemployed, three were depressed. Four participants with diagnosed MDD also had severe fatigue scores.

Cognitive performance

The raw accumulated cognitive scores ranged from 75 to 201 and mean (±SD) was 137.64 (±26.21). There was no significant difference in cognitive performance between whole MS cohort nor individual subtypes, and healthy controls. I found a trend difference (p=0.08) between MS subtypes in the performance in the CVLT component, which was lower in RRMS vs PPMS. One participant was unable to complete the BICAMS for personal reasons.

Symptoms change after DMTs initiation

Post commencement of DMT's (Ocrevus), 5 participants returned 4-6 months after their baseline scans and same protocol procedures as baseline were applied to the returnees (see results in figures 5.3, 5.4). With regard to fatigue, FSS Scores did appear to improve for re-scanned participants (n=5) when they returned for their post-treatment scans (after 4-6 months).

Improvements were also observed in the depression scores of returning participants (see figures 5.4) in both the BDI and MADRS scales (lower scores). Mean(±SD) scores for BDI baseline and returning participants were 24 (10.72) and 14 (8.96) respectively, while MADRS mean scores were 18.2 (10.62) and 9.0 (6.32) respectively. There were also significant differences between baseline scores and post DMT's for both. *[t(4)= 8.91, p = 0.001].* 95% CI *[6.61 to 12.59]* for BDI and *[t(4)= 3.59, p = 0.02].* 95% CI *[2.10 to 16.30].*

Regarding cognitive performance, 2 and 4 participants in total had improvements in SDMT and BVMT respectively, while all participants saw improvements in the CVLT component of BICAMS. There were improvements in total cognitive scores in all participants. Total cognitive mean(±SD) was 124.6 (28.85) at baseline, compared to 137.8 (28.45) after commencement of DMT's. On the conducted Paired sample t-test, the results indicate significant differences between total BICAMS performance scores at baseline and after commencement of DMT's *[t(4)= -4.27, p = 0.01].* 95% CI *[-21.78 to -4.62].* Individual BICAMS components did not show significant differences *(p>0.05).*

| | MS (whole group) | MS subtype | | Healthy Volunteers | Statistical test | | |
		RRMS	PPMS		MS vs HV	RR- vs PP-MS	Subtype PP vs HV / RR vs HV
N. of subjects	25	9	6	10	-	-	-
Gender (M:F)	8:15	1:8	2:4	3:5	Chi square: 0.08 (F)	-	-
Age (years, mean ± SD)	39.96 (13.40)	36.89 (13.90)	49.17 (7.81)	36.57 (15.34)	p<0.86	p<0.07	p<0.20 / p<0.79
EDSS (mean ± SD)	2.30 (1.6)	1.29 (0.56)	4.0 (1.3)	n/a	-	p<0.01*	-
Disease Duration (years, mean ± SD)	5.65 (5.66)	7.01 (7.11)	3.83 (2.32)	n/a	-	p<0.29	-
BICAMS Total Raw score (mean ± SD)	137.64 (26.21)	142.25 (27.33)	124 (26.05)	143.25 (24.69)	p<0.34	p<0.21	p<0.18 / p<0.94
Component 1 (SDMT)	47.91 (14.22)	49.75 (18.41)	41.17 (10.74)	48.75 (12.88)	p<0.52	p<0.29	p<0.35 / p<0.89
Component 2 (BVMT)	25.32 (7.91)	25.25 (4.62)	24.33 (10.01)	26.13 (9.64)	p<0.92	p<0.84	p<0.69 / p<0.83
Component 3 (CVLT)	64.41 (9.23)	67.25 (6.92)	58.50 (10.21)	66.0 (9.53)	p<0.18	p<0.08	p<0.13 / p<0.78
Diagnosis of Major Depression (n. of cases)	6	6	0	-	-	-	-
MADRS	16.1 (11.2)	17.8 (14.04)	13.5 (4.93)	1.0 (1.07)	p>0.004*	p<0.38	p>0.02* / p>0.001*
BDI	21.2 (14.1)	23.0 (18.29)	18.5 (2.59)	0.75 (1.04)	p>0.002*	p<0.47	p>0.01* / p>0.001*
FSS	33.53 (19.05)	30.78 (18.85)	37.67 (20.34)	1.88 (1.36)	p>0.001*	p<0.42	p>0.000* / p>0.001*

Table 10: Demographics and clinical characteristics of recruited patients at baseline. Unbracketed numbers-mean, numbers in brackets- Standard deviation, MADRS- Montgomery-Asberg Depression Rating Scale, BDI- Becks Depression Inventory, FSS- Fatigue Severity Scale, SDMT- Symbol Digit Modalities Test, BVMT- Brief Visuospatial Memory Test, CVLT- California Verbal Learning Test.

(A)
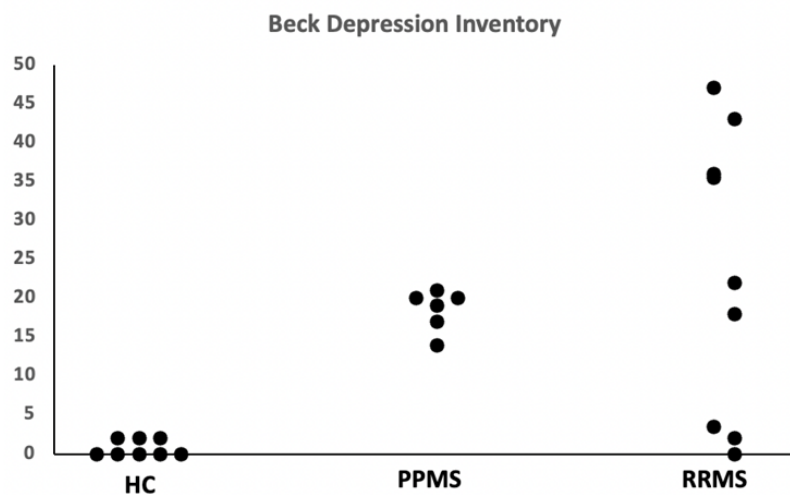
(B)
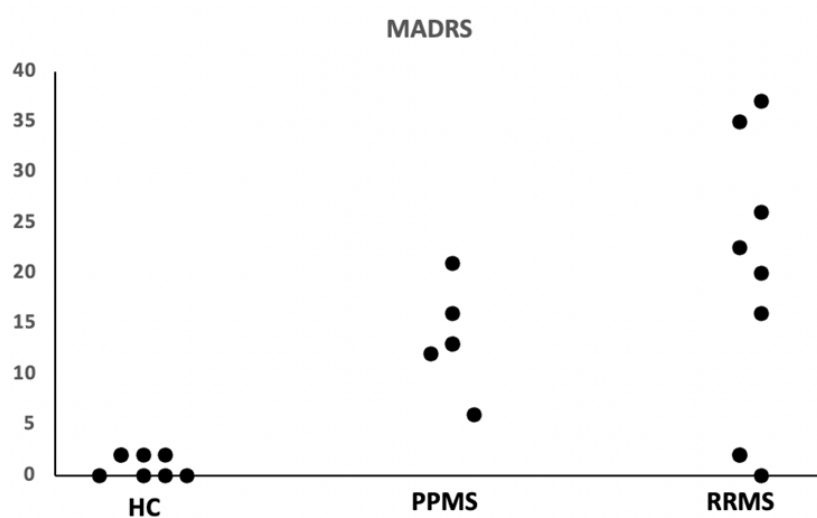
Figure 5. 1 Scatter plot of BDI (Becks Depression Inventory) and MS type (A), Scatter plot of MADRS (Montgomery-Asberg Depression Rating Scale) and MS type (B).

(C)
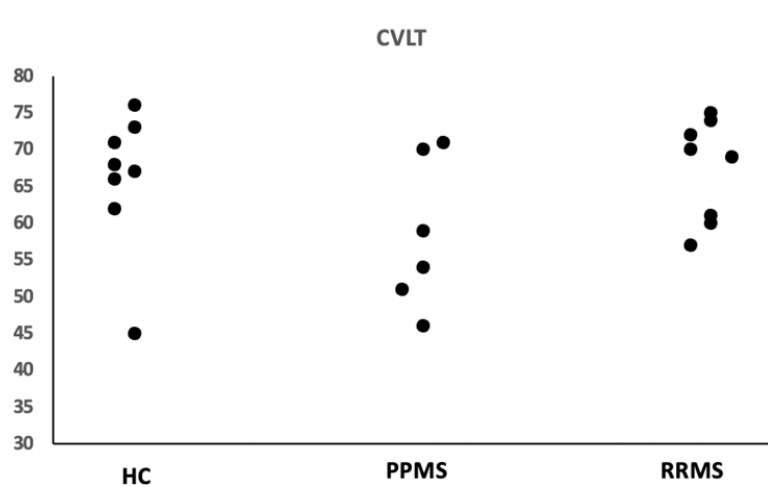
(D)
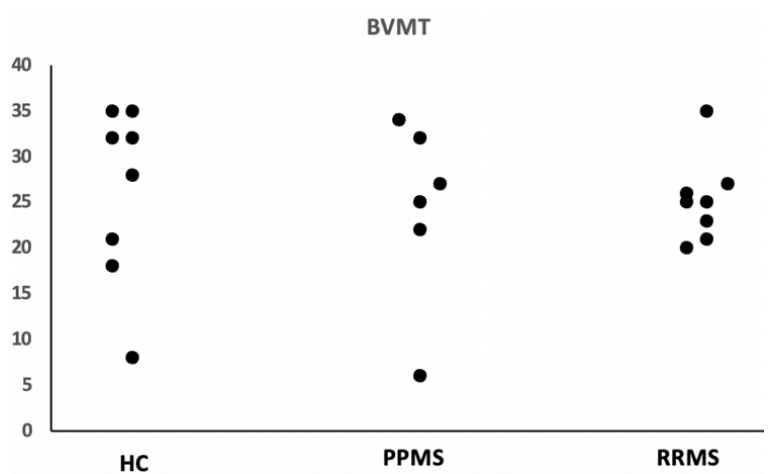
(E)
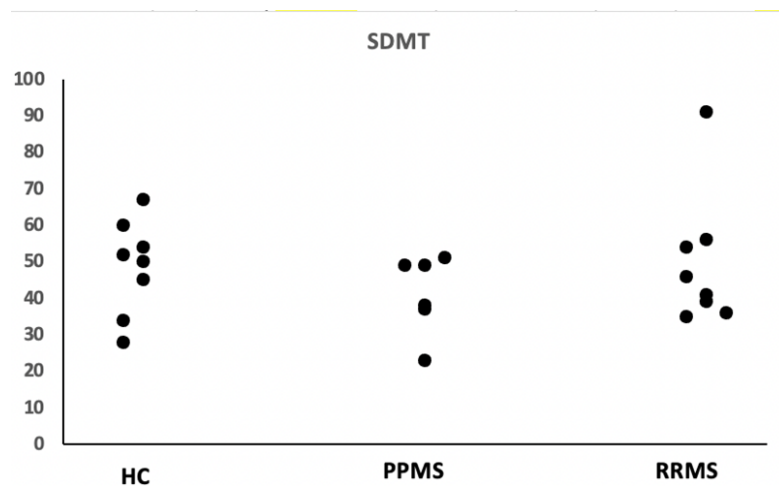
Figure 5. 2 Scatter plot of BICAMS components and MS types. CVLT- California Verbal Learning Test (C), BVMT- Brief Visuospatial Memory Test (D) and SDMT- Symbol Digit Modalities Test (E).

(A)

(B)

C)

(D)
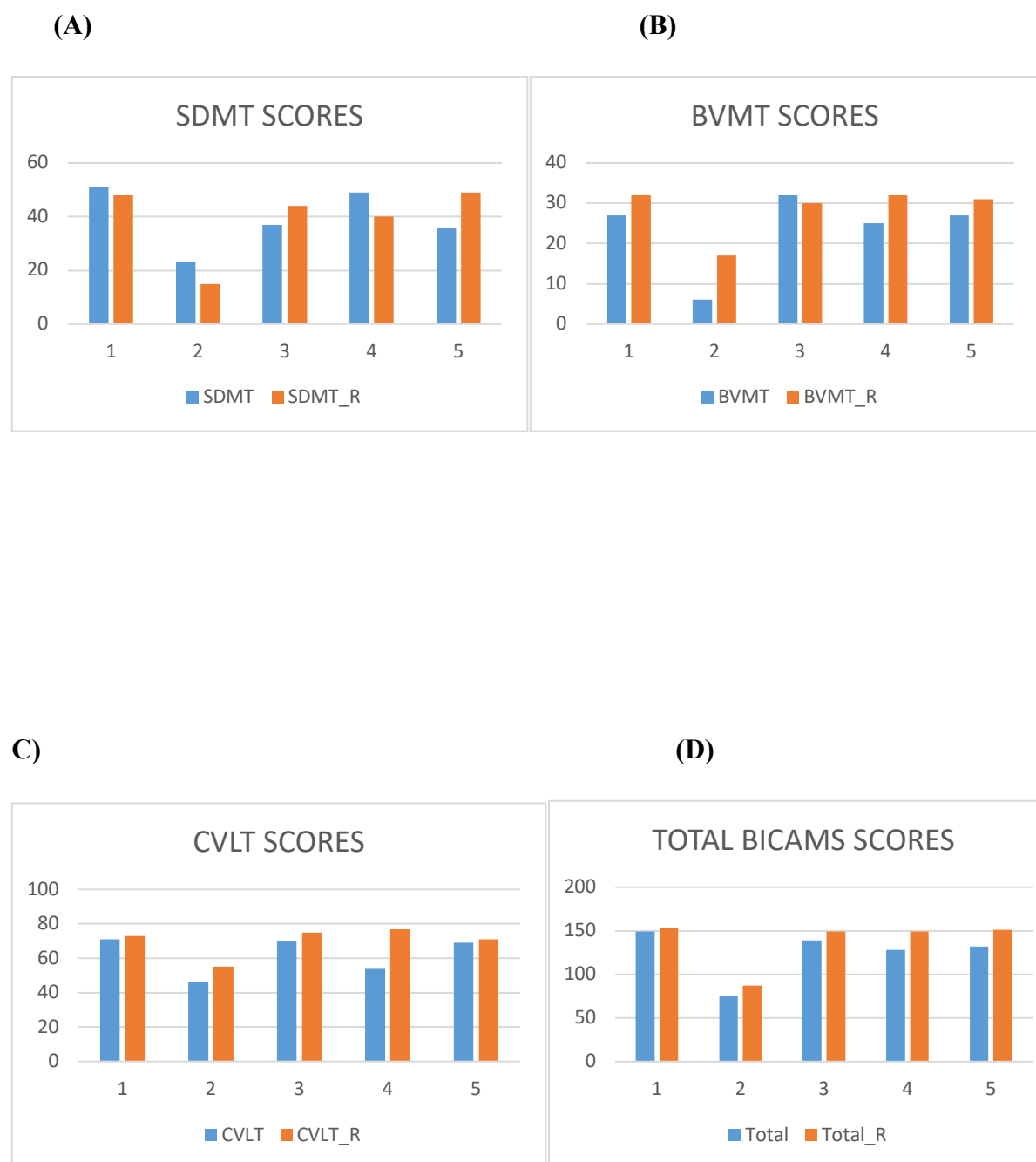
Figure 5. 3 Cluster columns comparing cognitive scores at baseline and post commencement of DMT's in 5 participants. Some improvement in performance noted in the total overall BICAMS scores of returning participants (_R)

S/N	Treatment	BDI	BDI_R	MADRS	MADRS_R
1	OCR	17	9	16	8
2	OCR	20	13	12	6
3	OCR	21	12	13	10
4	OCR	19	8	13	2
5	OCR	43	30	37	19

Table 11: Comparison between baseline and post-treatment depression scores. (OCR-Ocrevus, _R- return post treatment)
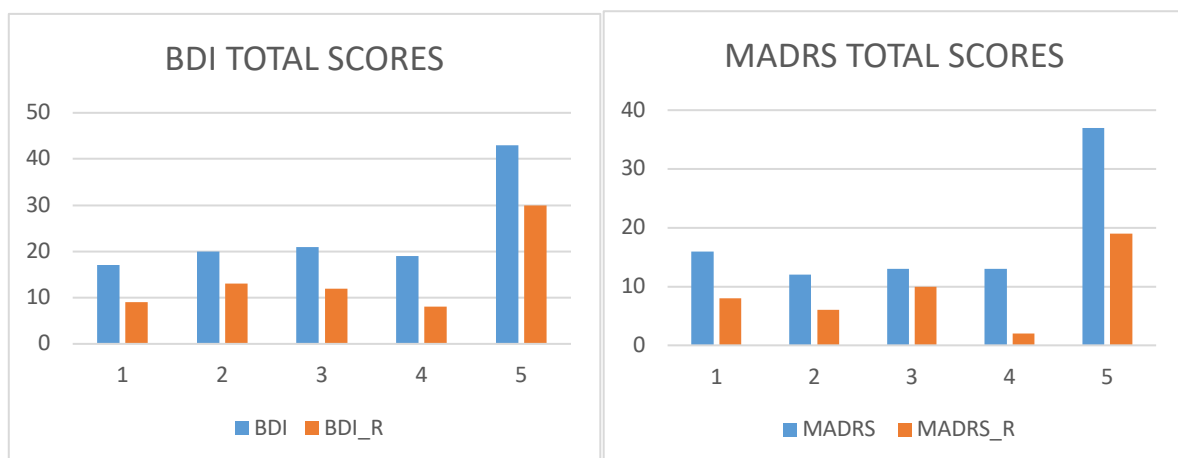
Figure 5. 4 Cluster columns comparing depression scores at baseline and post commencement of DMT's in 5 participants. Improvements also observed in scores of returning participants.

5.5 DISCUSSION

Our recruited participants presented with varying levels of disability depending on the MS subtype. As expected, participants with PPMS had higher EDSS values, with shorter duration of disease, relative to RRMS patients. Interestingly, however, the subtypes were different with regard to the prevalence of associated depression. Of the 40% of MS participants in this

study with a diagnosis of depression, all belonged to the RRMS subtype. Similar trend have been reported in other studies (Dekker et al., 2019; Rocca et al., 2017; Figueiredo et al., 2020). Mohammadi et al., 2015 reported higher rates of depression in women with RRMS compared to more progressive stages, with associated links to increased inflammatory components in RRMS. Albeit, other rationales might also be connected to this trend such as duration of disease, age, level of support and adjustment capabilities (Dennison et al., 2009), or perhaps due to a larger number of participants in RRMS, and hence, greater variance measures (Doshi & Chataway, 2017; Zeydan & Kantarci, 2020). Employment status varied significantly among the groups, with higher depression scores appearing amongst the unemployed.

The prevalence of fatigue in our recruited MS cohort was approximately 53% (8/15) which is consistent with available literature (Nagaraj et al., 2013; Kaya Aygünoğlu et al., 2015; Tarasiuk et al., 2022). Mean (±SD) fatigue scores were calculated as 33.3 (±19). Amongst MS related symptoms, fatigue is very frequent, and is understood to be contributory to distress and poorer quality of life (Fisk et al., 1994; Frankel et al., 2006; Krupp et al 2006). Severe fatigue has been portrayed in large studies to be predictive of worsening EDSS scores (Vaughn et al., 2020) and is perceived as one of the most serious symptoms impacting on quality of life and everyday activities (Tarasiuk et al., 2022). In line with predictions, 4 out of 6 MS participants in this study with diagnosis of depression also had severe fatigue (approximately 66%) which supports suggestions of co-morbidity or co-occurrence (Tarasiuk et al., 2022). However, the difference in MDD diagnosis prevalence amongst subtypes was not paralleled by similar differences in fatigue levels, as PPMS had numerically higher FSS scores than RRMS. This is an interesting finding as both depression and fatigue are viewed as having contributory immuno-inflammatory mechanisms behind their aetiology in MS, and in some cases, are difficult to differentiate. They could both present symptomatically with anhedonia and amotivation, hence comprise similar symptoms that match criteria for clinical depression. However, though both conditions (Depression and Fatigue) overlap with one another comorbidly in MS, they represent two distinct syndromes. Increased serum and CSF proinflammatory cytokines (interferon, interleukins and neopterin) have been implicated (Pokryszko-Dragan et al., 2012). Converging studies also report robust correlation between depression and fatigue (Patrick et al., 2009), including our study which showed correlations of fatigue with both BDI and MADRS scores. It is possible that underlying mechanisms contribute to depression and fatigue in a differential manner amongst MS subtypes.

Considering cognitive performance, there were no statistically significant differences amongst groups (MS and controls). There were also no definite relationships of cognitive scores with disease burden or progression. When analysing phenotypes separately, there was slightly poorer performance scores in the PPMS subtype compared to HC, though not statistically significant. This was not the case with the RRMS subtype whose mean performance scores was similar to HC's (see table 9). Lower PPMS performance scores compared to controls were observed in the SDMT ($p=0.35$) and the CVLT ($p=0.13$) components of the BICAMS. Performance Scores were also lower in PPMS compared to RRMS in the CVLT component, but again not statistically significant ($p=0.08$). As seen in the systematic review of the literature (Chapter 2), Herranz 2016 noted an increase in diffusion-based MD parameter correlated negatively with SDMT and CVLT scores in MS and CIS and was able to distinguish between memory preserved and memory impaired CIS patients. Both scales could thus be sensitive enough in characterising and distinguishing cognitive impairments between PPMS and HC's as highlighted in this study, though larger population sizes would be required to validate such evidence.

Some Research literature describe a cognitive reserve hypothesis in MS (Stern, 2002, 2012; Sumowski & Leavitt, 2013), that depicts extensive efficiency and capacity of neural networks (Stern et al., 2005; Sumowski et al., 2010), and is associated with enriching life experiences. Age could also be a determining factor in terms of cognition. The highest raw cognitive total score in the study was 210 which was from a 22-year-old RRMS participant, diagnosed with depression and employed. Fatigue and depression are also reported to impact on cognition (Takeda et al., 2021). However, there was no correlation of cognition to either FSS, BDI or MADRAS scores within our study.

Post baseline scans, treatments (first infusion) with Ocrevus were given around the 5th month by treating Neurologists and this may have coincided with the period following necessary assessments and prior necessary investigations (Hepatitis B, HIV and white blood cell count). The mechanism of action of Ocrevus is by B-cell depletion of monoclonal antibodies. CD20-positive-B lymphocytes are selectively targeted by binding to cellular surface proteins, which inevitably destroys the cells and protects myelin against damage from such cell lines. Clinical effects include decreased relapse rates in RRMS, and lower rates of progression in PPMS (Mulero et al., 2018). The inhibition of the secretion of proinflammatory cytokines by B-Cells could ideally be the pharmacodynamic mechanism and rationale behind improved

depression scores and enhanced total cognitive scores but establishing significant evidence would require standardised clinical trials on a much larger scale. Interestingly, there was also statistical significance associated with better total cognitive performances in the returning participants after first dose of Ocrevus, which may in effect, bolster suggestions that reductions in depressive scores could be tantamount to enhanced psychological performances or a general improvement in wellbeing that may follow initiation of life changing disease modifying treatment. One returnee participant, according to the MINI assessment, went from experiencing major depression symptoms to only mild symptoms, albeit, she had also begun cognitive behavioural therapy (CBT).

CHAPTER 6. DIFFUSION-WEIGHTED MR STUDY OF MICROSTRUCTURAL ALTERATIONS IN HIPPOCAMPAL SUBFIELDS ACROSS MS PHENOTYPES

6.1 INTRODUCTION

In prior chapters (Chapter 2), and as part of a Systematic review of the literature, I reviewed and discussed alterations in hippocampal quantitative neuroimaging measures derived from various imaging modalities of RRMS, PPMS and healthy controls, as well as their specific clinical and functional relevance. I have also further looked at clinical manifestation of depression and cognitive dysfunction in both MS types (Chapter 5). I now intend to explore the presence of microstructural changes (diffusion-weighted MRI parameters) and volumes in the right and left hippocampal subregions of our recruited MS data, contrasting patients to healthy controls, and also comparing PPMS and RRMS phenotypes whilst exploring potential correlations with clinical parameters.

 MS is principally viewed as an immune mediated neuroinflammatory condition, while PPMS is generally portrayed as a clinical variant (Hohlfield et al., 2016). Albeit, when considering a more primary neurodegenerative disease mechanistic process, as suggested by some researchers, this could then indeed indicate the reverse, placing PPMS as the primary condition and RRMS as a modified inflammatory process (Trapp et al., 2018). Some studies suggest an overlap of pathogenic mechanisms (Rice et al 2013, Abdelheck et al., 2017), with pre-existing lesions expanding gradually from the white matter and diffuse neurodegenerative processes occurring in the normal appearing white or grey matter (Lassman et al., 2012).

The separate study of MS subtypes will potentially contribute to better characterisation of the etiopathogenetic processes that are specific of each MS phenotype

Whilst this chapter focuses on DW-MRI in individual subfields, the next chapter (Chapter 7) will analyse diffusion of hippocampal metabolites (choline, NAA and Cr) obtained from DWMRS study of the anterior hippocampus, separately for RRMS and PPMS patients.

6.2 DEMOGRAPHICS AND SAMPLE.

Total recruited sample size (n=25) where split into 3 groups based on diagnosis and type of MS. PPMS (n=6), RRMS (n=9), HC (n=8). All participants were recruited via the University Hospital Sussex Neurology departments and from the University of Sussex. All participants completed an informed consent form. Clinical features and characteristics are further displayed in Table 8 as well as Chapters 4 and 5.

6.2.1 Image analysis

For the purpose of this thesis, only the DW-MRS and the diffusion imaging data were analysed.

Diffusion imaging data were pre-processed as follows. First they were denoised using the Marchenko-Pastur principal component analysis (MPPCA) algorithm (Veraart et al., 2016) implemented in the dwidenoise command in MRtrix (http://www.mrtrix.org). Next, they were corrected for susceptibility distortions using ToPUP and eddy-current and motion induced misregistration using 'eddy'. The resulting dataset was processed with the IQT scripts, in the same way described in Chapter 3. The same training dataset was used for the locally acquired data, as the MAPMRI model is not sensitive to the specific set of b-values, as long as the acquisition protocol is sufficient to provide a good estimation of the model parameters. As described in Chapter 3, a full dataset with increased resolution (0.673 mm) was synthesised from the MAPMRI coefficients and used to fit both, DTI and NODDI models. The directionally averaged b=1000 set was used for subfield segmentation. The segmentation was performed automatically in this case, using VolBrain and ASHS. Reason for utilizing automatic segmentation methods on prisma data was as a result of slightly lower contrast compared to HCP data. This affected the visibility of vital manual segmentation initiating land marks in the medial temporal regions, like the VHS (Vestigial Hippocampal Sulcus). These may stem from pathologically induced tissue effects in the region of interest (Hippocampus). Computation and analysis of diffusion parameters was done using ITK-SNAP software (Version 3.8).
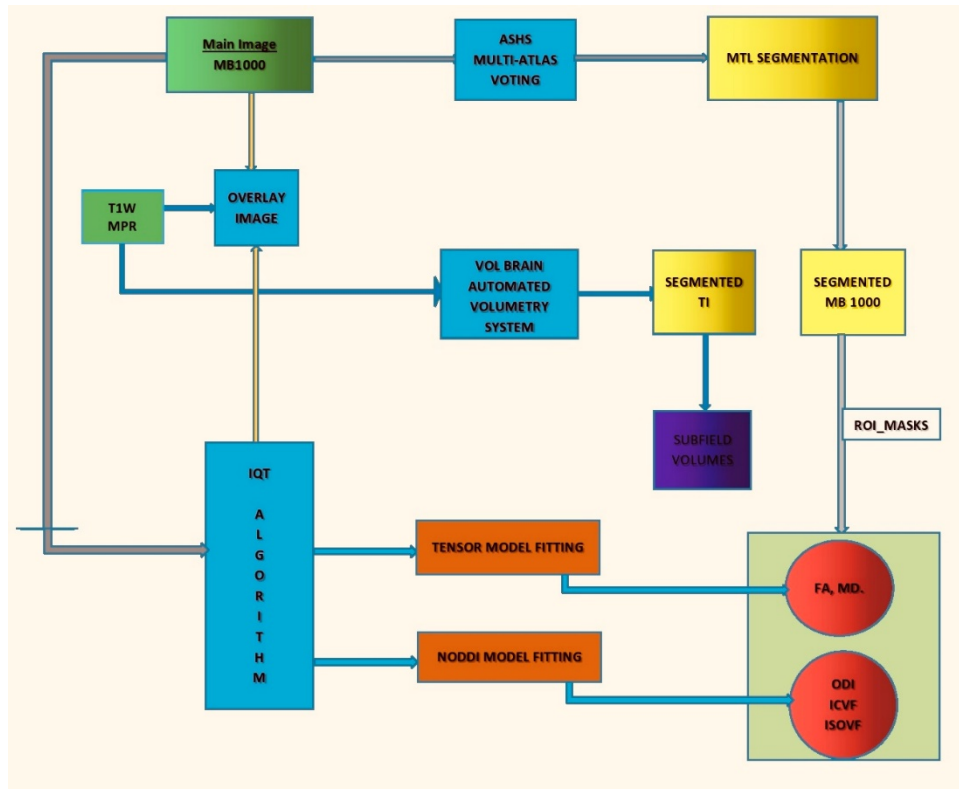
Figure 6. 1 Imaging Analysis Pipeline

6.2.2 Image Acquisition

MRI was obtained via a Siemens MAGNETOM Prisma 3T MRI Scanner. The protocol included a high-resolution T1 weighted volume (0.8 mm isotropic resolution, TR= 2400.0 ms, TE=2.22 ms, TI=1000 ms) , T2 weighted TSE sequence and T2 weighted-Fluid-Attenuated Inversion Recovery (TR=2400.0 ms, TE= 2.22ms, FOV= 256 x 256 x 256 mm^3, flip angle= 8 deg, matrix size = 192 x 192). All acquired in sagittal orientation and reconstructed in 3 orthogonal planes. Diffusion-weighted MRI was acquired with a multi-band pulsed gradient spin echo EPI (TE=2000 ms, TR=49.20 ms) with a voxel size of 1.35mm isotropic. The protocol was set up to match as closely as possible the HCP one. Only 2 b values of 1000 and 3000 s/mm^2, respectively, were used, each with 64 diffusion-weighted directions.

6.2.3 Post acquisition computational image processing

The resulting dataset was processed with the IQT scripts, in the same way described in Chapters 3 and 4. The same training dataset was used for the locally acquired data, as the MAPMRI model is not sensitive to the specific set of b-values, as long as the acquisition protocol is sufficient to provide a good estimation of the model parameters. As described in Chapter 3, a full dataset with increased resolution (0.673 mm) was synthesised from the MAPMRI coefficients and used to fit both, DTI and NODDI models. The directionally averaged b=1000 set was used for subfield segmentation.

6.2.4 Hippocampal Subfield Segmentation

An automated segmentation pipeline was used (See figure 6.1).

HIPS and volBrain; This automatic advanced pipeline was utilized to segment monomodal T1w data and obtain reports of the different individual hippocampal subfield volumes (CA1, CA2/CA3, DG/CA4, SLRM) from both left and right sides. The segmentations are based on multi-atlas patch-based label fusion segmentation adaptations (Manjón & Coupé, 2016); Zamani et al., 2020).

Developed by Yushkevich (Yushkevich et al., 2015), Automatic Segmentation of Hippocampal Subfields (ASHS) is a software tool designed specifically for the automatic segmentation of medial temporal lobe (MTL) structures, including the subfields of the Hippocampus. Accurate and reliable results of the segmentation are usually obtained, and these techniques have been validated in prior studies (Yushkevich et al., 2015a, b, de Flores et al., 2015). However, there were minor errors noted in a few data, which were identified and corrected manually using ITK-SNAP software tools. The error was mostly with voxels slightly exceeding subfield boundaries and may have derived from the deformable image registration process of Joint label fusion, the ASHS procedure where expert labelled segmentations (atlases) are automatically transferred to novel images (Wang et al., 2013). These errors were identified during quality checks. The Main Toolbar function of ITK-SNAP

was employed to manually redefine these boundaries based on neuroanatomical knowledge, and parameters derived were then automatically adjusted.

ASHS.

ASHS was utilized in obtaining diffusion parameters from the imaging data. Usually, the technique requires T1 and high resolution T2 MRI images (Cong et al., 2018). We adapted this procedure by replacing T2 with our high-resolution diffusion weighted image (MB1000), which had been pre-processed with IQT, further enhancing resolution. Multi-atlas segmentation was achieved by corrective learning (Wang et al., 2011) and Label fusion method (Wang et al., 2013). Segmented regions included CA1, DG, Subiculum, entorhinal cortex, perirhinal areas (BA35, BA36), Parahippocampal cortex (PHC), and Sulcus. I subsequently focused on relevant CA1 and DG subregions as well as PHC, which has been implicated in MS in some literature (Guerts et al., 2007) and is known to play vital roles in cognition (Aminoff et al., 2013; Bohbot et al., 2015). Obtained segmented masks were fitted on derived Diffusion maps to compute parameters for analysis, via ITK-SNAP 3.8.0 software.

VolBrain performs automatic segmentation on T1 weighted images using an advanced pipeline. Preprocessing utilizes the following steps to achieve automatic segmentation; Denoising, affine registration in MNI space, inhomogeneity corrections and normalization of intensity. A path based multi-atlas method is applied. HIPS is the VolBrain pipeline required for subfield segmentation of monomodal (T1) derived from multimodal (T1 + T2) MRI data (See figure 6.4 C). We obtained volumes from T1W data and compared these with both the volumes obtained from ASHS and manual segmentation.

6.2.5 Statistical analysis

The study used analysis of covariance (ANCOVA) to test for differences in hippocampal imaging measures between MS patients and non-affected participants, and between PPMS and RRMS, whilst correcting for age, levels of disability as well as other clinical and neuroimaging parameters was carried out between patient subtypes. Pearson's correlation test was used to investigate the relationship between imaging and clinical variables.

Statistical analyses involving multiple regions of interest within the hippocampus involved correction for multiple comparisons using false discovery rate (FDR) at 10%.

The assumption of normality for each continuous distribution was checked using Shapiro-Wilk tests. The statistical assumption of homogeneity of variance was checked using Levene's test. If both statistical assumptions were met, ANCOVA analysis was used to compare the controls and the two MS groups on continuous parameters. Post hoc testing using Tukey's test was employed when a significant main effect was found. Means and standard deviations were reported and interpreted for the ANCOVA analyses. If one or both statistical assumptions were violated, non-parametric Kruskal-Wallis tests were performed to test for significant effects (See Chapter 5). Dunn's tests were used in a post hoc fashion if a significant main effect was detected. Means and standard deviation were reported and interpreted for the analyses. Chi-square analysis was used to compare the groups on categorical variables (See Chapter 5). Frequency and percentage statistics were reported for the chi-square analyses. Statistical significance was assumed at an alpha value of 0.05 and all analyses were performed using Social Sciences (SPSS 23, IBM Corporation, Somers, New York.)

6.3 METHODS

Both data sets were processed with IQT scripts (as described in chapter 3). Same training data set was employed for both acquired data. On both occasions, spatial resolutions of acquired images were improved by IQT, but HCP data did appear more visually enhanced with hippocampal neuroanatomical landmarks more appreciable on the HCP data (see Fig 6.2 and Fig 6.3 as illustrative example). It was much more difficult to appreciate the Vestigial hippocampal sulcus (VHS), an important landmark for commencing hippocampal segmentation (Dalton et al.,2017) on the data acquired from the Prisma. The algorithm which works on single images recover information via extrapolation and image reconstruction and is spatial domain based. The pre-processed images had initially been acquired by high resolution. Any trade-offs between spatial resolution, SNR and acquisition times would have already been established prior to processing with IQT. Fig 6.4 demonstrates the different segmentation modalities and procedures employed (manual and automatic).

A.   **B.**
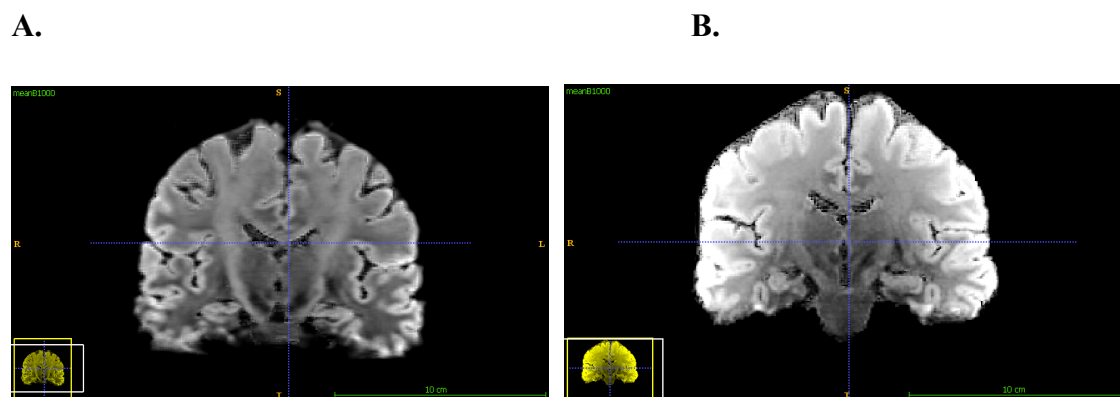
Figure 6. 2 Comparing results of images after application of IQT to HCP data (A) and data acquired on the Prisma (B)

A.   **B.**
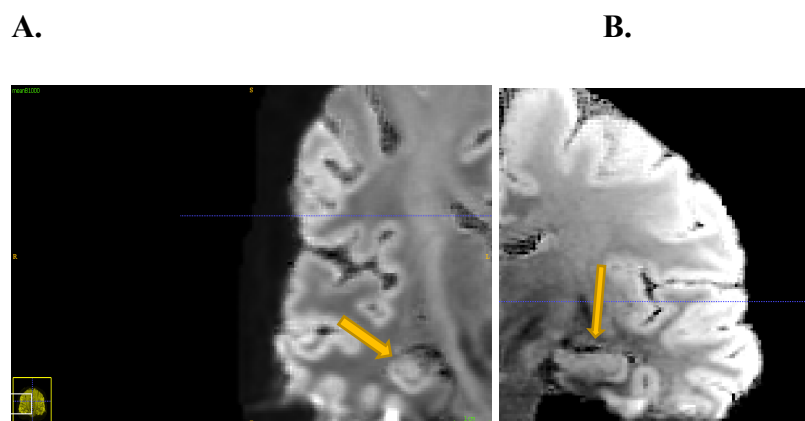
Figure 6. 3 Zooming into relevant region of interest (yellow arrow) on both sets of data at 6.5pixel/mm does away with blurring, but subregions of the hippocampus appear better appreciated on the HCP data (A) compared to the Prisma data (B).
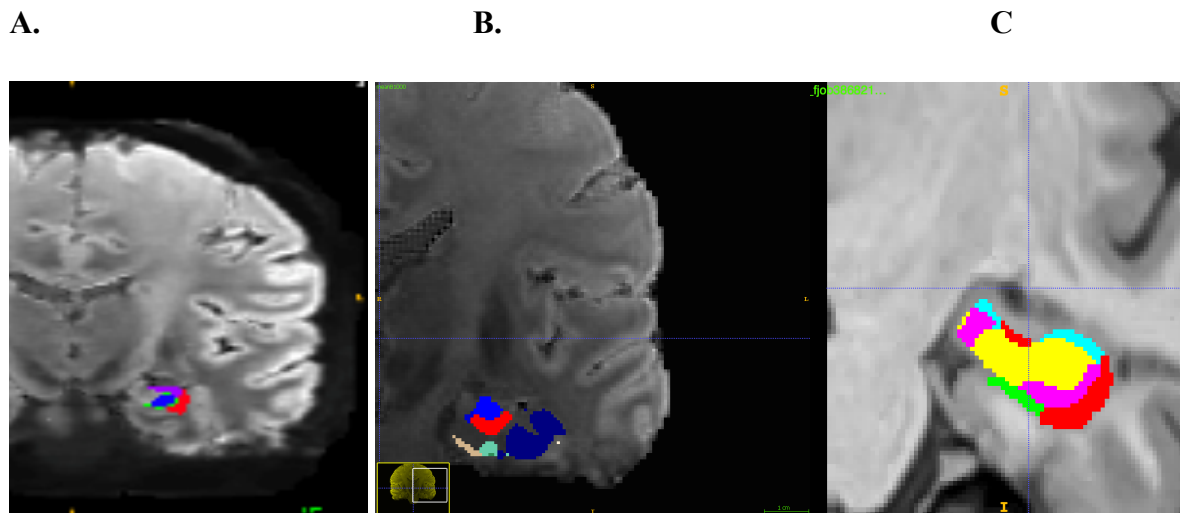
Figure 6. 4 Left hippocampus manual segmentation of HCP data (A) with representations of automatic segmentation (ASHS (B) and VolBrain (c)) of data from Prisma. HCP data- Data obtained from the Human Connectome Project. Prisma data- Data obtained from diffusion weighted imaging.

6.3.1 Between group differences

Some of the continuous outcomes violated statistical assumptions, so non-parametric analyses were used for some of the between-subjects comparisons (see table 9, Chapter 5). Non-parametric comparisons were employed for BDI, MADRS, FSS and in the analysis of mean diffusivity (MD) of the left hippocampal CA1. For the outcomes that met both assumptions, and to compare ordinal and continuous outcome variables, ANCOVA found significant main effects between PPMS and HC's (PPMS > HC) mostly on the left, but also on the right hippocampus. This occurred in the left CA1 MD $p = 0.019$, left DG MD, $p = 0.015$ and right PHC, $p = 0.032$. There was also significant group contrast in the right CA1 MD $p = 0.022$. Similarly, there were significant differences amongst left and right DG volumes ($p = 0.003$, $p = 0.023$ respectively) and left CA1 volume $p = 0.014$. Post hoc testing found a significant difference between controls and PPMS, $p = 0.025$. With age introduced as covariate, effects of MD in left CA1 and DG were still significant if left uncorrected, $p = 0.05$ or less. Significant effects remained after multiple corrections using FDR. There were no other significant main effects detected for any other continuous parameters. FA was not

altered and there were no significant findings with the diffusion indices in RRMS relative to PPMS or healthy controls. There were also no correlations to clinical variables. See **fig 6.5 below** for the distribution of diffusivity parameters in the left hippocampus across the three significant subfields (CA1, DG and PHC), across the three groups.
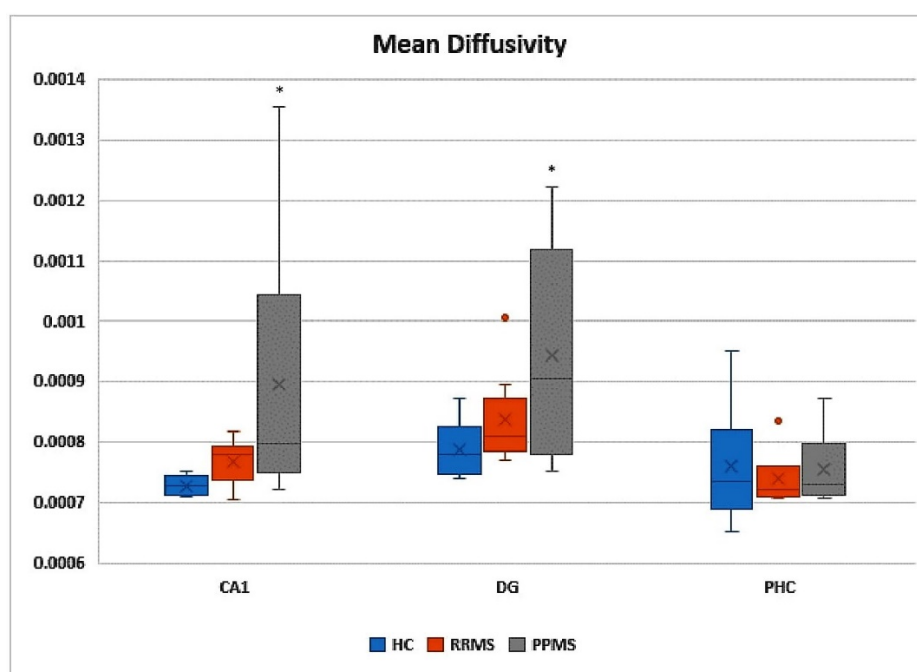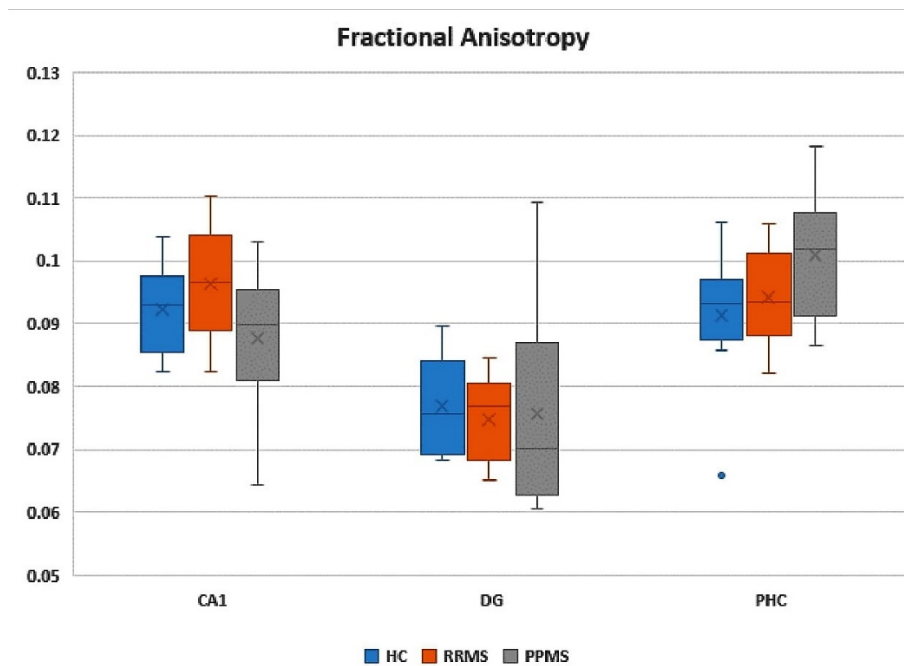
Figure 6. 5 Box and Whiskers plot comparison of MD and FA in the left hippocampal subfields (CA1, DG and PHC) in PPMS, RRMS and HC groups. (*p< 0.05, PPMS > HC).

6.3.2 Calculation of Cohen's d effect size and Sample size determination for future studies.

Effect sizes were estimated by calculating the Cohen's *d*, which was determined by calculating the mean difference between two groups and dividing obtained result by the standard deviation. **Cohen's *d* = (M$_2$ – M$_1$)/SD.** We chose the subfield with the strongest effect (CA1) and focused on MD, with a view to interpret the effect size between PPMS and HC. Sample size employed was 14, (PPMS, n=6, HC, n=8). Cohen's d estimate was calculated at approximately 0.5, depicting a medium effect size. The estimate derived was then used to inform power and sample size calculation for future studies, using the G*Power sample calculation software (Kang, 2021). Power was set to 80% (0.8), a percentage commonly applied to detect an effect size of 0.5 (Kang, 2021). An even ratio for the two selected groups was utilized (same number of participants in MS and control groups). Power calculation deduced a total of 64 participants in each group, a suggested sum total of 128 participants. Demonstration of distribution of plot is displayed below in Figure 6.6.
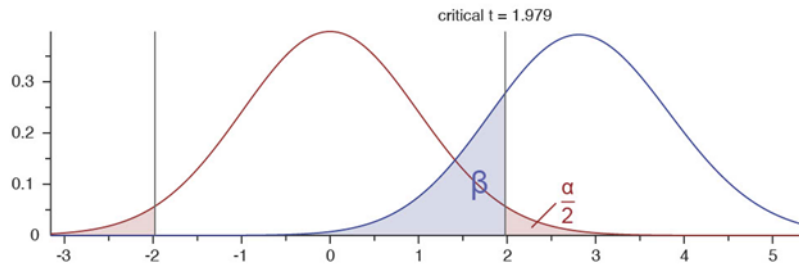
Figure 6. 6 Distribution of plot, Power sample size calculation.

6.4 DISCUSSION

Compared to controls, apart from the significant differences of BDI, MADRS and FSS which were applicable to both MS types (PPMS and RRMS) (see Chapter 5), the other major significant findings were only pertinent to PPMS and controls, only affected MD, and were predominantly seen in the left hippocampus. These findings were consistent with notable findings from the systematic review (Chapter 2), where significant increases in MD were observed in the left hippocampus of MS patients compared to controls (Roosendaal et al., 2010). There were increases in diffusion-based MD parameters in relevant included studies which correlated with progression in MS and reflected more sustained and progressive neurodegenerative pathology possibly elicited by microscopic barrier disruptions and extracellular fluid expansion. The lack of statistically significant changes in FA possibly further supports scope for a more significant role of FA in the earlier forms of MS pathology (CIS) where reductions are noted (Planche et al., 2016), or could indicate declining sensitivity during measurement, linked to grey matter neuro- axonal losses which are characteristic of MS disease progression. Arguably, it may also generally be due to inadequate population size. Mean diffusivity measures the rate and direction of water molecules within the brain tissue and is suggested to reflect indirect measures of structural integrity. Values obtained from MD are used to describe microstructural properties in cortical grey matter (Kwon et al., 2015) and serve as potential biomarkers for neurodegenerative processes (Andica et al., 2019).

The finding of MD alterations in hippocampal grey matter of PPMS patients exclusively is noteworthy and support the idea of separate pathogenetic mechanisms underlying PPMS and

RRMS respectively. There have been varying discussions on the patho-aetiological significance of PPMS, with reference to being either a piece of a broader spectrum of the actual clinical disorder (MS), or perhaps, an entirely distinct phenomena existing on its own (Trapp et al., 2008; Mahad et al., 2015). Distinguishing PPMS from the more prevalent RRMS is vital both clinically and radiologically, due specifically to the underlying contrasting pathological mechanisms, clinical and radiological features and in particular, a consequent difference in therapeutic response and application of pharmacological interventions. Currently, Ocrelizumab, a monoclonal antibody that eliminates specific B cells is the only treatment licensed for PPMS in the UK. Generally, PPMS is clinically viewed as a phase or type of MS that typically lacks recurrent remissions and exacerbations and is characterised by increasing neurological deficits. Compared to RRMS, PPMS has a much lower prevalence (10-15%), higher disability, equal female/male ratio, and onset is usually around the 5th decade, unlike RRMS which is more common in the 3rd decade and has a higher female predominance (Ebers, 2004; Rice et al., 2013; Scalfari et al., 2018). Radiologically, lesions are observed to be more prominent on the spinal cord in PPMS compared to presence in the brain as seen in RRMS. Further, and with respect to pathological mechanisms and pharmacological response, research evidence also suggests that substantial differences exist between PPMS and RRMS (Lassman et al., 2012; Claes et al., 2015; Dargahi et al., 2017). RRMS is known to cause more active, acute inflammation compared to PPMS (Lassmann et al., 2018). Substantially, acute and relapsing MS is reflected by intense BBB leakage chiefly affecting white matter, characterised by focal bulk invasion of T and B lymphocytes, whereas progressive MS depicts a more gradual neurodegenerative process appearing in either grey or white matter, characterised by intact blood brain barrier, and a moderate build-up of T and B lymphocytes in the connective tissue spaces (Lassman et al., 2012).

Indeed, PPMS is generally believed to affect the deep grey structures (Mesanos et al., 2011; Anderson et al., 2010). In keeping with available literature, grey matter pathology in MS is largely identified as more profound with PPMS and affects both cortical and subcortical areas (Filip et al., 2021). Atrophy, neuronal death and microglial activation are all synonymous with cortical pathological damage in comparison to white matter pathology where there is more vigorous and active inflammation (Peterson et al., 2001, Fisher et al., 2008). The left hemisphere of the brain has also been implicated more commonly in inflammation induced cognitive pathology (Harrison et al., 2015); Haroon et al., 2014). Interestingly, there was no

significant differences seen in the BICAMS cognitive scores amongst MS types and controls. MD in the CA1 and DG subfield of the left hippocampus, were the areas sensitive to changes, and were significantly different amongst the PPMS and control groups as observed in our pair wise comparisons, and possibly indicative of microstructural alterations in these areas. MD represents a directional average of diffusion coefficient and tends to increase when there is tissue loss or an increase in the content of free water. Expansion of extracellular fluid and micro-barrier disruptions as reflected by increases in MD are also indicative of progressive MS neurodegenerative pathology. Increases in MD are also known to correlate with neurological disability in MS. As indicated in the results, there were significant increases in statistical mean of MD in the above regions. Other regions showed group microstructural variations in diffusion parameter mean, but these were not statistically significant. Geurts, 2007 post-mortem studies does report hippocampal demyelination occurring in CA1, and also in the parahippocampal gyrus, with the presence of type III subpial cortical lesions (21.6%). Essentially, inflammation occurring in PPMS is reported to involve connective tissue spaces such as the meninges and large perivascular spaces (Lassman et al., 2018). Mixed lesions are also reported to extend from the PHC to CA1 in histological studies (Guerts et al., 2007). Finally, there was also statistical significance (p = 0.03) amongst groups (HC < PPMS) of differences in volumes of the left dentate gyrus. Mean volume was found to be larger in PPMS compared to controls. Interestingly, literature looking at DG expansion in MS via surface-based mesh modelling techniques, reported morphological alterations in DG, more prominent on the left side, corresponding to a larger radial distance when compared to controls (Rocca et al., 2015). Surface expansion in this regard has been suggested to reflect an inflammation adapted reactive subgranular zone attempting to remedy hippocampal circuitry functions (Rocca et al., 2015).

Overall, the specificity of alterations to the PPMS subtype we observed in our study, albeit limited by the extremely small sample size, is relevant to the distinction in aetio-pathogenesis of different MS subtypes. A potential limitation when considering IQT-enhanced pathological images compared to healthy brains, is the inability to capture very subtle parameter variations most especially with regards to multi-shell modalities like NODDI (Alexander et al., 2017), hence focus was mainly on DTI parameters in the Prisma data.

6.5 CONCLUSION

This study provides preliminary evidence of the sensitivity of diffusion MRI in distinguishing progressive MS from healthy controls on the basis of microstructural alterations and volume changes in hippocampal subfields. Notably, and of particular interest are group variations in CA1, and the dentate gyrus, demonstrating a key role of these regions in MS progression. Further research with larger population samples and other diffusion parameters would be useful.

CHAPTER 7. EXPLORING NEURONAL AND GLIAL MORPHOMETRIC ALTERATIONS IN THE ANTERIOR HIPPOCAMPUS OF MULTIPLE SCLEROSIS PATIENTS USING DIFFUSION-WEIGHTED MR SPECTROSCOPY.

7.1 INTRODUCTION

As elaborated in prior chapters, substantial experimental, clinical and postmortem evidence indicate hippocampal predilection and involvement in Multiple sclerosis (MS) neuro-inflammatory pathology, with consequential cognitive and affective sequalae. Excessive levels of demyelinated lesions have been Identified and subsequently reported within the hippocampus of a staggering 78% (15/19) of chronic postmortem MS brains (Geurts et al., 2007). Indeed, both immunochemical staining procedures and translocator protein PET imaging studies have clearly revealed additional elevated glial activity around hippocampal lesions and have thus been indicative of ongoing cellular neuroinflammatory or neuroprotective processes (Colasanti et al., 2016, Nistico et al 2013). MS experimental studies in mouse models have further shown elevated growth factors and progenator cellular activities reflective of astrocytic and oligodendrocyte involvement in the inflamed hippocampus (Azin et al., 2015). Elevated Glial fibrillary acidic proteins (GFAP) which are markers of astrocyte activation have also been reported in the hippocampus of EAE mice (Jukkola et al., 2013). Further, there is observed significant microglial involvement in synaptic pathology in the postmortem hippocampus of MS patients evidenced by lysosomal digestion and microglia engulfment (Tsouki & Williams, 2021), leading to a disruption in excitatory/ inhibition balance within the hippocampal synapses. More so, morphological changes in microglial cells have also been extensively reported in MS hippocampus, crucially in the early stages of the disease processes and have been further linked to specific hippocampal sub compartments or subregions. For instance, microglia hypertrophy in CA1 and hyper ramification in CA2/3, have been experimentally observed in early demyelinative processes (Roufagalas et al., 2021). Ultimately, metabolic dysfunction involving glial-neuronal dysregulation are perceived to drive neuronal death, and progressive disability in MS. Given its sub regional role in neurogenesis and apparent limited perfusion, further exaggerated in neuroinflammatory pathology, hippocampal subfields like CA1 and DG are

particularly and uniquely vulnerable to metabolic demands. In view of specific cellular responses (including changes in morphology and motility) which also apparently appear to be characterized by region specific heterogeneity within the hippocampus, cellular profiling with both sensitive and specific invivo techniques targeted towards analyzing regional quantitative microstructural measures becomes highly relevant as markers in early pathological identification, and also as future therapeutic mechanistic targets (Roufagalas et al., 2021). However, current modalities (TSPO-PET, DWI), though relatively sensitive, are either too dear, fraught with methodological complexities or are generally not specific enough with respect to compartmentalized cellular responses (De Marco et al., 2022).

Diffusion weighted MR Spectroscopy (DW-MRS) has been reported to be quite unique and provides a distinctive approach to investigating compartment specific microstructural changes in diseased tissue environments (Ronen et al., 2013, Kan et al., 2012). By directly measuring the apparent diffusion coefficients (ADC) of intracellular neuronal and glial metabolites with sufficient concentrations to establish MR signals, DW-MRS is reported to provide specific patterns of spectroscopy and information about cellular morphology in MRS experiments. NAA, for instance, is almost entirely located in the neurons, while choline is generally accepted to be more concentrated within glia cells (Choi et al., 2007). NAA has critical roles in myelin formation, being vital precursors in the synthesis of steroids and fatty acids (Wood et al., 2012), and is also widely accepted as a biological marker of neuronal health and density. Choline compounds are considered biomarkers in cellular proliferation and demyelination (Allaili et al., 2016). With regards MS pathology, mitochondrial dysfunction or neuronal axonal loss in thalamic grey matter has been associated to a decrease in the ADC of NAA, while cellular energy metabolic impairments have also been associated with decreases in total creatine (tCr) (Bodini et al., 2018). DW-MRS has also been used to successfully investigate changes in glial and axonal microstructure in the corpus-callosum of SLE patients (Ercan et al., 2016), and revealed group disparities in brain metabolites (creatine and choline) amongst SLE patients and healthy controls. However, the DW-MRS technique is not without limitations, as low concentrations of metabolites, especially applicable to certain regions of interests, do equate to lesser sensitivity and similar issues with spatial resolution when compared to other quantitative imaging modalities. Likewise, diffusion MRI on its own, lacks specificity of signal source due to the ubiquity of water in living tissue. Hence, despite the hippocampus being vastly implicated in neuroinflammatory/ neurodegenerative disease conditions, it has scarcely been evaluated with MRS modalities,

possibly due to a smaller surface area, its anatomical location (poor homogeneity) and apparent complexities (lower spectral resolution), as well as other potential technical challenges that span poor signal to noise ratios (Allaili et al., 2016) to issues with partial volume effects. This is further compounded with apparent difficulties in positioning of the voxel.

This study provides the first insight into the use of DWMRS on the hippocampus, and as an exploratory measure, utilizes the technique in measuring changes in the apparent diffusion coefficients (ADC) of glial (CHO) and neuronal (NAA) metabolites in the anterior hippocampus of MS participants and healthy controls. We also measured ADC's of Cr metabolites. Resultant peak analysis was carried out and the area under the peak for the above metabolites was recorded and calculated for analysis. Our principal aim as indicated in Chapter 1, was to foster a multi-modal approach, combining initial diffusion tensor measurements with diffusion measurements from DW-MRS, hereby enhancing on both sensitivity and specificity in effectively analyzing and comparing microstructural and cellular changes in recruited MS participants (grouped into subtypes: PPMS, RRMS) as well as healthy controls.

7.2 DW-MRS ACQUISITION/ANALYSIS

Supine position was adopted for participants during scanning and participants were encouraged not to move during the process. MRI and DW-MRS data were acquired with 3T (Siemens Magnetom Prisma, Siemens Healthineers, Erlangen, Germany). Acquired in sagittal orientation, and reconstructed in three orthogonal planes, T1W MPRAGE was acquired following a standard localizer (TR= 2400 ms; TE= 2.22 ms, TI= 1000 ms, flip angle = 8 deg, FOV 256 X 256 mm^2, matrix size 192 X 192). Voxel resolution of 1.35mm was placed on the left hippocampus, on the head, the body and parts of the hippocampal tail. VOI was selected based on prior experimental and clinical research depicting microglia activation in the hippocampus of MS brain (Colasanti et al., 2016, Politis et al., 2012). The DW-MRS sequence was a bipolar sequence based on a semi-LASER sequence and was utilized for DW-MRS (Genovese et al., 2021) with TE= 100 ms, TR= 3000 ms, band width= 2500 Hz, Vector size= 1024. Weighting conditions b= 0 s/mm^2 and the other three b= 3500 s/mm^2. The number of diffusion weighting directions were set at 3 and the number of gradient amplitude

values was set at 1. Diffusion gradients were applied in three orthogonal directions [1, 1, -0.5, 1], [-0.5, 1, 1], [-0.5, 1, 1] in the VOI co-ordinate system. B_0 shimming using FASTMAP (fast automatic schimming technique by mapping along projections) with echo planar signal trains were used for adjustments after the beginning of each voxel measurement (Gruetter and Tkac, 2000).

Spectral analysis was performed offline using Matlab (Mathworks, Natick MA, USA) and with Linear prediction singular value decomposition (LPSVD). Peak estimates at high b value were averaged and ADC computed from resulting mean values. $_tNAA$, $_tCHO$ and $_tCr$ were estimated at b= 0 s/mm^2 spectra.

The preprocessing Matlab package consisted of two stages; 1) Based on water data, the generation of eddy current correction (ECC) file. 2) The generation of output spectroscopic files and preprocessing of DWS data. Key subprocesses were also necessary which included the generation of weighted average FID data, frequency drift correction, zero-order phase correction, eddy current correction and water peak removal.

For eddy current correction, the Matlab command script **ecc_siemens** was utilized to generate the appropriate dialogue for the selection of gradient directions (3 for this study), number of gradient values, and also for determining SVD parameter and bandwidth. Command script **dws_siemens** was required for metabolite DWS data processing, to determine gradient directions, gradient values, zero filling factor, ECC water file, spectral registration, inclusion range, where to threshold and water removal.

Processing pipeline was then commenced, and panel of figures containing corrected spectra was generated for analysis.

7.2.1 Statistical Analysis

Statistical analysis of data was accomplished by the Statistical Package for the Social Sciences (SPSS 23, IBM Corporation, Somers, New York.) and the StataCorp LLC, College Station, Texas 77845 USA statistical program. Generalised linear model and Mann-Whitney u-test was applied in the analysis.

Data was expressed as Mean values and standard deviations. Parameters included were NAA, Cr, and CHO. Due to exploratory nature of study and in order to avoid type 2 errors, no correction for multiple testing was performed, as is conventional in such types of studies. Pearson correlation analysis was used to examine the relationship between metabolite concentration and diffusivity parameters. *p*-values of less than 0.05 were deemed significant statistically.

7.3 RESULTS

Mean metabolite ADC values, as well as their SD's, for all three groups (PPMS, RRMS and HC's) are shown in Table 11, and group ADC distribution for all three groups are demonstrated in Fig. 7.2. When the mean ADC's of all three groups were compared with ANOVA, there were no significant differences among the groups (tCho) ($P = 0.5071$), (tNAA) ($P = 0.9728$) and (tCr) ($P = 0.32471$). Pairwise comparisons showed that in the PPMS group, (tCho) was higher than in HC's (mean ADC (tCho) in PPMS = 8.0894E-05 ± 1.6404E-05 $\mu m^2/ms$, mean ADC (tCho) in HC = 6.0359E-05 ± 2.4923E-05 $\mu m^2/ms$, $P = 0.1891$), showing a moderately higher difference but not significantly so. There were also no statistically significant differences found in mean ADC (tNAA) and mean ADC (tCr) values between MS phenotypes and healthy controls. No significant differences were found between PPMS and RRMS metabolite mean ADC's. No correlations were found between metabolite ADC's and diffusivity indices.

A   **B**
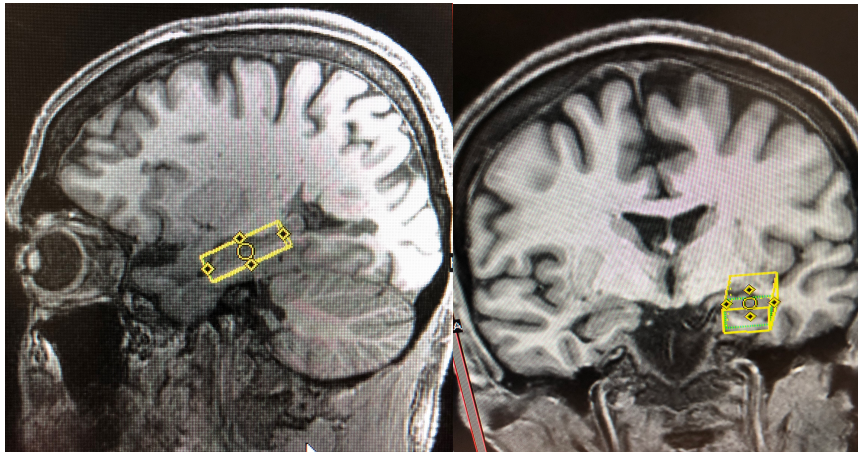
C
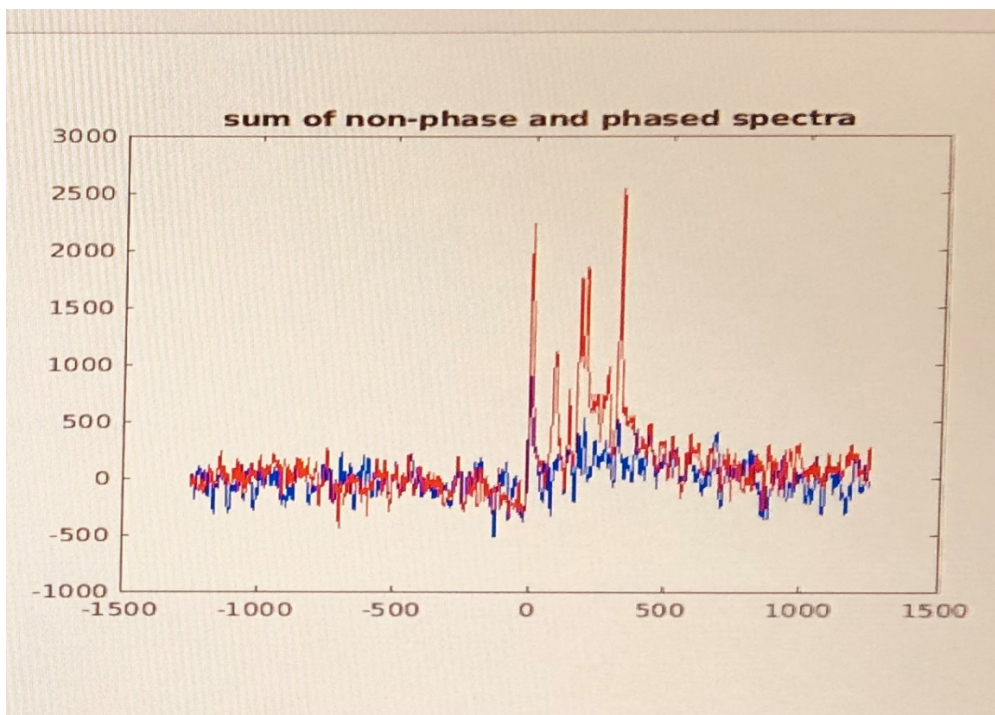
Figure 7. 1 Voxel location and Spectra (C). Sagittal (A) and Coronal (B). A and B show voxel location and angulation on the anterior hippocampus. C demonstrates the whole spectrum averaged before (blue) and after correction (red).

As represented in fig 7.1, the ADC of selected metabolites was quantified via a small 3mL voxel placed on the left hippocampus, covering the head, body and parts of the tail. These areas were particularly selected because they contain the relevant subfields investigated in prior chapters. Angulation of voxel was along the anterior-posterior axis of the hippocampus. Positioning of voxel was left-right 30mm, superior-inferior 10mm and anterior 10mm with all of the hippocampal head and body included. For interparticipant replication, voxel placement and location of the very first process was recorded and applied in other subsequent sessions.

High quality spectra without external contamination from the exterior, alongside effective water suppression was achieved in all cases, and the ADC's of NAA, Choline and Cr were computed using LPSVD (De Marco et al., 2022). (See 7.1, C, D).
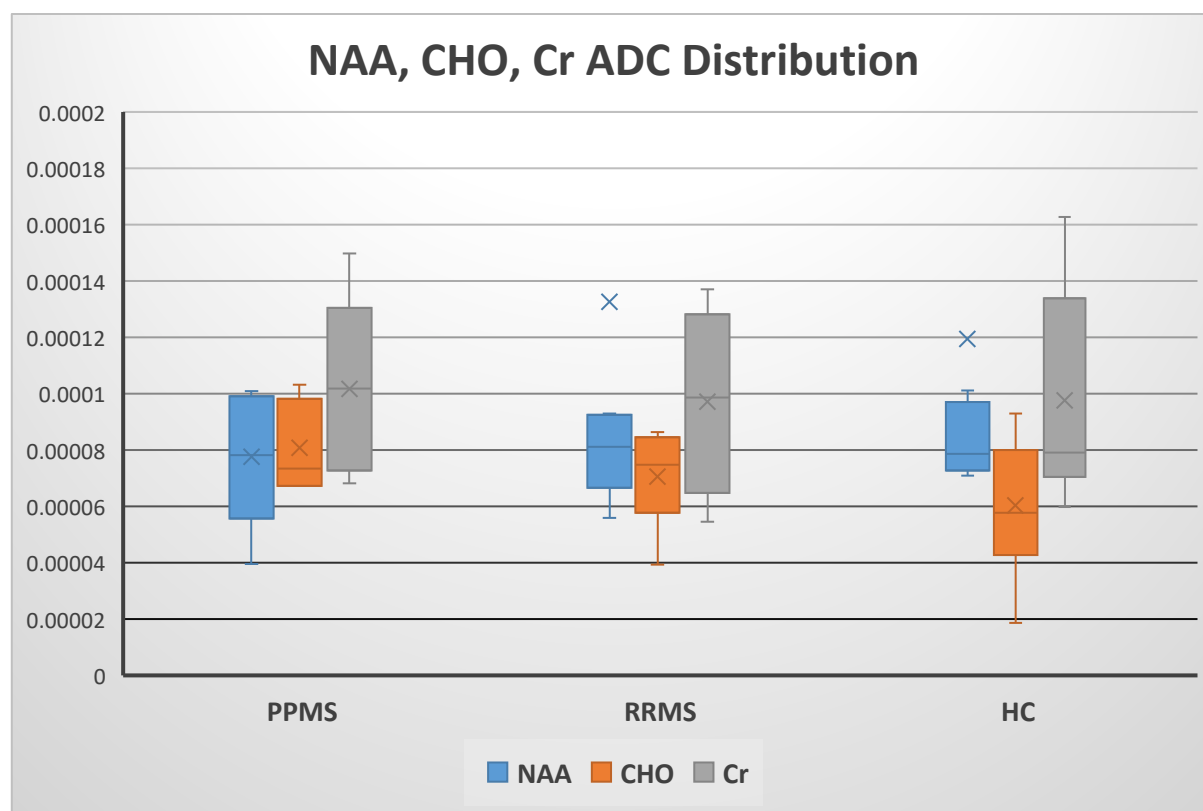
Figure 7. 2 ADC distribution of NAA, CHO and Cr in healthy controls, RRMS and PPMS participants.

ID NUMBERS	AMPLITUDE			FREQUENCIES			ADC		
ID	NAA	CHO	CR	NAA	CHO	CR	NAA	CHO	CR
30637[MS]	55475	49562	41112	2.0	3.2	3.0	1.44×10^{-4}	1.11×10^{-4}	5.99×10^{-4}
17352[HV]	39487	34412	32527	2.0	3.2	3.0	1.66×10^{-4}	2.05×10^{-4}	2.22×10^{-4}
31013[MS]	55593	Poor LW	Poor LW	1.9			5.27×10^{-4}		
30447[HV]	60295	46801	41413	1.9	3.2	3.0	1.65×10^{-4}	4.32×10^{-5}	1.38×10^{-4}
30822[MS]	38834	29839	23712	2.0	3.2	3.0	1.87×10^{-4}	2.62×10^{-4}	3.28×10^{-4}
28564[HV]	40173	31384	27090	1.9	3.2	3.0	1.74×10^{-4}	1.42×10^{-4}	1.41×10^{-4}
30745[MS]	50087	42066	42287	1.9	3.2	3.0	1.76×10^{-4}	1.56×10^{-4}	1.26×10^{-4}
24000[HV]	25203	?	?	1.9			9.07×10^{-4}		
31332[MS]	38253	30006	24814	1.9	3.2	3.0	1.98×10^{-4}	1.88×10^{-4}	2.59×10^{-4}
28544[HV]	33131	29248	14809	2.0	3.2	3.0	2.33×10^{-4}	1.72×10^{-4}	3.75×10^{-4}
31303[MS]	38993	27407	28651	2.0	3.2	3.0	9.15×10^{-5}	1.68×10^{-4}	1.78×10^{-4}
25[HV]	40167	49563	37129	1.9	3.1	3.0	1.94×10^{-4}	9.88×10^{-5}	1.74×10^{-4}
30770[MS]	43520	36810	22205	2.0	3.2	3.0	1.86×10^{-4}	1.93×10^{-4}	2.35×10^{-4}
30805[MS]	39854	25452	34700	2.0	3.2	3.0	2.12×10^{-4}	Poor LW on B=0	Poor LW on B=0

Table 12: Sample data, showing table of spectral quality, including Amplitude (Amp), Frequency, Linewidth (LW) and ADC values of NAA, CHO and Cr. ?-failed spectra, MS-Multiple Sclerosis, HV-Healthy Controls.

As seen in fig 7.2, Cr ADC appears to have the highest variability in diffusion coefficients across the three groups excluding the two outliers encountered in the NAA metabolite ADC. Choline coefficients are also greater in PPMS compared to RRMS and HC's. Results indicated that mean ADC's of all three metabolites (NAA, CHO, Cr) were not statistically significantly different between the three groups (p= 0.96, 0.21, 0.77) respectively.

Respective ADC means and standard deviations are reported in table 12 below.

	Groups	Mean	Std. Dev
NAA	HC	8.0204E-05	1.038E-05
	PPMS	7.7594E-05	2.4474E-05
	RRMS	7.9476E-05	2.6221E-06
	Total	7.9188E-05	1.4824E-05
CHO	HC	6.0359E-05	2.4923E-05
	PPMS	8.0894E-05	1.6404E-05
	RRMS	7.9429E-05	1.0125E-05
	Total	7.1018E-05	2.1553E-05
Cr	HC	9.7805E-05	3.7835E-05
	PPMS	0.00010173	3.2089E-05
	RRMS	8.4071E-05	2.561E-05
	Total	9.6366E-05	3.2328E-05

Table 13: Mean and Standard deviations of NAA, CHO and Cr ADC's. HC- Healthy controls (n=8), PPMS- Primary Progressive Multiple Sclerosis (n=6), RRMS- Relapsing Remitting Multiple Sclerosis (n=9).

7.4 DISCUSSION

This is one of the first studies examining compartment specific alterations in the microstructure of the hippocampus of MS patients scanned with 3 Tesla MRI. The study particularly explored diffusion related measurements of NAA, a predominantly neuronal/axonal metabolite and Choline, a glial metabolite, as well as Creatine which is thought to represent gliosis. There were observed differences in Choline ADC measurements amongst the three groups (RRMS, PPMS, HC), particularly identifiable in the PPMS group, but not statistically significant. These differences could be suggestive of activation and morphological changes of glial cells in hippocampal inflammation of this subgroup.

Growing research evidence stipulates glial activation as the central activity defining the neuroinflammatory process. Specifically, Microglial and Astrocytic morphological alterations, along with elevations in density are seen to be accordant with post-mortem data in a variety of prototypical autoimmune neuroinflammatory and neurodegenerative conditions (De Marco et al., 2022). Neuropathological mechanisms of functional conditions have also been linked with microglia and astrocytic alterations. Both neuro-resident immunocompetent cells are reported to undergo morphological and functional changes during the

neuroinflammatory processes, thus making it somewhat difficult and abstruse to distinguish which or the other was sensitive to the measurement of choline ADC in this study.

When activated, glia release proinflammatory cytokines, nitrogen and oxygen species; neurotoxic factors that impact on neurogenesis and transmission across neurons. Morphologically, activated microglia assume an amoeboid shape portraying retraction and thickening (Davis 1994), while astrocytes become larger and gain processes that overlap. Experimentally, Lignuel et al. 2019 linked myoinositol sensitivity to astrocytic hypertrophy perhaps signifying a more microglial/ Choline sensitivity as Choline was unaffected during Lignuel's research. The Cuprizone model of neuroinflammation also supports the phenomena of increases in myoinositol ADC's to changes in astrocytes while increases in choline corresponded more to changes in microglial (Genovese et al., 2021b).

Prior studies; preclinical, clinical and post-mortem have implicated the hippocampus in MS neuroinflammatory pathology. Indeed, histopathological research evidence further depicts activation and reactivity of microglia in the hippocampal inflammatory process. In addition, there have been suggestions of direct connections between gliosis and elevated concentrations of total choline (Brooks et al., 2010). Mixed lesions were identified as the predominant lesion type in a post-mortem study (15/19 MS brains), showing significant hippocampal involvement in MS pathology. Ongoing chronic inflammatory activity and demyelination were also reflected using immunochemistry studies, as was observed by the presence of HLADR-positive microglia at the lesion edges (Geurts 2007).

In similar studies looking at 45 recruited chronic MS participants, 28 were found to have extensive demyelination of the hippocampus. Microglial activation was observed in a few of the affected regions with chronic lesions being in the majority (Papadopoulos et al., 2009). In this study, significant hippocampal atrophy was identified and was evidenced by notable neuronal losses in the CA1/2/3 regions of the hippocampus spanning about 27-30%.

Essentially, there are more slowly expanding lesions in PPMS which is linked to chronic inflammation that continues to cause myelin and axonal damage (Arnold et al., 2021). On pathological exam, PPMS is also described as having high proportions of mixed lesions and an accumulation of activated microglial (Singhal et al., 2021). The resultant neurodegenerative Sequela in PPMS, composed of atrophic changes as well as loss of neuronal structure and function entails immuno-inflammatory processes that give rise to

neuronal damage and vascular injury. Glial reactivity which is evoked consequentially from tissue injury include microglial hypertrophy (Graeber & Streit, 2010).

Glial intracellular diffusivity is reported to be congruous with inflammation induced microglial activation and activities. There is expansion of cytosol diffusivity following increases in intracellular space and reduced intracellular tortuosity that results from morphological changes (soma thickening and cellular hypertrophy) which are linked to inflammation instigated microglial responses (Sofroniew, 2009).

Despite extensive identification of microglial activation at MS lesional sites by in vivo quantitative imaging using mostly TSPO-PET modalities (Colasanti et al., 2016, Politis et al., 2012), It is still generally and widely unclear as to their specific role. While often involved in the pathologic mechanistic process, they are also known to play neuroprotective and tissue repair roles (Davalos et al., 2005; Melton et al., 2003; Nimmerjahn et al., 2005; Taylor et al., 2005). Morphological changes akin to length and size reductions, reduction in arborization and decreased branching have been reported in post-mortem studies of neurodegenerative conditions (Davies et al., 2017). Changes have been classified as being rod like, amoeboid, activated and ramified (Leyh et al., 2021), with cellular functions (surveillance and maintenance in the brain) shown to be invariably associated with these changes (Giordano et al., 2021). Pre-clinical animal studies have specifically depicted the presence of rod microglia in CA1 in status epilepticus with hippocampal pathology (Wyatt-Johnson et al., 2017) also signifying the possibility of hippocampal subfield specificity with links to glial morphometric changes.

Compared to controls, reductions in NAA (creatine referenced in some reports) have been identified in grey matter mixed and unspecified lesions in relation to RRMS and progressive MS (Chard et al., 2002; Inglese et al., 2004; Kapeller et al., 2001; Tiberio et al., 2006; Wylezinska et al., 2003). Quantification of Cr metabolite during MS pathology is still widely indefinite as there are variations in the alteration of CNS concentrations during MS pathology. Reports indicate Cr reductions in the grey matter in RRMS lesions and also in the progressive grey matter (Bodini et al., 2018; Helms, 2001; Sijens & Oudkerk, 2005).

Ercan et al (2016) carried out similar studies to this, but using 7T MRI, and using a combination of DWMRS and DTI on the anterior body of the corpus callosum of patients with neuropsychiatric lupus (NPSLE), comparing to systemic SLE and controls. The study also considered average diffusivity measurements of similar metabolites (NAA, Choline and

Cr), and found significantly increased diffusion of total creatine and total choline, compared to HC's. This was in contrast to my study, were there was slight reductions in creatine ADC values during pathology more so in RRMS, than in PPMS. Contrasting diffusivity co-efficient patterns, perhaps, could be attributable to systematic contributions (ischaemia, micro-infarcts and strokes), and the role of astrocytes in SLE. Analogous to findings in this study and in general, there were indications of glial reactivity in response to inflammation. Notably, and also similar to this study, the Ercan study also had increases in mean diffusivity on DTI.

7.5 LIMITATIONS

There are several technical challenges associated with the medial temporal region of the brain in which the hippocampus is located (Choi & Frahm, 1999; Knight-Scott et al., 2003). For instance, several sinuses and the petrous bone are located adjacent to the hippocampus, and these result in larger susceptibility gradients with linewidths that are broader and associated with poorer homogeneity of β_0 magnetic field, and in relation to other brain regions like the corpus callosum, a reduction in spatial resolution.

Further, spectral quality as well as data reliability and reproducibility tend to be impacted upon due to the combination of poor SNR, reduced spectral resolution and the apparent difficulties in positioning voxels.

7.5 CONCLUSION

In this study, we show that obtaining DWMRS spectra in the hippocampus was achievable, enabling computation of Choline, NAA and Cr ADC in a small group of RRMS (n=6); PPMS (n=4) patients; and controls (n=7). Results show that application of DWMRS choline ADC is of interest, particularly in the PPMS group where there seems to be an early signal in a direction consistent with the hypothesis.

CHAPTER 8. SUMMARY, LIMITATIONS, HINDERANCES AND FUTURE DIRECTIONS

8.1 SUMMARY

The studies reported in this thesis were directed at investigating the use of Multi-modal MRI techniques in the characterization of hippocampal neuroinflammatory pathology in patients with MS. Chapter 2 of the thesis consisted of a systematic review of the literature which is currently published in the Journal of Clinical and Experimental Immunology (British Society of Immunology). The focus of the review was on imaging measures of hippocampal neuroinflammation in three selected prototypical autoimmune neuroinflammatory conditions which included the primary condition of focus, MS. A summary of the findings highlighted significant differences between MS patients and controls particularly with more progressive forms of MS. There were also notably, the exclusion of separate subfields in the analysis of microstructural alterations and immunocompetent cell density in MS hippocampal inflammation. Key observations were contrasting changes in radial distance in CA1 and DG, increases in diffusion-based MD parameters and reductions in diffusion-based FA consistent with ECF expansion and microscopic barrier disruptions. There were also correlations of these quantitative imaging markers with cognitive and affective alterations.

My second analysis reported in Chapter 3 initially highlighted the issues surrounding hippocampal imaging such as problems with neuroanatomical location and complexities of the hippocampal structure such as the inhomogeneity of the hippocampal interior. Partial volume effects, reductions in spatial resolution and diffusion weighting and problems with co-registration post-acquisition were also identified as issues with diffusion imaging in the hippocampus. In this chapter, I focused on a novel innovative approach (IQT), an algorithm that effected the resolution enhancement of acquired images from the Human Connectome Project (HCP). I then subsequently performed manual segmentation of selected hippocampal subfields using obtained directionally averaged b=1000smm^{-2} images and was able to deduce and compare diffusion parameter estimates (DTI and NODDI) separately across hippocampal subfields. The key findings of the analysis in this chapter was the difference in DTI and NODDI parameter distribution across the designated hippocampal subfields. I was also able to infer that the characterisation of microstructural alterations in hippocampal pathology

might be more accurate and precise at subfield levels compare to the more generally applied global analysis of the hippocampus.

In Chapter 4, I introduce my clinical study and present the methodology employed to apply clinical and imaging assessments to a cohort of patients with MS and healthy control subjects.

In Chapter 5, I did a clinical and behavioural study of all my recruited participants with the aim of characterising the clinical measures derived from cognitive and affective domains that reflect involvement of the hippocampus. I achieved this by administering and rating neuropsychiatric diagnostic questionnaires, and reported depressive, cognitive, fatigue and disability related scores across MS subtypes and healthy controls. I also compared cognitive and affective scores at baseline to post treatment with DMT's (Ocrevus). The summary of findings during this analysis included significant differences between MS subtypes and controls for BDI, MADRS and fatigue scores. Higher disability scores and a shorter duration of disease were noted amongst PPMS compared to RRMS and interestingly, rates of depression were only observed amongst the RRMS subtype (40%). There were also positive correlations between fatigue and depression scores.

In the fourth analysis (Chapter 6), I explored potential microstructural alterations (significant changes in diffusion parameters) with the right and left hippocampus of recruited MS subtypes, as well as with healthy controls. I also looked at significant changes in subfield volumes within these groups. I then explored possible correlations to clinical and demographic variables. I found mean diffusivity changes mostly in the left hippocampal subfields (CA1 and DG) and right parahippocampal gyrus (PHC). There were also some significant variations in volumes.

In the fifth and final set of analysis (Chapter 7), I explored the use of DWMRS in measuring the ADC's of three selected metabolites (NAA, CHO and Cr) within the hippocampus of the three established groups (PPMS, RRMS, HC's). I was able to obtain DWMRS spectra in the hippocampus of the above three metabolites and compute their ADC's from each group. The result of this analysis showed some early signals in the application of DWMRS choline ADC in the PPMS subtype which was consistent with evidence that depicts sensitivity to glial morphometric changes during neuroinflammation.

8.2 LIMITATIONS

In general, technical challenges deriving from the complexities of structures within the medial temporal lobes and limbic regions have limited and influenced the use of diffusion weighted imaging and spectroscopy techniques in highly specialised structures such as the hippocampus. Some of such limitations may have also had impacts on this study.

Firstly, the neuroanatomical location of the hippocampus for instance, places it in close proximity to other structures, including the CSF, and this could have led to partial volume effects that may have invalidated some of our quantitative measurements in diffusion. Additionally, the sinus and petrous bone located adjacent to the hippocampus could have had an impact on spectral resolution due to poor homogeneity of the β_0 magnetic field and large susceptibility gradients. To mitigate against the former, thorough checks were carried out on diffusion parameters obtained and, where excessive deviations were computed or observed as was the case in a few data; subfield delineation and segmentation of affected data were thoroughly re-inspected, and adequate soft-ware tools applied to manually correct these errors. For the later, B_0 shimming was performed using a fast-automatic shimming technique, FAST (EST) MAP (Gruetter and Tkac, 2000) for the minimization of B_0 variation. For high quality spectral results, analysis of spectra was transferred offline using customised software implemented in Matlab (Mathworks, Natick MA, USA). Linear prediction singular value decomposition (LPSVD) was applied for spectral analysis, with aspects of processing such as line broadening to increase SNR, Zero-filling factor for increased spectral resolution, water removal and correction methods for phase/frequency drift corrections.

Secondly, the minute size of the hippocampus and again its midbrain location was expected to contribute to lower SNR's. Indeed, uncertainties and difficulties with voxel positioning across participants may have put reliability of acquired results in question. Hence, records of exact voxel positioning and measurements were saved for initial data to ensure exact reproducibility on subsequent scans. A moderate to large voxel size was adopted compared to the size of the hippocampus to also ensure feasibility.

Thirdly and with regards to the clinical scales utilized in this study, adopting open designs meant that participants were not blinded to any procedures. These applied mostly to returnee participants and also to the cognitive scales. Already having experienced baseline processes,

participants who returned for post-treatment procedures may have invested more time and effort to enhance their performances prior to visiting the imaging centre to re-take the cognitive tests. Observer bias could have also been introduced due to the necessary interactions between investigator and participants, as well as due to non-blinding of the investigator. However, the cognitive tests purposely selected for the study, the BICAMS, is relatively immune from potential bias as it offers objective measures of cognitive performance (J. Campbell et al., 2016).

Lastly, the unavoidable and insufficient sample size of recruited participants to the study could have in effect reduced the statistical power of the study and limited my ability to draw any strong conclusions. It is possible that the inability to see significant effects in FA, RRMS, around the right hippocampus and in aspects of the DWMRS study in general, could be linked to being underpowered.

The important specific criteria which sought to recruit participants that were naïve to disease modifying treatments (DMT's) was somewhat problematic in recruitment (more so with the impact of Covid), but was equally crucial to determining pathologically induced changes unaltered by pharmacological interventions and free from confounds. Hence, a trade-off between recruitment of drug naïve, low EDSS, MS patients, to having a reasonable sample size, was preferred to keep the sample free and clean from drug and very high disability confounds.

I have also mostly focused on PPMS which is quite rare and difficult to recruit. A combination of time constraints with a limited window for recruitment which spanned first diagnosis to the start of DMT's left little room for manoeuvre in this regard.

I did employ some statistical applications to correct for any errors. While using complex analytical procedures (MANCOVA), I have avoided non-essential variables and also applied non-parametric tests for non-normally distributed data where necessary. I have also carried out false discovery rate analysis (FDR) to correct for multiple comparisons. I also estimated effect size in selected subfield and group, using deduced mean diffusivity parameters, to inform power and sample size calculations for future studies.

8.3 HINDERANCES, AND IMPACT OF COVID-19

This project had a few hinderances. Firstly, and most importantly, sample size, which mostly resulted from the impact of the COVID pandemic. This hampered planned recruitment strategies already put in place. Remote measures were immediately adapted to salvage the impact but having a clinical component requiring initial assessments and pre-screening did not allow for complete mitigation. Hence contact with eligible patients were limited. It took vigorous efforts to recruit and establish the current sample size. This included obtaining an honorary contract with the neurology department and weekly attendance at neurology multi-disciplinary team meetings. Efforts were also made to establish primary contacts with MS specialists who were having direct contact with recruitable MS patients. This worked to an extent but was also subject to too many intermediaries in terms of consultant neurologists, clinical fellows and specialist nurses, which ultimately had an effect on recruitment. There was also some degree of reluctance on available neurologists and specialist nurses to recruit patients with recent diagnosis of MS into the study possibly because of the immediate impact of learning of such a severe diagnosis.

The impact of the pandemic also had other silent effects, psychologically and emotionally which seemed to affect morale in general. Social distancing meant that scan appointments had to be rationed or delayed, and some pre-scan screening and procedures had to be adapted remotely.

Secondly, there were technical lapses which had some effects on the speed of data analysis, especially computational aspects. There was only one neuro-science server which was being utilised by several researchers, resulting into rotational use at various instances. Processing of commands or codes in itself were slowed to an extent and errors would amount in some instances due to this effect with re-coding where necessary. This slowed down data analysis in general and did not allow for processing of some diffusion parameters. To mitigate, technical support was sort from MRI physicists and other technical alternatives were also partly utilised. In future perhaps, multiple computational systems and servers could be employed.

8.4 CONCLUSION

The study initially and extensively investigated 'state of the art' quantitative imaging modalities used to investigate and analyse hippocampal inflammation in prototypical autoimmune neuroinflammatory conditions, via systematic review methodology. I was able to highlight on current imaging modalities in use, post-acquisition procedures and the relevance of subfield specificity and vulnerability to neuroinflammatory pathological mechanisms.

This work further demonstrated the sensitivity and specificity of multimodal quantitative imaging techniques in characterising hippocampal pathology in the subtypes of MS. The focus was on Diffusion weighted MRI and MRS modalities with the aim of investigating subfield volumetric, tensor derived and spectroscopy neuroimaging properties. Unique resolution enhancing procedures (IQT) were also employed post acquisition, and preliminary studies with data from the human connectome project were processed to elaborate on individual hippocampal subfield differences.

The severity of depression as well as other clinical and neurological scales were also measured and correlations sought amongst subtypes of MS and a control group.

I was able to show statically significant differences in diffusion parameters and regional volumes amongst hippocampal subregions, particularly between the PPMS cohort and controls, and within CA1 and DG and the PHC, which was not only consistent with MS literature, but also contributory as considerations of subfield specificity in MS hippocampal pathology is quite limited in the research literature.

Uniquely, and the possibly for the first time, I was also able to show sensitivity of choline ADC to glial morphometric changes in the hippocampus of a relatively small cohort of PPMS patients, using DWMRS techniques.

8.5 FUTURE WORK

This work has shown the relevance of the analysis of sperate hippocampal subfields in neuroinflammation with a primary focus on MS. It showed the sensitivity of two diffusion modalities (DWI and DWMRS) combined with an innovative post acquisition resolution enhancing algorithm (IQT) in detecting microstructural alterations in the MS hippocampus compared to healthy controls. Significant differences in mean diffusivity was observed in pathophysiological relevant subfields (CA1, DG) and also in PHC, with variations in computed parameters also noticeable across selected subfields.

Future applications of above methods and measures could have a role in clinical practice for more accurate and rapid disease diagnosis, and/or in the development of therapeutic endpoints for relevant clinical trials.

The distinct cytoarchitecture, neurochemistry and cellular functions of the hippocampal subfields are considered to be responsible for the unique roles involving multiple cognitive processes, including spatial navigation and episodic memory (Yassa et al., 2011, Bakker et al., 2008, Brown et al., 2014). Physiologically, and related to aging, the CA3 subfield has been linked with object recognition, while the granular cells of DG have also been linked to pattern separation (Dillon et al., 2017). Hence, there is reported selective vulnerability to notable neurodegenerative processes as seen in Alzheimer's disease (Braak, 1991).

Differential and selective subfield vulnerability have been equally defined in affective pathology such as with depressive disorders (Small et al., 2011), and in essence, could indeed be determined by quantitative measurements of neuroinflammatory induced microstructural alterations, as demonstrated in this study, and by using our selected imaging modalities with the analysis of neuroimaging correlates.

Therefore, reliable and valid sub regional segmentation of the hippocampus, a vital post acquisition analytical procedure, is thus highly essential to the study of cognitive and affective correlates in MS, and could in effect be key to the production of beneficial biomarkers for early diagnosis, better understanding of neuroinflammatory pathological mechanisms (such as MS), and indeed, provide therapeutic end points for clinical trials in this regard.

Regarding a future in diagnostics, and clinical usability; When hippocampal segmentation is manually orchestrated, the determination of relevant anatomical land marks within the hippocampal interion can be an excruciating venture, due to structural complexities and insufficient resolution, and even though generally regarded as gold standard, issues resulting from biases also unfortunately abound. With much larger datasets, the process could also be labour-intensive and very time consuming as I readily realised while implementing my protocol on initial physiological data. Unless skilled, dedicated and credible manpower is available, I do not recommend the application of manual segmentation in daily medical diagnostics.

With automatic segmentation however, though partial volume effects, costs and intensity non-uniformity of gray levels due to over inclusion of surrounding CSF and boundary voxels can equally invalidate automated methods of segmentation; a careful selection of images in Atlas based methods (utilised in this study), as well as proper evaluation procedures to validate methods and applied software, including manual oversight, could in effect, prepare grounds for the utilization of these methods in clinical environments.

In general, and considering possible applications of end points to potential clinical trials, I strongly recommend a focus on hippocampal imaging measures when assessing the efficacy of DMT's on secondary affective and cognitive symptoms. In essence, this research showed sensitivity of the selected imaging modalities to detect changes in mean diffusivity parameters and glial activation in PPMS but not in RRMS, which was possibly indicative of extracellular fluid expansion and cellular activity in the former. Compared to levels in controls, increasing mean diffusivity within CA1 and DG, as depicted in this study, may indeed correlate with disease progression, and could ultimately shed more light on treatment response. Being indirect measures of microstructural integrity, hippocampal diffusivity parameters as measured in this study could represent disease specific biomarkers and inform on whether relevant medications (DMT's) impact on their proposed targets or potentially alter the supposed course of the disease or even symptoms of the disease.

In future, further studies may explore additional hippocampal sub regions and a wider range of diffusivity parameters as seen with NODDI, as well as investigate other clinical correlates. In addition, a much larger recruitment of MS participants would greatly increase statistical power to detect significant subtle changes.

Future work could also take into consideration, data from other diffusion MRI techniques such as ASL and ASE and explore oxidative metabolism within the inflamed hippocampal subregions as well as additionally examine metabolite concentrations with Single-voxel proton MRS. The exploration of other metabolites (myoinositol, lactate) and any potential significant changes associated with inflammation in the hippocampus could also be examined. The effects of subfield analysis can also be compared to that of global analysis of the hippocampus in terms of sensitivity to detect microstructural changes.

APPENDICES

***i)* Role of COVID-19 in Neuro-inflammation and Demyelination: A possible viral post-delayed neuro-biological link to Multiple Sclerosis and Depression.**

Introduction

Neuroinflammation is a complex biological, immune mediated response, which stems from biochemical and cellular processes within the nervous system, and has been implicated with depression, stress, injury, infection and neurodegenerative conditions. The process of neuroinflammation has been linked experimentally with the Coronaviruses over time and has been observed in isolated cases after infection with COVID-19. Combined with the intense and overwhelming psycho-social stressors involved, the post pandemic era is predicted to see a massive rise in psychiatric illnesses, especially depression, as well as a possible potential increase in demyelinating conditions like Multiple Sclerosis (MS).

Current Covid-19 cases worldwide stand at a staggering 521 million with recorded death figures currently at 6.26 million and recovery figures as at 2020 was 25,446,698. These figures and demographics continue to change even as this article is being written up. Global spread has been swift with almost every country of the World now having reported at least one case of COVID-19. Modelling predictions as once reported by researchers at the Imperial College London estimated the reproduction number (R_O) to be between 2 and 2.6, with the capability of spread within 12 hours even before showing symptoms. The assumption at the time of the imperial report was that the rate of infection per country would increase exponentially, a doubling time of 5 days. The grim prediction, according to analysts from the Economic Intelligence Unit is that approximately 50% of the global populace will be infected due to the Pandemic. As it stands, millions of cases have been officially reported worldwide.

It goes without saying that the financial, social, economic, and most importantly, health impact have been catastrophic, and has continued to be felt worldwide with far reaching implications and consequences.

An important predictable effect from the entire ordeal experienced by all affected was an expected impact on psychological health, with the already vulnerable being more impacted than others (Druss, 2020). When exacerbated by an additional drastic reduction in access to already underfunded psychiatric and psychological services plus an expected rise in the risk of the prevalence of depression and anxiety; the potential fallout from the pandemic, mental health wise, was truly devastating (Holmes et al., 2020). Thus, there have been pockets of debates and reflections by both scientific and clinical communities alike, on what the likely long-term mental health related consequences of the pandemic could mean and potential measures to mitigate against the impact.

Reported major adverse consequences which stem from isolation, loneliness and direct contact with the virus include; anxiety, depression, undue distress, trauma driven stress responses, impairment in social and occupational functioning, self-harm and at the extremes; suicide (Holmes et al., 2020).

Alongside the psychosocial consequences of the COVID pandemic on global mental health, the direct neurobiological effects of COVID infection, and their potential etiopathogenetic role in the development of major psychiatric illness should also be considered.

Therefore as part of the remit of this thesis and considering the ongoing global impact of the pandemic, I will review existing evidence on the neurotropic characteristics of COVID19, and refer to rapidly growing literature reporting neurological sequelae of COVID19 infection. I will summarize laboratory findings from studies of other neurotropic coronaviruses illustrating the particular ability of triggering delayed neuroimmune responses that closely resemble those observed in neuroinflammatory autoimmune demyelinating diseases such as MS. Finally, I will refer to converging evidence from human and animal research indicating that those neuroimmune responses are involved in the genesis of affective and cognitive disorders and moderate the effects of stress on CNS integrity. I will also aim to provide mechanistic grounds for the hypothesis that the Covid19 will have direct and long-lasting detrimental effects on brain tissue integrity and function likely to result in the emergence of affective and cognitive sequelae in a significant proportion of affected individuals. Furthermore, I propose that the neuroimmunological response to COVID infection will

impact the susceptibility of affected individuals to the detrimental and pathogenetic effects of psychosocial stress.

Evidence that COVID-19 is neurotropic

Multiple cases with demonstrated acute CNS infections have been reported: the first case of viral encephalitis was reported by Beijing Ditan Hospital. The 56-year-old patient in question had severe symptoms including decreased consciousness and failed to respond to regular treatment. CT scan was uneventful, but gene sequencing of cerebrospinal fluid (CSF) sample confirmed the presence of the novel coronavirus. Neurological symptoms resolved after he was treated for viral encephalitis.

Another recorded case from the Henry Ford Health system in Michigan (USA) was of acute hemorrhagic necrotizing encephalopathy associated with COVID-19. In this case, the 58-year-old female patient involved had initially presented with a 3 day history of the tale signs of COVID-19 infection (fever, cough, muscle aches). She would later develop signs of confusion, lethargy, and disorientation. After a positive COVID-19 test, further Neuroimaging tests, which included a Brain CT revealed symmetric hypoattenuation within the bilateral medial thalami. Brain MRI also showed hemorrhagic rim enhancing lessions within the bilateral thalami, medial temporal lobes and subinsular regions. Patient was treated with intravenous immunoglobulins.

Reported evidence of the presence of neurological symptoms are also backed by various studies in recent literature. Presence of headaches (8% of 38 patients), nausea and vomiting (about 1%) have been reported (Li et al., 2020). A recent retrospective review by (Mao et al., 2020) looking at the neurological manifestations of 214 COVID-19 patients in Wuhan, China, also found central nervous system symptoms including headaches, epilepsy, impaired consciousness, cerebrovascular disease and muscle injury in 78 patients (36%). Seemingly, neuroimaging findings have also provided evidence. There have been recorded accounts of notable MRI findings reported in a group of patients (12/27 with acute findings and 10/27 with cortical FLAIR signal abnormality), during a retrospective study of 749 patients across 8 hospitals. Specifically, a contrast enhanced cranial 1.5T MRI of a 59-year-old patient involved in the study showed symmetric white matter hyperintensity and right frontal cortical

hyperintensity. There was also prominent linear hyperintensity within the frontal sulci. Another similar contrast enhanced image from the study, in a 48-year-old COVID patient with neurological symptoms showed bifrontal cortical hyperintensity. Pial subarachnoid prominent linear hyperintensity was also scattered in some of the right frontal sulci in the image of this patient. Withal, cerebrospinal fluid (CSF) obtained in 4 of the patients with cortical signal abnormalities showed elevated total proteins (Kandemirli et al., 2020).

Can Coronavirus help in understanding the CNS Immuno-effects of COVID-19?

Other Human coronaviruses have been found to have effects on the CNS that could potentially help frame a bio-mechanistic model of neuro-immune reactions to COVID-19.

The SARS-COV for instance, responsible for a prior epidemic in 2003, which shows close genetic similarities to COVID-19 (SARS-COV-2), exhibited the propensity to induce neurological disease. With regards SARS-COV, points of entry into the nervous system could be directly through the olfactory nerve or indirectly, through blood circulation and neuronal pathways. Post-mortem studies show infiltration of monocytes and lymphocytes in the vessel wall, ischemic changes of neurons and demyelination of nerve fibers. Following on, patients affected with COVID-19 have also exhibited neurological symptoms such as epilepsy, headaches, disturbed consciousness, sudden loss of smell and taste, which are all indicative of intracranial infections. In both SARS-COV and SARS COV-2 infections, utilizing genomic sequencing, viral presence have been duly confirmed in the cerebrospinal fluid (CSF), further supporting the notion of their capabilities to cause CNS damage, potentially via neuroinflammation (Wu et al., 2020).

More mechanistic explanations can be derived from several experimental models and research studies that demonstrate involvement of other Human Coronaviruses in the pathophysiology of autoimmune demyelinating neurological conditions, such as MS.

The mouse hepatitis virus (MHV), a member of the enveloped Coronaviridae, which shares similar nucleocapside protein properties with SARS-COV (Ding et al., 2017), have been implicated in ongoing myelin loss and have been shown to establish and sustain chronic CNS infection by cleverly avoiding CD8^{+} T cells which are important in controlling the acute phase of infections.

Experimentally, intracerebral innoculation of adult mice with MHV results in the infection of both glial and neuronal cells, resulting in encephalomyelitis and chronically, in the development of white matter pathology associated with focal CNS demyelinating lesions. Following infection, there is subsequent remyelination and recurrent demyelination, similar to MS like brain pathology. Intriguingly enough, MHV infection of rodents can amplify the course of Experimental autoimmune encephalomyelitis (EAE) (Talbot et al., 2001).

A potential coronavirus post-delayed neurobiological mechanistic approach spanning infection pathway to demyelination can thus be elaborated based on an MHV experimental model. Based on the MHV model, and on gaining entry into the CNS, infection and replication will occur in the ependymal cells lining the lateral ventricles (LV). This would be accompanied by spread of the virus into the parenchyma and subsequent infection of the glial cells (astrocytes, oligodendrocytes, and microglia). The glial cells (especially microglia) become activated, increase in number and undergo morphological changes. The activated cells signal and enhance the entry of innate components (neutrophils, macrophages, and natural killer (NK) cells) via the secretion of proinflammatory cytokines (TNF-α, IL-6 and CXCL10) and disruption of the blood brain barrier (BBB). Viral replication in the ependymal cells and drainage of viral antigen into the cervical lymphnodes through the cerebrospinal fluid is thought to activate the adaptive immune response. The adaptive phase ensues with further spread of the virus within the parenchyma. Virus specific CD4^{+}and CD8^{+} T cells are called into play. They secrete IFN-Υ and enhance the secretion of proinflammatory chemokines (CXCL9, CXCL10, CCL5) from astrocytes. These aim to reduce viral replication in the glia cells. There is a subsequent decrease in the number of inflammatory cells. However, viral persistence is associated with the retention of immune effectors in the CNS.

Host control of the MHV infection result in a slowly resolving but chronic CNS disease that is associated with neuroinflammation. The chronic pathological change is likened to the neuroinflammatory disease processes observed in Multiple Sclerosis (MS), the prototype of cellular immune mediated CNS disorders (Bergmann et al., 2006).

The neurotropic JHM strain of MHV is a well-accepted model of viral induced neurologic disease that imitates the histopathological and clinical characteristics of MS. In addition, the Human corona viruses, HC$_O$V group (229E and OC43) have exhibited neurotrophic properties and have been detected in neural tissue, in some cases of MS patients, using various scientific and investigatory procedures in identification (Talbot et al., 2001).

Potential COVID-19 Neuroinflamatory/ Immunological effects
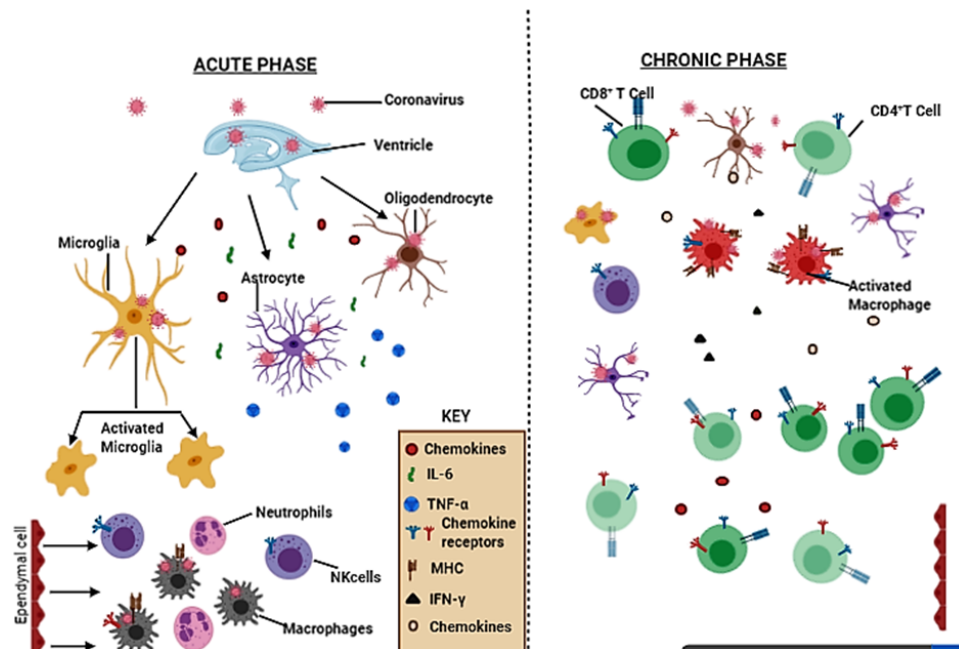
We thus speculate on the possibility of a rise in post-delayed virus-host auto-immune mediated demyelinating conditions such as MS, and further hypothesize that these neuro-inflammatory processes will lead to the genesis of affective and cognitive symptoms.

Immunological mechanisms leading to depression associated to autoimmune encephalitis

The Experimental autoimmune encephalomyelitis (EAE) is a known complex model in rodents during which neuro-immuno pathological mechanisms lead to inflammation, demyelination, axonal loss and gliosis; which are indeed key characteristics of MS like pathology (Constantinescu et al., 2011). Following interleukin -1β (IL-1β) perfusion, EAE models have been associated with synaptic pathology, alterations in GABAergic transmission, disruption of long-term potentiation (LTP) and alterations of synaptic plasticity in the hippocampus (Nisticò et al., 2013). Hippocampal neurogenesis in the rodents with EAE is also affected due to alterations in neuronal progenitor proliferation in the subgranular zone of the dentate gyrus (Giannakopoulou et al., 2013). Accumulating evidence from post-mortem analysis further implicates microglial mediated complement (C1q and C3) deposition in the loss of synapses and reduction in synaptic density (Michailidou et al., 2015).

Putative Interactions between COVID19-induced psychosocial stress and neuroinflammation

Central and additional to the interplay of the above biological factors is the impact of apparent psychological or life stressors, which have been imposed by COVID-19 infections in addition to the psychosocial impact of lock down. Based on the current scenario, probable evidence suggests that the intense psychological stress in everyone affected, as clearly experienced as a direct or indirect consequence of COVID-19 infections, will predictably promote the development of depressive disorders. Psychological stress is known to activate neuro-endocrine pathways that alter immune response. Stress on its own has been proposed to potentiate immunological priming during neuroinflammatory processes, via a signal cascade in the brain (HMGB-1, NLRP3) that amplifies neuroinflammatory response, modifies behavioral reaction and indeed, predisposes individuals to psychiatric disorders (Frank et al., 2016). Experimental pro-inflammatory challenges induced by viral infection alongside prior stressors can exacerbate neuroinflammatory reactions and manifest endophenotypic presentations tenable in psychiatric disorders such as changes in cognition and mood (Frank et al., 2016). Microglial, which secrete an array of inflammatory mediators including proinflammatory cytokines, chemokines, prostaglandins and reactive oxygen/nitrogen species, are reported to be set in a primed activation state by exposure to psychological stressors and are indicated as key in further inducing an exaggerated neuroinflammatory response. Essentially, microglia that become altered by stress-induced factors, display morphological and immunophenotypic cellular changes, that potentially lead to aberrant peripheral and central inflammatory processes. These processes have been seemingly demonstrated by observed monocyte trafficking to the brain in experimental models involving mice that underwent prolonged stress exposure and began to show anxiety like behaviors. Furthermore, though there is the lack of a clear-cut evidence indicating its role in the development and persistence of MS, existing literature continues to support a strong link of MS with stressful life events. Animal and human data reviewing the interaction of two major stress response systems (the hypothalamo-pituitary-adrenal axis and the autonomic nervous system) have been implicated, and are hypothesized to be associated with the pathogenesis and progression of MS (Gold et al., 2005).

Current research evidence also suggests that treatments or experimental challenges that raise pro-inflammatory cytokines induce symptoms of psychological distress, and potentially lead to depressive syndromes in the general population. Depression is found associated with higher levels of inflammatory biomarkers, cytokines, and expression of genes involved in the inflammatory response (Farooq et al., 2017). Furthermore, there is an increased incidence of affective disorders in immune mediated inflammatory disease cohorts (Marrie et al., 2017). These findings suggest that immune dysregulation and the activation of the inflammatory response system might play a causal role in the development of major depression. Mechanisms underlying the link between inflammation and depression include role of cytokines directly crossing the blood brain barrier, crosstalk between peripheral and central immune systems and the dysregulation of the hypothalamic-pituitary-adrenal axis (Miller and Raison, 2016).

Based on this evidence, we speculate that the vast number of Covid-19 infections globally, via a combination of both psycho-social and biological factors (Neuroinflammation), will lead to neuropsychiatric sequele, a depression Pandemic of some sort.

Basic diagram displaying potential interplay between combination of psychological and biological factors
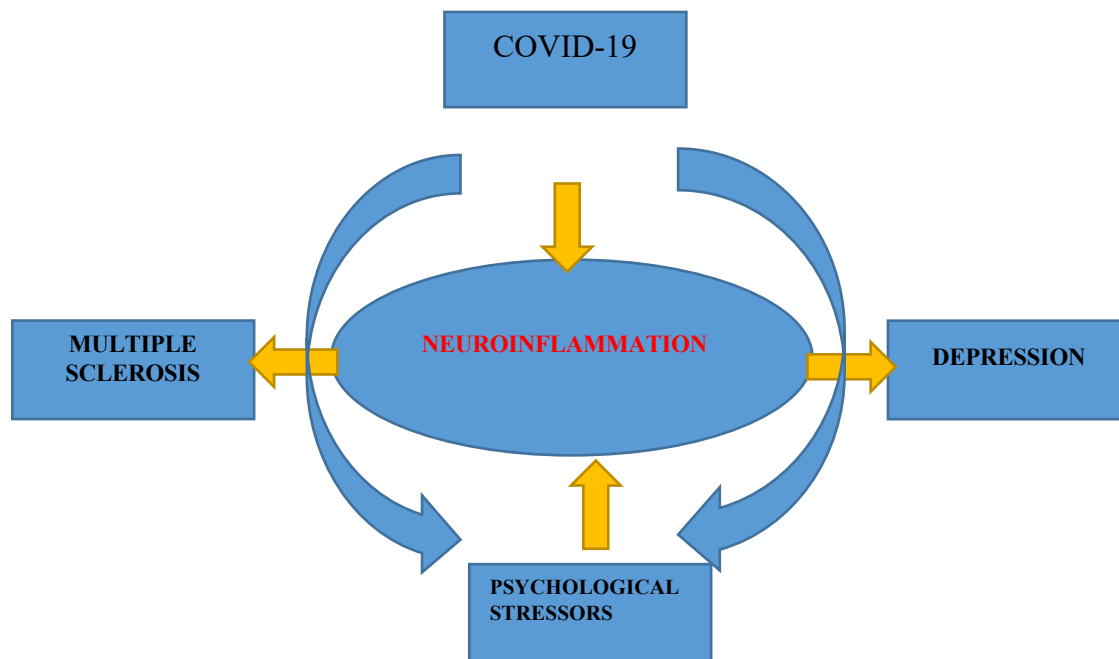
Conclusion and suggestions for future research

Coronaviruses have been previously implicated to delayed auto-immune responses which have been shown, using experimental models, to lead to neuroinflammation, demyelination and CNS tissue damage. Peripheral and central inflammation are biologically linked to Major depression. Chronic neuroinflammation, axonal damage and demyelination also characterise MS.

SARS-COV and currently, COVID-19 show similar neurotrophic pathologic potentials. Having pandemic status, the psycho-socio-economic impact alone has been devastating and will also induce stress mediated neuroinflammatory responses in the CNS.

Based on prior evidence and biological models, microglial activation and priming is thought to play a key role in mediating and exaggerating these overlapping processes. The hippocampus is also particularly affected and has been implicated in the cognitive and affective pathologies surrounding demyelinating conditions such as MS.

***ii) NeuPsychPal*: Proposed novel online computer app, as a psychological intervention for chronic neuroinflammatory and disabling illness.**

Introduction

Neupsychpal was founded in 2021 and is projected to be a jointly owned UK based mobile and online computer app which would be geared to address the psychological pitfalls that are secondary to chronic debilitating neurological conditions, with an initial focus on MS.

Problem Statement: There are over 2.5 million people across the globe currently suffering with MS.

Over 1 million in the US and 100 000 in the UK alone. Robust research evidence suggests a very high prevalence of depression amongst people living with MS, about 50% life time prevalence and 25% annual prevalence. Research evidence also further suggests worsening morbidity, prognosis and quality of life when both conditions occur co-morbidly.

Current or conventional psychological methods aimed at treating such complexes combined with a potential treatment resistant mode of depression is insufficient. Albeit, waiting times are fraught with difficulties and lengthy periods, making the general wellbeing of an already chronic and debilitating situation, even more gruesome.

In addition, these therapies seem too general, and appear not to be personalised enough.

Value Preposition: Neupsychpal is proposing to offer targeted psychotherapeutic modalities via a mobile app for long- term and debilitating health conditions (MS) which will comprise the;

- Coping with Pain and stress
- Behavioural activation

- Social Prescribing
- Psychoeducation

Proposed Methods

Description

Potential psychotherapeutic packages for those with chronic autoimmune neuroinflammatory conditions with MS as a prototype (see appendix for selected literature)

Terms used (PICO Elements)

Patient/Population/Problem	Intervention	Comparison	Outcome
Multiple sclerosis, MS, depression, depressed, depressive, comorbidity, comorbid	Psychotherapy, psychiatric treatments, counselling, mental health services, support packages, self help		

Limits applied

Age group	Language	Publication Type	Time limit
Adult Humans	English	No limit applied	1980 onwards

Summary of resources searched and results

Source	Number of results
Medline	110
Embase	260
PsycINFO	119
HMIC (Health Management Information Consortium)	16
Cochrane Central Register of Controlled Trials (CENTRAL) and Cochrane Database of Systematic Reviews (CDSR)	124
Total before de-duplication	629
Total after de-duplication	460

Observations, market opportunities and competitive advantage

It's evident that there's a rising demand for digital healthcare amidst the pandemic and digital era

Digital healthcare seems to target urban dwellers as they seem to live the 'busy life'- hence disposable income or class could play a role and should be considered within this sector. Notions of a costly and self-interested 'commercialised self-care' is also apparent.

Focus seems to be on treatment and not prevention. As many digital wellness apps are not able to target root causative effects of individual challenges, focus is more on 'management' of these conditions.

To be distinct, Neurospsychpal can go beyond being 'just another app', especially within the digital space and can offer more interpersonal solutions even within a virtual world. - Hybrid offerings to better cater to varying generational audiences, and possibility of more interpersonal offerings may be a competitive advantage.

Wellness is defined in different ways to different people, thus Neurospsychpal must clearly define its wellness offerings and unique benefits should be clearly identified- not only to better identify target customers, but also to set itself apart within the market.
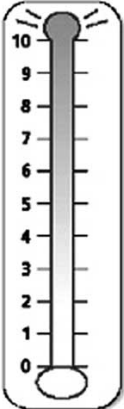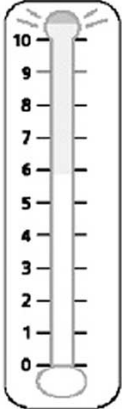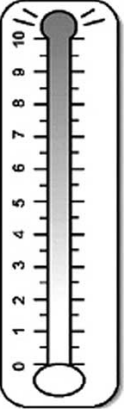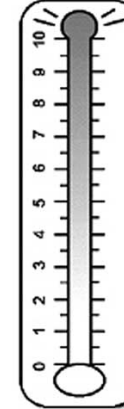
Many of the wellness apps are generic, thus a niche focus on MS-related mental health may be a unique strength

MS societies and national health organisations such as the NHS are reference points for MS patients and more general users, hence partnerships with these organisations may be benefitcial in reaching a greater audience and building trustworthiness.

iii) Emotional Thermometer

In the first four columns, please mark the number (0-10) that best describes how much emotional upset you have been experiencing in the past **two weeks**, including today.

In the next three columns please indicate how long you have been experiencing these emotional problems, how much impact they have had on you, and how much you need help for these.

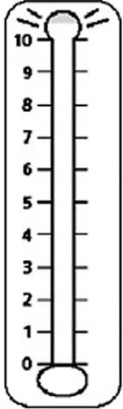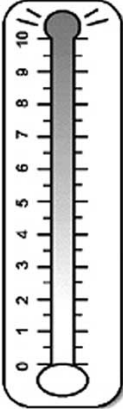| Emotional Upset			
1. Distress	2. Anxiety	3. Depression	4. Anger
10 = Extreme	10 = Extreme	10 = Extreme	10 = Extreme

Emotional Impact		
5. Duration	6. Burden	7. Need Help
10 = 10+ months	10 = Cannot function at all	10 = Desperately

0 = None	0 = None	0 = None	0 = None

0 = Just today	0 = No Effect on me	0 = Can manage myself

iv) Montgomery and Asberg Depression Rating Scale (MADRS)

Montgomery and Asberg Depression Rating Scale (MADRS)

The rating should be based on a clinical interview moving from broadly phrased questions about symptoms to more detailed ones which allow a precise rating of severity. The rater must decide whether the rating lies on the defined scale steps (0, 2, 4, 6) or between them (1,3,5).

It is important to remember that it is only on rare occasions that a depressed patient is encountered who cannot be rated on the items in the scale. If definite answers cannot be elicited from the patient all relevant clues as well as information from other sources should be used as a basis for the rating in line with customary clinical practice.

The scale may be used for any time interval between ratings, be it weekly or otherwise but this must be recorded.

1. Apparent Sadness
Representing despondency, gloom and despair, (more than just ordinary transient low spirits) reflected in speech, facial expression, and posture.

Rate by depth and inability to brighten up.

0 No sadness.
1
2 Looks dispirited but does brighten up without difficulty.
3
4 Appears sad and unhappy most of the time.
5
6 Looks miserable all the time. Extremely despondent.

2. Reported sadness
Representing reports of depressed mood, regardless of whether it is reflected in appearance or not. Includes low spirits, despondency or the feeling of being beyond help and without hope.

Rate according to intensity, duration and the extent to which the mood is reported to be influenced by events.

0 Occasional sadness in keeping with the circumstances.
1
2 Sad or low but brightens up without difficulty.
3
4 Pervasive feelings of sadness or gloominess. The mood is still influenced by external circumstances.
5
6 Continuous or unvarying sadness, misery or despondency.

3. Inner tension
Representing feelings of ill-defined discomfort, edginess, inner turmoil, mental tension mounting to either panic, dread or anguish.

Rate according to intensity, frequency, duration and the extent of reassurance called for.

0 Placid. Only fleeting inner tension.
1
2 Occasional feelings of edginess and ill defined discomfort.
3
4 Continuous feelings of inner tension or intermittent panic which the patient can only master with some difficulty.
5
6 Unrelenting dread or anguish. Overwhelming panic

4. Reduced sleep
Representing the experience of reduced duration or depth of sleep compared to the subject's own normal pattern when well.

0 Sleeps as usual.
1
2 Slight difficulty dropping off to sleep or slightly reduced, light or fitful sleep.
3
4 Sleep reduced or broken by at least two hours.
5
6 Less than two or three hours sleep

5. Reduced appetite
Representing the feeling of a loss of appetite compared with when well.

Rate by loss of desire for food or the need to force oneself to eat.

0 Normal or increased appetite.
1
2 Slightly reduced appetite.
3
4 No appetite. Food is tasteless.
5
6 Needs persuasion to eat at all.

v) Generalized Anxiety Disorder 7-item (GAD-7) scale

Generalized Anxiety Disorder 7-item (GAD-7) scale

Over the last 2 weeks, how often have you been bothered by the following problems?	Not at all sure	Several days	Over half the days	Nearly every day
1. Feeling nervous, anxious, or on edge	0	1	2	3
2. Not being able to stop or control worrying	0	1	2	3
3. Worrying too much about different things	0	1	2	3
4. Trouble relaxing	0	1	2	3
5. Being so restless that it's hard to sit still	0	1	2	3
6. Becoming easily annoyed or irritable	0	1	2	3
7. Feeling afraid as if something awful might happen	0	1	2	3
Add the score for each column	+	+	+	
Total Score (add your column scores) =				

If you checked off any problems, how difficult have these made it for you to do your work, take care of things at home, or get along with other people?

Not difficult at all _____
Somewhat difficult _____
Very difficult _____
Extremely difficult _____

Source: Spitzer RL, Kroenke K, Williams JBW, Lowe B. A brief measure for assessing generalized anxiety disorder. *Arch Inern Med.* 2006;166:1092-1097.

vi) Fatigue Severity Scale (FSS)

Fatigue Severity Scale (FSS)

This questionnaire contains nine statements that rate the severity of your fatigue symptoms. Read each statement and circle a number from 1 to 7, based on how accurately it reflects your condition during the past week and the extent to which you agree or disagree that the statement applies to you.

***A low value (e.g. 1) indicates strong disagreement with the statement, whereas a high value (e.g. 7) indicates strong agreement.

| *During the past week, I have found that:*	Disagree ⟷ Agree
1. My motivation is lower when I am fatigued	1 2 3 4 5 6 7
2. Exercise brings on my fatigue.	1 2 3 4 5 6 7
3. I am easily fatigued.	1 2 3 4 5 6 7
4. Fatigue interferes with my physical functioning.	1 2 3 4 5 6 7
5. Fatigue causes frequent problems for me.	1 2 3 4 5 6 7
6. My fatigue prevents sustained physical functioning.	1 2 3 4 5 6 7
7. Fatigue interferes with carrying out certain duties and responsibilities.	1 2 3 4 5 6 7
8. Fatigue is among my three most disabling symptoms.	1 2 3 4 5 6 7
9. Fatigue interferes with my work, family or social life.	1 2 3 4 5 6 7

Total Score: _____

vii) Epworth Sleepiness Scale

EPWORTH SLEEPINESS SCALE

How likely are you to doze off or fall asleep in the following situations, in contrast to feeling just tired? This refers to your usual way of life in recent times. Even if you have not done some of these things recently, try to work out how they would have affected you.

Check the box under the most appropriate response for each situation:

Date of Assessment ☐☐ ☐☐ ☐☐☐☐
Day   Month   Year

Time____

SITUATION	would never doze [0]	*slight* chance of dozing [1]	*moderate* chance of dozing [2]	high chance of dozing [3]
Sitting and reading	☐	☐	☐	☐
Watching TV	☐	☐	☐	☐
Sitting, inactive in a public place (e.g. a theater or a meeting)	☐	☐	☐	☐
As a passenger in a car for an hour without a break	☐	☐	☐	☐
Lying down to rest in the afternoon when circumstances permit	☐	☐	☐	☐
Sitting and talking to someone	☐	☐	☐	☐
Sitting quietly after a lunch without alcohol	☐	☐	☐	☐
In a car, while stopped for a few minutes in the traffic	☐	☐	☐	☐

viii) BICAMS

v **BICAMS tests**
Symbol digits modalities test A

Brief Visuospatial Memory Test
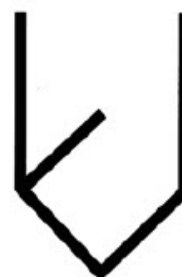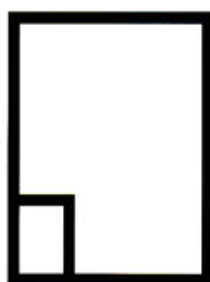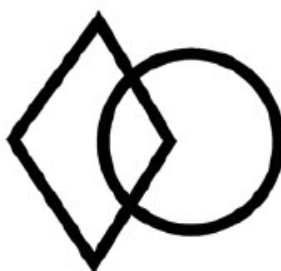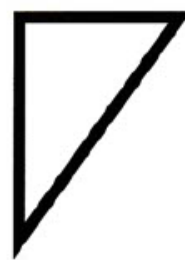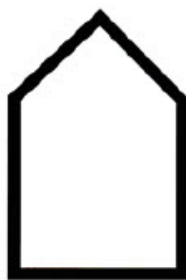
California Verbal Learning Test

List A Immediate Free Recall Trial 1

I'm going to read a list of words to you. Listen carefully, because when I'm through, I want you to tell me as many of the words as you can. You can say them in any order, just say as many of them as you can. Are you ready?

Read List A at an even pace, taking slightly longer than one second per word, so the entire list takes 18 to 20 seconds. Then say: **Go ahead.**

Trial 2

I'm going to read the same list again. Like before, tell me as many of the words as you can, in any order. Be sure to also say words from the list that you told me the first time.

Trials 3 and 4

I'm going to read the same list again. Like before, tell me as many of the words as you can, in any order, including words from the list you've said before.

Trial 5

I'm going to read the same list one more time. Like before, tell me as many of the words as you can, in any order, including words from the list you've said before.

Record all responses verbatim, in the order recalled. Prompt only once (e.g., Anything else?) at the end of each free and cued recall trial (i.e., after 15 seconds with no response or when the examinee says he/she cannot remember more words).

List A		Trial 1		Trial 2		Trial 3		Trial 4		Trial 5	
			Resp Type		Resp Type		Resp Type		Resp Type		Resp Type
truck	1	1		1		1		1		1	
	2	2		2		2		2		2	
spinach	3	3		3		3		3		3	
giraffe	4	4		4		4		4		4	
bookcase	5	5		5		5		5		5	
onion	6	6		6		6		6		6	
motorcycle	7	7		7		7		7		7	
cabinet	8	8		8		8		8		8	
zebra	9	9		9		9		9		9	
lamp	10	10		10		10		10		10	
coach	11	11		11		11		11		11	
celery	12	12		12		12		12		12	
cow	13	13		13		13		13		13	
desk	14	14		14		14		14		14	
boat	15	15		15		15		15		15	
squirrel	16	16		16		16		16		16	
cabbage	17	17		17		17		17		17	
	18	18		18		18		18		18	
	19	19		19		19		19		19	
	20	20		20		20		20		20	

Total Correct C
Total Repetitions R
Total Intrusions I

ix) Becks Depression Inventory_II

BDI - II

Instructions: This questionnaire consists of 21 groups of statements. Please read each group of statements carefully. And then pick out the one statement in each group that best describes the way you have been feeling during the past two weeks, including today. Circle the number beside the statement you have picked. If several statements in the group seem to apply equally well, circle the highest number for that group. Be sure that you do not choose more than one statement for any group, including Item 16
(Changes in Sleeping Pattern) or Item 18 (Changes in Appetite).

1. Sadness
   0. I do not feel sad.
   1. I feel sad much of the time.
   2. I am sad all the time.
   3. I am so sad or unhappy that I can't stand it.

2. Pessimism
   0. I am not discouraged about my future.
   1. I feel more discouraged about my future than I used to.
   2. I do not expect things to work out for me.
   3. I feel my future is hopeless and will only get worse.

3. Past Failure
   0. I do not feel like a failure.
   1. I have failed more than I should have.
   2. As I look back, I see a lot of failures.

   3. I feel I am a total failure as a person.

4. Loss of Pleasure
   0. I get as much pleasure as I ever did from the things I enjoy.
   1. I don't enjoy things as much as I used to.
   2. I get very little pleasure from the things I used to enjoy.
   3. I can't get any pleasure from the things I used to enjoy.

5. Guilty Feelings
   0. I don't feel particularly guilty.

1. I feel guilty over many things I have done or should have done.
2. I feel quite guilty most of the time.
3. I feel guilty all of the time.

6. Punishment Feelings 0. I don't feel I am being punished.
1. I feel I may be punished. 2. I expect to be punished.
3. I feel I am being punished.

7. Self-Dislike
0. I feel the same about myself as ever.
1. I have lost confidence in myself.
2. I am disappointed in myself.
3. I dislike myself.

8. Self-Criticalness
   0. I don't criticize or blame myself more than usual.
   1. I am more critical of myself than I used to be.
   2. I criticize myself for all of my faults.
   3. I blame myself for everything bad that happens.

9. Suicidal Thoughts or Wishes
   0. I don't have any thoughts of killing myself.
   1. I have thoughts of killing myself, but I would not carry them out.
   2. I would like to kill myself.
   3. I would kill myself if I had the chance.

10. Crying
   0. I don't cry anymore than I used to.
   1. I cry more than I used to.
   2. I cry over every little thing.
   3. I feel like crying, but I can't.

11. Agitation
   0. I am no more restless or wound up than usual.
   1. I feel more restless or wound up than usual.
   2. I am so restless or agitated, it's hard to stay still.
   3. I am so restless or agitated that I have to keep moving or doing something.

12. Loss of Interest
  0. I have not lost interest in other people or activities.
  1. I am less interested in other people or things than before.
  2. I have lost most of my interest in other people or things.
  3. It's hard to get interested in anything.

13. Indecisiveness
  0. I make decisions about as well as ever.
  1. I find it more difficult to make decisions than usual.
  2. I have much greater difficulty in making decisions than I used to.
  3. I have trouble making any decisions.

14. Worthlessness
  0. I do not feel I am worthless.
  1. I don't consider myself as worthwhile and useful as I used to.
  2. I feel more worthless as compared to others.
  3. I feel utterly worthless.

15. Loss of Energy
  0. I have as much energy as ever.
  1. I have less energy than I used to have.
  2. I don't have enough energy to do very much.
  3. I don't have enough energy to do anything.

16. Changes in Sleeping Pattern
  0. I have not experienced any change in my sleeping. 1a I sleep somewhat more than usual.

1b I sleep somewhat less than usual.
2a I sleep a lot more than usual.
2b I sleep a lot less than usual.
3a I sleep most of the day.
3b I wake up 1-2 hours early and can't get back to sleep.

17. Irritability
  0. I am not more irritable than usual.
  1. I am more irritable than usual.
  2. I am much more irritable than usual.
  3. I am irritable all the time.

18. Changes in Appetite
  0. I have not experienced any change in my appetite.
  1a My appetite is somewhat less than usual.
  1b My appetite is somewhat greater than usual.
  2a My appetite is much less than before.
  2b My appetite is much greater than usual.
  3a I have no appetite at all.
  3b I crave food all the time.

19. Concentration Difficulty
0. I can concentrate as well as ever.
1. I can't concentrate as well as usual.
2. It's hard to keep my mind on anything for very long.
3. I find I can't concentrate on anything.

20. Tiredness or Fatigue
0. I am no more tired or fatigued than usual.
1. I get more tired or fatigued more easily than usual.
2. I am too tired or fatigued to do a lot of the things I used to do.
3. I am too tired or fatigued to do most of the   things I used to do.

21. Loss of Interest in Sex
0. I have not noticed any recent change in my   interest in sex.
1. I am less interested in sex than I used to be.
2. I am much less interested in sex now.
3. I have lost interest in sex completely.

Total Score: _____

x) MRI Safety Questionnaire

Brighton and Sussex
medical school

Clinical Imaging Sciences Centre

MRI Safety Questionnaire

The MRI scanner uses a powerful magnetic field so we need to make sure that you are safe to enter the scanning room. Please remove all loose metal objects before your scan eg: keys, coins, credit cards, dentures, hearing aids, mobile phones / pagers, watches, hairclips, metallic body piercings and if you are requested change into the clothes provided.

Name	Date of Birth	Weight (kg)	Contact Number	Office Use Only CISC Number
	dd.mm.yyyy			

Address		Name and Address of GP

Do you have / ever had any of the following? If yes please include details and dates:	No	Yes	Details / Dates
Cardiac pacemaker/defibrillator?			
Heart surgery / valve replacement?			
Head surgery including that to the eye or ears (including a hydrocephalus shunt)?			
Any other surgery?			
Neurological stimulator or any other implanted medical device?			
Epilepsy?			
Skin patches? (HRT, nicotine, pain relief, contraceptive)			
Tattoos or permanent eye makeup? (See overleaf)			
Have you ever worked with metal? eg. Mechanics / metal sheet worker			
Have you EVER had metal fragments in your eyes?			
Shrapnel injury?			
Have you had a previous MRI scan at this centre?			

Women of child bearing age (12-65)		
Is there any chance of you being pregnant?	Yes	No

Patients / participants with false limbs or callipers please remove them before entering the MRI room. Inform a radiographer if you need assistance

I confirm that I have answered and understood the above questions and information, and that the information I have provided is correct to the best of my knowledge

Patient / Participant Signature (parent / guardian if under 16)	Date	Radiographer Signature	Date

Version 5
Created: Jan 2017
Review: Jan 2019

By JH

REFERENCES

Aboul-Enein, F., Krššák, M., Höftberger, R., Prayer, D., & Kristoferitsch, W. (2010). Reduced NAA-Levels in the NAWM of patients with MS is a feature of progression. A study with quantitative magnetic resonance spectroscopy at 3 Tesla. *PLoS ONE*, *5*(7). https://doi.org/10.1371/journal.pone.0011625

Albrecht, D. S., Granziera, C., Hooker, J. M., & Loggia, M. L. (2016). In Vivo Imaging of Human Neuroinflammation. In *ACS Chemical Neuroscience*. https://doi.org/10.1021/acschemneuro.6b00056

Alexander, D. C., Zikic, D., Ghosh, A., Tanno, R., Wottschel, V., Zhang, J., Kaden, E., Dyrby, T. B., Sotiropoulos, S. N., Zhang, H., & Criminisi, A. (2017). Image quality transfer and applications in diffusion MRI. *NeuroImage*. https://doi.org/10.1016/j.neuroimage.2017.02.089

Aminoff, E. M., Kveraga, K., & Bar, M. (2013). The role of the parahippocampal cortex in cognition. In *Trends in Cognitive Sciences* (Vol. 17, Issue 8). https://doi.org/10.1016/j.tics.2013.06.009

Anacker, C. (2014). *Adult Hippocampal Neurogenesis in Depression: Behavioral Implications and Regulation by the Stress System* (pp. 25–43). https://doi.org/10.1007/7854_2014_275

Anderson, V. M., Fisniku, L. K., Khaleeli, Z., Summers, M. M., Penny, S. A., Altmann, D. R., Thompson, A. J., Ron, M. A., & Miller, D. H. (2010). Hippocampal atrophy in relapsing-remitting and primary progressive MS: A comparative study. *Multiple Sclerosis*, *16*(9). https://doi.org/10.1177/1352458510374893

Appenzeller, S., Carnevalle, A. D., Li, L. M., Costallat, L. T. L., & Cendes, F. (2006). Hippocampal atrophy in systemic lupus erythematosus. *Annals of the Rheumatic Diseases*. https://doi.org/10.1136/ard.2005.049486

Arnold, D. L., & Matthews, P. M. (2002). MRI in the diagnosis and management of multiple sclerosis. In *Neurology*. https://doi.org/10.1212/wnl.58.8_suppl_4.s23

Assaf, Y., & Pasternak, O. (2008). Diffusion tensor imaging (DTI)-based white matter mapping in brain research: A review. In *Journal of Molecular Neuroscience*. https://doi.org/10.1007/s12031-007-0029-0

Azin, M., Mirnajafi-Zadeh, J., & Javan, M. (2015). Fibroblast growth factor-2 enhanced the recruitment of progenitor cells and myelin repair in experimental demyelination of rat hippocampal formations. *Cell Journal*, *17*(3).

Ballok, D. A., Woulfe, J., Sur, M., Cyr, M., & Sakic, B. (2004). Hippocampal damage in mouse and human forms of systemic autoimmune disease. In *Hippocampus*. https://doi.org/10.1002/hipo.10205

Barak, Y., & Achiron, A. (2002). Effect of interferon-beta-1b on cognitive functions in multiple sclerosis. *European Neurology*, *47*(1). https://doi.org/10.1159/000047940

Barkhof, F., Haller, S., & Rombouts, S. A. R. B. (2014). Resting-state functional MR imaging: A new window to the brain. In *Radiology* (Vol. 272, Issue 1). https://doi.org/10.1148/radiol.14132388

Bartsch, T., Döhring, J., Reuter, S., Finke, C., Rohr, A., Brauer, H., Deuschl, G., & Jansen, O. (2015). Selective neuronal vulnerability of human hippocampal CA1 neurons: Lesion evolution, temporal course, and pattern of hippocampal damage in diffusion-weighted MR imaging. *Journal of*

Cerebral Blood Flow and Metabolism.
https://doi.org/10.1038/jcbfm.2015.137

Bartsch, T., Schönfeld, R., Müller, F. J., Alfke, K., Leplow, B., Aldenhoff, J., Deuschl, G., & Koch, J. M. (2010). Focal lesions of human hippocampal CA1 neurons in transient global amnesia impair place memory. *Science*. https://doi.org/10.1126/science.1188160

Basser, P. J., Mattiello, J., & LeBihan, D. (1994). MR diffusion tensor spectroscopy and imaging. *Biophysical Journal*. https://doi.org/10.1016/S0006-3495(94)80775-1

Benedict, R. H. B., Amato, M. P., Boringa, J., Brochet, B., Foley, F., Fredrikson, S., Hamalainen, P., Hartung, H., Krupp, L., Penner, I., Reder, A. T., & Langdon, D. (2012). Brief International Cognitive Assessment for MS (BICAMS): international standards for validation. *BMC Neurology*, *12*. https://doi.org/10.1186/1471-2377-12-55

Benedict, R. H. B., Cookfair, D., Gavett, R., Gunther, M., Munschauer, F., Garg, N., & Weinstock-Guttman, B. (2006). Validity of the minimal assessment of cognitive function in multiple sclerosis (MACFIMS). *Journal of the International Neuropsychological Society*, *12*(4). https://doi.org/10.1017/S1355617706060723

Bergmann, C. C., Lane, T. E., & Stohlman, S. A. (2006). Coronavirus infection of the central nervous system: Host-virus stand-off. In *Nature Reviews Microbiology*. https://doi.org/10.1038/nrmicro1343

Bertholdo, D., Watcharakorn, A., & Castillo, M. (2013). Brain Proton Magnetic Resonance Spectroscopy: Introduction and Overview. In *Neuroimaging Clinics of North America*. https://doi.org/10.1016/j.nic.2012.10.002

Bodini, B., Branzoli, F., Poirion, E., García-Lorenzo, D., Didier, M., Maillart,

E., Socha, J., Bera, G., Lubetzki, C., Ronen, I., Lehericy, S., & Stankoff, B. (2018). Dysregulation of energy metabolism in multiple sclerosis measured in vivo with diffusion-weighted spectroscopy. *Multiple Sclerosis Journal*. https://doi.org/10.1177/1352458517698249

Bohbot, V. D., Allen, J. J. B., Dagher, A., Dumoulin, S. O., Evans, A. C., Petrides, M., Kalina, M., Stepankova, K., & Nadel, L. (2015). Role of the parahippocampal cortex in memory for the configuration but not the identity of objects: Converging evidence from patients with selective thermal lesions and fMRI. *Frontiers in Human Neuroscience*, *9*(AUGUST). https://doi.org/10.3389/fnhum.2015.00431

Boyle, E. A., & McGeer, P. L. (1990). Cellular immune response in multiple sclerosis plaques. *American Journal of Pathology*.

Brown, D. A., & Sawchenko, P. E. (2007). Time course and distribution of inflammatory and neurodegenerative events suggest structural bases for the pathogenesis of experimental autoimmune encephalomyelitis. *Journal of Comparative Neurology*, *502*(2). https://doi.org/10.1002/cne.21307

Brun, L., Pron, A., Sein, J., Deruelle, C., & Coulon, O. (2019). Diffusion mri: Assessment of the impact of acquisition and preprocessing methods using the brainvisa-diffuse toolbox. *Frontiers in Neuroscience*. https://doi.org/10.3389/fnins.2019.00536

Bulik, M., Jancalek, R., Vanicek, J., Skoch, A., & Mechl, M. (2013). Potential of MR spectroscopy for assessment of glioma grading. In *Clinical Neurology and Neurosurgery* (Vol. 115, Issue 2). https://doi.org/10.1016/j.clineuro.2012.11.002

Burdette, J. H., Durden, D. D., Elster, A. D., & Yen, Y. F. (2001). High b-value diffusion-weighted MRI of normal brain. *Journal of Computer Assisted*

Tomography, *25*(4). https://doi.org/10.1097/00004728-200107000-00002

Burgess, N., Maguire, E. A., & O'Keefe, J. (2002). The human hippocampus and spatial and episodic memory. In *Neuron* (Vol. 35, Issue 4). https://doi.org/10.1016/S0896-6273(02)00830-9

Cacciaguerra, L., Pagani, E., Mesaros, S., Dackovic, J., Dujmovic-Basuroski, I., Drulovic, J., Valsasina, P., Filippi, M., & Rocca, M. A. (2019). Dynamic volumetric changes of hippocampal subfields in clinically isolated syndrome patients: A 2-year MRI study. *Multiple Sclerosis Journal*. https://doi.org/10.1177/1352458518787347

Calabrese, P. (2006). Neuropsychology of multiple sclerosis: An overview. In *Journal of Neurology* (Vol. 253, Issue 1 SUPPL.). https://doi.org/10.1007/s00415-006-1103-1

Calsolaro, V., Matthews, P. M., Donat, C. K., Livingston, N. R., Femminella, G. D., Guedes, S. S., Myers, J., Fan, Z., Tyacke, R. J., Venkataraman, A. V., Perneczky, R., Gunn, R., Rabiner, E. A., Gentleman, S., Parker, C. A., Murphy, P. S., Wren, P. B., Hinz, R., Sastre, M., … Edison, P. (2021). Astrocyte reactivity with late-onset cognitive impairment assessed in vivo using 11C-BU99008 PET and its relationship with amyloid load. *Molecular Psychiatry*. https://doi.org/10.1038/s41380-021-01193-z

Campbell, I. L., Erta, M., Lim, S. L., Frausto, R., May, U., Rose-John, S., Scheller, J., & Hidalgo, J. (2014). Trans-signaling is a dominant mechanism for the pathogenic actions of interleukin-6 in the brain. *Journal of Neuroscience*. https://doi.org/10.1523/JNEUROSCI.2830-13.2014

Campbell, J., Langdon, D., Cercignani, M., & Rashid, W. (2016). A Randomised controlled trial of efficacy of cognitive rehabilitation in multiple sclerosis: A cognitive, behavioural, and MRI study. *Neural*

Plasticity, *2016*. https://doi.org/10.1155/2016/4292585

Canu, E., McLaren, D. G., Fitzgerald, M. E., Bendlin, B. B., Zoccatelli, G., Alessandrini, F., Pizzini, F. B., Ricciardi, G. K., Beltramello, A., Johnson, S. C., & Frisoni, G. B. (2010). Microstructural diffusion changes are independent of macrostructural volume loss in moderate to severe Alzheimer's disease. *Journal of Alzheimer's Disease*, *19*(3). https://doi.org/10.3233/JAD-2010-1295

Cao, G., Edden, R. A. E., Gao, F., Li, H., Gong, T., Chen, W., Liu, X., Wang, G., & Zhao, B. (2018). Reduced GABA levels correlate with cognitive impairment in patients with relapsing-remitting multiple sclerosis. *European Radiology*. https://doi.org/10.1007/s00330-017-5064-9

Cappellani, R., Bergsland, N., Weinstock-Guttman, B., Kennedy, C., Carl, E., Ramasamy, D. P., Hagemeier, J., Dwyer, M. G., Patti, F., & Zivadinov, R. (2014). Subcortical deep gray matter pathology in patients with multiple sclerosis is associated with white matter lesion burden and atrophy but not with cortical atrophy: A diffusion tensor MRI study. *American Journal of Neuroradiology*. https://doi.org/10.3174/ajnr.A3788

Cawley, N., Solanky, B. S., Muhlert, N., Tur, C., Edden, R. A. E., Wheeler-Kingshott, C. A. M., Miller, D. H., Thompson, A. J., & Ciccarelli, O. (2015). Reduced gamma-aminobutyric acid concentration is associated with physical disability in progressive multiple sclerosis. *Brain*. https://doi.org/10.1093/brain/awv209

Cercignani, M., Bammer, R., Sormani, M. P., Fazekas, F., & Filippi, M. (2003). Inter-sequence and inter-imaging unit variability of diffusion tensor MR imaging histogram-derived metrics of the brain in healthy volunteers. *American Journal of Neuroradiology*, *24*(4).

Cercignani, M., Bozzali, M., Iannucci, G., Comi, G., & Filippi, M. (2001). Magnetisation transfer ratio and mean diffusivity of normal appearing white and grey matter from patients with multiple sclerosis. *Journal of Neurology Neurosurgery and Psychiatry*. https://doi.org/10.1136/jnnp.70.3.311

Cercignani, M., Iannucci, G., Rocca, M. A., Comi, G., Horsfield, M. A., & Filippi, M. (2000). Pathologic damage in MS assessed by diffusion-weighted and magnetization transfer MRI. *Neurology*. https://doi.org/10.1212/WNL.54.5.1139

Chard, D. T., Griffin, C. M., Parker, G. J. M., Kapoor, R., Thompson, A. J., & Miller, D. H. (2002). Brain atrophy in clinically early relapsing-remitting multiple sclerosis. *Brain*. https://doi.org/10.1093/brain/awf025

Chen, M. K., & Guilarte, T. R. (2008). Translocator protein 18 kDa (TSPO): Molecular sensor of brain injury and repair. In *Pharmacology and Therapeutics*. https://doi.org/10.1016/j.pharmthera.2007.12.004

Chi, J. M., Mackay, M., Hoang, A., Cheng, K., Aranow, C., Ivanidze, J., Volpe, B., Diamond, B., & Sanelli, P. C. (2019). Alterations in blood-brain barrier permeability in patients with systemic lupus erythematosus. *American Journal of Neuroradiology*. https://doi.org/10.3174/ajnr.A5990

Choi, C. G., & Frahm, J. (1999). Localized proton MRS of the human hippocampus: Metabolite concentrations and relaxation times. *Magnetic Resonance in Medicine*, *41*(1). https://doi.org/10.1002/(SICI)1522-2594(199901)41:1<204::AID-MRM29>3.0.CO;2-7

Chwastiak, L., Ehde, D. M., Gibbons, L. E., Sullivan, M., Bowen, J. D., & Kraft, G. H. (2002). Depressive symptoms and severity of illness in multiple sclerosis: Epidemiologic study of a large community sample. *American Journal of Psychiatry*.

https://doi.org/10.1176/appi.ajp.159.11.1862

Cianfoni, A., Niku, S., & Imbesi, S. G. (n.d.). *Metabolite Findings in Tumefactive Demyelinating Lesions Utilizing Short Echo Time Proton Magnetic Resonance Spectroscopy*. www.ajnr.org

Claes, N., Fraussen, J., Stinissen, P., Hupperts, R., & Somers, V. (2015). B cells are multifunctional players in multiple sclerosis pathogenesis: Insights from therapeutic interventions. In *Frontiers in Immunology* (Vol. 6, Issue DEC). https://doi.org/10.3389/fimmu.2015.00642

Colasanti, A., Guo, Q., Giannetti, P., Wall, M. B., Newbould, R. D., Bishop, C., Onega, M., Nicholas, R., Ciccarelli, O., Muraro, P. A., Malik, O., Owen, D. R., Young, A. H., Gunn, R. N., Piccini, P., Matthews, P. M., & Rabiner, E. A. (2016). Hippocampal neuroinflammation, functional connectivity, and depressive symptoms in multiple sclerosis. *Biological Psychiatry*. https://doi.org/10.1016/j.biopsych.2015.11.022

Compston, A., & Coles, A. (2002). Multiple sclerosis. *Lancet*. https://doi.org/10.1016/S0140-6736(02)08220-X

Compston, A., & Coles, A. (2008). Multiple sclerosis. In *The Lancet*. https://doi.org/10.1016/S0140-6736(08)61620-7

Constantinescu, C. S., Farooqi, N., O'Brien, K., & Gran, B. (2011). Experimental autoimmune encephalomyelitis (EAE) as a model for multiple sclerosis (MS). In *British Journal of Pharmacology*. https://doi.org/10.1111/j.1476-5381.2011.01302.x

Crombe, A., Planche, V., Raffard, G., Bourel, J., Dubourdieu, N., Panatier, A., Fukutomi, H., Dousset, V., Oliet, S., Hiba, B., & Tourdias, T. (2018). Deciphering the microstructure of hippocampal subfields with in vivo DTI and NODDI: Applications to experimental multiple sclerosis. *NeuroImage*,

172, 357–368. https://doi.org/10.1016/j.neuroimage.2018.01.061

Cucurella, M. G., Rovira, A., Río, J., Pedraza, S., Tintoré, M. M., Montalbán, X., & Alonso, J. (2000). Proton magnetic resonance spectroscopy in primary and secondary progressive multiple sclerosis. *NMR in Biomedicine*. https://doi.org/10.1002/(SICI)1099-1492(200004)13:2<57::AID-NBM609>3.0.CO;2-5

Daducci, A., Canales-Rodríguez, E. J., Zhang, H., Dyrby, T. B., Alexander, D. C., & Thiran, J. P. (2015). Accelerated Microstructure Imaging via Convex Optimization (AMICO) from diffusion MRI data. *NeuroImage*, *105*. https://doi.org/10.1016/j.neuroimage.2014.10.026

Dalton, M. A., Zeidman, P., Barry, D. N., Williams, E., & Maguire, E. A. (2017). Segmenting subregions of the human hippocampus on structural magnetic resonance image scans: An illustrated tutorial. *Brain and Neuroscience Advances*. https://doi.org/10.1177/2398212817701448

Damoiseaux, J. S., Rombouts, S. A. R. B., Barkhof, F., Scheltens, P., Stam, C. J., Smith, S. M., & Beckmann, C. F. (2006). Consistent resting-state networks across healthy subjects. *Proceedings of the National Academy of Sciences of the United States of America*, *103*(37). https://doi.org/10.1073/pnas.0601417103

Dargahi, N., Katsara, M., Tselios, T., Androutsou, M. E., De Courten, M., Matsoukas, J., & Apostolopoulos, V. (2017). Multiple sclerosis: Immunopathology and treatment update. In *Brain Sciences* (Vol. 7, Issue 7). https://doi.org/10.3390/brainsci7070078

Davalos, D., Grutzendler, J., Yang, G., Kim, J. V., Zuo, Y., Jung, S., Littman, D. R., Dustin, M. L., & Gan, W. B. (2005). ATP mediates rapid microglial response to local brain injury in vivo. *Nature Neuroscience*, *8*(6).

https://doi.org/10.1038/nn1472

Davie, C. A., Barker, G. J., Thompson, A. J., Tofts, P. S., McDonald, W. I., & Miller, D. H. (1997). 1H magnetic resonance spectroscopy of chronic cerebral white matter lesions and normal appearing white matter in multiple sclerosis. *Journal of Neurology Neurosurgery and Psychiatry*. https://doi.org/10.1136/jnnp.63.6.736

Davies, D. S., Ma, J., Jegathees, T., & Goldsbury, C. (2017). Microglia show altered morphology and reduced arborization in human brain during aging and Alzheimer's disease. *Brain Pathology*, *27*(6). https://doi.org/10.1111/bpa.12456

Dawson, J. W. (1916). XVIII.—The histology of disseminated sclerosis. *Transactions of the Royal Society of Edinburgh*, *50*(3). https://doi.org/10.1017/S0080456800027174

de Graaf, R. A., Rothman, D. L., & Behar, K. L. (2007). High resolution NMR spectroscopy of rat brain in vivo through indirect zero-quantum-coherence detection. *Journal of Magnetic Resonance*, *187*(2). https://doi.org/10.1016/j.jmr.2007.06.001

De Marco, R., Ronen, I., Branzoli, F., Amato, M. L., Asllani, I., Colasanti, A., Harrison, N. A., & Cercignani, M. (2022). Diffusion-weighted MR spectroscopy (DW-MRS) is sensitive to LPS-induced changes in human glial morphometry: A preliminary study. *Brain, Behavior, and Immunity*. https://doi.org/10.1016/j.bbi.2021.10.005

Dekeyzer, S., De Kock, I., Nikoubashman, O., Vanden Bossche, S., Van Eetvelde, R., De Groote, J., Acou, M., Wiesmann, M., Deblaere, K., & Achten, E. (2017). "Unforgettable" – a pictorial essay on anatomy and pathology of the hippocampus. In *Insights into Imaging*.

https://doi.org/10.1007/s13244-016-0541-2

Dekker, I., Leurs, C. E., Hagens, M. H. J., van Kempen, Z. L. E., Kleerekooper, I., Lissenberg-Witte, B. I., Barkhof, F., Uitdehaag, B. M. J., Balk, L. J., Wattjes, M. P., & Killestein, J. (2019). Long-term disease activity and disability progression in relapsing-remitting multiple sclerosis patients on natalizumab. *Multiple Sclerosis and Related Disorders*, *33*. https://doi.org/10.1016/j.msard.2019.05.017

DeKraker, J., Köhler, S., & Khan, A. R. (2021). Surface-based hippocampal subfield segmentation. In *Trends in Neurosciences* (Vol. 44, Issue 11). https://doi.org/10.1016/j.tins.2021.06.005

Dennison, L., Moss-Morris, R., & Chalder, T. (2009). A review of psychological correlates of adjustment in patients with multiple sclerosis. In *Clinical Psychology Review* (Vol. 29, Issue 2). https://doi.org/10.1016/j.cpr.2008.12.001

Detre, J. A., Leigh, J. S., Williams, D. S., & Koretsky, A. P. (1992). Perfusion imaging. *Magnetic Resonance in Medicine*, *23*(1). https://doi.org/10.1002/mrm.1910230106

Dhikav, V., & Anand, K. (2012). Hippocampus in health and disease: An overview. *Annals of Indian Academy of Neurology*, *15*(4), 239. https://doi.org/10.4103/0972-2327.104323

Ding, Z., Fang, L., Yuan, S., Zhao, L., Wang, X., Long, S., Wang, M., Wang, D., Foda, M. F., & Xiao, S. (2017). The nucleocapsid proteins of mouse hepatitis virus and severe acute respiratory syndrome coronavirus share the same IFN-β antagonizing mechanism: Attenuation of PACT-mediated RIG-I/MDA5 activation. *Oncotarget*. https://doi.org/10.18632/oncotarget.17912

Doshi, A., & Chataway, J. (2017). Multiple sclerosis, a treatable disease. In

Clinical Medicine, Journal of the Royal College of Physicians of London (Vol. 17, Issue 6). https://doi.org/10.7861/clinmedicine.17-6-530

Droogan, A. G., Clark, C. A., Werring, D. J., Barker, G. J., McDonald, W. I., & Miller, D. H. (1999). Comparison of multiple sclerosis clinical subgroups using navigated spin echo diffusion-weighted imaging. *Magnetic Resonance Imaging*. https://doi.org/10.1016/S0730-725X(99)00011-9

Druss, B. G. (2020). Addressing the COVID-19 Pandemic in Populations with Serious Mental Illness. In *JAMA Psychiatry*. https://doi.org/10.1001/jamapsychiatry.2020.0894

Dudek, S. M., Alexander, G. M., & Farris, S. (2016). Rediscovering area CA2: Unique properties and functions. In *Nature Reviews Neuroscience* (Vol. 17, Issue 2). https://doi.org/10.1038/nrn.2015.22

Dutta, R., Chang, A., Doud, M. K., Kidd, G. J., Ribaudo, M. V, Young, E. A., Fox, R. J., Staugaitis, S. M., & Trapp, B. D. (2011). Demyelination causes synaptic alterations in hippocampi from multiple sclerosis patients. *Annals of Neurology*, *69*(3), 445–454. https://doi.org/10.1002/ana.22337

Ebers, G. C. (2004). Natural history of primary progressive multiple sclerosis. *Multiple Sclerosis*, *10*(SUPPL. 1). https://doi.org/10.1191/1352458504ms1025oa

Ekstrom, A. D., Bazih, A. J., Suthana, N. A., Al-Hakim, R., Ogura, K., Zeineh, M., Burggren, A. C., & Bookheimer, S. Y. (2009). Advances in high-resolution imaging and computational unfolding of the human hippocampus. *NeuroImage*, *47*(1). https://doi.org/10.1016/j.neuroimage.2009.03.017

ElSayed, M. E. S. K. A., El-Toukhy, M. M. B., Asaad, R. E., & El-Serafy, O. A. (2019). Diffusion tensor imaging for assessment of normally appearing

white matter of the brain and spinal cord in cases of multiple sclerosis: a multi-parametric correlation in view of patient's clinical status. *Egyptian Journal of Radiology and Nuclear Medicine*, 50(1). https://doi.org/10.1186/s43055-019-0031-x

Farooq, R. K., Asghar, K., Kanwal, S., & Zulqernain, A. (2017). Role of inflammatory cytokines in depression: Focus on interleukin-1β (Review). In *Biomedical Reports*. https://doi.org/10.3892/br.2016.807

Ferré, J. C., Bannier, E., Raoult, H., Mineur, G., Carsin-Nicol, B., & Gauvrit, J. Y. (2013). Arterial spin labeling (ASL) perfusion: Techniques and clinical use. In *Diagnostic and Interventional Imaging* (Vol. 94, Issue 12). https://doi.org/10.1016/j.diii.2013.06.010

Ferrucci, L., & Fabbri, E. (2018). Inflammageing: chronic inflammation in ageing, cardiovascular disease, and frailty. In *Nature Reviews Cardiology*. https://doi.org/10.1038/s41569-018-0064-2

Filip, P., Dufek, M., Mangia, S., Michaeli, S., Bareš, M., Schwarz, D., Rektor, I., & Vojtíšek, L. (2021). Alterations in Sensorimotor and Mesiotemporal Cortices and Diffuse White Matter Changes in Primary Progressive Multiple Sclerosis Detected by Adiabatic Relaxometry. *Frontiers in Neuroscience*, 15. https://doi.org/10.3389/fnins.2021.711067

Filip, P., Svatkova, A., Carpenter, A. F., Eberly, L. E., Nestrasil, I., Nissi, M. J., Michaeli, S., & Mangia, S. (2020). Rotating frame MRI relaxations as markers of diffuse white matter abnormalities in multiple sclerosis. *NeuroImage: Clinical*. https://doi.org/10.1016/j.nicl.2020.102234

Filippi, M., Cercignani, M., Inglese, M., Horsfield, M. A., & Comi, G. (2001). Diffusion tensor magnetic resonance imaging in multiple sclerosis. *Neurology*. https://doi.org/10.1212/WNL.56.3.304

Filippi, M., Iannucci, G., Tortorella, C., Minicucci, L., Horsfield, M. A., Colombo, B., Sormani, M. P., & Comi, G. (1999). Comparison of MS clinical phenotypes using conventional and magnetization transfer MRI. *Neurology*. https://doi.org/10.1212/wnl.52.3.588

Filippi, M., Rocca, M. A., Colombo, B., Falini, A., Codella, M., Scotti, G., & Comi, G. (2002). Functional magnetic resonance imaging correlates of fatigue in multiple sclerosis. *NeuroImage*, *15*(3). https://doi.org/10.1006/nimg.2001.1011

Finke, C., Kopp, U. A., Pajkert, A., Behrens, J. R., Leypoldt, F., Wuerfel, J. T., Ploner, C. J., Prüss, H., & Paul, F. (2016). Structural Hippocampal Damage Following Anti-N-Methyl-D-Aspartate Receptor Encephalitis. *Biological Psychiatry*. https://doi.org/10.1016/j.biopsych.2015.02.024

Finke, C., Prüss, H., Heine, J., Reuter, S., Kopp, U. A., Wegner, F., Bergh, F. T., Koch, S., Jansen, O., Münte, T., Deuschl, G., Ruprecht, K., Stöcker, W., Klaus-Peterwandinger, K. P., Paul, F., & Bartsch, T. (2017). Evaluation of cognitive deficits and structural hippocampal damage in encephalitis with leucine-rich, glioma-inactivated 1 antibodies. *JAMA Neurology*. https://doi.org/10.1001/jamaneurol.2016.4226

Fischer, J. S., Priore, R. L., Jacobs, L. D., Cookfair, D. L., Rudick, R. A., Herndon, R. M., Richert, J. R., Salazar, A. M., Goodkin, D. E., Granger, C. V., Simon, J. H., Grafman, J. H., Lezak, M. D., O'Reilly Hovey, K. M., Perkins, K. K., Barilla-Clark, D., Schacter, M., Shucard, D. W., Davidson, A. L., … Kooijmans-Coutinho, M. F. (2000). Neuropsychological effects of interferon β-1a in relapsing multiple sclerosis. *Annals of Neurology*, *48*(6). https://doi.org/10.1002/1531-8249(200012)48:6<885::AID-ANA9>3.0.CO;2-1

Fisk, J. D., Pontefract, A., Ritvo, P. G., Archibald, C. J., & Murray, T. J. (1994).

The Impact of Fatigue on Patients with Multiple Sclerosis. *Canadian Journal of Neurological Sciences / Journal Canadien Des Sciences Neurologiques*, *21*(1). https://doi.org/10.1017/S0317167100048691

Foong, J., Rozewicz, L., Chong, W. K., Thompson, A. J., Miller, D. H., & Ron, M. A. (2000). A comparison of neuropsychological deficits in primary and secondary progressive multiple sclerosis. *Journal of Neurology*. https://doi.org/10.1007/PL00007804

Frank, M. G., Weber, M. D., Watkins, L. R., & Maier, S. F. (2016). Stress-induced neuroinflammatory priming: A liability factor in the etiology of psychiatric disorders. In *Neurobiology of Stress*. https://doi.org/10.1016/j.ynstr.2015.12.004

Frankel, J. E., Bean, J. F., & Frontera, W. R. (2006). Exercise in the Elderly: Research and Clinical Practice. In *Clinics in Geriatric Medicine* (Vol. 22, Issue 2). https://doi.org/10.1016/j.cger.2005.12.002

Fukushima, S., Furube, E., Itoh, M., Nakashima, T., & Miyata, S. (2015). Robust increase of microglia proliferation in the fornix of hippocampal axonal pathway after a single LPS stimulation. *Journal of Neuroimmunology*, *285*. https://doi.org/10.1016/j.jneuroim.2015.05.014

Geurts, J. J. G., Bö, L., Roosendaal, S. D., Hazes, T., Daniëls, R., Barkhof, F., Witter, M. P., Huitinga, I., & Van Der Valk, P. (2007a). Extensive hippocampal demyelination in multiple sclerosis. *Journal of Neuropathology and Experimental Neurology*. https://doi.org/10.1097/nen.0b013e3181461f54

Geurts, J. J. G., Bö, L., Roosendaal, S. D., Hazes, T., Daniëls, R., Barkhof, F., Witter, M. P., Huitinga, I., & Van Der Valk, P. (2007b). Extensive hippocampal demyelination in multiple sclerosis. *Journal of*

Neuropathology and Experimental Neurology, *66*(9), 819–827.
https://doi.org/10.1097/nen.0b013e3181461f54

Geurts, J. J. G., Reuling, I. E. W., Vrenken, H., Uitdehaag, B. M. J., Polman, C.
H., Castelijns, J. A., Barkhof, F., & Pouwels, P. J. W. (2006). MR
spectroscopic evidence for thalamic and hippocampal, but not cortical,
damage in multiple sclerosis. *Magnetic Resonance in Medicine*.
https://doi.org/10.1002/mrm.20792

Giannakopoulou, A., Grigoriadis, N., Bekiari, C., Lourbopoulos, A., Dori, I.,
Tsingotjidou, A. S., Michaloudi, H., & Papadopoulos, G. C. (2013). Acute
inflammation alters adult hippocampal neurogenesis in a multiple sclerosis
mouse model. *Journal of Neuroscience Research*.
https://doi.org/10.1002/jnr.23226

Giordano, K. R., Denman, C. R., Dubisch, P. S., Akhter, M., & Lifshitz, J.
(2021). An update on the rod microglia variant in experimental and clinical
brain injury and disease. *Brain Communications*, *3*(1).
https://doi.org/10.1093/braincomms/fcaa227

Glanz, B. I., Holland, C. M., Gauthier, S. A., Amunwa, E. L., Liptak, Z.,
Houtchens, M. K., Sperling, R. A., Khoury, S. J., Guttmann, C. R. G., &
Weiner, H. L. (2007). Cognitive dysfunction in patients with clinically
isolated syndromes or newly diagnosed multiple sclerosis. *Multiple
Sclerosis*, *13*(8). https://doi.org/10.1177/1352458507077943

Göbel-Guéniot, K., Gerlach, J., Kamberger, R., Leupold, J., von Elverfeldt, D.,
Hennig, J., Korvink, J. G., Haas, C. A., & LeVan, P. (2020). Histological
Correlates of Diffusion-Weighted Magnetic Resonance Microscopy in a
Mouse Model of Mesial Temporal Lobe Epilepsy. *Frontiers in
Neuroscience*. https://doi.org/10.3389/fnins.2020.00543

Gold, S. M., Mohr, D. C., Huitinga, I., Flachenecker, P., Sternberg, E. M., & Heesen, C. (2005). The role of stress-response systems for the pathogenesis and progression of MS. In *Trends in Immunology*. https://doi.org/10.1016/j.it.2005.09.010

Gold, S. M., O'Connor, M. F., Gill, R., Kern, K. C., Shi, Y., Henry, R. G., Pelletier, D., Mohr, D. C., & Sicotte, N. L. (2014). Detection of altered hippocampal morphology in multiple sclerosis-associated depression using automated surface mesh modeling. *Human Brain Mapping*. https://doi.org/10.1002/hbm.22154

Gong, N. J., Wong, C. S., Chan, C. C., Leung, L. M., & Chu, Y. C. (2014). Aging in deep gray matter and white matter revealed by diffusional kurtosis imaging. *Neurobiology of Aging*, *35*(10). https://doi.org/10.1016/j.neurobiolaging.2014.03.011

González-Reimers, E., Martín-González, C., Romero-Acevedo, L., Quintero-Platt, G., Gonzalez-Arnay, E., & Santolaria-Fernández, F. (2019). Effects of alcohol on the corpus callosum. In *Neuroscience of Alcohol: Mechanisms and Treatment*. https://doi.org/10.1016/B978-0-12-813125-1.00015-5

Goubran, M., Ntiri, E. E., Akhavein, H., Holmes, M., Nestor, S., Ramirez, J., Adamo, S., Ozzoude, M., Scott, C., Gao, F., Martel, A., Swardfager, W., Masellis, M., Swartz, R., MacIntosh, B., & Black, S. E. (2020). Hippocampal segmentation for brains with extensive atrophy using three-dimensional convolutional neural networks. *Human Brain Mapping*. https://doi.org/10.1002/hbm.24811

Graeber, M. B., & Streit, W. J. (2010). Microglia: Biology and pathology. In *Acta Neuropathologica* (Vol. 119, Issue 1). https://doi.org/10.1007/s00401-009-0622-0

Granberg, T., Fan, Q., Treaba, C. A., Ouellette, R., Herranz, E., Mangeat, G., Louapre, C., Cohen-Adad, J., Klawiter, E. C., Sloane, J. A., & Mainero, C. (2017). In vivo characterization of cortical and white matter neuroaxonal pathology in early multiple sclerosis. *Brain*, *140*(11). https://doi.org/10.1093/brain/awx247

Granziera, C., Wuerfel, J., Barkhof, F., Calabrese, M., De Stefano, N., Enzinger, C., Evangelou, N., Filippi, M., Geurts, J. J. G., Reich, D. S., Rocca, M. A., Ropele, S., Rovira, À., Sati, P., Toosy, A. T., Vrenken, H., Gandini Wheeler-Kingshott, C. A. M., & Kappos, L. (2021). Quantitative magnetic resonance imaging towards clinical application in multiple sclerosis. In *Brain* (Vol. 144, Issue 5). https://doi.org/10.1093/brain/awab029

Grieve, S. M., Williams, L. M., Paul, R. H., Clark, C. R., & Gordon, E. (2007). Cognitive aging, executive function, and fractional anisotropy: A diffusion tensor MR imaging study. *American Journal of Neuroradiology*.

Grussu, F., Schneider, T., Tur, C., Yates, R. L., Tachrount, M., Ianuş, A., Yiannakas, M. C., Newcombe, J., Zhang, H., Alexander, D. C., DeLuca, G. C., & Gandini Wheeler-Kingshott, C. A. M. (2017). Neurite dispersion: a new marker of multiple sclerosis spinal cord pathology? *Annals of Clinical and Translational Neurology*, *4*(9). https://doi.org/10.1002/acn3.445

Gupta, A., Baradaran, H., Schweitzer, A. D., Kamel, H., Pandya, A., Delgado, D., Wright, D., Hurtado-Rua, S., Wang, Y., & Sanelli, P. C. (2014). Oxygen extraction fraction and stroke risk in patients with carotid stenosis or occlusion: A systematic review and meta-analysis. *American Journal of Neuroradiology*, *35*(2). https://doi.org/10.3174/ajnr.A3668

Hamsini, B. C., Reddy, B. N., Neelakantan, S., & Kumaran, S. P. (2018). Clinical Application of MR Spectroscopy in Identifying Biochemical

Composition of the Intracranial Pathologies. In *GABA And Glutamate - New Developments In Neurotransmission Research*. https://doi.org/10.5772/intechopen.71728

Harris, A. D., Roberton, V. H., Huckle, D. L., Saxena, N., Evans, C. J., Murphy, K., Hall, J. E., Bailey, D. M., Mitsis, G., Edden, R. A. E., & Wise, R. G. (2013). Temporal dynamics of lactate concentration in the human brain during acute inspiratory hypoxia. *Journal of Magnetic Resonance Imaging*. https://doi.org/10.1002/jmri.23815

Harrison, N. A., Cercignani, M., Voon, V., & Critchley, H. D. (2015). Effects of inflammation on hippocampus and substantia nigra responses to novelty in healthy human participants. *Neuropsychopharmacology*, *40*(4). https://doi.org/10.1038/npp.2014.222

Haussleiter, I. S., Brüne, M., & Juckel, G. (2009). Psychopathology in multiple sclerosis: Diagnosis, prevalence and treatment. In *Therapeutic Advances in Neurological Disorders* (Vol. 2, Issue 1, pp. 13–29). https://doi.org/10.1177/1756285608100325

Heaton, R. K., Nelson, L. M., Thompson, D. S., Burks, J. S., & Franklin, G. M. (1985). Neuropsychological Findings in Relapsing-Remitting and Chronic-Progressive Multiple Sclerosis. *Journal of Consulting and Clinical Psychology*, *53*(1). https://doi.org/10.1037/0022-006X.53.1.103

Heine, J., Prüß, H., Scheel, M., Brandt, A. U., Gold, S. M., Bartsch, T., Paul, F., & Finke, C. (2020). Transdiagnostic hippocampal damage patterns in neuroimmunological disorders. *NeuroImage: Clinical*. https://doi.org/10.1016/j.nicl.2020.102515

Helms, G. (2001). Volume correction for edema in single-volume proton MR spectroscopy of contrast-enhancing multiple sclerosis lesions. *Magnetic*

Resonance in Medicine. https://doi.org/10.1002/mrm.1186

Henf, J., Grothe, M. J., Brueggen, K., Teipel, S., & Dyrba, M. (2018). Mean diffusivity in cortical gray matter in Alzheimer's disease: The importance of partial volume correction. *NeuroImage: Clinical, 17*. https://doi.org/10.1016/j.nicl.2017.10.005

Herranz, E., Giannì, C., Louapre, C., Treaba, C. A., Govindarajan, S. T., Ouellette, R., Loggia, M. L., Sloane, J. A., Madigan, N., Izquierdo-Garcia, D., Ward, N., Mangeat, G., Granberg, T., Klawiter, E. C., Catana, C., Hooker, J. M., Taylor, N., Ionete, C., Kinkel, R. P., & Mainero, C. (2016). Neuroinflammatory component of gray matter pathology in multiple sclerosis. *Annals of Neurology*. https://doi.org/10.1002/ana.24791

Herrera-Rivero, M., Heneka, M. T., & Papadopoulos, V. (2015). Translocator protein and new targets for neuroinflammation. In *Clinical and Translational Imaging*. https://doi.org/10.1007/s40336-015-0151-x

Holmes, E. A., O'Connor, R. C., Perry, V. H., Tracey, I., Wessely, S., Arseneault, L., Ballard, C., Christensen, H., Cohen Silver, R., Everall, I., Ford, T., John, A., Kabir, T., King, K., Madan, I., Michie, S., Przybylski, A. K., Shafran, R., Sweeney, A., … Bullmore, E. (2020). Multidisciplinary research priorities for the COVID-19 pandemic: a call for action for mental health science. In *The Lancet Psychiatry*. https://doi.org/10.1016/S2215-0366(20)30168-1

Huang, W. J., Chen, W. W., & Zhang, X. (2017). Multiple sclerosis: Pathology, diagnosis and treatments (review). In *Experimental and Therapeutic Medicine*. https://doi.org/10.3892/etm.2017.4410

Hughes, E. G., Peng, X., Gleichman, A. J., Lai, M., Zhou, L., Tsou, R., Parsons, T. D., Lynch, D. R., Dalmau, J., & Balice-Gordon, R. J. (2010). Cellular

and synaptic mechanisms of anti-NMDA receptor encephalitis. *Journal of Neuroscience*. https://doi.org/10.1523/JNEUROSCI.0167-10.2010

Huijbregts, S. C. J., Kalkers, N. F., De Sonneville, L. M. J., De Groot, V., Reuling, I. E. W., & Polman, C. H. (2004). Differences in cognitive impairment of relapsing remitting, secondary, and primary progressive MS. *Neurology*, *63*(2). https://doi.org/10.1212/01.WNL.0000129828.03714.90

Hurtz, S., Chow, N., Watson, A. E., Somme, J. H., Goukasian, N., Hwang, K. S., Morra, J., Elashoff, D., Gao, S., Petersen, R. C., Aisen, P. S., Thompson, P. M., & Apostolova, L. G. (2019). Automated and manual hippocampal segmentation techniques: Comparison of results, reproducibility and clinical applicability. *NeuroImage: Clinical*, *21*. https://doi.org/10.1016/j.nicl.2018.10.012

Iannucci, G., Rovaris, M., Giacomotti, L., Comi, G., & Filippi, M. (2001). Correlation of multiple sclerosis measures derived from T2-weighted, T1-weighted, magnetization transfer, and diffusion tensor MR imaging. *American Journal of Neuroradiology*.

Ibrahim, M. A., Hazhirkarzar, B., & Dublin, A. B. (2021). Gadolinium Magnetic Resonance Imaging. In *StatPearls*.

Ingle, G. T., Stevenson, V. L., Miller, D. H., & Thompson, A. J. (2003). Primary progressive multiple sclerosis: A 5-year clinical and MR study. *Brain*. https://doi.org/10.1093/brain/awg261

Inglese, M., & Bester, M. (2010). Diffusion imaging in multiple sclerosis: Research and clinical implications. *NMR in Biomedicine*, *23*(7), 865–872. https://doi.org/10.1002/NBM.1515

Inglese, M., Liu, S., Babb, J. S., Mannon, L. J., Grossman, R. I., & Gonen, O. (2004). Three-dimensional proton spectroscopy of deep gray matter nuclei

in relapsing-remaining MS. *Neurology*.
https://doi.org/10.1212/01.WNL.0000133133.77952.7C

Ingo, C., Brink, W., Ercan, E., Webb, A. G., & Ronen, I. (2018). Studying
neurons and glia non-invasively via anomalous subdiffusion of intracellular
metabolites. *Brain Structure and Function*. https://doi.org/10.1007/s00429-
018-1719-9

Joffe, R. T., Lippert, G. P., Gray, T. A., Sawa, G., & Horvath, Z. (1987). Mood
Disorder and Multiple Sclerosis. *Archives of Neurology*, *44*(4), 376–378.
https://doi.org/10.1001/archneur.1987.00520160018007

Johns, M. W. (1991). A new method for measuring daytime sleepiness: The
Epworth sleepiness scale. *Sleep*, *14*(6).
https://doi.org/10.1093/sleep/14.6.540

Jongen, P. J., Wesnes, K., Van Geel, B., Pop, P., Sanders, E., Schrijver, H.,
Visser, L. H., Gilhuis, H. J., Sinnige, L. G., & Brands, A. M. (2014).
Relationship between working hours and power of attention, memory,
fatigue, depression and self-efficacy one year after diagnosis of clinically
isolated syndrome and relapsing remitting multiple sclerosis. *PLoS ONE*,
9(5). https://doi.org/10.1371/journal.pone.0096444

Jukkola, P., Guerrero, T., Gray, V., & Gu, C. (2013). Astrocytes differentially
respond to inflammatory autoimmune insults and imbalances of neural
activity. *Acta Neuropathologica Communications*, *1*(1).
https://doi.org/10.1186/2051-5960-1-70

Jurgens, H. A., Amancherla, K., & Johnson, R. W. (2012). Influenza Infection
Induces Neuroinflammation, Alters Hippocampal Neuron Morphology, and
Impairs Cognition in Adult Mice. *Journal of Neuroscience*.
https://doi.org/10.1523/JNEUROSCI.6389-11.2012

Kandemirli, S. G., Dogan, L., Sarikaya, Z. T., Kara, S., Akinci, C., Kaya, D., Kaya, Y., Yildirim, D., Tuzuner, F., Yildirim, M. S., Ozluk, E., Gucyetmez, B., Karaarslan, E., Koyluoglu, I., Demirel Kaya, H. S., Mammadov, O., Kisa Ozdemir, I., Afsar, N., Citci Yalcinkaya, B., … Kocer, N. (2020). Brain MRI Findings in Patients in the Intensive Care Unit with COVID-19 Infection. *Radiology*. https://doi.org/10.1148/radiol.2020201697

Kang, H. (2021). Sample size determination and power analysis using the G*Power software. In *Journal of Educational Evaluation for Health Professions* (Vol. 18). https://doi.org/10.3352/JEEHP.2021.18.17

Kapeller, P., McLean, M. A., Griffin, C. M., Chard, D., Parker, G. J. M., Barker, G. J., Thompson, A. J., & Miller, D. H. (2001). Preliminary evidence for neuronal damage in cortical grey matter and normal appearing white matter in short duration relapsing-remitting multiple sclerosis: A quantitative MR spectroscopic imaging study. *Journal of Neurology*. https://doi.org/10.1007/s004150170248

Kaya Aygünoğlu, S., Çelebi, A., Vardar, N., & Gürsoy, E. (2015). Correlation of fatigue with depression, disability level and quality of life in patients with multiple sclerosis. *Noropsikiyatri Arsivi*, *52*(3). https://doi.org/10.5152/npa.2015.8714

Kempuraj, D., Thangavel, R., Natteru, P. A., Selvakumar, G. P., Saeed, D., Zahoor, H., Zaheer, S., Iyer, S. S., & Zaheer, A. (2016). Neuroinflammation Induces Neurodegeneration. *Journal of Neurology, Neurosurgery and Spine*.

Kermode, A. G., Thompson, A. J., Tofts, P., Macmanus, D. G., Kendall, B. E., Kingsley, D. P. E., Moseley, I. F., Rudge, P., & Mcdonald, W. I. (1990). Breakdown of the blood-brain barrier precedes symptoms and other mri signs of new lesions in multiple sclerosis: Pathogenetic and clinical

implications. *Brain*. https://doi.org/10.1093/brain/113.5.1477

Khandaker, G. M., Zammit, S., Burgess, S., Lewis, G., & Jones, P. B. (2018). Association between a functional interleukin 6 receptor genetic variant and risk of depression and psychosis in a population-based birth cohort. *Brain, Behavior, and Immunity*, *69*. https://doi.org/10.1016/j.bbi.2017.11.020

Kidd, D., Thorpe, J. W., Thompson, A. J., Kendall, B. E., Moseley, I. F., Macmanus, D. G., McDonald, W. I., & Miller, D. H. (1993). Spinal cord mri using multi-array coils and fast spin echo: Ii. findings in multiple sclerosis. *Neurology*. https://doi.org/10.1212/wnl.43.12.2632

Kim, E. J., Pellman, B., & Kim, J. J. (2015). Stress effects on the hippocampus: A critical review. In *Learning and Memory* (Vol. 22, Issue 9). https://doi.org/10.1101/lm.037291.114

Kim, M. J., Lee, J. H., Juarez Anaya, F., Hong, J., Miller, W., Telu, S., Singh, P., Cortes, M. Y., Henry, K., Tye, G. L., Frankland, M. P., Montero Santamaria, J. A., Liow, J. S., Zoghbi, S. S., Fujita, M., Pike, V. W., & Innis, R. B. (2020). First-in-human evaluation of [11C]PS13, a novel PET radioligand, to quantify cyclooxygenase-1 in the brain. *European Journal of Nuclear Medicine and Molecular Imaging*. https://doi.org/10.1007/s00259-020-04855-2

Klaver, R., De Vries, H. E., Schenk, G. J., & Geurts, J. J. G. (2013). Grey matter damage in multiple sclerosis A pathology perspective. *Prion*, *7*(1). https://doi.org/10.4161/pri.23499

Knight-Scott, J., Haley, A. P., Rossmiller, S. R., Farace, E., Mai, V. M., Christopher, J. M., Manning, C. A., Simnad, V. I., & Siragy, H. M. (2003). Molality as a unit of measure for expressing 1H MRS brain metabolite concentrations in vivo. *Magnetic Resonance Imaging*, *21*(7).

https://doi.org/10.1016/S0730-725X(03)00179-6

Kocevar, G., Stamile, C., Hannoun, S., Roch, J. A., Durand-Dubief, F., Vukusic, S., Cotton, F., & Sappey-Marinier, D. (2018). Weekly follow up of acute lesions in three early multiple sclerosis patients using MR spectroscopy and diffusion. *Journal of Neuroradiology*. https://doi.org/10.1016/j.neurad.2017.06.010

Kodiweera, C., Alexander, A. L., Harezlak, J., McAllister, T. W., & Wu, Y. C. (2016). Age effects and sex differences in human brain white matter of young to middle-aged adults: A DTI, NODDI, and q-space study. *NeuroImage*, *128*. https://doi.org/10.1016/j.neuroimage.2015.12.033

Koo, T. K., & Li, M. Y. (2016). A Guideline of Selecting and Reporting Intraclass Correlation Coefficients for Reliability Research. *Journal of Chiropractic Medicine*, *15*(2). https://doi.org/10.1016/j.jcm.2016.02.012

Korostil, M., & Feinstein, A. (2007). Anxiety disorders and their clinical correlates in multiple sclerosis patients. *Multiple Sclerosis*, *13*(1). https://doi.org/10.1177/1352458506071161

Kotter, M. R., Li, W. W., Zhao, C., & Franklin, R. J. M. (2006). Myelin impairs CNS remyelination by inhibiting oligodendrocyte precursor cell differentiation. *Journal of Neuroscience*. https://doi.org/10.1523/JNEUROSCI.2615-05.2006

Krupp, L. B., Larocca, N. G., Muir Nash, J., & Steinberg, A. D. (1989). The fatigue severity scale: Application to patients with multiple sclerosis and systemic lupus erythematosus. *Archives of Neurology*, *46*(10). https://doi.org/10.1001/archneur.1989.00520460115022

Kumar, D. R., Aslinia, F., Yale, S. H., & Mazza, J. J. (2011). Jean-martin charcot: The father of neurology. *Clinical Medicine and Research*.

https://doi.org/10.3121/cmr.2009.883

Kurtzke, J. F. (1983). Rating neurologic impairment in multiple sclerosis: An expanded disability status scale (EDSS). *Neurology*. https://doi.org/10.1212/wnl.33.11.1444

Kutzelnigg, A., & Lassmann, H. (2014). Pathology of multiple sclerosis and related inflammatory demyelinating diseases. In *Handbook of Clinical Neurology*. https://doi.org/10.1016/B978-0-444-52001-2.00002-9

Kwon, Y., Kim, M., Kim, Y., Jung, H. S., & Jeoung, D. (2020). Exosomal MicroRNAs as Mediators of Cellular Interactions Between Cancer Cells and Macrophages. In *Frontiers in Immunology*. https://doi.org/10.3389/fimmu.2020.01167

Lampron, A., Larochelle, A., Laflamme, N., Préfontaine, P., Plante, M. M., Sánchez, M. G., Wee Yong, V., Stys, P. K., Tremblay, M. È., & Rivest, S. (2015). Inefficient clearance of myelin debris by microglia impairs remyelinating processes. *Journal of Experimental Medicine*. https://doi.org/10.1084/jem.20141656

Landtblom, A. M., Fazio, P., Fredrikson, S., & Granieri, E. (2010). The first case history of multiple sclerosis: Augustus d'Esté (1794-1848). In *Neurological Sciences*. https://doi.org/10.1007/s10072-009-0161-4

Langdon, D. W., Amato, M. P., Boringa, J., Brochet, B., Foley, F., Fredrikson, S., Hämäläinen, P., Hartung, H. P., Krupp, L., Penner, I. K., Reder, A. T., & Benedict, R. H. B. (2012). Recommendations for a brief international cognitive assessment for multiple sclerosis (BICAMS). In *Multiple Sclerosis Journal* (Vol. 18, Issue 6). https://doi.org/10.1177/1352458511431076

Leary, S. M., Davie, C. A., Parker, G. J. M., Stevenson, V. L., Wang, L.,

Barker, G. J., Miller, D. H., & Thompson, A. J. (1999). 1H magnetic resonance spectroscopy of normal appearing white matter in primary progressive multiple sclerosis. *Journal of Neurology*. https://doi.org/10.1007/s004150050507

Lecrubier, Y., Sheehan, D. V., Weiller, E., Amorim, P., Bonora, I., Sheehan, K. H., Janavs, J., & Dunbar, G. C. (1997). The Mini International Neuropsychiatric Interview (MINI). A short diagnostic structured interview: Reliability and validity according to the CIDI. *European Psychiatry*, *12*(5). https://doi.org/10.1016/S0924-9338(97)83296-8

Lee, Y., Park, Y., Nam, H., Lee, J. W., & Yu, S. W. (2020). Translocator protein (TSPO): The new story of the old protein in neuroinflammation. In *BMB Reports*. https://doi.org/10.5483/BMBRep.2020.53.1.273

Leyh, J., Paeschke, S., Mages, B., Michalski, D., Nowicki, M., Bechmann, I., & Winter, K. (2021). Classification of Microglial Morphological Phenotypes Using Machine Learning. *Frontiers in Cellular Neuroscience*, *15*. https://doi.org/10.3389/fncel.2021.701673

Li, Y. C., Bai, W. Z., & Hashikawa, T. (2020). The neuroinvasive potential of SARS-CoV2 may play a role in the respiratory failure of COVID-19 patients. In *Journal of Medical Virology*. https://doi.org/10.1002/jmv.25728

Liu, Z., & Li, Y. (2016). Cortical cerebral blood flow, oxygen extraction fraction, and metabolic rate in patients with middle cerebral artery stenosis or acute stroke. *American Journal of Neuroradiology*, *37*(4). https://doi.org/10.3174/ajnr.A4624

Lucchinetti, C., Brück, W., Parisi, J., Scheithauer, B., Rodriguez, M., & Lassmann, H. (2000). Heterogeneity of multiple sclerosis lesions: Implications for the pathogenesis of demyelination. *Annals of Neurology*.

https://doi.org/10.1002/1531-8249(200006)47:6<707::AID-ANA3>3.0.CO;2-Q

Ma, W., & Peng, L. (2021). Image quality transfer with auto-encoding applied to dMRI Super-Resolution. *Proceedings - 2021 4th International Conference on Advanced Electronic Materials, Computers and Software Engineering, AEMCSE 2021*. https://doi.org/10.1109/AEMCSE51986.2021.00169

Mackenzie, I. S., Morant, S. V., Bloomfield, G. A., MacDonald, T. M., & O'Riordan, J. (2014). Incidence and prevalence of multiple sclerosis in the UK 1990-2010: A descriptive study in the General Practice Research Database. *Journal of Neurology, Neurosurgery and Psychiatry*. https://doi.org/10.1136/jnnp-2013-305450

Mahad, D. H., Trapp, B. D., & Lassmann, H. (2015). Pathological mechanisms in progressive multiple sclerosis. In *The Lancet Neurology* (Vol. 14, Issue 2). https://doi.org/10.1016/S1474-4422(14)70256-X

Manjón, J. V., & Coupé, P. (2016). Volbrain: An online MRI brain volumetry system. *Frontiers in Neuroinformatics*, *10*(JUL). https://doi.org/10.3389/fninf.2016.00030

Mao, L., Jin, H., Wang, M., Hu, Y., Chen, S., He, Q., Chang, J., Hong, C., Zhou, Y., Wang, D., Miao, X., Li, Y., & Hu, B. (2020). Neurologic Manifestations of Hospitalized Patients with Coronavirus Disease 2019 in Wuhan, China. *JAMA Neurology*. https://doi.org/10.1001/jamaneurol.2020.1127

Marik, C., Felts, P. A., Bauer, J., Lassmann, H., & Smith, K. J. (2007). Lesion genesis in a subset of patients with multiple sclerosis: A role for innate immunity? *Brain*. https://doi.org/10.1093/brain/awm236

Marques, F., Sousa, J. C., Coppola, G., Falcao, A. M., Rodrigues, A. J., Geschwind, D. H., Sousa, N., Correia-Neves, M., & Palha, J. A. (2009). Kinetic profile of the transcriptome changes induced in the choroid plexus by peripheral inflammation. *Journal of Cerebral Blood Flow and Metabolism*. https://doi.org/10.1038/jcbfm.2009.15

Marrie, R. A., Walld, R., Bolton, J. M., Sareen, J., Walker, J. R., Patten, S. B., Singer, A., Lix, L. M., Hitchon, C. A., El-Gabalawy, R., Katz, A., Fisk, J. D., & Bernstein, C. N. (2017). Increased incidence of psychiatric disorders in immune-mediated inflammatory disease. *Journal of Psychosomatic Research*, *101*, 17–23. https://doi.org/10.1016/j.jpsychores.2017.07.015

Martinez-Martin, P. (2017). What is quality of life and how do we measure it? Relevance to Parkinson's disease and movement disorders. In *Movement Disorders* (Vol. 32, Issue 3). https://doi.org/10.1002/mds.26885

Mathiesen, H. K., Tscherning, T., Sorensen, P. S., Larsson, H. B. W., Rostrup, E., Paulson, O. B., & Hanson, L. G. (2005). Multi-slice echo-planar spectroscopic MR imaging provides both global and local metabolite measures in multiple sclerosis. *Magnetic Resonance in Medicine*. https://doi.org/10.1002/mrm.20407

Maurelli, M., Marchioni, E., Cerretano, R., Bosone, D., Bergamaschi, R., Citterio, A., Martelli, A., Sibilla, L., & Savoldi, F. (1992). Neuropsychological assessment in MS: clinical, neurophysiological and neuroradiological relationships. *Acta Neurologica Scandinavica*, *86*(2). https://doi.org/10.1111/j.1600-0404.1992.tb05052.x

McCunn, P., Gilbert, K. M., Zeman, P., Li, A. X., Strong, M. J., Khan, A. R., & Bartha, R. (2019). Reproducibility of Neurite Orientation Dispersion and Density Imaging (NODDI) in rats at 9.4 Tesla. *PLoS ONE*, *14*(4). https://doi.org/10.1371/journal.pone.0215974

McEwen, B. S., De Leon, M. J., Lupien, S. J., & Meaney, M. J. (1999). Corticosteroids, the aging brain and cognition. In *Trends in Endocrinology and Metabolism*. https://doi.org/10.1016/S1043-2760(98)00122-2

Melton, L. M., Keith, A. B., Davis, S., Oakley, A. E., Edwardson, J. A., & Morris, C. M. (2003). Chronic glial activation, neurodegeneration, and APP immunoreactive deposits following acute administration of double-stranded RNA. *GLIA*, *44*(1). https://doi.org/10.1002/glia.10276

Mews, I., Bergmann, M., Bunkowski, S., Gullotta, F., & Brück, W. (1998). Oligodendrocyte and axon pathology in clinically silent multiple sclerosis lesions. *Multiple Sclerosis*. https://doi.org/10.1177/135245859800400203

Michailidou, I., Willems, J. G. P., Kooi, E. J., Van Eden, C., Gold, S. M., Geurts, J. J. G., Baas, F., Huitinga, I., & Ramaglia, V. (2015). Complement C1q-C3-associated synaptic changes in multiple sclerosis hippocampus. *Annals of Neurology*. https://doi.org/10.1002/ana.24398

Michel, V., Yuan, Z., Ramsubir, S., & Bakovic, M. (2006). Choline transport for phospholipid synthesis. In *Experimental Biology and Medicine* (Vol. 231, Issue 5). https://doi.org/10.1177/153537020623100503

Miller, A. H., & Raison, C. L. (2016). The role of inflammation in depression: From evolutionary imperative to modern treatment target. In *Nature Reviews Immunology*. https://doi.org/10.1038/nri.2015.5

Minden, S. L., Orav, J., & Reich, P. (1987a). Depression in multiple sclerosis. *General Hospital Psychiatry*. https://doi.org/10.1016/0163-8343(87)90052-1

Minden, S. L., Orav, J., & Reich, P. (1987b). Depression in multiple sclerosis. *General Hospital Psychiatry*. https://doi.org/10.1016/0163-8343(87)90052-1

Minden, S. L., & Schiffer, R. B. (1990). Affective Disorders in Multiple Sclerosis Review and Recommendations for Clinical Research. *Archives of Neurology*, *47*(1), 98–104. https://doi.org/10.1001/archneur.1990.00530010124031

Ming, G., & Song, H. (2011). Adult Neurogenesis in the Mammalian Brain: Significant Answers and Significant Questions. *Neuron*, *70*(4), 687–702. https://doi.org/10.1016/j.neuron.2011.05.001

Moffett, J. R., Arun, P., Ariyannur, P. S., & Namboodiri, A. M. A. (2013). N-Acetylaspartate reductions in brain injury: Impact on post-injury neuroenergetics, lipid synthesis, and protein acetylation. In *Frontiers in Neuroenergetics* (Vol. 5, Issue DEC). https://doi.org/10.3389/fnene.2013.00011

Mohammadi, K., Rahnama, P., & Montazeri, A. (2015). Prevalence and risk factors for depression in women with multiple sclerosis: A study from Iran. *Annals of General Psychiatry*, *14*(1). https://doi.org/10.1186/s12991-015-0069-8

Moher, D., Liberati, A., Tetzlaff, J., Altman, D. G., Altman, D., Antes, G., Atkins, D., Barbour, V., Barrowman, N., Berlin, J. A., Clark, J., Clarke, M., Cook, D., D'Amico, R., Deeks, J. J., Devereaux, P. J., Dickersin, K., Egger, M., Ernst, E., … Tugwell, P. (2009). Preferred reporting items for systematic reviews and meta-analyses: The PRISMA statement. In *PLoS Medicine*. https://doi.org/10.1371/journal.pmed.1000097

Mollink, J., Kleinnijenhuis, M., Cappellen van Walsum, A. M. van, Sotiropoulos, S. N., Cottaar, M., Mirfin, C., Heinrich, M. P., Jenkinson, M., Pallebage-Gamarallage, M., Ansorge, O., Jbabdi, S., & Miller, K. L. (2017). Evaluating fibre orientation dispersion in white matter: Comparison of diffusion MRI, histology and polarized light imaging. *NeuroImage*, *157*.

https://doi.org/10.1016/j.neuroimage.2017.06.001

Montal, V., Vilaplana, E., Alcolea, D., Pegueroles, J., Pasternak, O., González-Ortiz, S., Clarimón, J., Carmona-Iragui, M., Illán-Gala, I., Morenas-Rodríguez, E., Ribosa-Nogué, R., Sala, I., Sánchez-Saudinós, M. B., García-Sebastian, M., Villanúa, J., Izagirre, A., Estanga, A., Ecay-Torres, M., Iriondo, A., … Fortea, J. (2018). Cortical microstructural changes along the Alzheimer's disease continuum. *Alzheimer's and Dementia*, *14*(3). https://doi.org/10.1016/j.jalz.2017.09.013

Montalban, X., & Rio, J. (2006). Interferons and cognition. *Journal of the Neurological Sciences*, *245*(1–2). https://doi.org/10.1016/j.jns.2005.08.022

Montgomery SA, A. M. (1979). The Montgomery-Asberg Depression Scale (MADRS). *British Journal Of Psychiatry*, *134*.

Moseley, M. E., Cohen, Y., Kucharczyk, J., Mintorovitch, J., Asgari, H. S., Wendland, M. F., Tsuruda, J., & Norman, D. (1990). Diffusion-weighted MR imaging of anisotropic water diffusion in cat central nervous system. *Radiology*, *176*(2). https://doi.org/10.1148/radiology.176.2.2367658

Muhlert, N., Atzori, M., De Vita, E., Thomas, D. L., Samson, R. S., Wheeler-Kingshott, C. A. M., Geurts, J. J. G., Miller, D. H., Thompson, A. J., & Ciccarelli, O. (2014). Memory in multiple sclerosis is linked to glutamate concentration in grey matter regions. *Journal of Neurology, Neurosurgery and Psychiatry*. https://doi.org/10.1136/jnnp-2013-306662

Nagaraj, K., Taly, A. B., Gupta, A., Prasad, C., & Christopher, R. (2013). Prevalence of fatigue in patients with multiple sclerosis and its effect on the quality of life. *Journal of Neurosciences in Rural Practice*, *4*(3). https://doi.org/10.4103/0976-3147.118774

Nazeri, A., Chakravart, M., Rotenberg, D. J., Rajji, T. K., Rathi, X.,

Michailovich, O. V., & Voineskos, A. N. (2015). Functional consequences of neurite orientation dispersion and density in humans across the adult lifespan. *Journal of Neuroscience, 35*(4). https://doi.org/10.1523/JNEUROSCI.3979-14.2015

Nguyen, D. L., Wimberley, C., Truillet, C., Jego, B., Caillé, F., Pottier, G., Boisgard, R., Buvat, I., & Bouilleret, V. (2018). Longitudinal positron emission tomography imaging of glial cell activation in a mouse model of mesial temporal lobe epilepsy: Toward identification of optimal treatment windows. *Epilepsia*. https://doi.org/10.1111/epi.14083

Ni, J. M., Chen, S., Liu, J. J., Huang, G., Shen, T. Z., & Chen, X. R. (2010). Regional diffusion changes of cerebral grey matter during normal aging-A fluid-inversion prepared diffusion imaging study. *European Journal of Radiology*. https://doi.org/10.1016/j.ejrad.2009.04.028

Nimmerjahn, A., Kirchhoff, F., & Helmchen, F. (2005). Neuroscience: Resting microglial cells are highly dynamic surveillants of brain parenchyma in vivo. *Science, 308*(5726). https://doi.org/10.1126/science.1110647

Nisticò, R., Mango, D., Mandolesi, G., Piccinin, S., Berretta, N., Pignatelli, M., Feligioni, M., Musella, A., Gentile, A., Mori, F., Bernardi, G., Nicoletti, F., Mercuri, N. B., & Centonze, D. (2013). Inflammation Subverts Hippocampal Synaptic Plasticity in Experimental Multiple Sclerosis. *PLoS ONE*. https://doi.org/10.1371/journal.pone.0054666

Notter, T., Schalbetter, S. M., Clifton, N. E., Mattei, D., Richetto, J., Thomas, K., Meyer, U., & Hall, J. (2021). Neuronal activity increases translocator protein (TSPO) levels. *Molecular Psychiatry*. https://doi.org/10.1038/s41380-020-0745-1

Nutma, E., Ceyzériat, K., Amor, S., Tsartsalis, S., Millet, P., Owen, D. R.,

Papadopoulos, V., & Tournier, B. B. (2021). Cellular sources of TSPO expression in healthy and diseased brain. *European Journal of Nuclear Medicine and Molecular Imaging*. https://doi.org/10.1007/s00259-020-05166-2

Nutma, E., Stephenson, J. A., Gorter, R. P., De Bruin, J., Boucherie, D. M., Donat, C. K., Breur, M., Van Der Valk, P., Matthews, P. M., Owen, D. R., & Amor, S. (2019). A quantitative neuropathological assessment of translocator protein expression in multiple sclerosis. *Brain*. https://doi.org/10.1093/brain/awz287

O'Donnell, L. J., & Westin, C. F. (2011). An introduction to diffusion tensor image analysis. In *Neurosurgery Clinics of North America*. https://doi.org/10.1016/j.nec.2010.12.004

Okell, T. W., Garcia, M., Chappell, M. A., Byrne, J. V., & Jezzard, P. (2019). Visualizing artery-specific blood flow patterns above the circle of Willis with vessel-encoded arterial spin labeling. *Magnetic Resonance in Medicine*, *81*(3). https://doi.org/10.1002/mrm.27507

Ouzzani, M., Hammady, H., Fedorowicz, Z., & Elmagarmid, A. (2016). Rayyan-a web and mobile app for systematic reviews. *Systematic Reviews*, *5*(1). https://doi.org/10.1186/s13643-016-0384-4

Owen, D. R., Narayan, N., Wells, L., Healy, L., Smyth, E., Rabiner, E. A., Galloway, D., Williams, J. B., Lehr, J., Mandhair, H., Peferoen, L. A. N., Taylor, P. C., Amor, S., Antel, J. P., Matthews, P. M., & Moore, C. S. (2017). Pro-inflammatory activation of primary microglia and macrophages increases 18 kDa translocator protein expression in rodents but not humans. *Journal of Cerebral Blood Flow and Metabolism*. https://doi.org/10.1177/0271678X17710182

Özarslan, E., Koay, C. G., Shepherd, T. M., Komlosh, M. E., Irfanoğlu, M. O., Pierpaoli, C., & Basser, P. J. (2013). Mean apparent propagator (MAP) MRI: A novel diffusion imaging method for mapping tissue microstructure. *NeuroImage*. https://doi.org/10.1016/j.neuroimage.2013.04.016

Pain, C. C., Piggott, M. D., Goddard, A. J. H., Fang, F., Gorman, G. J., Marshall, D. P., Eaton, M. D., Power, P. W., & de Oliveira, C. R. E. (2005). Three-dimensional unstructured mesh ocean modelling. *Ocean Modelling*. https://doi.org/10.1016/j.ocemod.2004.07.005

Pan, B., Qu, Q., Xu, X., & Shi, Z. (2022). Structure-Color Preserving Network for Hyperspectral Image Super-Resolution. *IEEE Transactions on Geoscience and Remote Sensing*, *60*. https://doi.org/10.1109/TGRS.2021.3135028

Papadopoulos, D., Dukes, S., Patel, R., Nicholas, R., Vora, A., & Reynolds, R. (2009). Substantial archaeocortical atrophy and neuronal loss in multiple sclerosis. *Brain Pathology*. https://doi.org/10.1111/j.1750-3639.2008.00177.x

Papp, K. V., Kaplan, R. F., Springate, B., Moscufo, N., Wakefield, D. B., Guttmann, C. R. G., & Wolfson, L. (2014). Processing speed in normal aging: Effects of white matter hyperintensities and hippocampal volume loss. *Aging, Neuropsychology, and Cognition*, *21*(2). https://doi.org/10.1080/13825585.2013.795513

Parker, T. D., Slattery, C. F., Zhang, J., Nicholas, J. M., Paterson, R. W., Foulkes, A. J. M., Malone, I. B., Thomas, D. L., Modat, M., Cash, D. M., Crutch, S. J., Alexander, D. C., Ourselin, S., Fox, N. C., Zhang, H., & Schott, J. M. (2018). Cortical microstructure in young onset Alzheimer's disease using neurite orientation dispersion and density imaging. *Human Brain Mapping*, *39*(7). https://doi.org/10.1002/hbm.24056

Patten, S. B., Beck, C. A., Williams, J. V. A., Barbui, C., & Metz, L. M. (2003). Major depression in multiple sclerosis: A population-based perspective. In *Neurology*. https://doi.org/10.1212/01.WNL.0000095964.34294.B4

Patti, F. (2009). Cognitive impairment in multiple sclerosis. In *Multiple Sclerosis* (Vol. 15, Issue 1). https://doi.org/10.1177/1352458508096684

Pereira, J. B., Valls-Pedret, C., Ros, E., Palacios, E., Falcón, C., Bargalló, N., Bartrés-Faz, D., Wahlund, L. O., Westman, E., & Junque, C. (2014). Regional vulnerability of hippocampal subfields to aging measured by structural and diffusion MRI. *Hippocampus*. https://doi.org/10.1002/hipo.22234

Pérez-Rodríguez, D. R., Blanco-Luquin, I., & Mendioroz, M. (2021). The participation of microglia in neurogenesis: A review. In *Brain Sciences* (Vol. 11, Issue 5). https://doi.org/10.3390/brainsci11050658

Perosa, V., Priester, A., Ziegler, G., Cardenas-Blanco, A., Dobisch, L., Spallazzi, M., Assmann, A., Maass, A., Speck, O., Oltmer, J., Heinze, H. J., Schreiber, S., & Düzel, E. (2020). Hippocampal vascular reserve associated with cognitive performance and hippocampal volume. *Brain*. https://doi.org/10.1093/brain/awz383

Petcharunpaisan, S. (2010). Arterial spin labeling in neuroimaging. *World Journal of Radiology*, *2*(10). https://doi.org/10.4329/wjr.v2.i10.384

Peterson, J. W., Bö, L., Mörk, S., Chang, A., & Trapp, B. D. (2001). Transected neurites, apoptotic neurons, and reduced inflammation in cortical multiple sclerosis lesions. *Annals of Neurology*. https://doi.org/10.1002/ana.1123

Pierpaoli, C., Jezzard, P., Basser, P. J., Barnett, A., & Di Chiro, G. (1996). Diffusion tensor MR imaging of the human brain. *Radiology*, *201*(3). https://doi.org/10.1148/radiology.201.3.8939209

Pinna, A., & Colasanti, A. (2021). The Neurometabolic Basis of Mood Instability: The Parvalbumin Interneuron Link—A Systematic Review and Meta-Analysis. In *Frontiers in Pharmacology*. https://doi.org/10.3389/fphar.2021.689473

Planche, V., Ruet, A., Coupé, P., Lamargue-Hamel, D., Deloire, M., Pereira, B., Manjon, J. V., Munsch, F., Moscufo, N., Meier, D. S., Guttmann, C. R. G., Dousset, V., Brochet, B., & Tourdias, T. (2017). Hippocampal microstructural damage correlates with memory impairment in clinically isolated syndrome suggestive of multiple sclerosis. *Multiple Sclerosis*. https://doi.org/10.1177/1352458516675750

Pokryszko-Dragan, A., Frydecka, I., Kosmaczewska, A., Ciszak, L., Bilińska, M., Gruszka, E., Podemski, R., & Frydecka, D. (2012). Stimulated peripheral production of interferon-gamma is related to fatigue and depression in multiple sclerosis. *Clinical Neurology and Neurosurgery*, *114*(8). https://doi.org/10.1016/j.clineuro.2012.02.048

Portnoy, S., Flint, J. J., Blackband, S. J., & Stanisz, G. J. (2013). Oscillating and pulsed gradient diffusion magnetic resonance microscopy over an extended b-value range: Implications for the characterization of tissue microstructure. *Magnetic Resonance in Medicine*, *69*(4). https://doi.org/10.1002/mrm.24325

Pucak, M. L., Carroll, K. A. L., Kerr, D. A., & Kaplin, A. I. (2007). Neuropsychiatric manifestations of depression in multiple sclerosis: Neuroinflammatory, neuroendocrine, and neurotrophic mechanisms in the pathogenesis of immune-mediated depression. *Dialogues in Clinical Neuroscience*, *9*(2). https://doi.org/10.31887/dcns.2007.9.2/mpucak

Razek, A. A. K. A., El-Serougy, L., Abdelsalam, M., Gaballa, G., & Talaat, M. (2018). Differentiation of residual/recurrent gliomas from postradiation

necrosis with arterial spin labeling and diffusion tensor magnetic resonance imaging-derived metrics. *Neuroradiology*, *60*(2). https://doi.org/10.1007/s00234-017-1955-3

Reboldi, A., Coisne, C., Baumjohann, D., Benvenuto, F., Bottinelli, D., Lira, S., Uccelli, A., Lanzavecchia, A., Engelhardt, B., & Sallusto, F. (2009). C-C chemokine receptor 6-regulated entry of TH-17 cells into the CNS through the choroid plexus is required for the initiation of EAE. *Nature Immunology*, *10*(5). https://doi.org/10.1038/ni.1716

Reuben, A., Brickman, A. M., Muraskin, J., Steffener, J., & Stern, Y. (2011). Hippocampal atrophy relates to fluid intelligence decline in the elderly. *Journal of the International Neuropsychological Society*, *17*(1). https://doi.org/10.1017/S135561771000127X

Rice, C. M., Cottrell, D., Wilkins, A., & Scolding, N. J. (2013). Primary progressive multiple sclerosis: Progress and challenges. In *Journal of Neurology, Neurosurgery and Psychiatry* (Vol. 84, Issue 10). https://doi.org/10.1136/jnnp-2012-304140

Ridha, B. H., Barnes, J., Bartlett, J. W., Godbolt, A., Pepple, T., Rossor, M. N., & Fox, N. C. (2006). Tracking atrophy progression in familial Alzheimer's disease: a serial MRI study. *Lancet Neurology*, *5*(10). https://doi.org/10.1016/S1474-4422(06)70550-6

Ringman, J. M., O'Neill, J., Geschwind, D., Medina, L., Apostolova, L. G., Rodriguez, Y., Schaffer, B., Varpetian, A., Tseng, B., Ortiz, F., Fitten, J., Cummings, J. L., & Bartzokis, G. (2007). Diffusion tensor imaging in preclinical and presymptomatic carriers of familial Alzheimer's disease mutations. *Brain*, *130*(7). https://doi.org/10.1093/brain/awm102

Roca, M., Manes, F., Gleichgerrcht, E., Ibáñez, A., González De Toledo, M. E.,

Marenco, V., Bruno, D., Torralva, T., & Sinay, V. (2014). Cognitive but not affective theory of mind deficits in mild relapsing-remitting multiple sclerosis. *Cognitive and Behavioral Neurology*, *27*(1). https://doi.org/10.1097/WNN.0000000000000017

Rocca, M. A., Comi, G., & Filippi, M. (2017). The role of T1-weighted derived measures of neurodegeneration for assessing disability progression in multiple sclerosis. *Frontiers in Neurology*, *8*(SEP). https://doi.org/10.3389/fneur.2017.00433

Rocca, M. A., Longoni, G., Pagani, E., Boffa, G., Colombo, B., Rodegher, M., Martino, G., Falini, A., Comi, G., & Filippi, M. (2015). In vivo evidence of hippocampal dentate gyrus expansion in multiple sclerosis. *Human Brain Mapping*. https://doi.org/10.1002/hbm.22946

Rodriguez-Vieitez, E., & Nordberg, A. (2018). Imaging neuroinflammation: Quantification of astrocytosis in a multitracer PET approach. In *Methods in Molecular Biology*. https://doi.org/10.1007/978-1-4939-7704-8_16

Rogers, J. M., & Panegyres, P. K. (2007). Cognitive impairment in multiple sclerosis: Evidence-based analysis and recommendations. In *Journal of Clinical Neuroscience* (Vol. 14, Issue 10). https://doi.org/10.1016/j.jocn.2007.02.006

Roosendaal, S. D., Hulst, H. E., Vrenken, H., Feenstra, H. E. M., Castelijns, J. A., Pouwels, P. J. W., Barkhof, F., & Geurts, J. J. G. (2010). Structural and functional hippocampal changes in multiple sclerosis patients with intact memory function. *Radiology*. https://doi.org/10.1148/radiol.10091433

Rossi, S., Studer, V., Motta, C., Polidoro, S., Perugini, J., Macchiarulo, G., Giovannetti, A. M., Pareja-Gutierrez, L., Calò, A., Colonna, I., Furlan, R., Martino, G., & Centonze, D. (2017). Neuroinflammation drives anxiety and

depression in relapsing-remitting multiple sclerosis. *Neurology*, *89*(13). https://doi.org/10.1212/WNL.0000000000004411

Roufagalas, I., Avloniti, M., Fortosi, A., Xingi, E., Thomaidou, D., Probert, L., & Kyrargyri, V. (2021). Novel cell-based analysis reveals region-dependent changes in microglial dynamics in grey matter in a cuprizone model of demyelination. *Neurobiology of Disease*, *157*. https://doi.org/10.1016/j.nbd.2021.105449

Rubin, R. D., Watson, P. D., Duff, M. C., & Cohen, N. J. (2014). The role of the hippocampus in flexible cognition and social behavior. In *Frontiers in Human Neuroscience* (Vol. 8, Issue SEP). https://doi.org/10.3389/fnhum.2014.00742

Russo, M. V., & McGavern, D. B. (2016). Inflammatory neuroprotection following traumatic brain injury. In *Science*. https://doi.org/10.1126/science.aaf6260

Sadovnick, A. D., Remick, R. A., Allen, J., Swartz, E., Yee, I. M. L., Eisen, K., Farquhar, R., Hashimoto, S. A., Hooge, J., Kastrukoff, L. F., Morrison, W., Nelson, J., Oger, J., & Paty, D. W. (1996). Depression and multiple sclerosis. *Neurology*. https://doi.org/10.1212/WNL.46.3.628

Sagi, Y., Tavor, I., Hofstetter, S., Tzur-Moryosef, S., Blumenfeld-Katzir, T., & Assaf, Y. (2012). Learning in the Fast Lane: New Insights into Neuroplasticity. *Neuron*. https://doi.org/10.1016/j.neuron.2012.01.025

Salat, D. H. (2013). Diffusion Tensor Imaging in the Study of Aging and Age-Associated Neural Disease. In *Diffusion MRI: From Quantitative Measurement to In vivo Neuroanatomy: Second Edition*. https://doi.org/10.1016/B978-0-12-396460-1.00012-3

Sbardella, E., Petsas, N., Tona, F., Prosperini, L., Raz, E., Pace, G., Pozzilli, C.,

& Pantano, P. (2013). Assessing the Correlation between Grey and White Matter Damage with Motor and Cognitive Impairment in Multiple Sclerosis Patients. *PLoS ONE*. https://doi.org/10.1371/journal.pone.0063250

Sbardella, E., Tona, F., Petsas, N., & Pantano, P. (2013). DTI Measurements in Multiple Sclerosis: Evaluation of Brain Damage and Clinical Implications. *Multiple Sclerosis International*, *2013*. https://doi.org/10.1155/2013/671730

Sbardella, E., Tona, F., Petsas, N., Upadhyay, N., Piattella, M. C., Filippini, N., Prosperini, L., Pozzilli, C., & Pantano, P. (2015). Functional connectivity changes and their relationship with clinical disability and white matter integrity in patients with relapsing-remitting multiple sclerosis. *Multiple Sclerosis*, *21*(13). https://doi.org/10.1177/1352458514568826

Scalfari, A., Romualdi, C., Nicholas, R. S., Mattoscio, M., Magliozzi, R., Morra, A., Monaco, S., Muraro, P. A., & Calabrese, M. (2018). The cortical damage, early relapses, and onset of the progressive phase in multiple sclerosis. *Neurology*, *90*(24). https://doi.org/10.1212/WNL.0000000000005685

Schmitt, F. (2015). Echo-Planar Imaging. In *Brain Mapping: An Encyclopedic Reference*. https://doi.org/10.1016/B978-0-12-397025-1.00006-3

Schnider, A., Bassetti, C., Gutbrod, K., & Ozdoba, C. (1995). Very severe amnesia with acute onset after isolated hippocampal damage due to systemic lupus erythematosus. In *Journal of Neurology, Neurosurgery and Psychiatry*. https://doi.org/10.1136/jnnp.59.6.644-a

Schultz, C., & Engelhardt, M. (2014). Anatomy of the hippocampal formation. In *The Hippocampus in Clinical Neuroscience* (Vol. 34). https://doi.org/10.1159/000360925

Serres, S., Anthony, D. C., Jiang, Y., Broom, K. A., Campbell, S. J., Tyler, D.

J., Van Kasteren, S. I., Davis, B. G., & Sibson, N. R. (2009). Systemic inflammatory response reactivates immune-mediated lesions in rat brain. *Journal of Neuroscience*. https://doi.org/10.1523/JNEUROSCI.0406-09.2009

Shaw, K., Bell, L., Boyd, K., Grijseels, D. M., Clarke, D., Bonnar, O., Crombag, H. S., & Hall, C. N. (2021). Neurovascular coupling and oxygenation are decreased in hippocampus compared to neocortex because of microvascular differences. *Nature Communications*. https://doi.org/10.1038/s41467-021-23508-y

Shen, Y., Bai, L., Gao, Y., Cui, F., Tan, Z., Tao, Y., Sun, C., & Zhou, L. (2014). Depressive symptoms in multiple sclerosis from an in vivo study with TBSS. *BioMed Research International*. https://doi.org/10.1155/2014/148465

Shi, Y., Cheng, K., & Liu, Z. (2019). Hippocampal subfields segmentation in brain MR images using generative adversarial networks. *BioMedical Engineering Online*. https://doi.org/10.1186/s12938-019-0623-8

Sicotte, N. L., Kern, K. C., Giesser, B. S., Arshanapalli, A., Schultz, A., Montag, M., Wang, H., & Bookheimer, S. Y. (2008). Regional hippocampal atrophy in multiple sclerosis. *Brain*. https://doi.org/10.1093/brain/awn030

Siegert, R. J., & Abernethy, D. A. (2005). Depression in multiple sclerosis: A review. In *Journal of Neurology, Neurosurgery and Psychiatry* (Vol. 76, Issue 4, pp. 469–475). BMJ Publishing Group. https://doi.org/10.1136/jnnp.2004.054635

Sijens, P. E., & Oudkerk, M. (2005). Clinical magnetic resonance spectroscopy. In *Imaging Decisions MRI*. https://doi.org/10.1111/j.1617-

0830.2005.00038.x

Singhal, T., O'Connor, K., Dubey, S., Pan, H., Chu, R., Hurwitz, S., Cicero, S., Tauhid, S., Silbersweig, D., Stern, E., Kijewski, M., Dicarli, M., Weiner, H. L., & Bakshi, R. (2019). Gray matter microglial activation in relapsing vs progressive MS: A [F-18]PBR06-PET study. *Neurology: Neuroimmunology and NeuroInflammation*. https://doi.org/10.1212/NXI.0000000000000587

Singhal, T., Rissanen, E., Ficke, J., Cicero, S., Carter, K., & Weiner, H. L. (2021). Widespread Glial Activation in Primary Progressive Multiple Sclerosis Revealed by 18F-PBR06 PET: A Clinically Feasible, Individualized Approach. *Clinical Nuclear Medicine*, *46*(2). https://doi.org/10.1097/RLU.0000000000003398

Soares, D. P., & Law, M. (2009). Magnetic resonance spectroscopy of the brain: review of metabolites and clinical applications. In *Clinical Radiology*. https://doi.org/10.1016/j.crad.2008.07.002

Soares, J. M., Marques, P., Alves, V., & Sousa, N. (2013). A hitchhiker's guide to diffusion tensor imaging. *Frontiers in Neuroscience*. https://doi.org/10.3389/fnins.2013.00031

Sofroniew, M. V. (2009). Molecular dissection of reactive astrogliosis and glial scar formation. In *Trends in Neurosciences* (Vol. 32, Issue 12). https://doi.org/10.1016/j.tins.2009.08.002

Sormani, M. P., Bonzano, L., Roccatagliata, L., Cutter, G. R., Mancardi, G. L., & Bruzzi, P. (2009). Magnetic resonance imaging as a potential surrogate for relapses in multiple sclerosis: A meta-analytic approach. *Annals of Neurology*. https://doi.org/10.1002/ana.21606

Sosa, R. A., Murphey, C., Robinson, R. R., & Forsthuber, T. G. (2015). IFN-γ

ameliorates autoimmune encephalomyelitis by limiting myelin lipid peroxidation. *Proceedings of the National Academy of Sciences of the United States of America*. https://doi.org/10.1073/pnas.1505955112

Sotiropoulos, S. N., Jbabdi, S., Xu, J., Andersson, J. L., Moeller, S., Auerbach, E. J., Glasser, M. F., Hernandez, M., Sapiro, G., Jenkinson, M., Feinberg, D. A., Yacoub, E., Lenglet, C., Van Essen, D. C., Ugurbil, K., & Behrens, T. E. J. (2013). Advances in diffusion MRI acquisition and processing in the Human Connectome Project. *NeuroImage*, *80*. https://doi.org/10.1016/j.neuroimage.2013.05.057

Spano, B., Giulietti, G., Pisani, V., Morreale, M., Tuzzi, E., Nocentini, U., Francia, A., Caltagirone, C., Bozzali, M., & Cercignani, M. (2018). Disruption of neurite morphology parallels MS progression. *Neurology: Neuroimmunology and NeuroInflammation*, *5*(6). https://doi.org/10.1212/NXI.0000000000000502

Spitzer, R. L., Kroenke, K., Williams, J. B. W., & Löwe, B. (2006). A brief measure for assessing generalized anxiety disorder: The GAD-7. *Archives of Internal Medicine*, *166*(10). https://doi.org/10.1001/archinte.166.10.1092

Stagg, C. J., Bachtiar, V., Amadi, U., Gudberg, C. A., Ilie, A. S., Sampaio-Baptista, C., O'Shea, J., Woolrich, M., Smith, S. M., Filippini, N., Near, J., & Johansen-Berg, H. (2014). Local GABA concentration is related to network-level resting functional connectivity. *ELife*. https://doi.org/10.7554/eLife.01465

Stamoula, E., Siafis, S., Dardalas, I., Ainatzoglou, A., Matsas, A., Athanasiadis, T., Sardeli, C., Stamoulas, K., & Papazisis, G. (2021). Antidepressants on Multiple Sclerosis: A Review of In Vitro and In Vivo Models. In *Frontiers in Immunology* (Vol. 12). https://doi.org/10.3389/fimmu.2021.677879

Stanisz, G. J., Webb, S., Munro, C. A., Pun, T., & Midha, R. (2004). MR Properties of Excised Neural Tissue Following Experimentally Induced Inflammation. *Magnetic Resonance in Medicine.* https://doi.org/10.1002/mrm.20008

Starr, J. M., Farrall, A. J., Armitage, P., McGurn, B., & Wardlaw, J. (2009). Blood-brain barrier permeability in Alzheimer's disease: a case-control MRI study. *Psychiatry Research - Neuroimaging.* https://doi.org/10.1016/j.pscychresns.2008.04.003

Stebbins, G. T. (2010). Diffusion Tensor Imaging in Parkinson's Disease. In *Encyclopedia of Movement Disorders*. https://doi.org/10.1016/B978-0-12-374105-9.00020-4

Stern, Y. (2002). What is cognitive reserve? Theory and research application of the reserve concept. *Journal of the International Neuropsychological Society*, *8*(3). https://doi.org/10.1017/S1355617702813248

Stern, Y. (2012). Cognitive reserve in ageing and Alzheimer's disease. In *The Lancet Neurology* (Vol. 11, Issue 11). https://doi.org/10.1016/S1474-4422(12)70191-6

Stern, Y., Habeck, C., Moeller, J., Scarmeas, N., Anderson, K. E., Hilton, H. J., Flynn, J., Sackeim, H., & Van Heertum, R. (2005). Brain networks associated with cognitive reserve in healthy young and old adults. *Cerebral Cortex*, *15*(4). https://doi.org/10.1093/cercor/bhh142

Stevenson, V. L., Miller, D. H., Rovaris, M., Barkhof, F., Brochet, B., Dousset, V., Dousset, V., Filippi, M., Montalban, X., Polman, C. H., Rovira, A., De Sa, J., & Thompson, A. J. (1999). Primary and transitional progressive MS: A clinical and MRI cross- sectional study. *Neurology.* https://doi.org/10.1212/wnl.52.4.839

Sumowski, J. F., & Leavitt, V. M. (2013). Cognitive reserve in multiple sclerosis. In *Multiple Sclerosis Journal* (Vol. 19, Issue 9). https://doi.org/10.1177/1352458513498834

Sumowski, J. F., Wylie, G. R., Deluca, J., & Chiaravalloti, N. (2010). Intellectual enrichment is linked to cerebral efficiency in multiple sclerosis: Functional magnetic resonance imaging evidence for cognitive reserve. *Brain*, *133*(2). https://doi.org/10.1093/brain/awp307

Swanberg, K. M., Landheer, K., Pitt, D., & Juchem, C. (2019). Quantifying the Metabolic Signature of Multiple Sclerosis by in vivo Proton Magnetic Resonance Spectroscopy: Current Challenges and Future Outlook in the Translation From Proton Signal to Diagnostic Biomarker. In *Frontiers in Neurology* (Vol. 10). https://doi.org/10.3389/fneur.2019.01173

Takeda, A., Minatani, S., Ishii, A., Matsuo, T., Tanaka, M., Yoshikawa, T., & Itoh, Y. (2021). Impact of depression on mental fatigue and attention in patients with multiple sclerosis. *Journal of Affective Disorders Reports*, *5*. https://doi.org/10.1016/j.jadr.2021.100143

Talbot, P. J., Arnold, D., & Antel, J. P. (2001). Virus-induced autoimmune reactions in the CNS. In *Current Topics in Microbiology and Immunology*. https://doi.org/10.1007/978-3-662-10356-2_12

Tarasiuk, J., Kapica-Topczewska, K., Czarnowska, A., Chorąży, M., Kochanowicz, J., & Kułakowska, A. (2022). Co-occurrence of Fatigue and Depression in People With Multiple Sclerosis: A Mini-Review. In *Frontiers in Neurology* (Vol. 12). https://doi.org/10.3389/fneur.2021.817256

Taylor, D. L., Jones, F., Chen Seho Kubota, E. S. F., & Pocock, J. M. (2005). Stimulation of microglial metabotropic glutamate receptor mGlu2 triggers tumor necrosis factor α-induced neurotoxicity in concert with microglial-

derived Fas ligand. *Journal of Neuroscience*, *25*(11).
https://doi.org/10.1523/JNEUROSCI.4456-04.2005

Testaverde, L., Caporali, L., Venditti, E., Grillea, G., & Colonnese, C. (2012). Diffusion tensor imaging applications in multiple sclerosis patients using 3T magnetic resonance: A preliminary study. *European Radiology*, *22*(5). https://doi.org/10.1007/s00330-011-2342-9

Thompson, A. G. B., Sheldon, R., Poole, N., Varela, R., White, S., Jones, P., Mulley, C., Berg, A., Blain, C. R. V., & Agrawal, N. (2019). A new way of rapidly screening for depression in multiple sclerosis using Emotional Thermometers. *Acta Neuropsychiatrica*. https://doi.org/10.1017/neu.2019.1

Thompson, A. J., Banwell, B. L., Barkhof, F., Carroll, W. M., Coetzee, T., Comi, G., Correale, J., Fazekas, F., Filippi, M., Freedman, M. S., Fujihara, K., Galetta, S. L., Hartung, H. P., Kappos, L., Lublin, F. D., Marrie, R. A., Miller, A. E., Miller, D. H., Montalban, X., … Cohen, J. A. (2018). Diagnosis of multiple sclerosis: 2017 revisions of the McDonald criteria. In *The Lancet Neurology*. https://doi.org/10.1016/S1474-4422(17)30470-2

Thompson, A. J., Kermode, A. G., Wicks, D., MacManus, D. G., Kendall, B. E., Kingsley, D. P. E., & McDonald, W. I. (1991). Major differences in the dynamics of primary and secondary progressive multiple sclerosis. *Annals of Neurology*. https://doi.org/10.1002/ana.410290111

Thompson, A. J., Polman, C. H., Miller, D. H., McDonald, W. I., Brochet, B., Filippi, M., Montalban, X., & De Sá, J. (1997). Primary progressive multiple sclerosis. In *Brain*. https://doi.org/10.1093/brain/120.6.1085

Thompson, A., Kobelt, G., Berg, J., Capsa, D., Eriksson, J., & Miller, D. (2017). New insights into the burden and costs of multiple sclerosis in Europe: Results for the United Kingdom. *Multiple Sclerosis Journal*,

23(2_suppl), 204–216. https://doi.org/10.1177/1352458517708687

Thorpe, J. W., Kidd, D., Moseley, I. F., Kendall, B. E., Thompson, A. J., MacManus, D. G., McDonald, W. I., & Miller, D. H. (1996). Serial gadolinium-enhanced MRI of the brain and spinal cord in early relapsing-remitting multiple sclerosis. *Neurology*. https://doi.org/10.1212/WNL.46.2.373

Tiberio, M., Chard, D. T., Altmann, D. R., Davies, G., Griffin, C. M., McLean, M. A., Rashid, W., Sastre-Garriga, J., Thompson, A. J., & Miller, D. H. (2006). Metabolite changes in early relapsing-remitting multiple sclerosis: A two year follow-up study. *Journal of Neurology*. https://doi.org/10.1007/s00415-005-0964-z

Tognarelli, J. M., Dawood, M., Shariff, M. I. F., Grover, V. P. B., Crossey, M. M. E., Cox, I. J., Taylor-Robinson, S. D., & McPhail, M. J. W. (2015). Magnetic Resonance Spectroscopy: Principles and Techniques: Lessons for Clinicians. In *Journal of Clinical and Experimental Hepatology*. https://doi.org/10.1016/j.jceh.2015.10.006

Toschi, N., De Santis, S., Granberg, T., Ouellette, R., Treaba, C. A., Herranz, E., & Mainero, C. (2019). Evidence for Progressive Microstructural Damage in Early Multiple Sclerosis by Multi-Shell Diffusion Magnetic Resonance Imaging. *Neuroscience*, *403*. https://doi.org/10.1016/j.neuroscience.2019.01.022

Trapp, B. D., & Nave, K. A. (2008). Multiple sclerosis: An immune or neurodegenerative disorder? In *Annual Review of Neuroscience*. https://doi.org/10.1146/annurev.neuro.30.051606.094313

Trapp, B. D., & Stys, P. K. (2009). Virtual hypoxia and chronic necrosis of demyelinated axons in multiple sclerosis. In *The Lancet Neurology* (Vol. 8,

Issue 3). https://doi.org/10.1016/S1474-4422(09)70043-2

Treit, S., Steve, T., Gross, D. W., & Beaulieu, C. (2018). High resolution in-vivo diffusion imaging of the human hippocampus. *NeuroImage*. https://doi.org/10.1016/j.neuroimage.2018.01.034

Tsouki, F., & Williams, A. (2021). Multifaceted involvement of microglia in gray matter pathology in multiple sclerosis. In *Stem Cells* (Vol. 39, Issue 8). https://doi.org/10.1002/stem.3374

Valero, J., Bernardino, L., Cardoso, F. L., Silva, A. P., Fontes-Ribeiro, C., Ambrósio, A. F., & Malva, J. O. (2017). Impact of Neuroinflammation on Hippocampal Neurogenesis: Relevance to Aging and Alzheimer's Disease. *Journal of Alzheimer's Disease*, *60*(s1), S161–S168. https://doi.org/10.3233/JAD-170239

Van Waesberghe, J. H. T. M., Kamphorst, W., De Groot, C. J. A., Van Walderveen, M. A. A., Castelijns, J. A., Ravid, R., Lycklama À Nijeholt, G. J., Van Der Valk, P., Polman, C. H., Thompson, A. J., & Barkhof, F. (1999). Axonal loss in multiple sclerosis lesions: Magnetic resonance imaging insights into substrates of disability. *Annals of Neurology*. https://doi.org/10.1002/1531-8249(199911)46:5<747::AID-ANA10>3.0.CO;2-4

Van Walderveen, M. A. A., Kamphorst, W., Scheltens, P., Van Waesberghe, J. H. T. M., Ravid, R., Valk, J., Polman, C. H., & Barkhof, F. (1998). Histopathologic correlate of hypointense lesions on T1-weighted spin- echo MRI in multiple sclerosis. *Neurology*. https://doi.org/10.1212/WNL.50.5.1282

Vasek, M. J., Garber, C., Dorsey, D., Durrant, D. M., Bollman, B., Soung, A., Yu, J., Perez-Torres, C., Frouin, A., Wilton, D. K., Funk, K., DeMasters, B.

K., Jiang, X., Bowen, J. R., Mennerick, S., Robinson, J. K., Garbow, J. R., Tyler, K. L., Suthar, M. S., … Klein, R. S. (2016). A complement-microglial axis drives synapse loss during virus-induced memory impairment. *Nature*. https://doi.org/10.1038/nature18283

Vasic, V., & Schmidt, M. H. H. (2017). Resilience and vulnerability to pain and inflammation in the hippocampus. In *International Journal of Molecular Sciences* (Vol. 18, Issue 4). MDPI AG. https://doi.org/10.3390/ijms18040739

Vaughn, C. B., Kavak, K. S., Dwyer, M. G., Bushra, A., Nadeem, M., Cookfair, D. L., Ramanathan, M., Benedict, R. H. B., Zivadinov, R., Goodman, A., Krupp, L., Motl, R. W., Weinstock-Guttman, B., Kolb, C., Robb, J. F., Jubelt, B., Gerber, A., Kister, I., Ryerson, L. Z., … Picone, M. A. (2020). Fatigue at enrollment predicts EDSS worsening in the New York State Multiple Sclerosis Consortium. *Multiple Sclerosis Journal*, *26*(1). https://doi.org/10.1177/1352458518816619

Venkatesh, A., Stark, S. M., Stark, C. E. L., & Bennett, I. J. (2020). Age- and memory- related differences in hippocampal gray matter integrity are better captured by NODDI compared to single-tensor diffusion imaging. *Neurobiology of Aging*, *96*. https://doi.org/10.1016/j.neurobiolaging.2020.08.004

Venneti, Sriram; Lopresti, Brian J; Wiley, C. A. (2006). The peripheral benzodiazepine receptor in microglia: from pathology to imaging. *Progress in Neurobiology*.

Veraart, J., Novikov, D. S., Christiaens, D., Ades-aron, B., Sijbers, J., & Fieremans, E. (2016). Denoising of diffusion MRI using random matrix theory. *NeuroImage*, *142*. https://doi.org/10.1016/j.neuroimage.2016.08.016

Veronica Witte, A., Kerti, L., Margulies, D. S., & Flöel, A. (2014). Effects of resveratrol on memory performance, hippocampal functional connectivity, and glucose metabolism in healthy older adults. *Journal of Neuroscience*, *34*(23). https://doi.org/10.1523/JNEUROSCI.0385-14.2014

Vicente-Rodríguez, M., Singh, N., Turkheimer, F., Peris-Yague, A., Randall, K., Veronese, M., Simmons, C., Karim Haji-Dheere, A., Bordoloi, J., Sander, K., Awais, R. O., Årstad, E., NIMA Consortium, Cash, D., & Parker, C. A. (2021). Resolving the cellular specificity of TSPO imaging in a rat model of peripherally-induced neuroinflammation. *Brain, Behavior, and Immunity*. https://doi.org/10.1016/j.bbi.2021.05.025

Vrenken, H., Pouwels, P. J. W., Ropele, S., Knol, D. L., Geurts, J. J. G., Polman, C. H., Barkhof, F., & Castelijns, J. A. (2007). Magnetization transfer ratio measurement in multiple sclerosis normal-appearing brain tissue: Limited differences with controls but relationships with clinical and MR measures of disease. *Multiple Sclerosis*. https://doi.org/10.1177/1352458506075521

Wang, Y., Coughlin, J. M., Ma, S., Endres, C. J., Kassiou, M., Sawa, A., Dannals, R. F., Petri, M., & Pomper, M. G. (2017). Neuroimaging of translocator protein in patients with systemic lupus erythematosus: A pilot study using [11C]DPA-713 positron emission tomography. *Lupus*. https://doi.org/10.1177/0961203316657432

Weston, P. S. J., Simpson, I. J. A., Ryan, N. S., Ourselin, S., & Fox, N. C. (2015). Diffusion imaging changes in grey matter in Alzheimer's disease: A potential marker of early neurodegeneration. In *Alzheimer's Research and Therapy* (Vol. 7, Issue 1). https://doi.org/10.1186/s13195-015-0132-3

Williamson, L. L., & Bilbo, S. D. (2013). Chemokines and the hippocampus: A new perspective on hippocampal plasticity and vulnerability. In *Brain,*

Behavior, and Immunity. https://doi.org/10.1016/j.bbi.2013.01.077

Winston, G. P. (2012). The physical and biological basis of quantitative parameters derived from diffusion MRI. *Quantitative Imaging in Medicine and Surgery*, *2*(4). https://doi.org/10.3978/j.issn.2223-4292.2012.12.05

Wolinsky, J. S., Narayana, P. A., Johnson, K. P., Pruitt, A. A., Kolson, D., Gonzalez-Scarano, F., Bird, S. J., Pfohl, D., Grossman, R., Mannon, L., Ford, C. C., Greinel, E., Padilla, R., Lisak, R. P., Khan, O., Tselis, A. C., Kamholtz, J., Garbern, J., Lewis, R., … Gorbova, M. (2001). United States open-label glatiramer acetate extension trial for relapsing multiple sclerosis: MRI and clinical correlates. *Multiple Sclerosis*. https://doi.org/10.1191/135245801667520627

Wood, E. T., Ronen, I., Techawiboonwong, A., Jones, C. K., Barker, P. B., Calabresi, P., Harrison, D., & Reich, D. S. (2012). Investigating axonal damage in multiple sclerosis by diffusion tensor spectroscopy. *Journal of Neuroscience*, *32*(19). https://doi.org/10.1523/JNEUROSCI.0044-12.2012

Woodcock, E. A., Schain, M., Cosgrove, K. P., & Hillmer, A. T. (2020). Quantification of [11C]PBR28 data after systemic lipopolysaccharide challenge. *EJNMMI Research*. https://doi.org/10.1186/s13550-020-0605-7

Wu, Y., Xu, X., Chen, Z., Duan, J., Hashimoto, K., Yang, L., Liu, C., & Yang, C. (2020). Nervous system involvement after infection with COVID-19 and other coronaviruses. In *Brain, Behavior, and Immunity*. https://doi.org/10.1016/j.bbi.2020.03.031

Wujek, J. R., Bjartmar, C., Richer, E., Ransohoff, R. M., Yu, M., Tuohy, V. K., & Trapp, B. D. (2002). Axon loss in the spinal cord determines permanent neurological disability in an animal model of multiple sclerosis. *Journal of Neuropathology and Experimental Neurology*.

https://doi.org/10.1093/jnen/61.1.23

Wyatt-Johnson, S. K., Herr, S. A., & Brewster, A. L. (2017). Status epilepticus triggers time-dependent alterations in microglia abundance and morphological phenotypes in the hippocampus. *Frontiers in Neurology*, *8*(DEC). https://doi.org/10.3389/fneur.2017.00700

Wylezinska, M., Cifelli, A., Jezzard, P., Palace, J., Alecci, M., & Matthews, P. M. (2003). Thalamic neurodegeneration in relapsing-remitting multiple sclerosis. *Neurology*. https://doi.org/10.1212/01.WNL.0000069464.22267.95

Wyss-Coray, T. (2016). Ageing, neurodegeneration and brain rejuvenation. In *Nature*. https://doi.org/10.1038/nature20411

Yamamoto, J., & Tonegawa, S. (2017). Direct Medial Entorhinal Cortex Input to Hippocampal CA1 Is Crucial for Extended Quiet Awake Replay. *Neuron*, *96*(1). https://doi.org/10.1016/j.neuron.2017.09.017

Yegorov, Y. E., Poznyak, A. V., Nikiforov, N. G., Sobenin, I. A., & Orekhov, A. N. (2020). The link between chronic stress and accelerated aging. In *Biomedicines*. https://doi.org/10.3390/BIOMEDICINES8070198

Yi, S. Y., Barnett, B. R., Torres-Velázquez, M., Zhang, Y., Hurley, S. A., Rowley, P. A., Hernando, D., & Yu, J. P. J. (2019). Detecting microglial density with quantitative multi-compartment diffusion MRI. *Frontiers in Neuroscience*, *13*(FEB). https://doi.org/10.3389/fnins.2019.00081

Yin, P., Liu, Y., Xiong, H., Han, Y., Kumar Sah, S., Zeng, C., Wang, J., & Li, Y. (2018). Structural abnormalities and altered regional brain activity in multiple sclerosis with simple spinal cord involvement. *British Journal of Radiology*. https://doi.org/10.1259/bjr.20150777

Yushkevich, P. A., Piven, J., Hazlett, H. C., Smith, R. G., Ho, S., Gee, J. C., &

Gerig, G. (2006). User-guided 3D active contour segmentation of anatomical structures: Significantly improved efficiency and reliability. *NeuroImage*, *31*(3). https://doi.org/10.1016/j.neuroimage.2006.01.015

Yushkevich, P. A., Pluta, J. B., Wang, H., Xie, L., Ding, S. L., Gertje, E. C., Mancuso, L., Kliot, D., Das, S. R., & Wolk, D. A. (2015). Automated volumetry and regional thickness analysis of hippocampal subfields and medial temporal cortical structures in mild cognitive impairment. *Human Brain Mapping*, *36*(1). https://doi.org/10.1002/hbm.22627

Zeydan, B., & Kantarci, O. H. (2020). Impact of Age on Multiple Sclerosis Disease Activity and Progression. In *Current Neurology and Neuroscience Reports* (Vol. 20, Issue 7). https://doi.org/10.1007/s11910-020-01046-2

Zhang, H., Schneider, T., Wheeler-Kingshott, C. A., & Alexander, D. C. (2012). NODDI: Practical in vivo neurite orientation dispersion and density imaging of the human brain. *NeuroImage*. https://doi.org/10.1016/j.neuroimage.2012.03.072

Zheng, F., Cui, D., Zhang, L., Zhang, S., Zhao, Y., Liu, X., Liu, C., Li, Z., Zhang, D., Shi, L., Liu, Z., Hou, K., Lu, W., Yin, T., & Qiu, J. (2018). The volume of hippocampal subfields in relation to decline of memory recall across the adult lifespan. *Frontiers in Aging Neuroscience*. https://doi.org/10.3389/fnagi.2018.00320

Zrzavy, T., Endmayr, V., Bauer, J., Macher, S., Mossaheb, N., Schwaiger, C., Ricken, G., Winklehner, M., Glatter, S., Breu, M., Wimmer, I., Kovacs, G. G., Risser, D. U., Klupp, N., Simonitsch-Klupp, I., Roetzer, T., Rommer, P., Berger, T., Gelpi, E., … Höftberger, R. (2021). Neuropathological Variability within a Spectrum of NMDAR-Encephalitis. *Annals of Neurology*. https://doi.org/10.1002/ana.26223